

**PRECLINICAL EVALUATION OF MERIVA (A
FORMULATION OF CURCUMIN) AS A PUTATIVE
AGENT FOR CHEMOPREVENTION OF LUNG
CANCER**

**Thesis submitted for the degree of
Doctor of Philosophy
at the University of Leicester**

by

**Jagdish Mahale, M.Pharm
Department of Cancer Studies
University of Leicester**

September 2016

Abstract

Preclinical evaluation of Meriva (a formulation of curcumin) as a putative agent for chemoprevention of lung cancer

Jagdish Mahale

Curcumin, a naturally occurring dietary polyphenol, has been investigated for several years for its role in chemoprevention of cancer. There are emerging evidences that curcumin may have a potential role in prevention and treatment of lung cancer. Curcumin in its natural form is poorly absorbed, extensively metabolised and rapidly excreted. Meriva, a phospholipid formulation of curcumin, promises to enhance its bioavailability. The work described in this thesis investigates whether Meriva offers pharmacokinetic advantage over unformulated curcumin, elucidate a possible mechanism of action for curcumin and determine efficacy of Meriva *in vivo* using xenograft model of lung cancer.

Meriva offered superior curcumin and curcumin metabolites levels in mice plasma and lungs at two different dose levels (high and low). The levels were 5-16 fold higher for Meriva as compared to unformulated curcumin. A HPLC-UV method developed and validated for simultaneous quantification of curcumin and metabolites was found to reliable and reproducible.

In vitro, a 3D organotypic model was used to demonstrate important role stromal components, namely fibroblasts, play in cell invasion and metastasis. Curcumin treatment of organotypic cultures significantly inhibited tumour cell invasion. Curcumin also modulated a number of key proteins in HGF/MET signalling axis.

Nude mice were administered either control diet or diet supplemented with 0.226% w/w Meriva one week after A549:MRC5 (1:5) cell inoculation. Meriva significantly inhibited tumour growth versus control ($p < 0.05$). The expression of p53, Ki-67 and cleaved caspase-3 which were significantly altered following Meriva intervention.

These results together provide evidence that Meriva at a clinical relevant dose regime may be investigated in prevention and treatment of lung cancer.

Acknowledgement

This thesis becomes a reality with kind support and help of many individuals. I would like to extend my sincere thanks to all of them.

Foremost I would like to express my sincere gratitude to my supervisors, Professor Karen Brown and Dr Lynne Howells. Without their guidance this thesis would not have been completed. I would also like to express my appreciation to Dr. Stewart Sale for all his help during the first year of my research and for his continued interest in my work subsequent to his unexpected departure from the university. My deepest appreciation is extended to Professor Andreas Gescher and Dr. Hong Cai for the time and effort they invested in different aspects of my research, to facilitate my success. I would also like to express my thanks to Dr. Emma Horner-Glister, Dr. Catherine Adreadi, Dr. Jennifer Higgins, Maria Szpek and Melanie Haberle who in a number of ways contributed to the completion of my research. I am also very grateful for the support and the discussions with my fellow colleagues, Kelly, Jonny, Dhafer, Karzan, Ankur, Gintare, Con and Christina; it all contributed to a memorable experience.

Without the help and support of my family, my dream of completing a PhD would not have become a reality. My family and friends have been my strongest supporters during my sojourn in the UK. I am very thankful for their unwavering support and confidence in my abilities. I would also like to extend a special thanks to a very special person in my life Miss Nikita Derle for always being there for me. Finally I would like to extend the highest praise and thanks to God for the grace and opportunity to 'stay the course' that has culminated in this thesis.

List of contents

Abstract	i
Acknowledgements	ii
List of Contents	iii
Table of Contents	iii
List of Figures	viii
List of Tables	xii
List of Abbreviations	xiv
List of Publications and Conference Abstracts	xvii

Table of Contents

1	Introduction.....	1
1.1	Lung Cancer	1
1.1.1	Epidemiology of lung cancer	1
1.2	Risk factors for lung cancer	2
1.2.1	Tobacco Smoking	2
1.2.2	Passive Smoking.....	2
1.2.3	Environmental/Occupational factors.....	3
1.2.4	Family history	4
1.2.5	Age.....	5
1.2.6	Diet.....	5
1.2.7	Other lung diseases	5
1.3	Anatomy of the human Lung.....	6
1.4	Classification of lung cancer	6
1.4.1	Non-small cell lung cancer (NSCLC).....	7
1.4.2	Small cell lung cancer	8
1.5	Signs and symptoms of lung cancer	9

1.5.1	Symptoms of localised lung cancer.....	9
1.5.2	Symptoms of locally advanced disease	9
1.5.3	Symptoms of metastatic disease.....	9
1.6	Screening for lung cancer	9
1.7	Diagnosis of lung cancer	10
1.8	Staging of Lung cancer.....	12
1.8.1	Number staging system.....	12
1.8.2	TNM staging system	13
1.9	Management of Lung cancer	14
1.9.1	Surgery.....	14
1.9.2	Radiotherapy.....	14
1.9.3	Chemotherapy.....	14
1.10	Molecular pathogenesis of lung cancer	15
1.10.1	EGFR mutations	16
1.10.2	KRAS mutations.....	17
1.10.3	EML4-ALK Mutations.....	17
1.10.4	HGF/MET signalling.....	18
1.11	Prevention of lung cancer.....	22
1.11.1	Chemoprevention.....	23
1.11.2	Chemopreventive agents for lung cancer	28
1.11.3	Chemoprevention trials: Reason for failure.....	32
1.12	Curcumin	34
1.12.1	Possible mechanism of action of curcumin	35
1.12.2	Preclinical studies of curcumin and lung cancer	38
1.12.3	Clinical studies of curcumin	42
1.12.4	Pharmacokinetics and metabolism of curcumin.....	43
1.12.5	Preclinical models of lung cancer.....	53

2	Materials and Methods	58
2.1	Materials	58
2.1.1	Chemicals and Reagents	58
2.1.2	Polyacrylamide gel composition	58
2.1.3	Buffers.....	59
2.2	Methods.....	61
2.2.1	Synthesis of curcumin metabolites.....	61
2.2.2	Comparative pharmacokinetic study of curcumin and Meriva in mice - High dose study	64
2.2.3	Modification of extraction method to improve efficiency	66
2.2.4	Comparative pharmacokinetic study of curcumin and Meriva in mice using new validated method - Low dose study.....	67
2.2.5	Healthy volunteer turmeric food pharmacokinetic study	67
2.2.6	Cell Culture	68
2.2.7	Xenograft study and lysate preparation.....	78
2.3	Statistical analysis	80
3	Pharmacokinetic and Metabolism study of curcumin and Meriva	81
3.1	Introduction.....	81
3.2	Curcumin and metabolite concentration in plasma and lung tissue following a single oral dose - High dose pharmacokinetic study.	83
3.2.1	Enzymatic conversion of plasma and lung samples.....	90
3.3	Full validation of the improved HPLC-UV method for simultaneous detection and quantification of curcumin, curcumin glucuronide and curcumin sulfate.....	97
3.3.1	Accuracy and precision	97
3.3.2	Recovery	98
3.3.3	Linearity.....	100
3.3.4	Selectivity and sensitivity.....	100

3.3.5	Stability.....	102
3.4	Curcumin and metabolite concentration in plasma and lung tissue following a single oral dose - Low dose pharmacokinetic study	105
3.4.1	Enzymatic conversion of plasma and lung samples.....	110
3.5	Healthy human volunteer turmeric food Study.....	115
3.6	Discussion	119
4	<i>In-vitro</i> effect of curcumin on HGF/MET signalling axis	125
4.1	Introduction.....	125
4.2	Effect of curcumin on proliferation of A549 and MRC5 cells.....	126
4.3	Effect of MRC5 fibroblasts on invasiveness of A549 cells	129
4.4	Effect of curcumin treatment on invasion of A549 cells	137
4.5	Effect of conditioned media on the HGF/MET pathway	139
4.6	Effect of curcumin treatment on the HGF-MET pathway	142
4.7	Effect of curcumin treatment on HGF stimulated HGF-MET pathway 147	
4.7.1	Optimisation of HGF stimulation conditions.....	147
4.8	Effect of curcumin treatment on HGF expression in MRC5 fibroblasts 153	
4.9	Discussion	154
5	<i>In vivo</i> efficacy of Meriva in lung cancer xenograft	159
5.1	Introduction.....	159
5.2	Effect of MRC5 fibroblasts on A549 lung cancer cells growth in nude mice 160	
5.3	Determination of cell population sub-type in co-culture xenograft tumours	161
5.4	Effect of Meriva consumption on A549:MRC5 co-culture xenografts in nude mice.....	164

5.5	Modulation of HGF/MET pathway and downstream proteins by Meriva in tumour tissue	167
5.6	Modulation of the apoptotic proteins, p21, p27, p53, Bax and Bcl-2 by Meriva in tumour tissue	170
5.7	Modulation of the autophagy proteins LC3-I, LC3-II and inflammatory marker COX-2 by Meriva in tumour tissue	173
5.8	Effect of Meriva on cell proliferation and apoptosis in paraffin-embedded xenograft tumour tissue using immunohistochemical staining..	174
5.9	Curcumin and metabolite levels in xenograft tumours and lung tissue following consumption of Meriva.	177
5.10	Discussion	179
6.	Concluding Discussion	184
7	References	192

List of figures

Figure 1.1 Scheme linking tobacco smoke carcinogens and lung cancer.....	3
Figure 1.2 Anatomy of lung.....	6
Figure 1.3 Flowchart for diagnosis of lung cancer.	11
Figure 1.4 Common mutations in lung cancer	16
Figure 1.5 HGF/Met Pathway	19
Figure 1.6 Functional crosstalk of HGF-MET signalling pathway with EGFR and VEGFR signalling pathway.	22
Figure 1.7 Intervention of chemopreventive agents at different stages of lung cancer.....	24
Figure 1.8 Potential genetic targets for chemoprevention of lung cancer	25
Figure 1.9 The classical and current view of carcinogenesis and chemoprevention targets.	27
Figure 1.10 CAF-tumour cell crosstalk.....	28
Figure 1.11 Structure of curcuminoids	35
Figure 1.12 Molecular targets of curcumin.....	36
Figure 1.13 Metabolism of curcumin following different routes of administration.	48
Figure 1.14 Difference between a phytosome and a liposome.	51
Figure 2.1 Organotypic co-culture set-up.....	73
Figure 3.1 Representative HPLC-UV chromatograms of mouse plasma following oral gavage dosing of unformulated curcumin or Meriva.	85
Figure 3.2 Concentrations of curcumin metabolites in mouse plasma following oral dosing with unformulated curcumin or Meriva.....	86
Figure 3.3 Representative HPLC-UV chromatograms of extracts from mouse lung homogenate following oral gavage dosing of unformulated curcumin or Meriva.....	87
Figure 3.4 Concentrations of curcumin and curcumin metabolites in mouse lungs following oral dosing with unformulated curcumin or Meriva.....	88
Figure 3.5 Representative HPLC-UV chromatograms of mouse plasma following oral gavage dosing of unformulated curcumin or Meriva and enzymatic conversion.	91
Figure 3.6 Concentrations of curcuminoids in mouse plasma following oral dosing with unformulated curcumin or Meriva and enzymatic conversion.	92

Figure 3.7 Representative HPLC-uvchromatograms of extracts from mouse lung homogenate following oral dosing of unformulated curcumin or Meriva and enzymatic conversion.	93
Figure 3.8 Concentrations of curcuminoids in mouse lung homogenate following oral dosing with unformulated curcumin or Meriva and enzymatic conversion.	94
Figure 3.9 Representative HPLC chromatogram of curcumin and metabolites spiked in to plasma and lung homogenate.....	101
Figure 3.10 LC-MS/MS multiple reaction monitoring (MRM) transition in mouse plasma following oral Meriva dosing.	106
Figure 3.11 Representative HPLC chromatograms of mouse plasma following oral gavage dosing of unformulated curcumin or Meriva (low dose).	107
Figure 3.12 Concentrations of curcumin metabolites in mouse plasma following oral dosing with unformulated curcumin or Meriva (low dose).	108
Figure 3.13 Representative HPLC-UV chromatograms of mouse plasma following oral gavage dosing of unformulated curcumin or Meriva and enzymatic conversion.	111
Figure 3.14 Concentrations of curcuminoids in mouse plasma following oral dosing with unformulated curcumin or Meriva and enzymatic conversion (low dose).....	112
Figure 3.15 Representative HPLC-UV chromatograms of mouse lung homogenate following oral gavage dosing of unformulated curcumin or Meriva and enzymatic conversion.	113
Figure 3.16 Concentrations of curcuminoids in mouse lung homogenate following oral dosing with unformulated curcumin or Meriva and enzymatic conversion (low dose).....	114
Figure 3.17 Turmeric containing sandwich, flapjack and soup used for the healthy human volunteer study.....	116
Figure 3.18 Representative HPLC-UV chromatograms of turmeric and turmeric food.....	117
Figure 3.19 Representative HPLC-UV chromatograms of healthy human plasma following consumption of turmeric containing food.	118
Figure 4.1 Effect of curcumin on the growth of A549 lung cancer cells.	127
Figure 4.2 Effect of curcumin on the growth of MRC5 lung fibroblasts.	128

Figure 4.3 Effect of different tumour cell:fibroblast ratios on tumour cell invasion.	130
Figure 4.4 Effect of fibroblasts on invasion on different lung cancer cell invasion.	132
Figure 4.5 Invasive behaviour of A549 tumour cells and MRC5 fibroblasts under different organotypic conditions.	134
Figure 4.6 Immunohistochemical staining of organotypics with MNF 116 cytokeratin.	136
Figure 4.7 Effect of curcumin treatment on invasion of A549 cells in a 3D organotypic co-culture model.	138
Figure 4.8 Expression of MET receptor related proteins in A549 cells treated with MRC5 conditioned media.	140
Figure 4.9 Expression of downstream proteins of HGF-MET pathway in A549 cells treated with MRC5 conditioned media.	141
Figure 4.10 Expression of MET receptor related proteins in A549 cells treated with curcumin.	143
Figure 4.11 Expression of downstream proteins of HGF-MET pathway in A549 cells treated with curcumin.	144
Figure 4.12 Expression of MET receptor related proteins in MRC5 fibroblasts treated with curcumin.	145
Figure 4.13 Expression of downstream proteins of HGF-MET pathway in MRC5 fibroblasts treated with curcumin.	146
Figure 4.14 Expression of MET receptor related proteins in A549 cells after stimulation with HGF.	148
Figure 4.15 Expression of downstream proteins of HGF-MET pathway in A549 cells after stimulation with HGF.	149
Figure 4.16 Expression of MET receptor related proteins in A549 cells after pre- treatment with curcumin and stimulation by HGF.	151
Figure 4.17 Expression of downstream proteins of HGF-MET pathway in A549 cells after pre-treatment with curcumin and stimulation by HGF.	152
Figure 4.18 Expression of HGF in MRC5 fibroblasts after treatment with curcumin.	153
Figure 5.1 Effect of MRC5 fibroblasts on growth of A549 tumour cells in nude mice	160

Figure 5.2 Representative flow cytometry scatter plots for the MNF 16 cytokeratin assay in mouse tumour xenograft cells.....	162
Figure 5.3 Histological appearance of A549:MRC5 (1:5) co-culture xenograft tumours.....	163
Figure 5.4 Effect of dietary Meriva or Epikuron on tumour growth in nude mice.	165
Figure 5.5 Effect of dietary Meriva or Epikuron on body weight in nude mice.	165
Figure 5.6 Kaplan-Meier survival curves for nude mice on 0.226% Meriva diet or control Epikuron diet.	166
Figure 5.7 Effect of Meriva on the expression c-MET in A549:MRC5 co-culture xenograft tumours in nude mice.....	168
Figure 5.8 Effect of Meriva on the expression MAPK, pMAPK, Akt and pAkt in A549:MRC5 co-culture xenograft tumours in nude mice	169
Figure 5.9 Effect of Meriva on the expression of p21, p27 and p53 in A549:MRC5 co-culture xenograft tumours in nude mice.....	171
Figure 5.10 Effect of Meriva on the expression of Bax and Bcl-2 in A549:MRC5 co-culture xenograft tumours in nude mice.....	172
Figure 5.11 Effect of Meriva on the expression of LC3 and COX-2 in A549:MRC5 co-culture xenograft tumours bearing nude mice.....	173
Figure 5.12 Effect of 0.226% Meriva diet on Ki-67 expression in A549:MRC5 co-culture xenograft tumours bearing nude mice.....	175
Figure 5.13 Effect of 0.226% Meriva diet on cleaved caspase 3 expression in A549:MRC5 co-culture xenograft tumours bearing nude mice.	176
Figure 5.14 Representative HPLC-UV chromatogram of mouse xenograft tumour and lungs post Meriva feeding.	178

List of Tables

Table 1.1 TNM classification of lung cancer	13
Table 1.2 Treatment options and 5 year survival statistics for NSCLC	15
Table 1.3 Selected preclinical and clinical studies of agents targeting MET in lung cancer.....	20
Table 1.4 Dual EGFR–MET inhibition studies in lung cancer xenograft models	22
Table 1.5 Clinical studies for chemoprevention of lung cancer	32
Table 1.6 A selection of preclinical <i>in vitro</i> and <i>in vivo</i> studies of curcumin in lung cancer models.	39
Table 1.7 Clinical studies of curcumin to illustrate safety and efficacy	42
Table 1.8 Preclinical and clinical pharmacokinetic studies of curcumin	46
Table 1.9 Conditional transgenic mouse model.	55
Table 2.1 Composition of the polyacrylamide gels used in Western blotting. ..	58
Table 2.2 Buffers and their constituent ingredients	59
Table 2.3 Antibodies for western blot.....	60
Table 2.4 Xenograft study group distribution	79
Table 3.1 Average curcumin and curcumin metabolite concentrations in mouse plasma and lungs following oral dosing at 240 mg/kg dose.....	89
Table 3.2 Average curcumin and metabolite concentrations in mouse plasma and lungs after 240 mg/kg dose and enzymatic conversion.	95
Table 3.3 Recovery, intra-day and inter-day accuracy and precision for determination of curcumin, curcumin glucuronide and curcumin sulfate in mouse plasma and lung	99
Table 3.4 Assay accuracy and precision for the measurement of curcumin, curcumin glucuronide and curcumin sulfate at the lower limit of quantification (LLOQ).....	101
Table 3.5 Long term stability of curcumin, curcumin glucuronide and curcumin sulfate in mouse plasma and lung homogenate.....	103
Table 3.6 Freeze thaw stability of curcumin, curcumin glucuronide and curcumin sulfate in mouse plasma and lung homogenate.....	104
Table 3.7 Average curcumin metabolite concentrations in mouse plasma following oral dosing at 70 mg/kg dose.....	109

Table 3.8 Average curcuminoid concentrations in mouse plasma and lungs after 70 mg/kg oral dosing and enzymatic conversion.	115
--	-----

List of Abbreviations

ADC	Adenocarcinoma
Akt	alpha serine/threonine-protein kinase
ATBC	Alpha Tocopherol Beta Carotene
AUC	Area under the concentration-time curve
BaP	benzo[a]pyrene
bDMC	bis-demethoxycurcumin
bFGF	basic fibroblasts growth factor
BRAF	rapidly accelerated fibrosarcoma gene B
CAF	Cancer Associated Fibroblasts
CARET	Carotene and Retinol
COPD	chronic pulmonary obstructive disease
COX	cyclooxygenase
DAB	Diaminobenzidine
DMC	demethoxycurcumin
DMSO	Dimethyl sulfoxide
DNA	Deoxyribonucleic acid
ECM	extracellular matrix
EGFR	epidermal growth factor receptor
EML-ALK4	echinoderm microtubule-associated protein-like 4 anaplastic lymphoma kinase
EMT	epithelial to mesenchymal transition
ERK	extracellular signal-regulated kinases
FAP	fibroblast activation protein
FCS	Fetal calf serum

FDA	Food and Drug Administration
FITC	Fluorescein isothiocyanate
FSP	fibroblast specific protein
H&E	Haematoxylin and eosin
HGF	Hepatocyte growth factor
H-NMR	Proton nuclear magnetic resonance
HPLC-UV	High performance liquid chromatography-UV
IC50	Half maximal inhibitory concentration
IGF	Insulin growth factor
IL	Interleukins
KRAS	Kirsten ras oncogene
LC3	Microtubule-associated protein 1 light chain 3
LCC	Large cell carcinoma
LC-MS/MS	Liquid chromatography-tandem mass spectrometry
LOD	Limit of detection
LOQ	Limit of quantitation
MAPK	mitogen-activated protein kinase
MET	Mesenchymal epithelial transition
MMP	matrix metalloproteinases
MSC	mesenchymal stem cells
mTOR	mechanistic target of rapamycin
NF- κ B	Nuclear factor kappa B
NSCLC	Non-small cell lung cancer
PAH	polyaromatic hydrocarbons
PBS	Phosphate buffered saline
PDGFR	platelet-derived growth factor receptor

PI3K	phosphatidylinositol-3-kinase
ROS	Reactive oxygen species
RPMI	Roswell Park Memorial Institute
RSD	Relative standard deviation
SCC	Squamous cell carcinoma
SCID	Severe combined immune deficiency
SCLC	Small cell lung cancer
SELECT	Selenium and Vitamin E Cancer Prevention Trial
STAT	signal transducer and activator of transcription
SULT	Sulfotransferase
TEMED	N,N,N',N'-tetramethylethylenediamine
TGF	Transforming growth factor
TKI	Tyrosine kinase inhibitor
TLC	Thin layer chromatography
TME	Tumour Microenvironment
TNF- α	tumour necrosis factor- α
TNM	Tumour/nodes/metastases
UGT	Uridine diphosphate glucuronosyltransferase
UV	Ultraviolet
VEGF	Vascular endothelial growth factor
α -SMA	alpha-smooth muscle actin

List of publications and conference abstract

- 1) Jagdish Mahale, Lynne M Howells et al. 2015. The role of stromal fibroblasts in lung carcinogenesis: A target for chemoprevention? *International Journal of Cancer*. 138. 30-44.
- 2) Lynne M Howells, Jagdish Mahale et al. 2014. Translating curcumin to the clinic for lung cancer prevention: evaluation of the pre-clinical evidence for its utility in primary, secondary and tertiary prevention strategies. *Journal of Pharmacology and Experimental Therapeutics*. 350. 483-94
- 3) Jagdish Mahale et al. 2015. Targeting the Tumour Microenvironment: A potential role for curcumin in lung cancer chemoprevention. *Journal of Thoracic oncology*. 10 (9). S732. (Abstract)
- 4) Jagdish Mahale et al. 2015. Dietary dose of curcumin-phospholipid formulation prevents tumour growth in a co-culture xenograft mouse model of lung cancer. *Mutagenesis*. 30 (6). 856. (Abstract)
- 5) Jagdish Mahale, et al. 2013. Meriva[®], a formulation of curcumin, exhibits superior curcumin and metabolite levels in comparison to unformulated curcumin in the lungs of mice: Implications for its use in lung cancer chemoprevention. *Respiratory Research Conference, University of Loughborough, UK.*

1 Introduction

1.1 Lung Cancer

Lung cancer develops when normal lung cells sustain genetic damage that eventually leads to uncontrolled cell proliferation. Most lung cancers begin in the cells lining the bronchi of the lungs. If not detected early, lung cancers have the capacity to aggressively invade neighbouring tissues or metastasize to distant parts of the body. Incidences of lung cancer were shown to increase sharply in the early decades of the 1900's, which was initially attributed to infectious disease states such as tuberculosis and influenza, or chronic pathologies such as bronchitis. However, in 1950, the first landmark epidemiological studies in the UK and USA demonstrated an association between cigarette smoking and lung cancer [1, 2]. Since then, extensive research has revealed a myriad of genetic and environmental factors that play a causative role in this disease.

1.1.1 Epidemiology of lung cancer

An estimated 14.1 million people were diagnosed with cancer worldwide in 2012, out of which lung cancer accounted for 13% of all the cases diagnosed. Worldwide, lung cancer is the leading cause of cancer death in men and the second leading cause of cancer death in women, with an estimated 1 million deaths in men and nearly 500,000 deaths in women in 2012 [3]. In the UK, lung cancer is the second most common cancer diagnosed amongst men and women. In the UK in 2012, approximately 43,500 people were diagnosed and almost 35,000 people died from lung cancer. Whilst incidence of lung cancer in the UK has been decreasing in men, it is steadily increasing in women, with more women dying from lung cancer than from breast cancer. Lung cancer has a poor prognosis, primarily because over two-thirds of patients are diagnosed at a later stage when curative treatment is not possible. Overall five year survival after diagnosis is less than 10%. This figures increases to 49% for non-small cell lung cancer and 31% for small cell lung cancer if the disease is diagnosed at stage 1. (<http://www.cancerresearchuk.org/health-professional/cancerstatistics/statistics-by-cancer-type/lung-cancer>).

1.2 Risk factors for lung cancer

1.2.1 Tobacco Smoking

Tobacco smoking is the most common known cause of lung cancer accounting for more than 85% of lung cancer cases. The relationship between tobacco smoking and lung cancer is well established. Over 4000 chemicals have been identified in cigarette smoke out of which 60 have been classified as chemical carcinogens. The most potent of these carcinogens are polycyclic aromatic hydrocarbons (PAH), n-nitroamines and aromatic amines [4]. As shown in Figure 1.1, these carcinogens when inhaled via smoking, get converted to forms that react with DNA and the resulting metabolically activated DNA adducts initiate genetic mutations known to cause lung cancer. The metabolic activation and deactivation of these adducts differs between individuals and determine the risk of developing cancer [5]. The risk of developing lung cancer from cigarette smoking is influenced by many factors such as the age at which the person started smoking, total length of time the person was exposed to tobacco smoke and the number of cigarettes smoked. However, the risk reduces greatly by 25-50% on quitting smoking for 10 years. Smoking cessation at a younger age also significantly reduces the risk [6]. Studies have shown that women who smoke are more susceptible to developing lung cancer than men who smoke. This is probably due to higher levels of PAH DNA adducts and lower DNA repair capacity observed in female lung cancer patients [7]. Overall, one in nine smokers develops lung cancer in their lifetime [8]. The cumulative risk of developing lung cancer for a smoker in their life time is 13-16% compared to less than 1% for a non-smoker in Europe [9].

1.2.2 Passive Smoking

Passive smoking is involuntary exposure to tobacco smoke present in the environment. The second-hand smoke inhaled by passive smokers is the mixture of smoke exhaled by smokers and burning tobacco, exposing the passive smokers to the same carcinogens to that of an active smoker. In the US, it is estimated that 3000 people die of lung cancer every year due to passive smoking [10]. Children and women in particular are more vulnerable to health risks associated with passive smoking [11]. A study has shown that individuals with

smoking partners are at 30% greater risk of developing lung cancer than those with non-smoking partners [12].

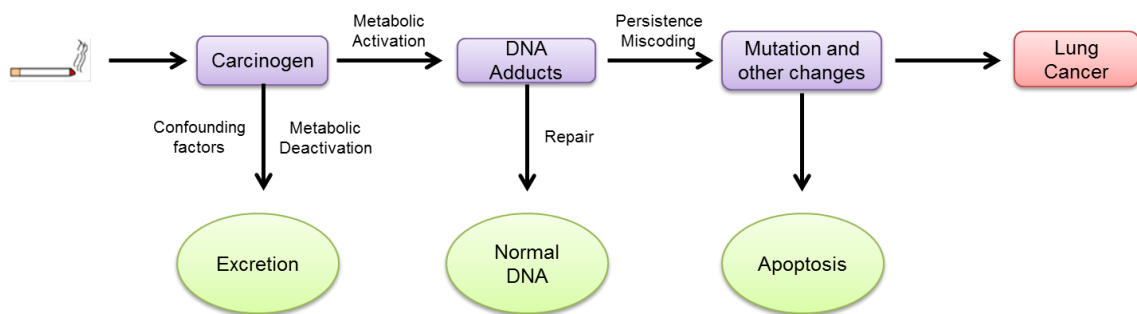


Figure 1.1 Scheme linking tobacco smoke carcinogens and lung cancer.

(Adapted from Hetch SS, [13])

1.2.3 Environmental/Occupational factors

Carcinogens present in the environment or workplace are capable of inducing genetic changes that could lead to development of cancer. Some of the most common environmental/occupational factors that contribute to lung carcinogenesis are discussed below.

1.2.3.1 Air Pollution

Outdoor air pollution has been associated with various respiratory diseases including lung cancer for decades, and contains many carcinogenic components such as diesel engine exhaust, solvents, metals, gases, dust and fine particulate matter. Exposure to air pollution is estimated to contribute to 223,000 lung cancer deaths per year worldwide [14]. The urban and rural factor study showed that people living in cities are at increased risk of developing lung cancer due to the presence of higher levels of environmental carcinogens [15, 16].

1.2.3.2 Asbestos fibres

The first evidence linking asbestos with lung cancer emerged in 1955 following a retrospective cohort study [17]. Since then, further studies have confirmed the relationship of lung cancer incidence to asbestos exposure. It is the most common occupational cause of thoracic cancers primarily due to mesothelioma cases. Asbestos is a natural fibrous mineral which occurs in 6 different forms including amosite, crocidolite, anthophyllite, tremolite and actinolite [18]. All the

forms of asbestos have been identified as carcinogenic. Approximately 4-12% of lung cancer cases globally can be attributed to occupational exposure of asbestos [19]. Apart from working in asbestos mines the risk of asbestos exposure comes primarily from asbestos particles released from buildings where two thirds of the total asbestos produced is used [20]. Some countries have banned asbestos use but there are still many countries that use/mine asbestos for commercial purposes.

1.2.3.3 Polycyclic aromatic hydrocarbons (PAHs)

Increased lung cancer risk from both occupational and environmental exposure to PAHs has been well documented [21, 22]. PAHs are formed by incomplete burning of organic matter. Environmental exposure to PAHs comes from combustion of diesel fuel, oil, coal, biomass fuels and tobacco. Occupational exposure to PAHs includes aluminium production, iron and steel foundry work, coke production and coal gasification [23]. PAHs are a group of over 100 chemicals amongst which benzo[a]pyrene (BaP) has been classified as one the most potent carcinogen when analysed in the assay systems such as mouse skin, human cell mutagenicity assays [24].

Other occupational carcinogens include arsenic, radon, beryllium, nickel, chromium, cadmium and silica dust.

1.2.4 Family history

A significant number of lung cancer incidences are among people who do not have any known personal, occupational or environmental exposure to risk factors. These can be associated with the genetic make-up of individuals which define if they are susceptible or resistant to developing lung cancer. Large cohort studies have shown that the risk of developing lung cancer is 1.5 times higher for those with a family history of the disease [25, 26]. For example, *RGS17* gene having a role in developing tolerance to opioid analgesic drugs, was identified as a major candidate for familial lung cancer susceptibility [27]. Another study in which 16 incidence of lung cancer were observed across 3 generations within the same family, identified that the *MAST1* gene, having a role in regulating cell growth and apoptosis, was likely to be associated with lung cancer susceptibility [28].

1.2.5 Age

Lung cancer is a slow and multistep carcinogenic process and can take up to 30 years to develop into the full form of invasive cancer. Hence lung cancer incidence is strongly related to age, with the average age at the time of diagnosis being over 70 years [18]. Nine out of ten cases of lung cancer in the UK are diagnosed at the age of 60 and above, with less than two percent of lung cancer cases diagnosed before the age of 45. The five year survival rate for patients with a lung cancer diagnosis in England ranges from 38-45% in 15-39 year-olds, to 5% in 80-99 year-old patients (<http://www.cancerresearchuk.org/health-professional/cancer-statistics/statistics-by-cancer-type/lung-cancer/incidence>).

1.2.6 Diet

The World Cancer Research Fund Report on food and nutrition (2015) suggested that there is probable evidence between fruit and vegetable intake and protection against lung cancer. A diet rich in fruits and vegetables has been found to reduce the risk of lung cancer incidence with a protective effect stronger in current smokers than former smokers [29]. Consumption of cruciferous vegetables like cabbage and broccoli which are rich in isothiocyanate content has been reported to have a protective effect against lung cancer [30]. Overall, no or low intake of fruits and vegetable have been reported to increase the risk of lung cancer incidence by 3-fold [31]. A prospective study on dietary intake of flavonoids, known for their anti-proliferative and antioxidant properties, has shown that lung cancer risk is lower in men with high flavonoid intake [32]. Consumption of certain dietary items like red and processed meat, saturated fats and lipids has been shown to increase risk of lung cancer [33].

1.2.7 Other lung diseases

Patients with chronic pulmonary obstructive disease (COPD) are at a significantly increased risk for both the development of primary lung cancer, as well as poor outcome after lung cancer diagnosis and treatment. Other lung diseases including pneumonia, tuberculosis, interstitial fibrosis and asthma also contribute to increased risk of lung cancer [18].

1.3 Anatomy of the human Lung

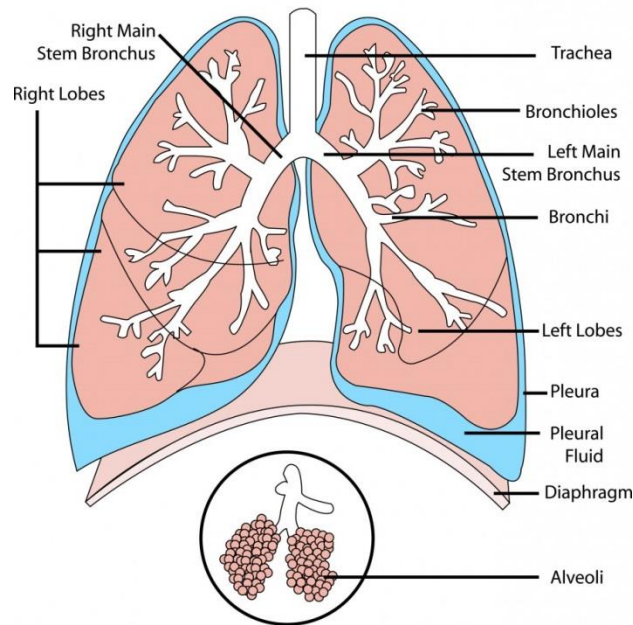


Figure 1.2 Anatomy of lung

Figure taken from <http://healthfavo.com/human-lung-anatomy.html>

Inhaled air enters into lungs via the trachea which branches into the left and right primary bronchus, each of which further branches into bronchi and bronchioles. The process of gas exchange occurs in alveoli which are microscopic structures at the end of the bronchioles. The thin-walled alveoli are connected to small blood vessels which allow oxygen to enter into the bloodstream and carbon dioxide to be exhaled from the body. Inside the chest are two thin layers of tissue called pleura. One layer covers the lungs and the other layer lines the inside of the chest. Pleural fluid is found between these two layers of pleura, and acts as a lubricant for the lungs during breathing. The right lung is divided into three lobes, right, middle and lower whereas left lung is divided into two lobes upper and lower (<http://www.innerbody.com/anatomy/respiratory/lungs>).

1.4 Classification of lung cancer

Lung cancer arises from the abnormal epithelial cells that line the airways of the lung. It can be broadly classified into two main types based on size and appearance of malignant cells observed under the microscope: small cell lung cancer (SCLC) and non-small cell lung cancer (NSCLC). Classification then determines appropriate intervention pathways. The new histological and

morphological WHO classification divides lung cancer into more than 80 different sub-classes [34].

1.4.1 Non-small cell lung cancer (NSCLC)

NSCLC is the most common type of lung cancer, making up 80-85% of all cases [35]. It typically grows and spreads more slowly than SCLC. NSCLC traditionally includes adenocarcinoma, squamous cell carcinoma and large cell carcinoma. The other less frequent forms are adeno-squamous carcinoma and large cell neuroendocrine tumours [36].

1.4.1.1 Adenocarcinoma

Adenocarcinoma (ADC) is the most common lung cancer subtype and accounts for approximately 40% of all lung cancer cases worldwide. It also develops more frequently in women and in individuals who have never smoked. ADC cells are glandular in appearance and produce a thick fluid called mucin. Adenocarcinomas can be further classified into tumours which exhibit lepidic, acinar, papillary, micropapillary or solid growth patterns or a mixture of these patterns [37]. They are more frequently observed in peripheral nodules and are approximately ≤ 4 cm in diameter. ADC in situ (AIS) is a subset of adenocarcinoma that begins in the alveoli. It is defined as a small to moderately sized (≤ 3 cm), solitary neoplastic lesion with pure lepidic growth showing no signs of invasion. It grows slowly and is less likely to metastasize than other forms of NSCLC. Atypical adenomatous hyperplasia (AAH) is a precursor lesion to adenocarcinoma in situ (AIS) usually 0.5 cm in diameter or less with lepidic proliferation of cells lining alveolar walls. If diagnosed at the AAH or AIS stage, 5 year disease free survival rate is 100% [38]. Adenocarcinoma is also the most commonly diagnosed subtype in people less than 50 years of age [39].

1.4.1.2 Squamous cell carcinoma

Squamous cell carcinoma (SCC) also known as epidermoid carcinoma, is the most common cancer type in current and former smoking men and accounts for ~30% of lung cancer cases. Over 90% of SCC cases are diagnosed in cigarette smokers. The tumours are mainly centrally located and are often larger than 4 cm in diameter. SCC is characterised by intercellular bridging and/or keratinisation of the individual cells. The four subtypes of SCC are papillary, clear

cell, small cell and basaloid. SCC is often preceded for years by squamous-cell metaplasia or dysplasia in the respiratory epithelium of the bronchi, which later transforms to carcinoma in situ. These tumours metastasize but often later than other forms of NSCLC. SCC is frequently diagnosed in individuals above 65 years old [39].

1.4.1.3 Large cell carcinoma

The cells of large cell carcinoma (LCC) are the largest of the various types of NSCLC. The cells are generally highly undifferentiated or immature in appearance. It is the least common type of NSCLC with early metastasis to the mediastinum and brain. It is a fast growing form that grows near the surface of the lung. They are found in approximately 10% of lung cancer cases. This form of NSCLC can occur in any part of the lung and the prognosis for large cell carcinoma is generally less favourable than for other forms of NSCLC. There are several variants of large cell carcinoma including clear cell LCC, basaloid LCC, lymphoepithelioma-like carcinoma, and large cell neuroendocrine carcinoma. All types predominate in smokers, except lymphoepithelioma-like carcinoma. The average age at diagnosis for LCC is about 60 and is more common among men [39].

1.4.2 Small cell carcinoma

The malignant epithelial cells of small cell carcinoma are abnormally small and are round, oval or spindle-like in shape. Small cell carcinoma accounts for 15% of all lung cancer cases. It is strongly associated with smoking and less than 1% of cases are diagnosed in never smokers. Small cell carcinoma is an aggressive form of cancer which grows quickly and tends to spread to lymph nodes and metastasize to other organs early in the disease process. Most people with small cell carcinoma have metastases to bone, liver or brain at the time of diagnosis. Small cell carcinoma often occurs in one of the larger airways and therefore tumours are often located centrally. Combined small cell carcinoma is a variant of small cell carcinoma combined with additional component that consists of any of the histologic types of NSCLC. Most cases of small cell carcinoma occur in individuals aged 60-80 years [39].

1.5 Signs and symptoms of lung cancer

Most of the lung cancer cases are diagnosed at later stages, but signs and symptoms can occur in the same individuals at an early stage of disease. The most common signs and symptoms of lung cancer are as follows [40], [41].

1.5.1 Symptoms of localised lung cancer

Unexplained or persistent cough for more than 3 weeks, worsening chest pain, coughing up sputum with signs of blood in it, unintentional weight loss, difficulty in breathing, wheezing and persistent fatigue are common symptoms of localised disease.

1.5.2 Symptoms of locally advanced disease

The symptoms associated with locally advanced disease are due to invasion of structures in or near the lungs, or from cancerous spread to regional lymph nodes. These include hoarse voice, difficulty swallowing, shoulder pain, swelling of face and neck.

1.5.3 Symptoms of metastatic disease

When lung cancer spreads to distant organs it may cause symptoms related to that organ. For example, bone metastasis may cause pain in the hip and back; metastasis to brain/spinal cord may lead to neurologic changes such as headache, weakness, numbness of arms or legs, dizziness, body balance, seizures; liver metastasis may cause jaundice, pain in the ribs; metastasis to skin/lymph nodes may cause lumps on the surface of the body.

1.6 Screening for lung cancer

Lung cancer screening is a strategy to identify cancer at an early stage before it becomes symptomatic, potentially leading to higher cure rates. At present, there is no national screening programme for lung cancer in most countries including the UK. Previous screening trials utilizing chest x-rays and/or sputum cytology have not been shown to decrease the risk of dying from lung cancer [42, 43]. The only recommended screening test for lung cancer by the US Preventive Task Force is low-dose computed tomography (LDCT). Their largest lung cancer screening trial showed that screening of high risk persons is effective in reducing the mortality from lung cancer. Individuals with more than 30 pack-years and

aged between 55 and 74 years at the time of randomization were included in this study. They found a relative mortality reduction of 20% when this high-risk group was screened with LDCT scan compared to chest radiography [44].

Although LDCT allows good characterisation of lung cancer at early stages there have been concerns about the use of this technique for screening purposes. One drawback of this technique is a high rate (9-50%) of false positive results as reported by different screening studies using LDCT [45]. False positive results lead to overdiagnosis, more invasive tests such as needle biopsies, surgery and increased risk of exposure to radiation. It also causes the individual unnecessary stress and anxiety. The cost involved in follow-up from CT scans is also very high [46]. Because the risks outweigh benefits, in the US LDCT screening is recommended only for former or current heavy smokers who are at higher risk of developing lung cancer. Currently, no screening technique is available for non-smokers.

1.7 Diagnosis of lung cancer

Once individuals show signs and symptoms associated with lung cancer, they undergo a series of diagnostic tests to confirm presence of disease. The findings of the diagnostic tests provide information on type and stage of lung cancer, which is crucial for deciding the correct treatment pathway. The National Institute for Clinical Excellence (NICE), UK recommends the following guideline for diagnosis of lung cancer (Figure 1.3).

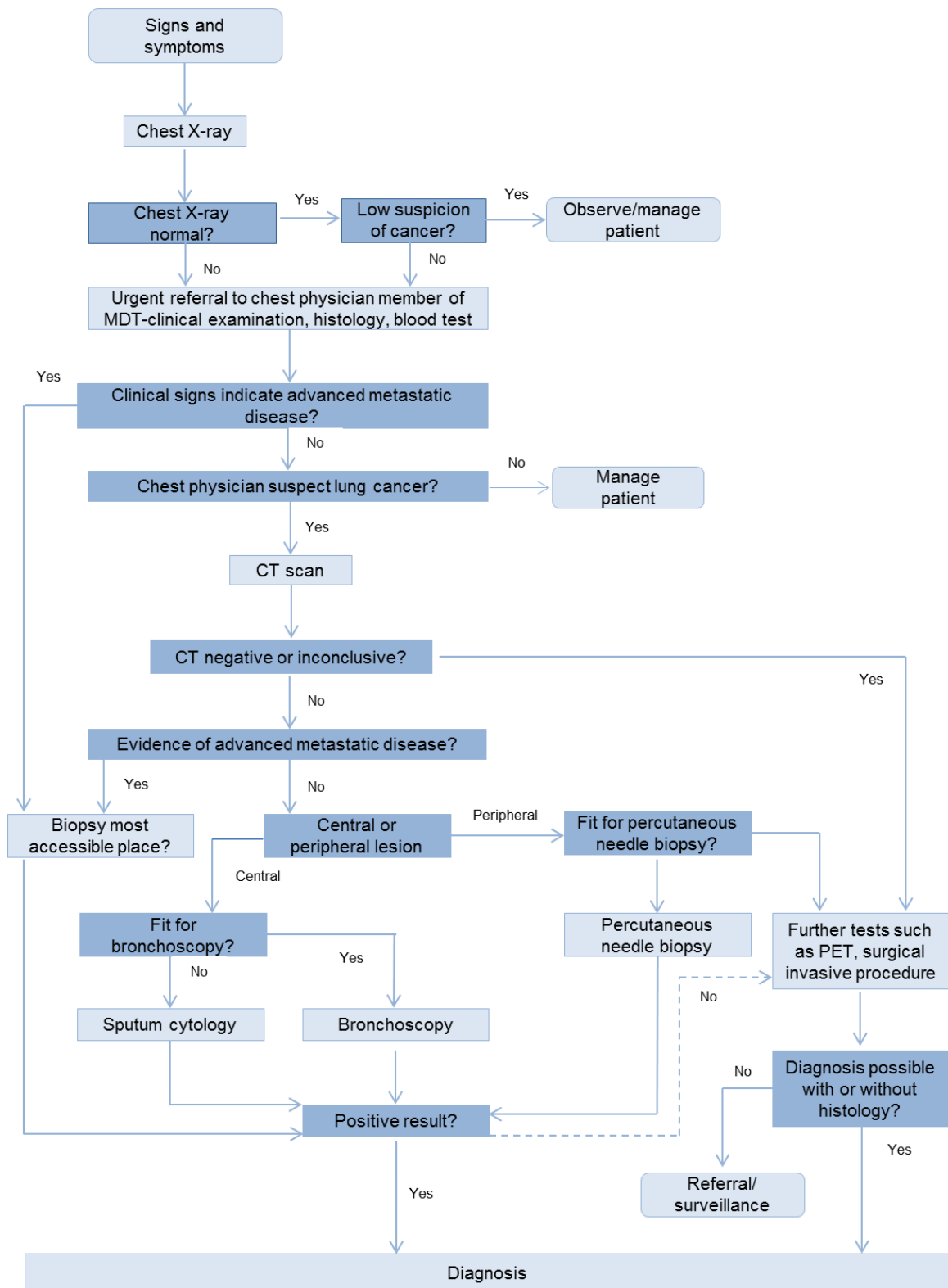


Figure 1.3 Flowchart for diagnosis of lung cancer.

Adapted from National Institute for Clinical Excellence (NICE) guidelines, UK.

1.8 Staging of Lung cancer

Lung cancer staging is a procedure by which size, position and spread of cancer is determined. Two types of staging system are used: number staging and the TNM staging system (Table 1.1).

1.8.1 Number staging system

The number staging divides cancer into four different types [47, 48]

Stage 1: The cancer is small and has not spread to lymph nodes. Stage 1 is further divided into 2 subtypes:

Stage 1A: Tumour size is up to 3 cm

Stage 1B: Tumour size between 3-5 cm and cancer may have spread to bronchus or pleura

Stage 2: This stage is divided into two subtypes.

Stage 2A: Tumour size between 5-7cm and has not spread to lymph nodes or tumour size 5 cm or less and may have spread to lymph nodes close to the affected lung.

Stage 2B: Tumour size larger than 7 cm but has not spread to lymph nodes or tumour size between 5-7 cm and has spread to lymph nodes close to the affected lung.

Stage 3: This stage is divided into two subtypes.

Stage 3A: Tumour size more than 7 cm and has spread to lymph nodes close to affected lung, chest wall, diaphragm or pleura. There may be two or more tumours in the same lobe of the lung.

Stage 3B: Similar to 3A. Tumour size more than 7 cm and has spread to lymph nodes opposite of affected lung.

Stage 4: Tumour present in both sides of the lung and has metastasized to other organs such as bones, liver, brain and lymph nodes.

1.8.2 TNM staging system

The TNM staging system defines lung cancer staging by the local extent of the primary tumour (T), involvement of associated lymph nodes (N), and whether or not metastases (M) exist [48].

Table 1.1 TNM classification of lung cancer

Primary Tumours (T)	
TX	Primary tumour cannot be assessed
T0	No evidence of primary tumour
Tis	Carcinoma in situ
T1a	Tumour 2 cm or less in greatest dimension
T1b	Tumour more than 2 cm but 3 cm or less in greatest dimension
T2a	Tumour more than 3 cm but 5 cm or less in greatest dimension
T2b	Tumour more than 5 cm but 7 cm or less in greatest dimension
T3	Tumour more than 7 cm or one that directly invades
T4	Tumour of any size that invades
Regional Lymph Nodes (N)	
NX	Regional lymph nodes cannot be assessed
N0	No regional lymph node metastases
N1	Metastasis in ipsilateral peribronchial and/or ipsilateral hilar lymph nodes and intrapulmonary nodes
N2	Metastasis in ipsilateral mediastinal and/or subcarinal lymph node(s)
N3	Metastasis in contralateral mediastinal, contralateral hilar, ipsilateral or contralateral scalene, or supraclavicular lymph node(s)
Distant Metastasis (M)	
M0	No distant metastasis
M1	Distant metastasis
M1a	Separate tumour nodule(s) in a contralateral lobe, tumour with pleural nodules
M1b	Distant metastasis (in extrathoracic organs)

1.9 Management of Lung cancer

1.9.1 Surgery

Surgical procedures performed for treating lung cancer include lobectomy (removal of a lobe), pneumonectomy (removal of entire lung) and segmentectomy (removal of only a small part of lung). Surgery is the most common treatment option for patients with stage 1 or stage 2 cancers. Surgery is performed for stage 3A cancer in some instances but almost never performed for stage 3B and stage 4 cases (Table 1.2) [49].

1.9.2 Radiotherapy

In the treatment of stage 1 and stage 2 lung cancers, radiotherapy is considered only when surgical resection is not possible because of limited pulmonary reserve or the presence of comorbidities. Radiotherapy can be given by an external source where radiation is aimed at the affected part of the lung, or as internal radiotherapy where a catheter with a radiation source is introduced into the affected part of the lung [50].

1.9.3 Chemotherapy

Chemotherapy forms the mainstay for treatment of more than 80% of lung cancer cases. Chemotherapy for stage 1 and stage 2 cancers is given when surgery is not possible [49]. It may also be given as an adjuvant therapy after surgery or in combination with radiotherapy to increase the chances of cure and reduce the possibility of relapse. The drugs available for management of lung cancer in the UK are cisplatin, carboplatin, etoposide, afatinib, vinorelbine, gemcitabine, crizotinib, paclitaxel, docetaxel, erlotinib, gefitinib and pemetrexed (tvscn.nhs.uk/.../Cancer-Lung-Chemotherapy-Regimen-3.4-March-2015.pdf).

Table 1.2 Treatment options and 5 year survival statistics for NSCLC

Stage	Standard Management	Survival
1A and B	Surgical resection	75% (1A) 55% (1B)
2A and B	Surgical resection	50% (2A) 40% (2B)
3A	Chemoradiotherapy Surgical resection in selective cases	10-35%
3B	Chemoradiotherapy	5%
4	Chemotherapy	Less than 5%

Table adapted from data provided in <http://reference.medscape.com/features/slideshow/lung-cancer#17>

1.10 Molecular pathogenesis of lung cancer

In recent years, modest improvements in clinical outcome of lung cancer treatment have been achieved by treating patients with targeted therapy directed against specific driver mutation. These driver mutations are responsible for both initiation and maintenance of cancer [51]. The presence of individual driver genes are often found to be mutually exclusive to one another. There have been more than 20 driver mutations identified in all forms of cancer. The commonly known oncogenic driver mutations in lung cancer are shown in Figure 1.4. The major mutations include epidermal growth factor receptor (*EGFR*), echinoderm microtubule-associated protein-like 4 anaplastic lymphoma kinase (*EML-ALK4*), *KRAS*, and *MET* and are briefly discussed below.

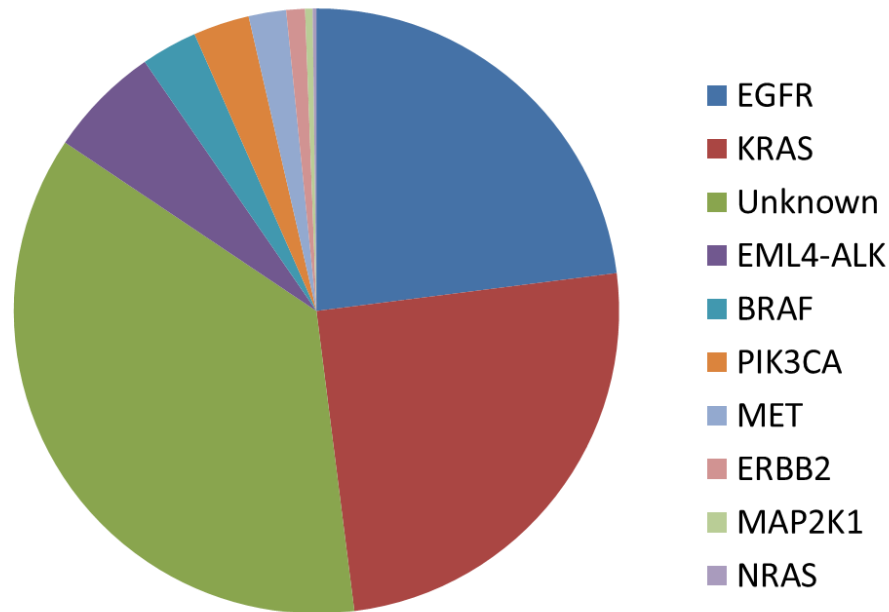


Figure 1.4 Common mutations in lung cancer

Abbreviations: EGFR, epidermal growth factor receptor; EML4-ALK, echinoderm microtubule-associated protein-like 4 anaplastic lymphoma kinase; KRAS, Kirsten ras oncogene; MAP2K1, mitogen-activated protein kinase 1; BRAF, rapidly accelerated fibrosarcoma gene B; NRAS, Neuroblastoma RAS oncogene; PIK3CA, phosphatidylinositol-4,5-Bisphosphate 3-Kinase; MET, mesenchymal epithelial transition

Figure made from different references [53, 64, 71].

1.10.1 EGFR mutations

EGFR belongs to transmembrane receptor tyrosine kinase family that is activated on binding of its ligand, epidermal growth factor (EGF). The binding of the ligand induces homodimerisation and autophosphorylation of the receptor resulting in downstream activation of numerous cellular processes including cell proliferation, cell survival, cell motility and cell invasion [52]. Approximately 15% of all NSCLCs in patients with European or African ethnicities, 35% of NSCLCs in East Asians, and 50% of NSCLCs in never smokers are *EGFR* mutation positive [53]. The activating *EGFR* mutations have been identified in exons 18 to 21 of the tyrosine kinase domain, about 90% of which are deletions in exon 19, and point mutation in exon 21. Patients harbouring *EGFR* mutation at exon 18, 19 and 21 respond well to gefitinib and erlotinib treatment which act by preferentially binding to mutant EGFR thus preventing phosphorylation of the receptor by adenosine triphosphate (ATP). However, treatment leads to

development of resistance and relapse is often observed after approximately one year of treatment [54], [55]. The most common mechanism for developing resistance is acquisition of a second-site resistance mutation at exon 20 and amplification of the receptor tyrosine kinase MET [56], [57]. Second generation EGFR-targeting drugs such as the selective and irreversible inhibitor of EGFR, afatinib, are able to overcome this resistance [58].

1.10.2 KRAS mutations

KRAS encodes a GTPase signalling protein that plays a critical role in the RAS/MAPK signalling pathway, downstream of many growth factor receptors, including EGFR. Mutation of the *KRAS* gene results in constitutive activation of RAS/MAPK signalling pathway which plays a critical role in cell proliferation, survival, and differentiation [59]. *KRAS* mutations are found in 15-25% of Asian and 25-50% of Caucasian NSCLC patients [53]. They occur more frequently in lung adenocarcinomas patients (approximately 30%) and are strongly associated with smoking. More than 97% of *KRAS*-mutant cases affect exon 2 and 3 [60]. Since *KRAS* is downstream of EGFR, it plays a key role in predicting efficacy of EGFR inhibitors. Mutated *KRAS* has been frequently associated with lower efficacy of EGFR inhibitors (cetuximab or panotumumab) or development of resistance to agents like erlotinib and gefitinib [59], [61]. *KRAS* mutations are present in approximately 25-30% of cases that are non-responsive to tyrosine kinase inhibitors (TKI). The response rate to EGFR-TKI is 3% for *KRAS* mutant patient as compared to 26% for patients without mutation [62]. Hence, *KRAS* mutation plays an important role in response as well as resistance to TKI therapy. Currently there is no agent that specifically targets *KRAS* and development of such agents is under intensive investigation.

1.10.3 EML4-ALK Mutations

EML4-ALK is a protein formed by fusion between intron 19 of receptor tyrosine kinase gene *ALK* and intron 13 of *EML4* [63]. The key downstream pathways of *ALK* include MAPK, PI3/AKT and STAT which are involved in cell proliferation and survival [59]. Frequency of *EML4-ALK* mutation is 2.3-6.7% in Asians and 1-3% among Caucasians. They are more commonly observed in adenocarcinoma patients who are light smokers or never smokers and tend to be of a younger age [64, 65, 66]. *ALK*-rearranged tumours have been found to be resistant to the

EGFR-TKI gefitinib and erlotinib [65]. Crizotinib, a dual ALK and MET inhibitor has been approved for treatment of patients with EML4-ALK translocations. However, as with other NSCLC therapies, resistance to crizotinib develops over time [67].

1.10.4 HGF/MET signalling

MET is a receptor tyrosine kinase composed of an extracellular α -chain and a transmembrane β -chain linked by a disulphide bond. Hepatocyte growth factor (HGF) is the natural and only known agonist of the Met receptor. The intracellular segment of MET the β -chain consists of a juxtamembrane domain which contains phosphorylation site pMet1003 which regulates ubiquitination and degradation of the MET receptor. The tyrosine kinase domain has phosphorylation sites pMet1234 and pMet1235 which positively modulate enzyme activity, and the c-terminal contains phosphorylation sites pMet1349 and pMet1356 which serve as multifunctional docking sites for downstream proteins (Figure 1.5). Binding of HGF to the MET receptor results in receptor homodimerization, and phosphorylation of its tyrosine kinase sites subsequently activate downstream pathways involved in cell proliferation, survival, invasion, motility, angiogenesis, metastasis and epithelial to mesenchymal transition (EMT) [68, 69]. MET overexpression has been frequently associated with NSCLC.

In a study by Ma et al., MET was overexpressed, activated, or mutated in NSCLC cell lines and tumour tissues. Expression of c-Met was found in 100% of NSCLC tumour tissues and 61% of samples showed overexpression of MET. Phosphorylated MET was preferentially observed in the invasive tumour samples [70]. High *MET* gene copy number has been detected in 1–11% of NSCLC cases and has been associated with poor prognosis [71, 72]. *MET* amplification has been reported in approximately 20% of EGFR-TKI resistant tumours. It drives and maintains the PI3K/AKT pathway, bypassing EGFR blockade by TKIs. [73]. Higher circulating levels of HGF and overexpression of MET have been found in 40-50% of patients with advanced lung cancer [74]. Currently there are many agents that are being investigated as MET inhibitors. Table 1.3 lists some of these studies.

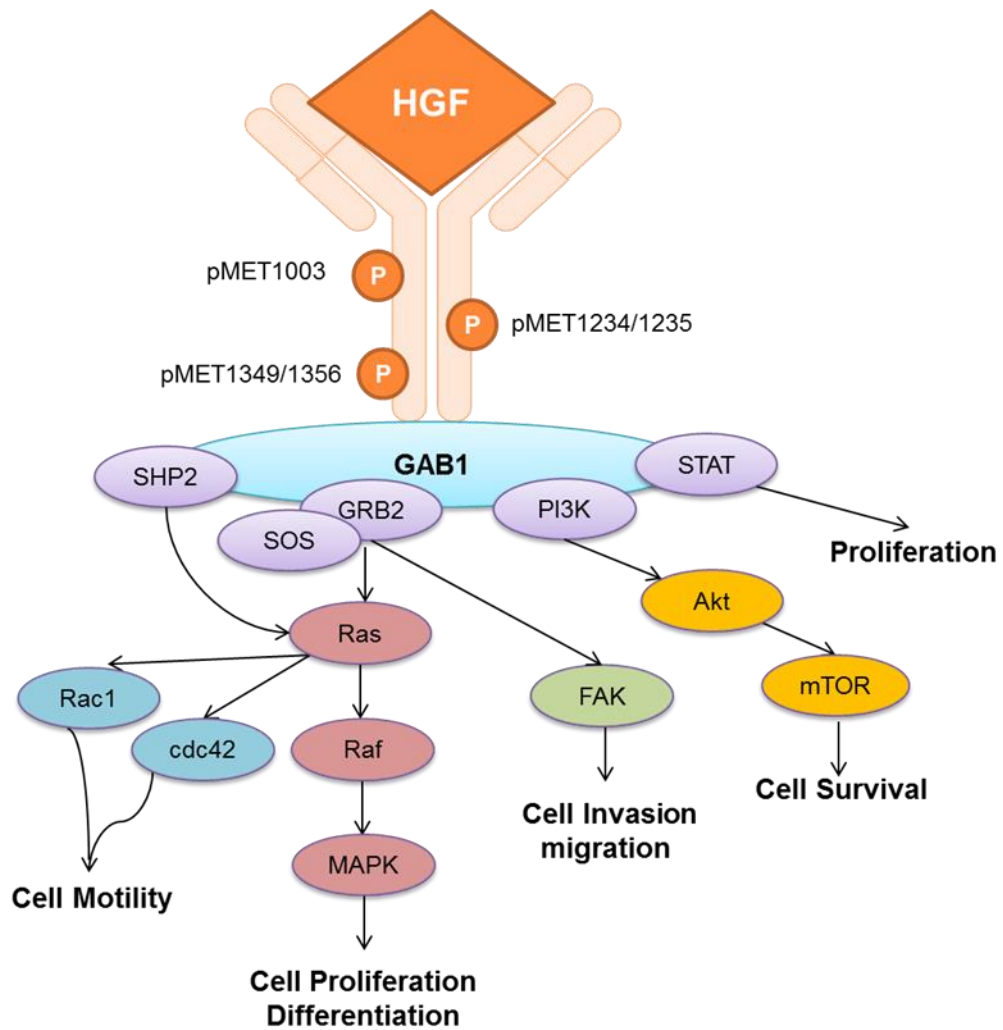


Figure 1.5 HGF/Met Pathway

Abbreviations: Akt, alpha serine/threonine-protein kinase; CDC42, cell division control protein 42 homolog; FAK, focal adhesion kinase; Gab1, Grb2-associated adaptor protein; Grb2, growth factor receptor-bound protein 2; HGF, hepatocyte growth factor; MAPK, mitogen-activated protein kinase; MET, mesenchymal epithelial transition; mTOR, mechanistic target of rapamycin; PI3K, phosphatidylinositol-3-kinase; Rac1, Ras-related C3 botulinum toxin substrate 1; Raf, rapidly accelerated fibrosarcoma; RAS, rat sarcoma; SHP2, SRC homology protein tyrosine phosphatase 3; SOS, son of sevenless; STAT, signal transducer and activator of transcription.

Table 1.3 Selected preclinical and clinical studies of agents targeting MET in lung cancer.

Preclinical Studies		
Agent	Observations	Ref
LY2801653	<p>1) Growth inhibition in tumour cell lines and patient-derived tumour xenograft models</p> <p>2) Significantly inhibited primary tumour growth and metastasis and increased survival in orthotopic mouse model</p> <p>3) Inhibited the constitutive activation of MET pathway signalling and inhibition of cell proliferation, anchorage-independent growth, migration, and invasion in H441 cell line</p>	[75]
PHA665752	<p>1) Inhibits tumourigenicity and angiogenesis in mouse lung cancer xenografts</p> <p>2) Reverses lung premalignancy induced by mutant <i>KRAS</i></p>	[76, 77]
SU11274	<p>1) Induces Apoptosis through the Increase of p53 Protein</p> <p>2) Inhibition of c-MET activation</p>	[78, 79]
Tivantinib	Effectively abrogated constitutive and HGF-induced MET phosphorylation in lung cancer cell lines. Inhibited pAkt, ERK1/2, STAT-3. Inhibited proliferation and induced apoptosis.	[80]
H224G11	NSCLC tumour xenograft growth significantly inhibited.	[81]
NK4 (HGF Antagonist)	Significantly inhibited <i>in vivo</i> tumour growth and distant metastasis	[82]
Clinical Studies		
Cabozantinib+ Erlotinib	30% reduction in tumour burden in 17% patients	[83]
Ficlatuzumab+ gefitinib	Partial response in 5 and stable disease in 4 patients (<i>n</i> =15)	[84]

Onartuzumab + erlotinib	Combination demonstrated benefit over erlotinib alone in patients with MET-overexpressing tumours	[83]
Rilotumumab (HGF inhibitor)	Currently undergoing	[74]

Abbreviations: Akt, alpha serine/threonine-protein kinase; ERK, extracellular signal-regulated kinases; HGF, hepatocyte growth factor; MET, mesenchymal epithelial transition; STAT Signal transducer and activator of transcription

1.10.4.1 HGF/MET crosstalk with other pathways

In addition to its role as an oncogenic driver, it has been demonstrated that substantial functional crosstalk exists between HGF/MET and other signalling pathways including EGFR and VEGFR signalling which are of primary importance in lung cancer (Figure 1.6). It has been shown that autocrine activation of EGFR by TGF- α can cause phosphorylation of MET. Cross-talk between the TGF- α /EGFR and the HGF/c-Met pathways can induce signal amplification and promote cell growth in a unidirectional way [85]. HGF can induce EGFR-TKI resistance in NSCLC cells by restoring the PI3K/Akt signalling pathway. Both EGFR and MET can activate one another independent of their agonist [86], and MET cross-talks and cooperates with other members of the EGF receptor family, including HER2, to enhance cell invasion. Overall, MET amplification is found in 20% of EGFR-TKI resistant patients [73]. The HGF/MET pathway can induce expression of VEGF-A by activation of MEK and PI3K pathways thereby promoting angiogenesis. [87, 88]. These shared downstream signalling pathways and extensive cross-talk are some of the primary reasons for development of resistance against targeted therapies. Combination therapies of EGFR and MET TKIs have shown promising results in *in vivo* preclinical studies and some of them are now under clinical investigation (Table 1.3 and 1.4).

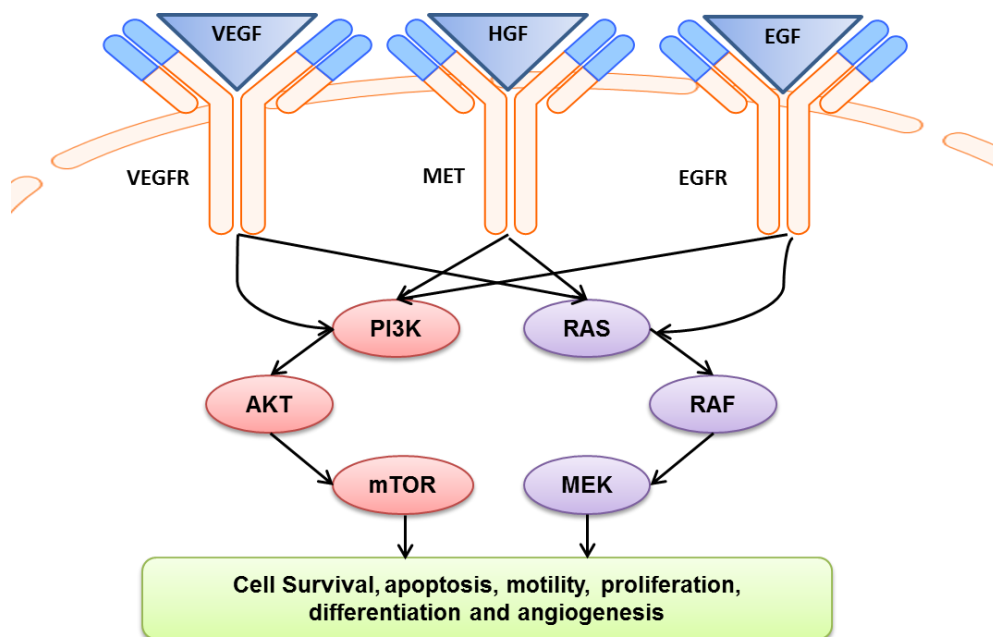


Figure 1.6 Functional crosstalk of HGF-MET signalling pathway with EGFR and VEGFR signalling pathway.

Abbreviations: Akt, alpha serine/threonine-protein kinase; EGF, epidermal growth factor; EGFR, epidermal growth factor receptor; HGF, hepatocyte growth factor; MEK, MAPK/ERK kinase; MET, mesenchymal epithelial transition; mTOR, mechanistic target of rapamycin; PI3K, phosphatidylinositol-3-kinase; Raf, rapidly accelerated fibrosarcoma; RAS, rat sarcoma; VEGF, vascular endothelial growth factor; VEGFR, vascular endothelial growth factor receptor.

Table 1.4 Dual EGFR–MET inhibition studies in lung cancer xenograft models

Agent	Target	In Vivo activity	Ref
Crizotinib+gefitinib	MET, ALK	Additive	[89]
SGX52+erlotinib	MET	Additive	[90]
MGCD26+erlotinib	MET VEGFR	Additive	[94]
Cabozantinib+gefitinib/erlotinib	MET, VEGFR	Synergistic	[94]
SU11274+erlotinib	MET	Synergistic	[91]

Table adapted from Robinson *et al* [92].

1.11 Prevention of lung cancer

There is no doubt that smoking cessation is the most important preventable risk factor for lung cancer. The primary reason for addiction to tobacco smoking is nicotine present in tobacco. The addictive potency of nicotine has been described as equal to that of heroin or cocaine and therefore overcoming nicotine addiction is the single most important factor in quitting smoking [93].

Pharmacological interventions such as nicotine replacement therapy in the form of nicotine gums, patches, nasal sprays, tables, lozenges and inhalers are effective as part of a strategy to promote smoking cessation. Public awareness programmes, education, counselling and advertisement restrictions are some of the methods used to discourage people from smoking [94, 95]. A recent WHO report suggests that even though global trends of tobacco smoking are declining, several low-income and middle-income countries are at risk of worsening tobacco epidemics and hence rapid and effective action is needed to achieve a WHO goal of less than 5% adults using tobacco products worldwide.

1.11.1 Chemoprevention

1.11.1.1 General concept

Chemoprevention can be defined as the use of natural or chemically synthesized compounds to prevent, inhibit or reverse the process of carcinogenesis [96]. The rationale for chemoprevention is based on two main concepts; multistep carcinogenesis and field cancerization. Multistep carcinogenesis is the progression of normal bronchoepithelial cells to metaplasia, and then to increasing grades of dysplasia (mild, moderate, and severe), culminating in carcinoma in situ and invasive squamous cell carcinoma. The field cancerization concept states that histologically normal-appearing tissues adjacent to malignant lesions contain molecular abnormalities similar to those seen in tumour tissue. This translates into increased risks of developing neoplastic lesions in other areas or sites of the field [97]. The aim of cancer chemoprevention is to intervene within this multistep carcinogenic process using agents that have the ability to modulate molecular and cellular targets that can inhibit one or more stages of cancer development.

Chemoprevention can be broadly classified into three different types (Figure 1.7). Primary chemoprevention involves the administration of agents to the healthy population or to those without overt disease but with particular risk factors. Secondary chemoprevention includes individuals with premalignant lesions and administration of agents to prevent progression to invasive cancer. Tertiary chemoprevention is to prevent recurrence or second primary cancers in individuals who have undergone successful treatment of early disease [98].

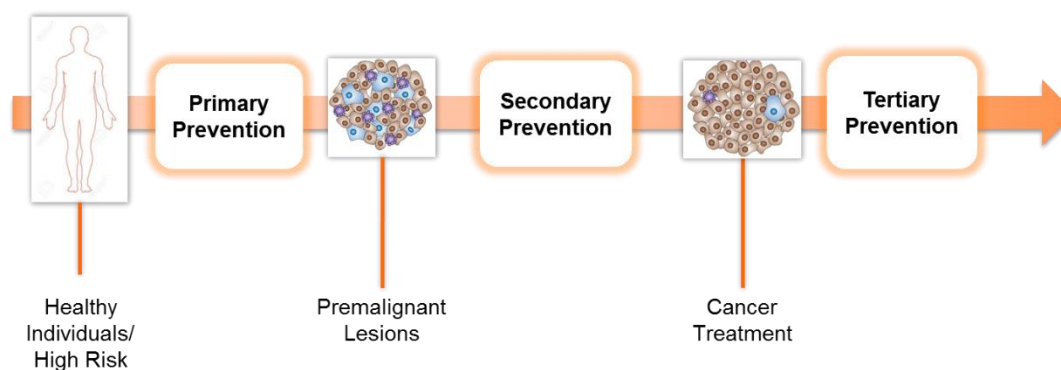


Figure 1.7 Intervention of chemopreventive agents at different stages of lung cancer.

1.11.1.2 Scope for chemoprevention in lung cancer

Since the risk-factors for lung cancer are well established and many of the molecular events in lung carcinogenesis and some precursor lesions have been identified, this is an ideal disease for chemoprevention. Development of lung cancer spans over several decades, and this long latency period provides an opportunity for intervention with chemopreventive agents to inhibit, delay or reverse the process of carcinogenesis. Rapid improvements in the understanding of the molecular and biological basis of lung carcinogenesis have raised new possibilities for development of chemopreventive agents. Former smokers who are at higher risk would be a suitable target population for primary chemoprevention. Advances in endoscopy techniques and radiology have increased the possibility to diagnose intraepithelial neoplasia and lung cancer at much earlier stages. This can help identify target population for secondary chemoprevention. Patients with a history of lung cancer are at a 40% risk of recurrence of disease [99, 100]. Tertiary chemoprevention can be useful for inhibiting or delaying the recurrence of disease and could possibly improve quality of life for this cohort.

1.11.1.3 Potential targets for lung cancer chemoprevention

An understanding of the mechanisms of action of chemopreventive agents is critical for the clinical development of the agent. The molecular targets and interactive signalling pathways altered during lung carcinogenesis can be attractive targets for chemoprevention, and agents that can modulate these targets can effectively be developed as chemopreventive agents. A strong rationale also exists for use of combinations of agents that can act on multiple

targets in an additive or synergistic manner [101]. Figure 1.8 summarises some potentially important targets for lung cancer chemoprevention. Apart from targets mentioned in figure 1.8, potential chemopreventive agents should also be investigated for their protective effects against early carcinogenic events such as prevention of DNA damage, DNA repair mechanism and ability to reduce DNA adduct formation.

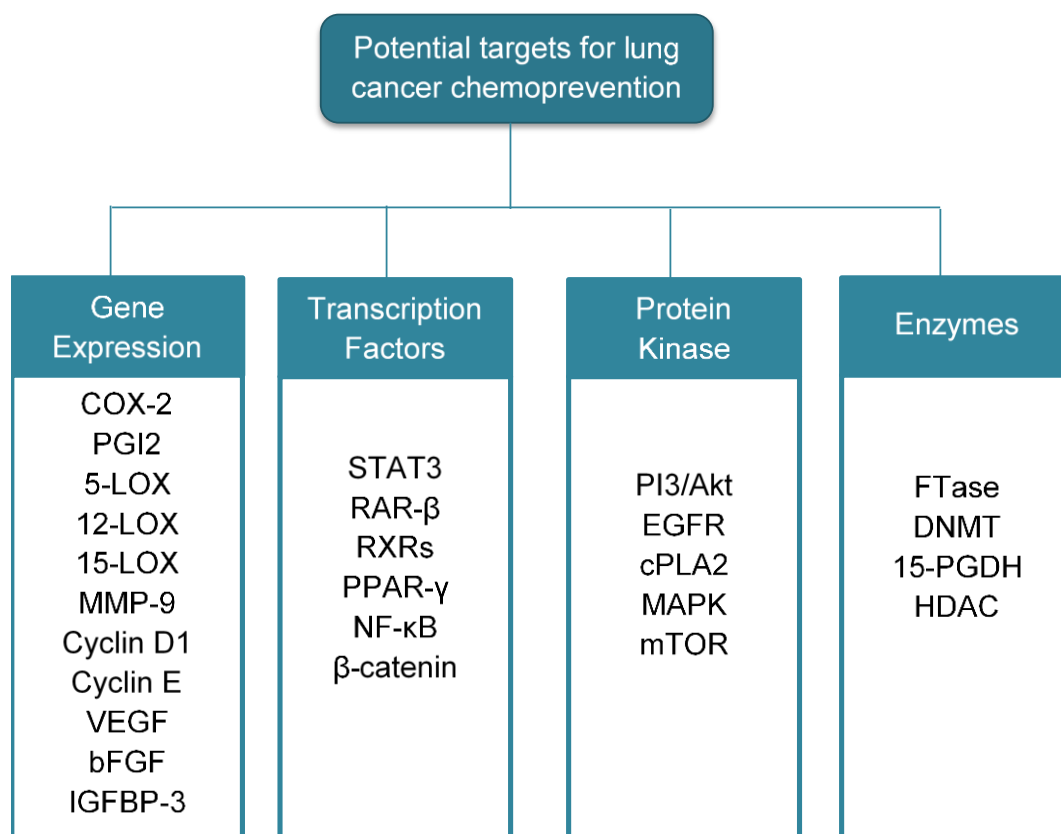


Figure 1.8 Potential genetic targets for chemoprevention of lung cancer

Figure made from information provided in Stewart *et al* [102].

Abbreviations: bFGF, basic fibroblasts growth factor; COX, cyclooxygenase; cPLA2, cytosolic phospholipase A2; DNMT, DNA methyl transferase; EGFR, endothelial growth factor receptor; FTase, farnesyltransferase; HDAC, histone deacetylase IGFBP-3, insulin like growth factor binding protein 3; LOX, lipoxygenase; MAPK, mitogen activated protein kinase MMP, matrix metalloproteinase; mTOR, mechanistic target of rapamycin; NF- κ B, nuclear factor- κ B; PGDH, hydroxyprostaglandin dehydrogenase; PGI2, prostaglandin 2; PI3, phosphoinositide 3 kinase; PPAR- γ , peroxisome proliferator activated receptor- γ ; RAR, retinoic acid receptor- β ; RXRs, retinoid x receptors; STAT, signal transducer and activator of transcription; VEGF, vascular endothelial growth factor.

1.11.1.4 Tumour Microenvironment (TME): A potential target for lung cancer prevention

TME is a complex system of many cellular and non-cellular components. There is increasing evidence that these components interact with each other and participate in maintenance and development of the tumour. Hence, targeting TME is emerging as an attractive strategy for preventive and therapeutic interventions for many cancer sites, including lung [103]. Figure 1.9 alludes to the complexity of potential therapeutic targets in a TME amongst which cancer associated fibroblasts play a prominent role.

1.11.1.4.1 Cancer Associated Fibroblasts (CAFs)

Under normal conditions, fibroblasts exist in an inactive state and form a structural network by synthesizing several components of the extracellular matrix (ECM), including collagens, laminin, and fibronectin. They also secrete ECM-degrading proteases such as matrix metalloproteinases (MMPs), and play a crucial role in maintaining an ECM homeostasis by regulating ECM turnover. During the process of wound healing, the fibroblasts become activated, which elicits tissue remodelling and expression of surface markers such as α -smooth muscle actin (α -SMA), platelet-derived growth factor receptor (PDGFR), fibroblast specific protein (FSP)-1, fibroblast activation protein (FAP), as well as stromal-derived factor-1 (SDF-1: CXCL12) and its receptor CXCR4. Upon completion of the healing process, these fibroblasts are removed by apoptosis or go back to their original state. However, in a TME, the fibroblasts remain activated and are referred to as cancer associated fibroblasts (CAFs). CAFs are able to influence vital tumourigenic functions such as cell proliferation, angiogenesis, inflammation and metastasis [104].

CAFs stimulate the production of matrix remodelling proteins, thereby degrading the ECM and allowing invasion of tumour cells into surrounding tissue areas. They suppress the immune response by recruiting inflammatory cells such as neutrophils, monocytes, macrophages to the tumour as well as by modifying immune cell function. CAFs release increased amounts of growth factors and cytokines, including vascular endothelial growth factor (VEGF), transforming growth factor- α (TGF- α), hepatocyte growth factor (HGF), platelet derived growth

factor (PDGF), SDF-1, and several interleukins (IL-1, IL-6, IL-8), which in turn promotes tumour angiogenesis and metastasis.

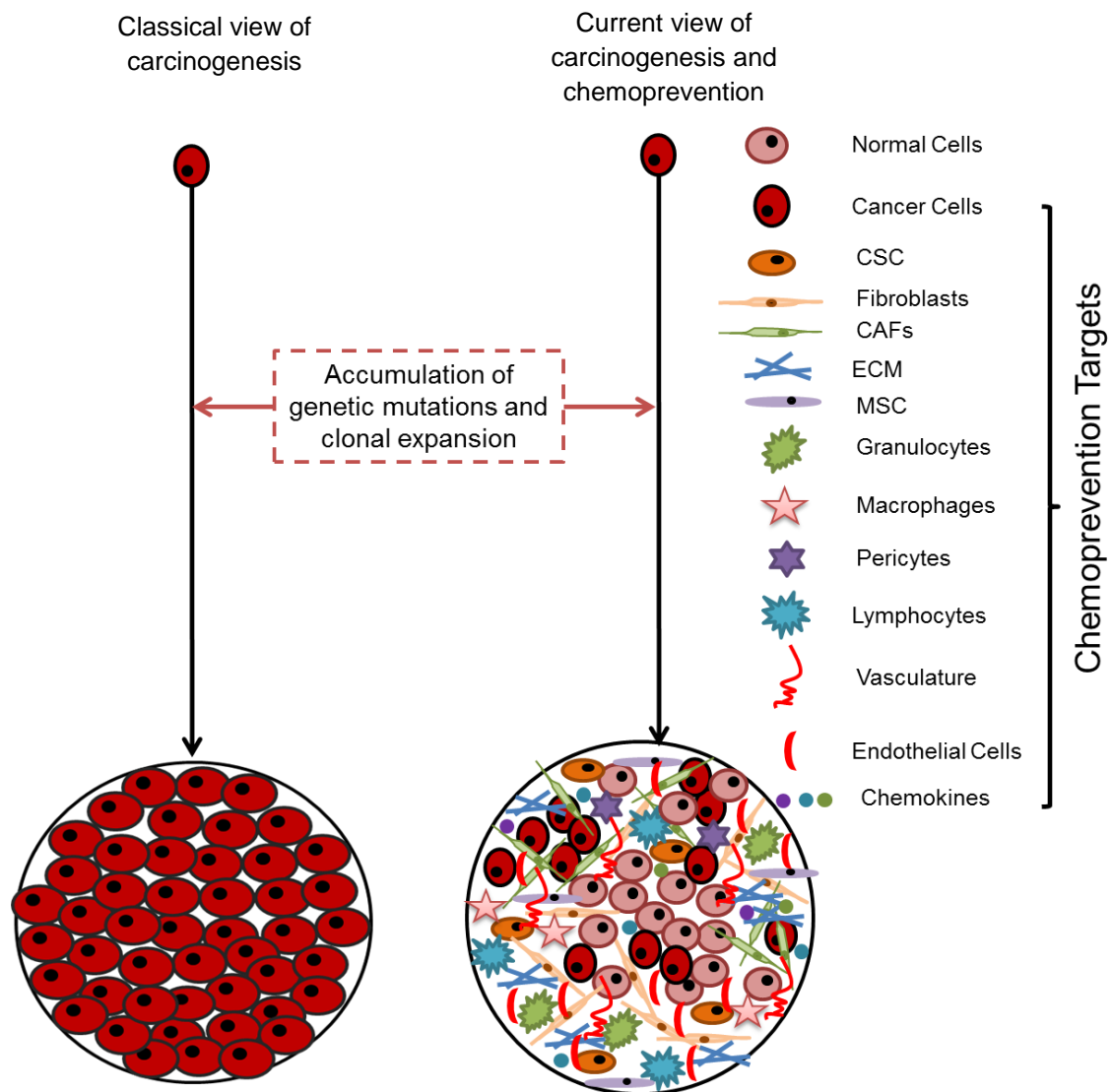


Figure 1.9 The classical and current view of carcinogenesis and chemoprevention targets.

Figure adapted from Deep and Agarwal [105]. Classically, tumours have been viewed as a homogenous mass of rapidly growing cells. The current view considers tumour as a complex system of many cell types that interact with each other.

Abbreviations: CSC, cancer stem cells; CAFs, cancer associated fibroblasts; ECM, extracellular matrix; MSC, mesenchymal stem cells.

CAFs interact with neighbouring tumour cells to recruit pro-carcinogenic signalling cascades including SDF-1/CXCR4 and HGF/MET signalling pathways that regulate tumour growth, cell migration, invasion and site-specific metastasis.

proven efficacy in preclinical models, and be acceptable for long-term human consumption [106]. A risk benefit ratio should also be considered as these agents would be taken by healthy individuals and it is likely that many of those won't develop cancer. For these reasons, repurposed drugs already in use for other indications and natural products with well safety profiles are ideal candidate. Some of the compounds that have been studied clinically for chemoprevention of lung cancer are described in the following section.

1.11.2.1 Retinoids and carotenoids

Retinoids are derivatives of vitamin A (retinol) which can be natural or synthetic compounds having a chemical structure similar to that of vitamin A. Retinoids exert their effect on gene expression by activating two main subtypes of nuclear receptors, retinoic acid receptors (RARs) and retinoid X receptors (RXRs) which play an important role in cell growth, apoptosis, and differentiation [107]. Carotenoids are a class of over 600 natural molecules that are found largely in fruit and vegetables and serve as precursors to retinols. Carotenoids possess strong antioxidant and immune-modulatory activity. Among carotenoids, beta-carotene has been the most extensively studied. Retinoids and carotenoids together have been the focus of large chemoprevention trials [96]. The rationale behind using retinoids as chemopreventive agents came from the successful treatment of premalignant lesions of oral leukoplakia and cervical dysplasia [108]. Epidemiological studies showed an inverse relation between serum levels of β carotene and cancer risk [109]. This evidence led to a number of large clinical trials including the Alpha Tocopherol Beta Carotene (ATBC) study, Carotene and Retinol (CARET) study and Physicians Health Study (PHS). In the ATBC trial, 29,133 men between the ages of 50-69 years of age and current smokers were recruited. The patients received either α -tocopherol, β -carotene or both. The trial results showed an 18% increase in lung cancer incidence and 8% increase in mortality among men who continued to smoke and received β -carotene supplementation, and no effect for α -tocopherol [110]. The results were confirmed in the CARET study (18,314 sample size), revealing a 28% higher rate of lung cancer and 17% higher overall death rate in those participants taking β – carotene in smokers and workers exposed to asbestos [111]. The reasons for failure of these trials are discussed in section 1.11.3. The PHS study recruited

male US physicians, 40–84 years of age without any history of cancer and were current, former or never smokers. The study used only β carotene as intervention and showed no effect on lung cancer incidence [112]. These three trials have been the largest lung cancer chemoprevention trials to date and were met with disappointing results.

1.11.2.2 Vitamin E (α -Tocopherol)

Vitamin E has been shown to have potent inhibitory activity on cell proliferation in various cancer cell lines including lung cancer. Preclinical studies have shown that Vitamin E possesses immune-modulatory and antioxidant properties [113], [114]. Apart from this, epidemiological studies also suggest that vitamin E intake has a protective effect against various pathologies, including cancer [115]. In the ATBC study, vitamin E supplementation alone did not have any effect on lung cancer incidence. This is the only chemopreventive study using vitamin E and further studies need to be implemented to evaluate its use.

1.11.2.3 Selenium

The role of selenium as a chemopreventive agent for lung cancer came to light when it was primarily being investigated for prevention of skin cancer with incidence of lung cancer as a secondary endpoint. A total of 1312 patients with a history of skin carcinoma received oral selenium for an average of 4.5 years. Selenium supplementation resulted in a 44% decrease in lung cancer incidence [116]. Another epidemiologic study suggested that increased selenium intake in populations with low selenium levels may decrease the risk of lung cancer [117]. However, subsequent chemopreventive trials using selenium did not show any effect on lung cancer incidence. The SELECT (selenium and vitamin E cancer prevention trial) study showed no significant effect on lung cancer prevention [118]. In the Linxian General Population Trial, 29,584 healthy adults aged 40-69 years were given a combination of α -tocopherol, β carotene and selenium. This combined intervention strategy revealed no beneficial effect on lung cancer incidence [119]. Similarly, a tertiary prevention study of selenium in patients with previous lung-cancer resection showed no decrease in lung-cancer recurrence [120]. The varying results for selenium trials led to the conclusion that selenium supplementation is beneficial only in population with low baseline selenium levels

as seen in the study by Reid et al [108]. It is also important to take into consideration the paradoxical activity of selenium while designing clinical studies for selenium. It can induce two fundamental types of effects: antioxidant, through its incorporation into selenoenzymes; and pro-oxidant, through the direct effects of selenocompounds [121].

1.11.2.4 N-acetylcysteine (NAC)

NAC has been reported to detoxify reactive electrophiles and free radicals through conjugation or reduction reactions, stimulate DNA repair and inhibit invasion in *in vitro* models. Preclinical and clinical studies have shown that the carcinogen-DNA adducts formed by cigarette smoke is inhibited by NAC [122, 123]. Considering this, the EUROSCAN clinical trial (European Study on Chemoprevention with Vitamin A and N-Acetylcysteine) was designed to test whether vitamin A and NAC could improve the prognosis of patients treated for lung cancer by preventing second primary tumours. The study recruited 2592 patients and had 93.5% patients who were either current or former smokers. The study failed to show any preventive effect of NAC on lung cancer incidence [124].

1.11.2.5 Anti-inflammatory agents

A number of anti-inflammatory agents have been investigated with respect to potential for chemopreventive effect in lung cancer. Iloprost and Celecoxib have both been shown to favourably alter prognostic biomarkers. Iloprost, a synthetic analogue of prostaglandin 2, was shown to improve endobronchial dysplasia in former smokers [125]. The COX-2 inhibitor celecoxib decreased the proliferative marker Ki-67 in lung tissue biopsies of former smokers. The decreases in Ki-67 correlated with a reduction and/or resolution of lung nodules [126]. Aspirin intake at low doses of 100 mg on alternate days, has been associated with lower incidence of lung cancer in a Women's Health Study [127]. However, the VITAL study which investigated use of regular-strength aspirin in 72,000 people found an elevated risk for SCLC with aspirin use [128].

1.11.2.6 EGFR inhibitors and Farnesyl Transferase inhibitors (FTI).

EGFR and FTI inhibitors are an upcoming class of compounds that are currently being investigated for their chemopreventive properties. Gefitinib (EGFR inhibitor) and tipifarnib (FTI inhibitor) are currently undergoing trials for lung

cancer prevention in patients with surgically resected early stage tumours (www.clinicaltrials.gov). Sputum atypia and Ki-67 labelling index will be the primary and secondary end-points for these trials. Some other compounds that have been studied for lung cancer chemoprevention, together with their outcomes are listed in table 1.5.

Table 1.5 Clinical studies for chemoprevention of lung cancer

Agent	Study group/end point	Patient no.	Conclusion	Ref
Enzastaurin	Former smokers	40	Non-significant	[129]
Sulindac	NSCLC/current or former smokers	61	Non-significant	[130]
13 cis RA+/- AT	Sputum atypia	75	Non-significant	[131]
Oltipraz	Chronic smokers	77	Non-significant	[132]
Budesonide	Smokers	112	Non-significant	[133]
Anethole Dithiolethione	Smokers with bronchial dysplasia	112	Potentially effective	[134]
Retinamide	Squamous metaplasia and dysplasia	82	Non-significant	[135]
BC/RA	Sputum atypia	755	Non-significant	[136]
Isotretinoin	Metaplasia	86	Non-significant	[137]
Folate + Vitamin B12	Squamous metaplasia	57	Beneficial	[138]
Etretinate	Sputum atypia	150	Negative	[139]
Folate + Vitamin B12	Sputum atypia	73	Reversal of sputum atypia	[140]

Abbreviations: AT, alpha-tocopherol; B12, vitamin B12; BC, beta-carotene; RA, retinoic acid.

1.11.3 Chemoprevention trials: Reason for failure

Almost all of the clinical trials for chemoprevention of lung cancer have met with disappointing results. Although these studies were based largely on epidemiological evidence, they highlighted the importance of having extensive

preclinical studies for improving our understanding of mechanisms of action that can confirm the preventive activity of the agent at doses that are clinically relevant. Many *in vivo* studies report results at a dose that are impossible to use in a clinical settings [141]. Hence, preclinical studies evaluating efficacy at a suitable dose with minimal toxicity should be undertaken. Another important consideration is selection of appropriate preclinical models. Models closely mimicking the human disease state should be developed to screen potential chemopreventive agents. Success of chemoprevention strategies largely depends on identification of optimal target populations. Although the clinical trials previously discussed had the correct rationale in selecting high risk populations, such cohort selection should be performed with great caution. Additional factors such as differences in risk determined by age, genetic make-up, lifestyle, history and differences between genders are also important considerations. The adverse results of ATBC and CARET study were widely attributed to the pro-oxidant effect of β -carotene on chemicals from cigarette smoke producing a free radical-rich environment in the lung. The pro-oxidant effect was suggested to be due to the high dose of 30 mg of β -carotene. This dose was 5 times the recommended daily allowance of β -carotene [142]. An *in vivo* study using cigarette smoke inhalation by ferrets showed that β -carotene, at an equivalent dose of 30 mg, led to squamous metaplasia and also facilitated the binding of cigarette smoke-derived carcinogens to DNA. On the contrary, a low pharmacological dose of 6 mg of β -carotene, attainable from a human diet high in fruits and vegetables, was found to have a mild protective effect against cigarette smoke-induced squamous metaplasia [143]. The dose of cigarette smoke to the ferrets was equivalent to human exposure who smoked 1.5 packs of cigarettes per day. These results highlight the importance of selection of appropriate preclinical models, correct dosing and optimal target populations. The lack of proper end-points can also be a hindrance in trials. For lung cancer there are currently no validated biomarkers. The most commonly used biomarkers are histologic changes based on multi step progression [144]. Establishing biomarkers that correlate with the disease and investigating their modulation by potential chemopreventive agents would be useful in predicting the outcome of a clinical trial. Biomarkers circulating in plasma, serum or present in sputum, if properly validated, could constitute the gold standard for a non-

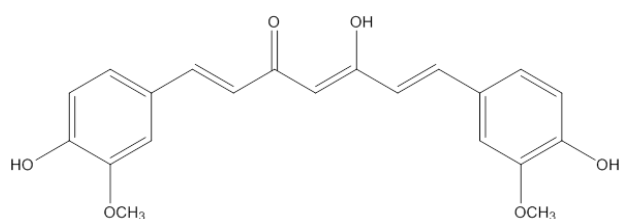
invasive cancer diagnostics. Such biomarkers include, circulating tumour cells, cell free DNA, microRNA, methylated DNA [145]. If surrogate biomarkers are identified such trials could be performed much quicker, with far fewer subjects and at a much lower cost. Future chemoprevention trials should therefore investigate compounds that have evidence of preclinical efficacy, safety and a well characterised pharmacokinetic profile. One such compound is curcumin.

1.12 Curcumin

Curcumin (Figure 1.11) is a dietary polyphenol derived from the rhizomes of turmeric (*Curcuma longa*), an Indian spice, commonly used as a food flavouring and food colouring agent. It has been investigated for activity against a spectrum of pathologies including, cancer, diabetes, cardiovascular disease, Alzheimer's, Parkinson's, skin diseases, multiple sclerosis and arthritis (reviewed in [146]). The beneficial properties of curcumin are complimented by a safe toxicological profile. Clinical studies have shown that it can be tolerated up to a very high dose of 12 grams a day with very few or no side effects [147]. The U.S. Food and Drug Administration has classified curcumin as a "generally regarded as safe" compound. Dietary intake of turmeric has been associated with reduced risk of cancer in humans [148]. Epidemiological studies show that the rates for colorectal, prostate and lung cancers in India are some of the lowest in the world [149]. Similarly, lower incidences of colon, breast, prostate and lung cancer amongst the British Indian population as compared to the British White population were observed [150]. It has been suggested that these lower incidences may be partially due to dietary intake of curcumin in the form of turmeric, in addition to overall dietary and lifestyle factors. The total intake of curcumin at which these beneficial effects are observed in Asian population is however difficult to predict as different studies report varying amount of turmeric intake through diet. These values range from 0.2 grams/person/day to 5 grams/person/day [148, 151, 152].

Commercially available curcumin is a mixture of 77% curcumin, 18% demethoxycurcumin (DMC) and 5% bis-demethoxycurcumin (bDMC) and together these three compounds are called curcuminoids [153]. Curcumin has been investigated as an agent for treatment and prevention for different forms of

cancer including lung, melanoma, head and neck, breast, colon, pancreatic, prostate, and ovarian cancers reviewed in [154, 155].



	R1	R2
Curcumin	OCH ₃	OCH ₃
DMC	OCH ₃	H
bDMC	H	H

Figure 1.11 Structure of curcuminoids

1.12.1 Possible mechanisms of action of curcumin

The *in vitro* and *in vivo* efficacy of curcumin against variety of cancers including lung is of particular interest due to its ability to induce a variety of pharmacological effects including apoptotic, anti-proliferative, anti-oxidant, and antiangiogenic effects. Curcumin has the ability to modulate multiple cancer-related targets including that of transcription factors, enzymes, cytokines, and growth factors (Figure 1.12). A few of the important mechanism of actions are briefly discussed here.

1.12.1.1 Curcumin inhibits tumour initiation

Reactive oxygen species (ROS) and reactive nitrogen species (RNS) produced by activated neutrophils have been detected in almost all forms of cancers, where they promote many aspects of tumor initiation, development and progression. Curcumin inhibits the induction of nitric oxide synthase in activated macrophages and has been shown to be a potent scavenger of free radicals like nitric oxide [156]. Curcumin also blocks nuclear factor-kappa B (NF-κB) activation which is involved in induction of inducible nitric oxide synthase (iNOS), one of the causes of oxidative stress and tumour initiation [157]. Dietary supplementation with curcumin in male ddY mice, a model for postprandial hypertriglyceridemia, has been shown to increase cytochrome p450, phase II detoxifying enzymes and antioxidant enzyme activity suggesting a preventive role in early carcinogenic events [158].

1.12.1.2 Curcumin inhibits cell proliferation and induces apoptosis

Apart from tumour initiation, NF- κ B is also a positive mediator of cell growth and proliferation. It modulates the up-regulation of several pro-survival proteins such as cyclin D1, Bcl-2, Bcl-xL, c-myc, cyclooxygenase-2 (COX-2). Inhibitory kappa B alpha (I κ B α) kinase (IKK) and Akt activation are required for NF- κ B gene expression. Curcumin blocks phosphorylation of I κ B α and Akt to inhibit NF- κ B protein expression [159, 160]. Activated STAT3 has been found to be present in the majority of cancers including lung, and plays an important role in cancer progression. Curcumin inhibits STAT3 activation and suppresses the expression of an array of pro-survival proteins including survivin, Bcl-XL and cyclin B1 [161, 162]. Cell proliferation induced by growth factors IL-2, IL-6 and PDGF are also known to be inhibited by curcumin [163].

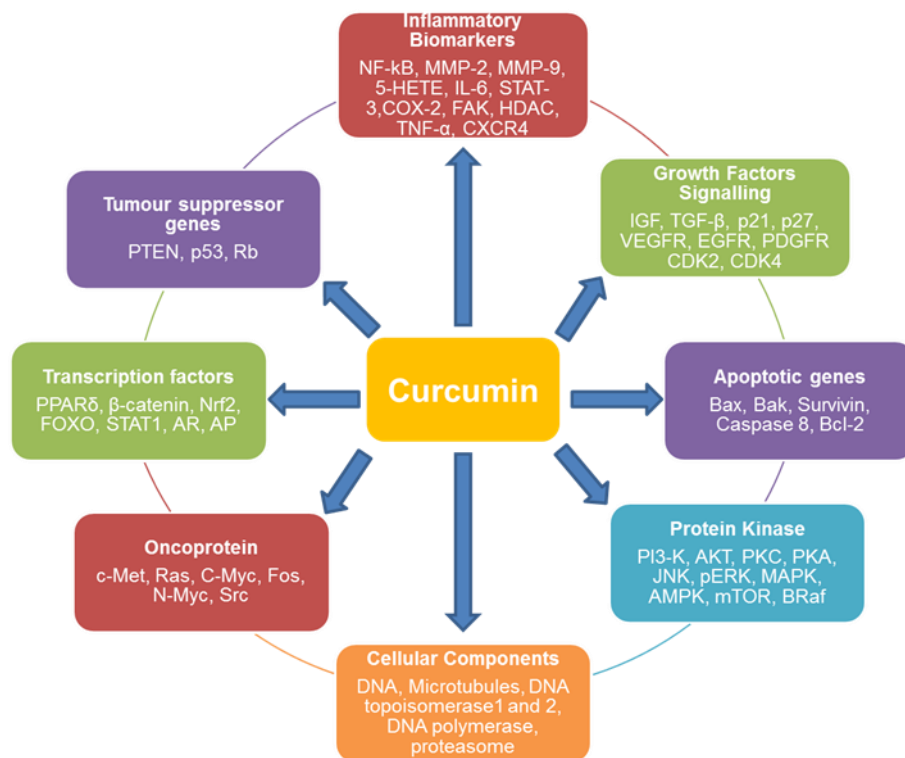


Figure 1.12 Molecular targets of curcumin

Figure adapted from Hasima et al [164].

Abbreviations: AP, activating protein; AR, androgen receptor; Akt, alpha serine/threonine-protein kinase; AMPK, AMP-activated protein kinase; Bcl-2, b-cell lymphoma 2; Bax, Bcl-2 associated X protein; Raf, rapidly accelerated fibrosarcoma; CXCR4, chemokine receptor type 4; CDK, cyclin dependant kinase; c-Myc, c-mycproto-oncogene; COX, cyclooxygenase; EGFR, epidermal growth factor receptor; ERK, extracellular regulatory kinase; FAK, focal adhesion kinase; HDAC, histone deacetylases; HETE, hydroxyecosatetraenoic acid; IGF, insulin growth factor; IL,

interleukin; JNK, c-Jun N-terminal protein kinases; PDGFR, platelet derived growth factor receptor; MAPK, mitogen activated phospho-kinase; MET, mesenchymal epithelial transition; MMP, matrix metalloproteinase; mTOR, mechanistic target of rapamycin; NF- κ B, nuclear factor kappa B; Nrf2, nuclear factor erythroid 2-related factor; PPAR- γ , peroxisome proliferator activated receptor- γ ; PI3K, phosphor inositol 3 kinase; PK, phosphor-kinase; PTEN, phosphatase and tensin homolog; STAT, signal transducer and activation of transcription; TGF- β , transforming growth factor β ; TNF- α , tumour necrosis factor- α , VEGFR, vascular endothelial growth factor receptor.

Curcumin promotes inhibition or arrest at all stages of the cell cycle. Cyclin dependant kinases (CDK) which regulate cell cycle progression are inhibited by curcumin by inducing expression of CDK inhibitors p16, p21, and p27. Curcumin induces down-regulation of cyclin D and prevents cells progressing from the G1 to the S phase, thus favouring apoptosis. In lung cancer cell lines, curcumin causes arrest at G2/M, G1/S, G0/G1, and the sub G1 phase [165-167]. These effects are accompanied by upregulation of pro-apoptotic genes *BAX* and *BAD* and downregulation of anti-apoptotic genes *BCL-2* and *BCL-XL*. Another mechanism of action by which curcumin induces apoptosis is by regulating tumour suppressor genes. Curcumin inhibits cell cycle progression by inducing p53, phosphatase and tensin homolog deleted on chromosome ten (PTEN) and retinoblastoma (*RB1*) protein expression in prostate cancer cells. In p53 deficient lung cancer cell lines, curcumin induces apoptosis by alternative p53 independent molecular pathways associated with translocation of BAX, BAK and caspase activation [168].

1.12.1.3 Curcumin inhibits invasion, metastasis and angiogenesis

Curcumin has been found to reduce the invasion and subsequent metastasis of cancer cells in cellular and animal models. During lung cancer metastasis, the invasive tumour cells have to penetrate a number of cellular barriers including the basement membrane. The major component of the basement membrane is type IV collagen. A group of proteolytic matrix metalloproteinases (MMPs) enzymes, especially MMP-2 and MMP-9, are involved in degradation of type IV collagen. The levels of these MMPs are found to be elevated in several forms of malignant cancers. VEGF is an important inducer of angiogenesis and VEGF overexpression and has been confirmed in different forms of human cancers

including NSCLC and SCLC [169]. *In vitro*, curcumin inhibits the migration and invasion of human lung cancer cells through inhibition of MMP-2, MMP-9 and VEGF [170]. These effects are exerted through down regulation of the MEK/ERK pathway. Other pathways by which curcumin is known to exert its anti-metastatic and anti-angiogenic properties are via inhibition of PI3/Akt/mTOR and NF- κ B pathways [171]. Growth factors that play a contributing role in VEGF mediated angiogenesis including EGF, FGF and TGF are also inhibited by curcumin [172-174] Recent studies have shown that curcumin suppresses migration and invasion of highly metastatic lung cancer cells by upregulation of E-cadherin, and downregulation of β catenin and vimentin expression [175].

1.12.2 Preclinical studies of curcumin and lung cancer

Curcumin has been investigated in different *in vitro* and *in vivo* studies to validate its use for prevention and treatment of lung cancer. Apart from the preclinical studies demonstrating mechanisms by which curcumin acts on lung cancer as discussed above, a number of other key *in vivo* and *in vitro* studies of curcumin and lung cancer are listed in Table 1.6.

Table 1.6 A selection of preclinical *in vitro* and *in vivo* studies of curcumin in lung cancer models.

<i>In Vitro</i> Studies		
Model	Effect of curcumin	Ref
Beas-2B bronchial epithelial cells	Decrease in EGFR expression in Beas-2B bronchial epithelial cells	[176]
Fetal rat lung fibroblasts	Prevention of hypoxia, pERK and induction of apoptosis in fetal rat lung fibroblasts	[177]
Human bronchial epithelial cells	Prevention of inflammation in human bronchial epithelial cells in response to fine particulate matter	[178]
Primary lung fibroblasts derived from scleroderma patients	Apoptosis in scleroderma but not normal lung fibroblasts.	[179]
Calu-3 human bronchial epithelial cells	Curcumin prevents cadmium-induced upregulation of IL-6 and IL-8, with reduction in pERK1/2 in bronchial epithelial cells.	[180]
Beas-2B bronchial epithelial cells	Prevention of cigarette smoke induced activation of NF-kB in Beas-2B bronchial epithelial cells	[181]
Human lung cancer cells	Curcumin increased cytotoxicity of erlotinib in erlotinib-resistant PC-9, H1975, H1650 cell lines.	[182]
Human lung adenocarcinoma cells	Induces LC3-II resulting in autophagy in A549 and IMP-90	[183]
Human lung adenocarcinoma cells	Curcumin sensitizes cells to redox-mediated apoptosis and increased p38 MAPK phosphorylation.	[184]

Human lung adenocarcinoma cells	Decreased invasion and migration associated with increased expression of the tumour suppressor HLJ-1.	[185]
<i>In Vivo studies</i>		
C57BL/6J mice exposed to cigarette smoke	Curcumin significantly decreased neutrophils and macrophages in broncho-alveolar lavage	[186]
Male TO mice exposed to diesel exhaust particles (DEP)	Curcumin inhibited inflammatory cell infiltration in lungs and systemic inflammation	[187]
C57BL/6 mice with intratracheal inoculation of <i>Staphylococcus aureus</i>	Decreased lung injury caused by decreasing inflammatory cell infiltration, decreasing alveolar wall thickening and consequent oedema	[188]
Male Laka mice exposed to benzo[a]pyrene (BP)	Curcumin in combination with piperine shows pronounced antioxidant effects by preventing BP-induced superoxide dismutase, catalase and glutathione depletion and decreased lung edema.	[189, 190]
A549 xenograft	Synergistically enhanced the anti-tumour efficacy of docetaxel in A549 xenograft	[191]
VEGF-overexpressing transgenic mice	Decreased pulmonary function damage, pulmonary inflammation and mRNA levels of VEGFR, c-myc, EGFR, ERK2, and cyclin D	[192]
C57BL/6 mice with tracheal instillation of lewis lung carcinoma cells	Prevented pulmonary fibrosis following thoracic irradiation	[193]

NCI-H460 xenografts	Inhibits tumour growth	[194]
Orthotopic mouse model of lung cancer	Curcumin-cyclodextrin complex potentiates the effects of gemcitabine to significantly decrease tumour volume and proliferative index.	[195]
Bleomycin-induced pulmonary fibrosis in rats	Significantly downregulated Collagen-I, TGFb1, and iNOS	[196]
Mice exposed to BP	Inhibits BP induced activation of NF-κB and MAPK signaling and Cox-2 transcription in lung tissues of mice. Reduced number of tumour nodules in lungs.	[197]
A549 xenograft	Curcumin-loaded hydrogel nanoparticle have enhanced anti-cancer activity.	[198]
Orthotopic NSCLC xenografts	Induced apoptosis and inhibited growth	[167]

1.12.3 Clinical studies of curcumin

In response to *in-vitro* and *in-vivo* studies of curcumin alluding to its chemopreventive and therapeutic effects, a number of clinical trials have addressed the safety and efficacy of curcumin in different types of cancer. Table 1.7 summarizes some of the completed clinical trials of curcumin to illustrate safety and efficacy. Clinical trials are still in their early phases of investigation but early trials have shown promise for use of curcumin in neoplastic and pre-neoplastic diseases such as multiple myeloma, pancreatic cancer and colon cancer.

Table 1.7 Clinical studies of curcumin to illustrate safety and efficacy

Disease/ Condition	Phase	Observation	Ref
Radiation Dermatitis	I/II	Curcumin reduced the severity of radiation dermatitis in breast cancer patients	[199]
Colorectal Neoplasia	II	A significant 40% reduction in aberrant crypt foci	[200]
High-risk or pre- malignant lesions	I	Histologic improvement of precancerous lesions in patients with recently resected bladder cancer, oral leucoplakia, intestinal metaplasia, cervical intra-epithelial neoplasia. Curcumin is not toxic to humans up to 8,000 mg/day when taken by mouth for 3 months.	[201]
Colorectal cancer	II	59% reduction in the activity of glutathione transferase and radiologically stable disease in 5 patients	[202]
Prostatic hyperplasia	II	Reduction of signs and symptoms of the disease evaluated by International Prostate Symptom Score	[203]
Myeloid leukaemia	II	Nitric oxide levels significantly decreased with turmeric as adjuvant co-treatment with imatinib	[204]

Colorectal cancer	II	Enhanced expression of p53, decreased levels of TNF- α	[205]
Pancreatic Cancer	I	Curcumin plus gemcitabine treatment elicited partial response in 9% patient and 36% patients had stable disease.	[206]
Breast Cancer	I	Partial response with docetaxel plus curcumin treatment	[207]
Pancreatic Cancer	II	Biological activity in 2/21 patients. 1 patient had 73% tumour regression. Downregulation of NF-kB, COX-2, and pSTAT3 in peripheral blood mononuclear	[208]

Ongoing clinical trials of curcumin for various malignancies include lung cancer, cervical cancer, colorectal adenoma, pancreatic cancer, breast cancer, chronic lymphocytic leukaemia, small lymphocytic lymphoma, multiple myeloma, multiple sclerosis, prostate cancer and familial adenomatous polyposis (<https://clinicaltrials.gov/ct2/results?term=curcumin&pg=1>).

1.12.4 Pharmacokinetics and metabolism of curcumin

For successful development of a chemopreventive agent an understanding of its pharmacokinetic profile is very important. The data obtained from preclinical and clinical pharmacokinetic studies helps in determining the dose required to achieve a therapeutic response in humans. Curcumin pharmacokinetic studies to date have suggested that curcumin is extensively metabolised, irrespective of the route of administration [153]. Following oral administration, curcumin is absorbed into the intestine and partially metabolised by intestinal enzymes and bacteria. The remaining curcuminoids and metabolites are further metabolised in the liver which is the major site of metabolism for curcumin [209]. In addition, curcuminoids are also metabolised in extra hepatic tissues including the kidneys which also express limited amounts of drug metabolising enzymes [210].

The first pharmacokinetic study of curcumin was performed in 1978 by Wahlström and Blennow in which they showed that an oral dose of 1g/kg of curcumin in Sprague-Dawley rats resulted in 75% of curcumin excreted in faeces with negligible amount in urine. Measurements of blood plasma levels and biliary excretion showed that curcumin was rapidly metabolised, poorly absorbed from the gut and excreted largely unchanged [211]. Since then, numerous pharmacokinetic studies in mice, rats and humans using a range of doses and different routes of administration have been performed. All of the studies point towards negligible amounts of curcumin in plasma and its metabolites as the predominant species. At high oral doses ranging from 100 mg/kg to 2 g/kg in rats a maximum serum concentration of 0.6-3.6 μM was observed. In clinical studies, an oral dose of 2g in healthy human volunteers resulted in either undetectable or extremely low (0.01 μM) plasma levels of curcumin. In another clinical study, oral dosing of 4–8 g of curcumin in humans showed peak plasma levels of 0.41–1.87 μM at 1-2 hour post dosing at 1-2 hours post dosing [201]. A selection of pharmacokinetic studies is listed in Table 1.8.

The major pathways that have been identified in curcumin metabolism are O-conjugation and reduction. The O-conjugation products are mainly observed following oral administration and include curcumin glucuronide, curcumin sulfate, curcumin glucuronide-sulfate and di-substituted conjugates. The presence of conjugative enzymes uridine diphosphate glucuronosyltransferases (UGTs) and sulfotransferases (SULTs) in liver, kidney and intestine extensively metabolise curcumin to form glucuronide and sulfate conjugates respectively [212, 213]. Pan *et al.* reported that 99% of curcumin is present as a glucuronide conjugate following oral administration in rats [214]. At an oral dose of 340 mg/kg in rats, the levels of curcumin glucuronide were 20 times, and curcumin sulfate were 4 times greater than free curcumin in plasma [215]. The reduction products are observed mainly following intravenous and intraperitoneal administration and include tetrahydrocurcumin, hexahydrocurcumin and octahydrocurcumin. Other minor products are dihydrocurcumin glucuronide, tetrahydrocurcumin glucuronide, ferulic acid and dihydroferulic acid [216]. The enzymes responsible for the metabolic reduction have been found to reside in the cytosol of liver and intestine and include alcohol dehydrogenases [217]. Surprisingly, curcumin

appears not to be metabolized by cytochrome P450, because no products of demethylation or hydroxylation were detected after incubation of curcumin with rat liver microsomes [218].

1.12.4.1 Biological activities of curcumin metabolites

Considering the fact that metabolites are the predominant species after curcumin administration, it is conceivable that they may possess some bioactivity. However, there have been relatively few studies investigating the biological effects of curcumin metabolites. Curcumin glucuronide was not found to be cytotoxic in HepG2 cells at high concentration of 25 μ M. It did not affect mRNA expression of acyl-CoA oxidase 1 (ACOX1), catalase (CAT) or amphiregulin (AREG) but had a significant effect on glutathione-S-transferase theta 1 (GSTT1) mRNA expression [219]. A similar study showed that curcumin glucuronides possessed very little anti-oxidant and anti-proliferative activity, and elicited no effect on the NF- κ B pathway [220, 221]. Curcumin sulfate was shown to have only weak prostaglandin E2 inhibitory activity [222]. However, tetrahydrocurcumin (THC) has been reported to have a bioactivity equivalent to that of curcumin. Some studies have shown that THC is a stronger antioxidant and is more efficacious than curcumin in preventing azoxymethane-induced colon cancer [223, 224]. THC can induce G2/M cell cycle arrest and apoptosis involving p38 MAPK activation in human breast cancer cells [225]. It also been demonstrated to have an inhibitory effect against tumour angiogenesis by downregulation of VEGF [226], and induces autophagic cell death through modulation of the PI3K/Akt/mTOR and MAPK signalling pathway in human leukaemia cells [227]. Hexahydrocurcumin (HHC) and octahydrocurcumin (OHC) have also been shown to have activity against colorectal cancer cell lines [228, 229]. Considering that curcumin undergoes extensive and rapid metabolism, yet pharmacological activity is still observed, it is reasonable to assume that metabolites might be converted back into parent compound on reaching target tissues, as has been observed for other putative chemopreventive agents such as resveratrol [230].

Table 1.8 Preclinical and clinical pharmacokinetic studies of curcumin

Species	Dose	Route	Plasma/tissue	Peak levels achieved (μM)	Ref
Rat	400 mg/kg	Oral	Plasma	< 1.3	[231]
			Kidney, liver	< 2	
Mouse	100 mg/kg	i.p	Plasma	6.12	[214]
			liver	0.08 \pm 0.007	
			spleen	0.07 \pm 0.002	
			Kidney	0.02 \pm 0.002	
			brain	0.001	
			intestine	0.3 \pm 0.01	
Mouse	100 mg/kg	oral	Plasma	0.68	[232]
		i.p	Plasma	2.5 \pm 0.2	
			Intestine	0.2 \pm 0.023	
			Liver	0.73 \pm 0.20	
			Brain	0.2.9 \pm 0.04	
			Heart	0.9.1 \pm 0.1	
			Muscles	0.84 \pm 0.6	
			Lungs	0.16 \pm 0.03	
			Kidneys	0.78 \pm 0.03	
Rat	2g/kg	Oral	Stomach	145 \pm 13.8	[231]
			Small intestine	159.5 \pm 29.9	
			Caecum	140.2 \pm 36.7	
			Large Intestine	13.8 \pm 6.8	
Rat	340 mg/kg	Oral	Plasma	0.0065 \pm 0.0045	[215]
Rat	1g/kg	Oral	Plasma	1.3	[233]
Rat	2 g/kg	Oral	Plasma	3.67 \pm 0.62	[234]
Rat	500 mg/kg	Oral	Plasma	0.06 \pm 0.01	[235]
Rat	10 mg/kg	i.v	Plasma	0.9 \pm 0.1	[235]
Human	2 g	Oral	Plasma	0.006 \pm 0.005	[234]
Human	4-8 g	Oral	Plasma	0.4–3.6	[201]
Human	10 g	Oral	Plasma	0.13	[147]

Human	12 g	Oral	Plasma	0.13	[236]
Human	3.6 g	Oral	Plasma	0.01±0.006	[236]
Human	0.4-3.6 g	Oral	Colorectum	0.01–0.05	[237]
Human	2.35 g	Oral	Colon	0.35	[238]
Human	8 g	Oral	Plasma	0.07-1.1	[239]

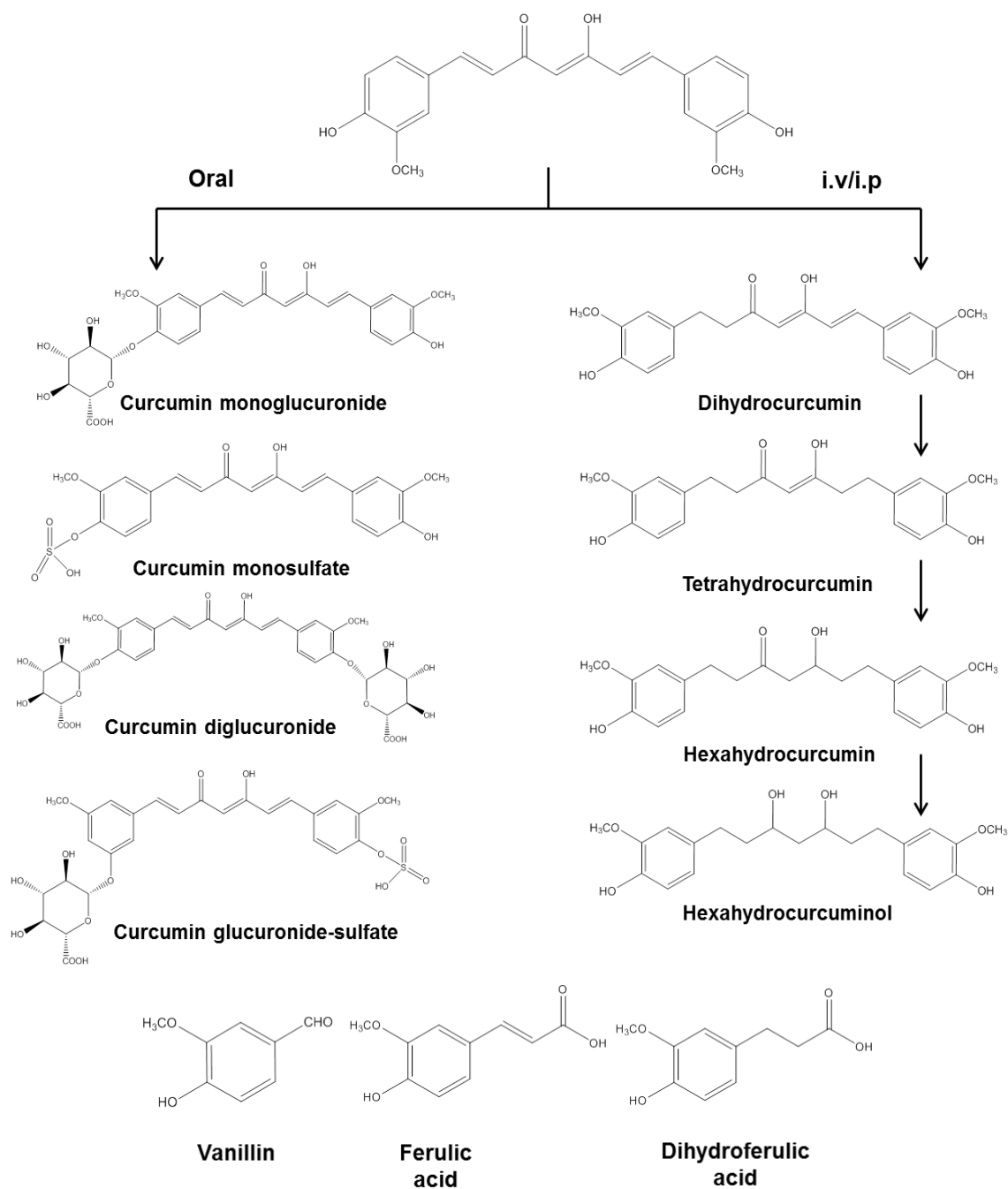


Figure 1.13 Metabolism of curcumin following different routes of administration.

Conjugated metabolites form the major species observed in plasma following oral administration whereas reduced metabolites are present in low amounts. Reduced metabolites are mostly seen after i.v/i.p administration in combination with conjugated metabolites.

1.12.4.2 Safety and tolerability of curcumin

Safety and tolerability of curcumin has been investigated in several studies. The US-FDA classifies curcumin as a 'generally regarded as safe' compound [240]. In rats, an intravenous dose of 5 g/kg and oral dose of 1.8g/kg for 90 days did not show any toxicity [211, 241]. In humans 8g oral dose for 3 months was found to be acceptable and well tolerated [201]. In another study doses ranging from 0.4-3.6 g for 4 months showed mild side effects like diarrhoea and nausea in some patients [242]. A healthy volunteer study with a single oral dose of 12 g was also found to be safe with grade 1 diarrhoea as the only toxicity observed in 1 out of 34 patient [147].

1.12.4.3 Development of curcumin formulations for clinical use

The overall properties of curcumin make it an excellent candidate for further investigation as an agent prevention and treatment of lung cancer. However, its low bioavailability brings into question its potential for application in clinical settings, and has necessitated development of a formulation of curcumin with enhanced bioavailability. Bioavailability of a drug can be enhanced by increasing the absorption, protecting it from extensive metabolism and by increasing its water solubility. Several formulations have been developed on the basis of these approaches. One successful approach was via co-administration of curcumin with piperine, which is a known hepatic and intestinal metabolic inhibitor. Its co-administration with curcumin increased serum levels of curcumin by 20 fold in humans [234]. Long term consumption of piperine however, can lead to clinical complications such as reduced metabolic clearance and adverse drug interactions [243]. Other alternatives include nanoparticle and liposome phospholipid formulation. Development of curcumin nanoparticle formulations (10-200 nm particle size) has received unprecedented attention and has also shown to increase curcumin bioavailability by 4 to 30 fold in rodents by increasing its solubility and absorption [244-246]. Polylactic-co-glycolic acid (PLGA) and PLGA-polyethylene glycol (PEG) (PLGA-PEG) blended nanoparticles containing curcumin increased the bioavailability 50 fold when orally administered in rats [247]. Single oral doses of nanoformulations may furnish

higher levels of curcumin temporarily; however, the health effects of long term administration of nanoparticles are as yet, unknown.

Liposomes are one of the most successful drug delivery platforms and have played a significant role in improving therapeutic delivery of a number of drugs [248]. Liposomes consist of closed bilayer phospholipid with a hydrophilic head and a hydrophobic tail, mostly phosphatidylcholine, bearing compartments for encapsulating any target drugs irrespective of its solubility. The lipids in the human cell membrane are also chiefly phospholipids such as phosphatidylcholine giving liposomes excellent biocompatibility. Liposome protect the target drug from direct degradation/metabolism and also increase its absorption. Liposomal formulation of curcumin, Lipocurc, has been successful in increasing the bioavailability of curcumin. An intravenous infusion of liposomal curcumin in Beagle dogs resulted in 6-9 fold higher plasma levels of THC as compared to native curcumin [249].

However, Phytosome[®], a patented technology developed by Indena (Milan, Italy), fundamentally based on liposome principle has more advantages to offer. The basic difference between them is that liposomes entrap the drugs either in the aqueous core of the phospholipid bilayer or at the bilayer interface and no chemical bonds are formed (Figure 1.14). This gives limited possibility of molecular interaction between the surrounding lipids. In phytosome, drug is an integral part of the lipid bilayer and is stabilised through with hydrogen bonds with polar head of the phospholipids. Furthermore, in liposomes the content of phospholipids is much higher, about five times more than phytosome, making phytosomes more preferable for oral clinical dosages [250].

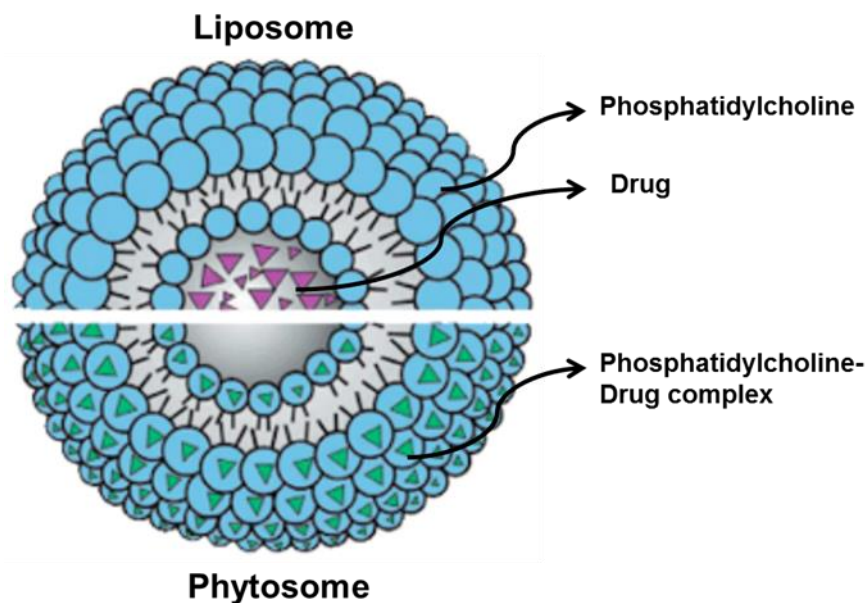


Figure 1.14 Difference between a phytosome and a liposome.

Figure taken from <http://www.phytosome.info/phyto-vs-lipo.html>

1.12.4.4 Meriva®- A phytosome formulation of curcumin

Phytosomal preparations may offer preferential drug delivery over that of liposomal platforms. This is primarily due to the higher phospholipid content of phytosomes, and the way in which the drug is mobilised throughout the phytosomal complex, rather than being present just in the aqueous core as observed in liposomes. Meriva, developed by Indena, is a formulation of curcumin prepared by mixing curcumin with a de-oiled powdered soybean lecithin enriched with 30% phosphatidylcholine in a 1:2 weight ratio. Two parts of microcrystalline cellulose are then added to improve formulation characteristics. The phosphatidylcholine and microcrystalline cellulose portion together is called Epikuron 130P. The overall ratio of curcumin to Epikuron 130P in Meriva is approximately 1:4. The phosphatidylcholine has a highly polarized head, with the negative charge of a phosphate group and the positive charge of the choline ammonium group. The polar groups present on curcumin and phosphatidylcholine form a complex with each other via hydrogen bonding and dipole interactions. As a result, the water-labile β -diketone moiety of curcumin is shielded from hydrolytic degradation and increases its stability in the intestinal pH range of 7-8. Apart from hydrolytic degradation, the lipophilic character of the curcumin–phosphatidylcholine complex also facilitates the rapid exchange of

curcumin across biological membranes in the gastro-intestinal tract via formation of a phospholipid monolayer on the mucosal surface [251]. This supports the transition of curcumin across lipophilic membranes into cells resulting in improved absorption.

Preclinical studies showed greater than a 20-fold increase in absorption of curcumin from Meriva as compared to unformulated curcumin [215]. Similar results were observed in clinical study involving health human volunteers where the overall curcuminoid absorption was about 29-fold higher for Meriva as compared to the unformulated curcumin [252]. It can be hypothesized that Meriva may furnish target tissues with superior level of curcuminoids and may prove more advantageous for therapeutic interventional studies for targets distant to the gastrointestinal tract, including lung.

1.12.5 Preclinical models of lung cancer

Preclinical studies are essential for the development and testing of conventional and novel therapeutic agents. The preclinical models commonly employed include cell lines, xenograft mouse models and transgenic mouse models. Use of preclinical models mimicking TME, such as 3D or organotypic co-culture models are also on the rise due to the advantages they offer over conventional cell line models. The preclinical models used within this thesis are discussed briefly below.

1.12.5.1 Cell lines

Cell lines form the mainstay of preclinical research with over 8,000 citations for lung cancer models [253]. As per the Sanger Institute database, there are 179 lung cancer cell lines available for preclinical research. (http://cancer.sanger.ac.uk/cell_lines/browse/tissue#sn=lung&ss=all&hn=&sh=&in=t&src=tissue&all_data=n). Cell lines have played a crucial role in elucidating the molecular and translational biology of lung cancer. They are useful in *in vitro* research as they retain oncogenic driver mutations, are an inexpensive tool for early drug screening and testing of targeted therapies and easy to maintain. One of the disadvantages of using cell lines is that they are grown as two-dimensional cultures and do not reflect the complex TME seen in human disease. Considering their importance in reflecting genetic make-up of disease, there is a need to develop models that could bridge the *in vitro-in vivo* gap. Three-dimensional (3D) models have been developed in an effort to minimise this gap.

1.12.5.2 3D/Organotypic co-culture models

3D models aim to better mimic the characteristics of a solid tumour *in vitro*, than conventional 2D models. As previously discussed, the tumour itself provides a complex environment comprising a host of cellular and non-cellular components, cell-cell interaction and cell-matrix interactions. It is important to accommodate these factors in preclinical models used for drug testing. In conventional 2D models, cells are grown as a monolayer on plastic plates in uniform nutrient and oxygen rich conditions. These conditions do little to reflect the hypoxic, heterogeneous conditions observed within a tumour. 3D models attempt to reproduce these tumour conditions as closely as possible. A widely used strategy

is to implant cells from standard 2D culture within a 3D matrix scaffold. Matrix scaffolds are typically made up of natural materials including collagen, laminin and hyaluronic acid which form the main components of ECM [254]. Amongst the natural scaffold material, collagen type 1 is commonly used because of its abundance, ubiquity, and biocompatibility. Matrices for 3D growth often use a mixture of collagen, Matrigel and growth factors to further approximate the ECM. Matrigel matrix is a reconstituted basement membrane preparation that is extracted from the Engelbreth-Holm-Swarm (EHS) mouse sarcoma, a tumour rich in ECM proteins. It contains a mixture of 60% laminin, 30% collagen IV, and 8% entactin and the remaining portion consists of heparin sulfate proteoglycan (perlecan), TGF- β , EGF, IGF, FGF, tissue plasminogen activator, and other growth factors which occur naturally in the EHS tumour. There are also residual MMPs derived from the tumour cells [255, 256]. Stromal cells such as fibroblasts can be incorporated into the artificial matrix (gels) to further mimic the TME as closely as possible. The porous nature of the gels allows cells to invade through the gel matrix by degrading the gel matrix. While the 3D culture systems hold great promise for applications in drug discovery and cancer cell biology there are still many shortcomings that need to be overcome. 3D models still lack vasculature which plays a vital role in tumor growth/survival and drug delivery. Variability in biologically derived matrices often cause non-reproducible experimental results. They are also much more expensive and laborious for large-scale studies and high throughput assays than traditional 2D culture [257].

1.12.5.3 Xenograft Mouse model

Xenograft models require subcutaneous injection of human cancer cells into an immunocompromised mouse such as athymic nude or severe-compromised immunodeficient (SCID) mice. The lack of a competent immune system in these mice provides a permissive environment allowing human-derived cancer cells to grow into a tumour. Commonly used cells for lung xenograft include A549, H1975, H1299, H226, HCC4006, HCC827 representing a variety of *K-Ras*, *EGFR*, and *p53* mutations [258]. Xenograft models are the mostly widely used models to examine tumour response to therapy *in vivo* prior to translation into clinical trials. The disadvantage of these models is the lack of a functional immune system and the site of propagation (subcutaneous) which does not

represent the human counterpart of disease. Orthotopic injections can be used to overcome the limitation of propagation of site, but they are technically more challenging, expensive and have post-surgery mortality of 5% and a 10% chance of tumour engraftment failure [258].

1.12.5.4 Transgenic mouse models

Transgenic mouse models are genetically modified animals created by the insertion (*knock-in*) or deletion (*knockout*) of a DNA sequence/fragment that results in functional gain or loss of endogenous genes. These models play an important role in understanding the role a particular gene in lung tumourigenesis. Some of the widely used transgenic models of lung cancer are listed in Table 1.9.

Table 1.9 Conditional transgenic mouse model.

Model Design	Transgene	Promoter	Cancer type	Ref
Tumour Suppressors	Rb, p53	Knock-in	SCLC	[259]
	p53	Knock-in	ADC	[259]
K-ras	LSL-K-rasG12D	Knock-in	ADC, EH	[260]
	K-ras4b G12D rTA	Tet-O CCSP	ADC	[261]
	K-ras V12	β -actin	ADC	[259]
Growth factor	FGF-3	UASG	Alveolar 2 CH	[262]
	GLp65	SP-C		

Table adapted from Liu and Johnston, 2006 [263].

Abbreviations: ADC, adenocarcinoma; CH, cell hyperplasia; EH, epithelial hyperplasia; LSL, lox-stop-lox rrTA, reverse tetracycline transactivator; UASG, upstream activating sequence

Hypothesis

Curcumin, a constituent of spice turmeric, has demonstrated anti-cancer properties in several *in vitro* and *in vivo* studies against different forms of cancer including that of lungs (Chapter 1.12). Preclinical and clinical studies have shown that curcumin is rapidly and extensively metabolised irrespective of the route of administration (Chapter 1.12.4). Attempts are being made to develop curcumin formulations that can enhance its bioavailability. We hypothesise that if curcumin, either in formulated or unformulated form reaches the lung, it can potentially be developed as an agent for prevention of lung cancer. A validated and sensitive analytical method for simultaneous detection of curcumin and metabolites could be used for accurate quantification for levels achieved in lungs and plasma. If curcumin or its formulation reaches lungs, *in vitro* 3D models mimicking tumour like condition can be utilised to study mechanism of action of curcumin against lung cancer. The *in vitro* findings can be used to assess *in vivo* efficacy of curcumin or its formulation at a clinically relevant dosage regimen.

Aims and Objectives

The overall aim of this project is to perform preclinical evaluation of Meriva, a phospholipid formulation of curcumin, and standard curcumin, generating pharmacokinetic and pharmacodynamic data, which might assist in the decision making as to whether curcumin can potentially be developed as an agent for chemoprevention of lung cancer. The *in vitro* and *in vivo* models used for the work described in this thesis are in context of tertiary prevention.

The specific research objectives to test our hypothesis and achieve the overall aim were:

- 1) HPLC methods until now were validated using curcumin only and their efficiency in analysing curcumin metabolites was not known. Hence, the first aim was to develop and validate a robust analytical method that can simultaneously and accurately quantify concentrations of curcumin, curcumin glucuronide and curcumin sulfate (*Chapter 3*).

- 2) To compare the levels of curcumin and curcumin metabolites achieved in mouse plasma and lungs following oral administration of Meriva or unformulated curcumin (*Chapter 3*).
- 3) To explore potential mechanisms of action of curcumin in a tertiary chemoprevention setting (*Chapter 4*).
- 4) To investigate the *in vivo* efficacy of a dietary intake of Meriva, on tumour development and survival in a xenograft mouse model of lung cancer (*Chapter 5*).

2 Materials and Methods

2.1 Materials

2.1.1 Chemicals and Reagents

Unless otherwise stated, all chemicals and solvents for general laboratory consumption were purchased from Fisher Scientific (Loughborough, UK) and Sigma (Poole, UK). For cell culture, the growth medium, trypsin and fetal calf serum (FCS) were obtained from Life Technologies (Paisley, UK) and tissue culture plastic-ware was from Appleton Woods (Birmingham, UK). Buffers used in Sodium Dodecyl Sulphate Polyacrylamide Gel Electrophoresis (SDS-PAGE), 10X TRIS/Glycine SDS Running Buffer, 10X TRIS/Glycine Transfer Buffer, ProtoGel (30%) 37.5:1 Acrylamide to Bisacrylamide Stabilised Solution, 4X ProtoGel Resolving Buffer and ProtoGel Stacking Buffer, were all purchased from Geneflow (Lichfield, UK). Antibodies were obtained from Santa Cruz (Heidelberg, Germany) or Cell Signaling (Hertfordshire, UK) as indicated in Table 2.1. Columns for HPLC and Mass Spectrometry (MS) were obtained from Waters (Hertfordshire, UK) and Thermo Scientific (Loughborough, UK) respectively. Curcumin and Meriva used for *in vitro* and *in vivo* studies were a kind gift from Indena S.p.A., Milan, Italy.

2.1.2 Polyacrylamide gel composition

Table 2.1 Composition of the polyacrylamide gels used in Western blotting.

Gel Components	5 % Stacking	8 % Resolving	10 % Resolving	12 % Resolving
Water (mL)	5.7	9.5	8.1	6.8
4X ProtoGel Resolving Buffer (mL)	-	5	5	5
ProtoGel Stacking Buffer (mL)	2.5	-	-	-
ProtoGel 30 % Acrylamide (mL)	1.7	5.3	6.7	8
10 % APS (mL)	0.100	0.200	0.200	0.200
TEMED (mL)	0.015	0.015	0.015	0.015

The above volumes were sufficient for 2 gels. The stacking gel was poured onto the set resolving gel in the gel cassettes and 10 or 15 well combs inserted in the stacking gel before setting. APS – ammonium persulfate, TEMED - N,N,N',N' - Tetramethylethylenediamine

2.1.3 Buffers

Table 2.2 Buffers and their constituent ingredients

Buffer	Composition
Blocking Buffer	5 % milk (Marvel dried skimmed milk, Spalding, UK) dissolved in 1X PBST (see below)
Citrate Buffer	10 mM citric acid monohydrate in dH ₂ O and pH adjusted to 6.0 with 2 M sodium hydroxide (NaOH) solution
Complete Cell Lysis Buffer	1 complete mini protease inhibitor cocktail tablet and 1 PhosStop phosphatase inhibitor cocktail tablet dissolved in 10 mL of complete lysis – M reagent (Roche Diagnostics Sussex, UK).
Phosphate Buffered Saline (PBS)	1X working solution contained 10 PBS tablets (Oxoid, Hampshire, UK) dissolved in 1000 mL dH ₂ O
PBS-Tween-20 (PBST)	1X working solution contained 10 PBS tablets dissolved in 1000 mL dH ₂ O with 1 mL Tween-20
Running Buffer	1X working solution contained 25 mM Tris, 192 mM glycine and 0.1 % w/v sodium dodecyl sulphate (SDS)
Sample Buffer, Laemmli 2X concentrate	Contained 4 % SDS, 20 % glycerol, 10 % 2 – mercaptoethanol, 0.004 % bromophenol blue and 0.125 M Tris HCl, pH adjusted to 6.8
Transfer Buffer	1X working solution contained 25 mM Tris, 192 mM glycine and 20 % v/v methanol (Fisher Scientific, Loughborough, UK)

Table 2.3 Antibodies for western blot

Antibody		Supplier	Host	Dilution
Actin (1-19)		Santa Cruz	Goat	1:1000
Akt		Cell Signaling	Rabbit	1:1000
Bax		Cell Signaling	Mouse	1:1000
Bcl2		Cell Signaling	Mouse	1:1000
Cleaved caspase 3		Cell Signaling	Rabbit	1:100
cMet		Cell Signaling	Rabbit	1:1000
COX2		Cell Signaling	Rabbit	1:1000
Cytokeratin MNF116		Cell Signaling	Rabbit	1:50
Ki-67		Santa Cruz	Goat	1:1000
LC3		Cell Signaling	Rabbit	1:1000
MAPK		Cell Signaling	Rabbit	1:1000
p21		Cell Signaling	Rabbit	1:1000
p27		Cell Signaling	Rabbit	1:1000
p53		Cell Signaling	Rabbit	1:1000
pAkt		Cell Signaling	Rabbit	1:1000
pMAPK		Cell Signaling	Rabbit	1:1000
pMet1003		Cell Signaling	Rabbit	1:1000
pMet1234		Cell Signaling	Rabbit	1:1000
pMet1349		Abcam	Rabbit	1:1000
Secondary Antibodies	Anti-goat IgG-HRP	Santa Cruz	Goat	1:20000
	Anti-mouse IgG-HRP	Santa Cruz	Donkey	1:10000
	Anti-rabbit IgG-HRP	Santa Cruz	Goat	1:5000

2.2 Methods

2.2.1 Synthesis of curcumin metabolites

Curcumin metabolites were synthesized in Department of Chemistry, University of Leicester under the supervision of Dr. Rob Britton.

2.2.1.1 Curcumin monosulfate

Curcumin monosulfate was synthesized as per the method described by Irving et al [238]. Briefly, 1 g (2.72 mmol) of curcumin was dissolved in 25 mL solvent containing pyridine:dimethylformaldehyde (DMF) in the ratio of 1:3. Then 830 mg (1.83 mmol) of sulphur trioxide - DMF complex was added to the solution which was reacted for 4 h at 37°C on a sand bath with constant stirring. The resulting reaction mixture was allowed to cool and 580 mg (5.47 mmol) of sodium bicarbonate was added and thin layer chromatography (TLC) was performed for crude separation of new compounds supported by MS/MS. The reaction mixture was filtered and dried *in vacuo*. The crude reaction mixture was purified by flash column chromatography using silica (silica 60) and ethanol/ dichloromethane (1:9→3:7) as mobile phase. The fractions collected were pooled together in a round bottomed flask and evaporated to dryness.

For TLC, normal-phase silica aluminium backed plates (Merck) were used. Detection was achieved by using an ultraviolet (UV) light at a wavelength of 254 nm and visualisation of separation was by dipping the plates in vanillin solution. The mobile phase for TLC separation was ethanol/ dichloromethane in the ratio of 3:7.

2.2.1.1.1 Characterisation of curcumin monosulfate

The identity of the synthesized compound was confirmed by high performance liquid chromatography LC-MS/MS and proton nuclear magnetic resonance (¹H-NMR). In HPLC-UV, a single peak of curcumin sulfate was detected with a retention time of 19.3 minutes. No other peaks were detected. Chromatography conditions are described in section 2.2.2.4. Single reaction monitoring (SRM) of the *m/z* 447 > 217 confirmed the identity of curcumin monosulfate. Chemical shifts obtained from ¹HNMR analysis correlated with the structure of the compound.

2.2.1.2 Curcumin monoglucoronide

Curcumin glucuronide was synthesized as per the method described by Pal et al [221]. It was a multistep synthesis process and identity of the product at each step was confirmed by MS and ¹HNMR analysis.

Step 1: β-D-Glucopyranosiduronic acid 4-formy-2- methoxyphenyl methyl ester, triacetate (Product A)

Vanillin (0.434 g, 2.85 mmol) and acetobromo-α-d-glucuronic acid methyl ester (2 g, 5.03 mmol) were dissolved in distilled quinolone at 0°C. Silver oxide (0.695 g, 2.99 mmol) was added in portions, allowing it to react after addition of each portion. The mixture was stirred in the dark at 0°C for 30 min and then for another 90 min at room temperature. Acetic acid (36 mL) was added and stirred for 5 min. The mixture was then passed through a celite pad and washed with ethyl acetate. Ethyl acetate fractions were evaporated to dryness and separated by flash column chromatography using silica and hexane/ethyl acetate (7:3→2:8) as mobile phase, to give product A.

Step 2: 5-Hydroxy-1-(4-hydroxy-3-methoxyphenyl)-1,4- hexadien-3-one (Product B)

2,4-Pentanedione (3.3 mL, 32.07 mmol) and boric anhydride (2 g, 28.7 mmol) were dissolved in ethyl acetate (30 mL), and the solution was stirred at 80°C for 30 min. To this mixture an ethyl acetate solution (40 mL) of the vanillin 4 (2.2 g, 14.4 mmol) and tributyl borate (1.6 mL, 5.96 mmol) was added. After stirring for 30 min at 85°C, n-butylamine (0.5 mL, 5.04 mmol) was added which was allowed to stir at 105°C for 1.5 hours. Then the reaction mixture was treated with 1 N HCl (10 mL) at 50°C and stirred at the same temperature for 1 hour. Reaction mixture was cooled and then extracted with ethyl acetate, washed with water and dried over Na₂SO₄. Flash chromatography over silica using hexane/ethyl acetate (2:1) as mobile phase was followed by recrystallization from ethanol and water, and gave product B.

Step 3: Curcumin β -D-glucopyranosiduronic acid 2,3,4-tri-O-acetyl methyl ester (Product C)

Product B (0.725 g, 3.1 mmol) and boric anhydride (0.3 g, 4.65 mmol) were dissolved in ethyl acetate (8 mL) at 50°C and stirred for 1.5 hours at 70°C. To this, product A (870 mg, 1.86 mmol) and tributyl borate (1.25 mL, 4.65 mmol) was added. After stirring for 1 hour, the mixture was treated with n-butylamine (306 μ L, 3.10 mmol) and allowed to react for 20 min. The temperature was increased to 85°C and the the mixture was allowed to react for 45 min and then overnight at room temperature. Following day 11 mL of 0.5 N HCl was added and allowed to react at 50°C for 30 min. The reaction mixture was cooled, washed with brine, extracted with ethyl acetate, and then dried over magnesium sulfate. The product was separated via flash chromatography using hexane/ethyl acetate (2:1 \rightarrow 1:1 \rightarrow 1:2) and gave product C.

Step 4: Curcumin monoglucoronide

To a cooled solution of Product C (160 mg, 0.24 mmol) in methanol (4.48 mL), 1 N NaOH solution was added drop-wise (4.48 mL, 4.4 moles). The resulting solution was then stirred for 3 h at 0°C and the pH of the solution was adjusted to 3–4 by adding 50% aqueous formic acid. The resulting yellow solid was filtered under vacuum and dried overnight in a desiccator under vacuum to give curcumin monoglucoronide.

2.2.1.2.1 Characterisation of curcumin monoglucoronide

The identity of the synthesized compound was confirmed by HPLC-UV, LC-MS/MS and $^1\text{H-NMR}$. In HPLC-UV, a single peak of curcumin monoglucoronide was detected with a retention time of 15.8 min. No other peaks were detected. SRM of the m/z 543 > 217 confirmed the identity of curcumin monoglucoronide. Chemical shifts obtained from $^1\text{HNMR}$ analysis correlated with the structure of the compound.

2.2.2 Comparative pharmacokinetic study of curcumin and Meriva in mice - High dose study

2.2.2.1 Dosing and plasma/lung tissue collection

Experiments were carried out under animal project license 60/4370 granted to University of Leicester by UK home office. The experimental design was vetted by the Leicester University Local Ethical Committee for Animal Experimentation and met the standards required by the United Kingdom Coordinating Committee for Cancer Research (UKCCCR) for animal welfare. C57 BL/6J male mice 6 weeks of age were obtained from Charles River Laboratories, UK and kept at 20-30°C temperature, 40%-60% humidity under a 12 hour light/dark cycle on standard 5LF2 pellet diet.

Dosing suspensions were prepared in 1% methylcellulose. Animals were fasted overnight and received unformulated curcumin or Meriva at 240 mg/kg in terms of curcumin equivalents. Animals were anaesthetised by isoflurane and at 0.08, 0.25, 0.5, 0.75, 1, 1.5, 3, 6 and 24 hours, blood samples were collected by cardiac puncture and immediately placed on ice. Animals were then sacrificed by cervical dislocation and lung tissues were collected, snap frozen in liquid nitrogen and then stored at -80°C until analysis. Blood samples were centrifuged at 17,000 x *g* for 10 min, and supernatant plasma was stored at -80°C until analysis. Group size was three mice per time point.

2.2.2.2 Extraction method for determining curcumin and curcumin metabolites in mice plasma and lungs

A pre-validated and published method from the group was used for determining levels of curcumin and metabolites in mouse plasma and lung following a single oral dose [215]. Briefly, to a 100 µL aliquot of plasma, 200 µL of 2% acetic acid and 700 µL of PBS was added. Samples were loaded on Strata-X polymeric reverse phase columns (Phenomenex, UK), washed with 1 mL of 25:25:1 methanol: water: glacial acetic and eluted with 1 mL methanol containing 2% glacial acetic acid under vacuum. Eluant was evaporated to dryness at 45°C in a SPD1010 SpeedVac System (Thermo Scientific, UK) and re-suspended in 100 µL 50:50 ammonium acetate (10 mM, pH 4.5):acetonitrile. Re-suspended samples were centrifuged, the supernatant transferred to HPLC vials and 50 µL

injected onto the HPLC column for analysis. Standard solutions of curcumin (0.1-10 µg/mL) were prepared in 100 µL of blank plasma to obtain a standard curve. The extraction efficiency of curcumin was 58%. The quantitation of curcumin and metabolites was based on the curcumin standard curve.

For curcumin extraction from lung tissues, 200 µL of lung homogenate (homogenised in PBS in the ratio of 1:2) was mixed with 400 µL of 9:1 acetone:formic acid, the mixture vortexed and incubated at -20°C for 30 min. The samples were then centrifuged at 17,000 x g for 20 min at 4°C. The supernatant was transferred to fresh eppendorf tubes and evaporated to dryness at 45°C in a SpeedVac system and the residue re-suspended in 100 µL 50:50 ammonium acetate:acetonitrile. The samples were vortexed vigorously, centrifuged for 3 min and the supernatant transferred into HPLC vials whereupon an aliquot of 50 µL of each sample was injected onto the HPLC column for analysis. Standard solutions of curcumin (0.1-10 µg/mL) were prepared in 100 µL of lung homogenate obtained from the control animal group and extracted as described above to obtain a standard curve. The extraction efficiency of curcumin was 73%. The quantitation of curcumin and metabolites was based on the curcumin standard curve.

2.2.2.3 Conversion of curcumin metabolites to parent curcuminoids

To assess the overall curcuminoid levels, plasma and lung samples were enzymatically treated to convert curcumin metabolites into parent curcumin. The enzyme solution containing mixture of two enzymes β-glucuronidase and sulfatase was dissolved in 0.1M phosphate buffer (pH 6.8) in such a way that 100 µL of final solution contained 1800 units of β-glucuronidase and 160 units of sulfatase. To 100 µL aliquots of plasma or lung homogenate, 100 µL of β-glucuronidase/sulfatase solution was added. The samples were vortexed vigorously and incubated at 37°C for 3.5 h. After incubation the samples were extracted as described above.

2.2.2.4 Chromatography conditions

The HPLC system consisted of a Waters Alliance 2695 system with a built-in quaternary pump, degasser and autosampler, coupled with a Waters 2487 Dual λ UV/VIS absorbance detector. The detection wavelength for curcumin and

metabolites was 426 nm. Curcumin was separated on an Atlantis[®] dC18 reverse phase-HPLC column (4.6x150 mm, particle size 3 µm) using gradient elution and an Atlantis[®] dC18 guard column (4.6x20 mm, particle size 3 µm) maintained at 25°C. Mobile phase A consisted of 10 mM ammonium acetate (pH 4.5) and mobile phase B consisted of acetonitrile. Initial conditions were 90% mobile phase A at 0 min progressing to 60% at 15 min, 15% at 25 min, 0% at 30 min, to 90% at 30.10 min, which was continued until the end of the run (40 min). The flow rate was 1 mL/min, autosampler temperature was 4°C and the injection volume was 50 µL. Data acquisition was undertaken using Empower software (Version 2.0).

2.2.3 Modification of extraction method to improve efficiency

The existing method was validated using curcumin standards only and was less efficient in extraction when applied to curcumin metabolites (extraction efficiency 48% for curcumin glucuronide and 20% for curcumin sulfate). Hence, the method was partly modified to improve the extraction efficiency for metabolites. The existing liquid phase extraction method used for tissue extraction was applied to plasma samples and both the sample types underwent extraction procedure twice. Briefly, to 100 µL of plasma or lung homogenate spiked with curcumin (0.075-7.5 µg/mL), curcumin sulfate and curcumin glucuronide (0.1-10 µg/mL), 200 µL of 9:1 acetone:formic acid was added. The mixture was vortexed for 10 seconds and then kept at -20°C for 30 min. The mixture was then centrifuged at 17, 000 x g for 20 min at 4°C. The supernatant was transferred to a new eppendorf and the precipitate underwent the extraction procedure again. The supernatant from both the extractions was pooled and evaporated to dryness using a SPD100 SpeedVac system. The dried residue was re-suspended in 100 µL of 50:50 ammonium acetate:acetonitrile, vortexed for 10 seconds, centrifuged 17000 x g for 3 min, supernatant transferred to HPLC vials and 50 µL was injected onto the column. The chromatography conditions remained same as described in section 2.2.2.4.

2.2.3.1 Validation of new extraction method

It was necessary to establish that the new extraction method was reliable and produced consistent results while allowing analysis of a large number of

samples. Hence, a full method validation was performed as per parameters set by the Food and Drug Administration (FDA), USA guidelines to ensure the reliability and reproducibility of the method. These parameters include accuracy, precision, linearity, extraction efficiency, sensitivity, specificity and stability. The parameters were tested using chromatography conditions described in section 2.2.2.4 and the results of method validation are described in results chapter section 3.3.

2.2.4 Comparative pharmacokinetic study of curcumin and Meriva in mice using new validated method – Low (clinically relevant) dose study

The human effective dose (HED) of curcumin in the pharmacokinetic study described in section 2.2.2 was 1.35 g for a 70 kg adult. (calculated on the basis of body surface area [264]). The new validated method was applied to investigate the pharmacokinetics of curcumin and Meriva in mice at a low clinically relevant HED of 400 mg in terms of curcumin. Based on body surface area, the equivalent dose for mice was 70 mg/kg. Dosing and plasma/tissue collection was performed as per procedure described in section 2.2.2.1, the only difference being in the time-points of sample collection which were 0.25, 0.5, 1, 1.5 and 3 hours post dosing. The samples were extracted as per the procedure described in section 2.2.3 and were analysed using chromatography conditions described in section 2.2.2.4.

2.2.5 Healthy volunteer turmeric food pharmacokinetic study

This study was undertaken to investigate the pharmacokinetics of curcumin when taken in the form of food containing turmeric. The food used for the study consisted of sandwich, sweet (flapjack) and soup. All food was prepared by the University of Leicester Catering Department and each portion contained 1 gram of turmeric.

2.2.5.1 Study Design

Three male and one female volunteer (aged 26-35 years) were recruited into the study following approval from the University of Leicester local ethics committee (reference lh28-3072). Two male and one female volunteers were White British and one male volunteer was Asian (Indian). All volunteers were without any

relevant medical conditions (including allergies or food intolerance) and were not on any medication. All volunteers gave written informed consent for the study. The volunteers were asked to refrain from all turmeric containing food or drinks for the 24 hours preceding and during the study, and were required to fast for 12 hours prior to study commencement. After the first blood draw at 0 hours, each volunteer consumed three portions of turmeric-containing food consisting of soup, sandwich and a sweet. The subsequent blood draws were at 0.5, 1, 2, 4, 8 and 24 hours post food consumption. Blood samples were collected in heparinised tubes and centrifuged at 3300 x g for 10 min at 4°C. Plasma was separated and aliquoted into 1 mL volumes then stored at -80°C until further use. All blood samples were processed within 30 min from the time of collection. The study consent from volunteers was obtained by Dr. Lynne Howells and blood samples were collected by Dr. Sameena Khan.

2.2.5.2 Plasma and food analysis

Plasma and food samples were extracted and analysed as per method described in section 2.2.2.4 and 2.2.3. Bread and flapjack were powdered using mortar and pestle and soup was freeze dried prior to extraction. Pre-weighed quantities were then extracted.

2.2.6 Cell Culture

A549 cells derived from 58-year-old Caucasian male human lung adenocarcinoma tissue and MRC5 fibroblasts derived from normal lung tissue of a 14-week-old male foetus were used for *in vitro* studies. A549 were cultured in Roswell Park Memorial Institute (RPMI) 1640 and MRC5 were cultured in Dulbecco's Modified Eagle's medium (DMEM) 6429 and both contained L-glutamine, supplemented with 10 % foetal calf serum (FCS). A549 were sourced from American Type Culture Collection (ATCC) and MRC5 were a kind gift from Cancer Science Division, University of Southampton. Both cell lines tested negative for mycoplasma.

2.2.6.1 Resuscitating cells from liquid nitrogen

Frozen stocks of cells stored in liquid nitrogen were flash thawed at 37°C prior to resuspension in 9 mL of fresh media, and subsequently centrifuged at 350 x g for 3 min at room temperature. The supernatant was discarded and the cells re-

suspended in 12 mL of media, transferred to a 75 cm³ flask and allowed to grow to 70-80% confluency before passaging.

2.2.6.2 Maintenance and passaging of cells

A549 and MRC5 cell lines were maintained under incubation condition of 100% humidity, 5% CO₂ at 37°C. Cells were passaged on reaching 70-80% confluency and were not used beyond passage 30 to reduce the possibility of genetic and/or phenotypic alterations. For passaging of cells, media was aspirated and cells were washed twice with 5 mL PBS followed by addition of 3 mL trypsin/EDTA (Invitrogen, Paisley, UK) to detach the cells. The trypsinised cells were incubated for not more than 5 min at 37°C. Once detached, 7 mL media was added to neutralise the trypsin. The cell suspension was centrifuged at 350 x *g* for 3 min at room temperature and re-suspended in 10 mL of fresh media. Cells were counted using a Z2 Coulter Particle Count and Size Analyser (Beckman Coulter, High Wycombe, UK) and seeded as per required density. The approximate doubling times of the cells were 24 hours for A549 and 40 hours for MRC5.

2.2.6.3 Cell treatment

The stock solution of curcumin was prepared at a concentration of 20 mM in dimethyl sulfoxide (DMSO) and stored at -20 °C. The stock solution was stored in 100 µL aliquots and discarded after single use. The final concentration of DMSO in the treatment medium was always less than 0.1% v/v and vehicle control for each experiments contained DMSO in a v/v concentration identical to treatment groups. Post treatment cells were washed twice with PBS and harvested by scrapping with lysis buffer on ice.

2.2.6.4 Cell proliferation assay

Cell proliferation was assessed by cell counting as per method described in Hill et al. [265]. The cells were seeded at a density of 1 x 10³ cells/well in 1 mL of growth medium, onto 24-well plates, in 4 wells to a give quadrupole count per concentration. The cells were allowed to adhere overnight prior to treatment with 1, 2.5, 5 or 10 µM curcumin or DMSO (control) in a final volume of 2 mL. Following 72, 96, 120 and 144 hours incubation at 37 °C, the growth medium was removed from the wells and the cells washed twice with 1 mL PBS. Trypsin/EDTA (0.5 mL) was added to each well and the plates incubated at 37

°C for 5 min to detach the cells. Once the cells were detached, the trypsin/EDTA was neutralised by adding 0.5 mL of growth medium. The cell suspension from each well was added to a coulter counter cup with 9 mL isoton and cells were counted. Cell numbers were calculated as percentage of the DMSO control and plotted against curcumin concentration. A linear line equation was used to calculate the log concentration at 50% of cell number. The antilog concentration was subsequently calculated to give the 50% inhibitory concentration (IC50) value. Each cell proliferation assay was performed independently in triplicate on separate days with different passages.

2.2.6.5 Organotypic co-culture Assay

The organotypic co-culture assay was used to study effects of tumour cell-fibroblast interactions on cell invasion and investigate effect of curcumin on this. The protocol for organotypic assay was provided by Cancer Sciences Unit, Faculty of Medicine, University of Southampton and further optimised as per experimental conditions. Spatulas, forceps, nylon membranes (2.5 x 2.5 cm size, made from nylon sheets supplied by Tetko Inc., New York, USA), stainless steel metal grids (made from A4 metal sheets supplied by The Mesh Company, Warrington, UK) were autoclaved before use. The stainless steel wire mesh was cut into 3 x 2.5 cm squares and folded 0.5cm on the longer side to make the metal grid. A 10X DMEM media was prepared by dissolving 1.35 g of DMEM powder and 0.37 g sodium bicarbonate in 10 mL water and sterile filtering it through a 20 micron syringe top filter. A keratinocyte growth media (KGM), rich in growth factors, was prepared as follows: A 10 g vial of α -minimum essential medium (MEM) powder and 2.2 g of sodium bicarbonate was dissolved in 1 litre of water. The solution was sterile filtered through 0.2 μ M Nalgene Rapid-Flow filters (Thermo Scientific, UK) into 2 bottles of 440 mL each. To each of the 440 mL α -MEM bottle, following sterile filtered solutions mention in table below were added.

FCS	50 mL
EGF	500 μ L (10 μ g/mL)
Insulin	250 μ L (10 mg/mL)
Hydrocortisone	2 mL (100 μ g/mL)
Adenine	5 mL (6.6 mg/mL)
Glutamax™	5 mL

EGF and hydrocortisone solutions were prepared in α -MEM solution. Insulin and adenine solutions were prepared in water. The experiment required 3 days to set up and the day-wise procedure was as follows:

Day 1, Preparation of gels: MRC5 fibroblast suspension was prepared containing 250 000 cells/100 μ L. In a 15 mL Falcon tube on ice, the following volumes were added and mixed to typically obtain 3 gels.

Rat Tail Collagen	1050 μ L
Matrigel	1050 μ L
10X DMEM	300 μ L
FCS	300 μ L
MRC5 Suspension	300 μ L

The solution was mixed on ice until it formed a homogenously coloured solution. One mL of gel mixture was added to each well of 24-well plate and the plates incubated for 1 hour at 37°C. Volumes were adjusted accordingly, depending on the number of gels to be prepared. After an hour of incubation the gel solidified, and 1 mL of 10% DMEM was added to the top of the gel and incubated overnight at 37°C.

Day 2, Adding A549/MRC5 cells and preparing nylon membranes: A cell suspension containing a mixture of A549 and MRC5 cells in varying proportion was prepared to give a final concentration of 750 000 cells/mL. Media on gels

prepared the day before was aspirated and replaced with the cell suspension, and incubated overnight allowing cell attachment to the gel.

The prior to use, nylon membranes were coated with matrigel/collagen to give them a smooth texture and prevent damage to the gel when placed on the metal grid. The coating solution was prepared in a 15 mL Falcon tube on ice and contained:

Rat Tail Collagen	1050 μ L
Matrigel	150 μ L
FCS	150 μ L
10% DMEM	150 μ L

The solution was mixed on ice until it formed a homogenously coloured solution. The pH was adjusted using 0.1 M NaOH until the colour of the solution become orange indicating neutral pH. Nylon membrane were placed in a 10 cm petri plate, 250 μ L of gel solution added to each nylon membrane, and the membranes incubated for 30 min at 37°C. Once the gel mixture solidified, 10 mL of sterile 1% glutaraldehyde solution prepared in PBS was added to each plate to fix the gel mixture to the nylon membrane. The plates were wrapped in parafilm and kept in kept at 4°C for one hour prior to washing thrice with PBS and once with 10% DMEM. After washing, 10% DMEM was added to the plate, which was then stored at 4°C overnight.

Day 3, Sterile stainless steel grids were placed in wells of a 6-well plate, and a collagen coated nylon membrane s placed onto each metal grid, collagen side up. Gels were then carefully lifted from the 24-well plates and transferred using a sterile spatula, onto the nylon sheets. KGM media treated/untreated with curcumin was then carefully added to each 6 well plate in sufficient volume to reach the under-surface of the nylon sheet without spilling onto it. Media was changed every 2 days and after 12 days, gels were fixed in formalin and embedded in paraffin blocks.

To determine optimum ratio of tumour cells and fibroblasts, A549:MRC5 cells were seeded in different ratios of 5:1, 2:1, 1:1, 1:2 and 1:5. For analysis, 10 μ m

organotypic sections were mounted on polysine slides and stained with haematoxylin and eosin.

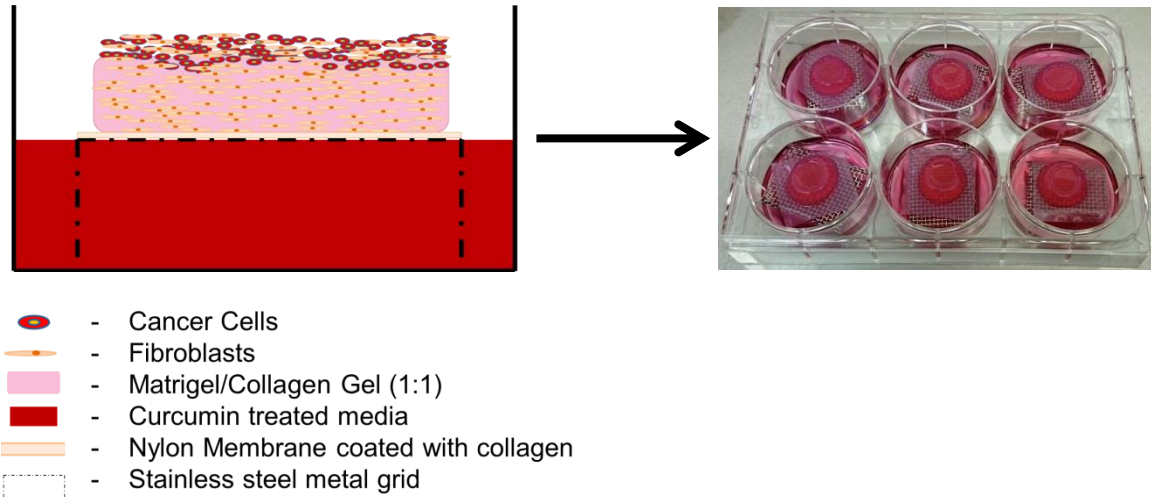


Figure 2.1 Organotypic co-culture set-up

2.2.6.5.1 Quantification of invasion

A semi-quantitative method was used to quantify invasion of cancer cells. The H&E stained slides were scanned using a NanoZoomer-XR digital slide scanner (Hamamatsu Photonics, Japan) and a series of images taken across the whole section at 20X magnification using imaging software NDPView (Version 2.0). The images were then quantified using imaging software ImageJ (Version 1.49) by using the following formula:

$$\text{Percentage Invasion} = \frac{\text{Total Invaded Area}}{\text{Total Area}} * 100$$

The invaded and non-invaded areas were added up to give percentage invasion across the whole section.

2.2.6.5.2 Immunohistochemical staining with MNF-16 cytokeratin

Formalin-fixed gels were stained for MNF16 cytokeratin using the MNF16 cytokeratin polyclonal antibody from Dako (Ely, UK). The paraffin-embedded sections (10 μm) mounted on polysine-coated slides were de-waxed by incubating at 65 $^{\circ}\text{C}$ for 20 min. The sections were hydrated by first immersing the slides in xylene (Genta Medical, York, UK) for 3 min (2X), followed by immersion

in a graded series of industrial methylated spirit (IMS) (Genta Medical, York, UK) rinses (99 % - 2X for 3 min and 95 % - 2X for 3 min). The slides were then washed in running tap water for 5 min. The antigen was unmasked by microwaving the slides on high power in 10 mM citrate buffer (pH 6.0) for 20 min. The Novocastra™ Novolink™ Polymer Detection System (Leica Biosystems, Newcastle Upon Tyne, UK) was used for visualisation. The endogenous peroxidase activity was inactivated by adding 100 µL of peroxidase block directly on the sections for 10 min. The slides were washed in PBS (2X for 5 min) before adding 100 µL of the protein block for 10 min to block nonspecific binding. Slides were washed in PBS as before and the sections incubated with the MNF-16 cytokeratin antibody (diluted 1:50 in 3 % w/v bovine serum albumin and 1 % v/v Triton X - 100 in PBS) for 2 hours at room temperature. . The negative control was mouse immunoglobulin fraction (normal) (Dako, Ely, UK). After washing the sections in PBS (2X for 5 min), 100 µL of post primary block was added for 5 min, followed by PBS washing (2X for 5 min) and addition of 100 µL of the Novolink™ Polymer for 30 min.. Whilst undertaking further PBS washes, 3,3'-diaminobenzidine (DAB) was prepared by adding 5 µL DAB chromogen to 100 µL Novolink™ DAB substrate buffer. DAB working solution (100 µL) was added to the sections for 5 min to react with the peroxidase and produce a brown stain. Following a 5 min wash with running tap water the sections were counterstained with Mayer's Haematoxylin for 1 min and washed again for another 5 min in running tap water. The sections were finally dehydrated back through the graded IMS and xylene. Coverslips were added to the slides using DPX (distyrene, plasticizer, xylene) mountant. The slides were scanned using the NanoZoomer-XR digital slide scanner slide scanner and images were taken at 20X zoom.

2.2.6.6 Treatment and preparation of whole cell lysates

A549 and MRC5 cells were seeded at a density of 2×10^6 in a 10 cm petri plate and allowed to adhere for 24 hours. The cells were treated with 5 µM curcumin and harvested at 1, 2, 4, 8, 16 and 24 hours post treatment. The 5 µM dose was selected on the basis of the results from cell proliferation assay. The control plates received DMSO only. The plates were kept on ice and cells washed twice in 5 mL PBS prior to addition of 200 µL of lysis buffer and harvesting by scraping. The cell suspension was kept on ice for 30 minutes to assist lysis and then

centrifuged at 17 000 x g at 4 °C for 20 min. The supernatant containing the proteins from the cell lysis was collected as the whole cell lysate. The protein concentration of the lysate was determined using the Bicinchoninic acid (BCA) protein assay as described in section 2.2.6.9.

2.2.6.7 HGF stimulation of MET pathway

A549 cells were seeded at a density of 2×10^6 in a 10 cm petri plate and allowed to adhere for 24 hours. The media for serum control plates was replaced with fresh 10% FCS media and rest of the plates were serum starved for 24 hours. After 24 hours, cells were treated with serum free media containing HGF (50 ng/mL) and cells were harvested at 15 min, 30 min, 1, 2 and 4 hour as described in section 2.2.6.3

2.2.6.8 Generation of MRC5 fibroblast conditioned media and assessing effect on MET pathway

MRC5 fibroblasts were seeded in a 175 cm³ flask and on reaching 70-80% confluency, the cells were washed twice with PBS. Serum free media was added and the cells incubated for 24 hours. The conditioned media generated was added to serum starved A549 cells and cells were harvested at 0.5, 1, 2 and 4 hour.

2.2.6.9 BCA Protein Assay

The Pierce BCA protein assay kit (Thermo Scientific, Loughborough, UK) was used to determine the concentration of proteins in lysates as per manufactures instructions. Serial dilutions of BSA ranging from 0 to 1 mg/mL were used to prepare a standard curve. Lysates of unknown concentration were serially diluted with distilled water (for example, 1:10, 1:50, 1:100) to ensure that the absorbance of the lysates was within the linear range of the BSA standard curve. Ten µL of distilled water, BSA standard solutions and serially diluted lysates was added to separate wells on a 96 well microplate in triplicate. Two hundred µL of the BCA working solution, prepared by mixing 50 parts of BCA Reagent A with 1 part of BCA Reagent B, was added to each well and mixed thoroughly. The microplate was covered and incubated at 37 °C for 30 min. Subsequently, the microplate was cooled to room temperature before reading the absorbance at 595 nm on a Fluostar Optima plate reader (BMG Labtech Ltd, Aylesbury, UK). The standard

curve generated was used to determine the protein concentration of the unknown lysates.

2.2.6.10 SDS-PAGE and Western Blotting

After determining protein concentration using the BCA assay, whole cell lysates were mixed with an equivalent volume of 2X Laemmli sample buffer and equivalent volumes across all samples were made up with distilled water to give a 1 $\mu\text{g}/\mu\text{L}$ of protein. Samples were boiled at 100 °C for 5 min and briefly centrifuged before loading 20 μL /well on to a polyacrylamide gel. The percentage resolving buffer used in the gel was dependent on the molecular weight of the protein of interest. A pageruler prestained protein ladder (Thermo Scientific, Loughborough, UK) was added to the first and last wells in each gel to indicate the relative sizes of the separated proteins in the cell lysate.

The Bio-Rad mini gel electrophoresis system (Hertfordshire, UK) was used for SDS-PAGE. All gels were placed in to running buffer and electrophoresis performed at 120 V until the dye front was approximately 5-10 mm from the end of the gel. The gels were then removed from the plates and allowed to equilibrate in transfer buffer for 10 min before being assembled in the transfer cassette. The separated proteins were transferred for 90 min onto a nitrocellulose membrane of pore size 0.2 μM (GE Healthcare, Buckinghamshire, UK) at 100 V.

Upon completion of the transfer, the nitrocellulose membrane was placed in blocking buffer for 2 hours on a rocking platform at room temperature. The membrane was then incubated with the primary antibody of interest at the concentrations indicated in Table 2.3. Incubation was carried out overnight in the cold room on a rocking platform. Following the incubation period the nitrocellulose membrane was washed in PBST (1X for 10 min and 2X for 5 min). The corresponding secondary antibody (Table 2.3) was then added to the membrane for 1 h at room temperature on a rocking platform. The secondary antibody was then removed and washed with PBST (1X for 10 min and 1X for 5 min). The last wash was with water for 5 min. Equal volumes of EZ-ECL solution A and EZ-ECL solution B from the EZ-ECL chemiluminescence detection kit for HRP (Biological Industries, Israel) were mixed together and allowed to equilibrate for 5 min. The membrane was subsequently incubated with the EZ-ECL mixture

for 1-2 min at room temperature. Excess ECL was drained, the membrane wrapped in cling film and placed protein side up in a hypercassette. In a dark room the membrane was exposed to ECL hyperfilm (GE Healthcare, Buckinghamshire, UK) for an appropriate time based on signal intensity and then developed using a Curix 60 Agfa-Gevaert (Germany). Membranes were re-probed for actin, a house-keeping protein used as the loading control. For re-probing, the nitrocellulose membrane was first washed in PBST for 10 min on a rocking platform at room temperature, followed by incubation in stripping buffer (ThermoScientific, Loughborough, UK) at room temperature for 10 min on a rocking platform. The stripped membrane was then washed once in PBST for 10 min before repeating the Western blotting procedure as outlined previously. The protein band densities were determined using ImageJ software version 1.49.

2.2.6.11 HGF enzyme-linked immunosorbent assay (ELISA)

Effect of curcumin treatment on HGF levels secreted by MRC5 fibroblasts was determined by using a Human HGF ELISA Kit (Invitrogen, California, USA). MRC5 fibroblasts were seeded at density of 1×10^3 cells/well in 1 mL of growth medium, onto 24-well plates in triplicate well. The cells were allowed to adhere overnight before treatment with 1, 2.5, or 5 μ M curcumin or DMSO control in a final volume of 1 mL media. After 7 days of treatment, media was collected and stored at -20°C until further use. Cells in each well were counted as described in section 2.2.6.4.

The wells of the microtiter strips were pre-coated with monoclonal antibody specific for human HGF. Fifty μ L of incubation buffer and 50 μ L of either HGF standards, control samples or media collected post 7 days of treatment, was added appropriately to each well and incubated for 3 hours at room temperature. After washing the wells with washing buffer (provided in the kit), 100 μ L of biotinylated monoclonal antibody specific to HGF was added and incubated at room temperature for 1 hour. The plates were washed with washing buffer to remove excess antibody and 100 μ L of Streptavidin-Horse Redox Peroxidase enzyme was added and plates were incubated for 30 min. The wells were washed with washing buffer to remove all the unbound enzyme and 100 μ L of chromogen substrate solution was added to each well and incubated for another 30 min in dark. The chromogen solution reacted with bound enzyme to produce

a blue colour, the intensity of which was directly proportional to the concentration of HGF present in the sample. After 30 min, 100 μ L of stop solution was added to each well and the plate was read at 450 nm absorbance using a Fluostar Optima plate reader (BMG Labtech). A standard curve of HGF standard concentration versus optical density was obtained and the concentration of HGF in samples was calculated. The HGF concentration was then normalised with cell number for that particular sample.

2.2.7 Xenograft study and lysate preparation

Male Balb/c nude mice (20-22 g body weight, 6 weeks old) were supplied by Charles River, UK. For housing conditions and licensing refer section 2.2.2.1. Animals were divided into two groups of ten animals each and were identified by ear punching. A total of 4.8×10^6 A549 and MRC5 cells in the ratio of 1:5 were suspended in 100 μ L mixture of matrigel and serum free media (1:1, v:v) and subcutaneously injected into the right dorsal flank of the mice under isoflurane inhalation anaesthesia. Once the tumours become palpable (7 days post injection) animals were switched to study diet. Table 2.4 represents the different groups in the study. There were two additional groups of 5 animals each which received subcutaneous injection of either A549 (8×10^5 cells) or MRC5 (4×10^6 cells) only. Animals were assessed for their health and weight weekly. Tumour volume was measured every 5 days using digital Vernier callipers. Tumour volume was calculated using the formula: *tumour volume* = *length* \times *width*²/2, where length is the largest tumour diameter and width is the smallest tumour diameter. Tumour volume was assessed until day 30 and the animals were then observed for a survival study. Animals were culled only when tumour size reached 17 mm³ in length, or exhibited weight loss of more than 20%. Animals were sacrificed by exsanguination under terminal anaesthesia with blood collection via cardiac puncture. Tumours were harvested and immediately divided into three portions: half the tumour was fixed in 10% w/v formalin to use for immunohistochemical analysis and the other two quarters were snap frozen in liquid nitrogen and stored at -80°C until further use for HPLC and western blot analysis. Lungs were also harvested, snap frozen in liquid nitrogen and stored at -80°C until further use for HPLC. The Meriva dose were equivalent to dose used in the pharmacokinetic study described in section 2.2.4. The dose was calculated

assuming a 20 gram mice ate 3 grams of diet every day. The dose in terms curcumin equivalent was approximately 0.044%.

Table 2.4 Xenograft study group distribution

Group	Number of cells		Number of animals	Study Diet (Irradiated)
	A549	MRC5		
I	8x10 ⁵	4x10 ⁶	10	Epikuron in AIN93G (0.180%)
II	8x10 ⁵	4x10 ⁶	10	Meriva in AIN93G (0.226%)
III	-	4x10 ⁶	5	AIN93G only
IV	8x10 ⁵	-	5	AIN93G only

Tumour tissues for western blot were weighed cut into small pieces, and homogenised in lysis buffer (1:4, w:v) The homogenate was placed on ice for 30 min and centrifuged (20 min, 17 000 x g, 4 °C). Protein concentrations of the tumour lysates were measured by BCA assay as described in section 2.2.6.9. The lysates were stored at -20°C until further use.

2.2.7.1 Preparation of single cell suspension from xenograft tumours

Tumour samples were minced on ice using scalpels and incubated with 200 units/mL of collagenase type 4 in serum free media (Worthington Biochemical, US) for 1 hour at 37°C. After incubation, the cells were centrifuged at 350 x g for 10 minutes. The supernatant was removed and the cells were re-suspended in 20 mL Hanks Balanced Salt Solution (Invitrogen, UK). The suspension was then passed through 70µM filter. After determining the cell number, the cells were centrifuged at 350 x g for 10 minutes and re-suspended in freezing media consisting of 10% DMSO in fetal calf serum (FCS) and frozen in liquid nitrogen until further use.

2.2.7.2 Staining of cells for flow cytometry

Frozen cells were thawed at room temperature and washed once with PBS. The cells were incubated with primary MNF-16 cytokeratin antibody (1:100) prepared in 3% BSA in PBS and incubated in dark for 1 hour at room temperature. The cells were washed once with PBS and then incubated with secondary Alexa Fluor 488 goat anti-mouse antibody (Life Technologies, USA) for 0.5 hours at 4°C. The

cells were washed once with PBS and re-suspended in 500µL PBS. The flow cytometry analysis was undertaken using a BD FACS Aria II with Diva software (Version 6.0). The assays included a negative control, a positive control and test samples.

2.2.7.3 Immunohistochemical staining of tumours for Ki-67 and cleaved caspase-3

Immunohistochemical staining of tumour sections was performed as per procedure described in section 2.2.6.5.2. The antibody dilution for Ki-67 was 1:1000 at room temperature for 2 hours and for cleaved-caspase-3 was 1:100 at room temperature for 2 hours.

2.3 Statistical analysis

Data from all *in vitro* studies are presented as the mean of at least 3 independent experiments \pm standard deviation (SD). Student's T-test in Excel 2013 was used for all *in vitro* data when comparing the treatment group to the control group only. Survival curves generated from the animal survival study were compared by the log-rank test (Prism 6), while the body weights and tumour volumes were compared by a mixed effects linear regression (performed by Dr. Maria Viskaduraki, Bioinformatics and Biostatistics Analysis Support Hub, University of Leicester). Data were considered to be statistically significant if $p \leq 0.05$.

3 Pharmacokinetic and Metabolism study of curcumin and Meriva

3.1 Introduction

Preclinical studies of curcumin, *in vitro* and *in vivo*, suggest a strong rationale for its use as a preventive agent for different forms of cancer including lung. In order to translate a chemopreventive candidate from a preclinical to clinical setting, it is necessary to establish the absorption, biotransformation and distribution profile to ensure that biologically effective concentrations of the active compound(s) can reach the desired target site. Pharmacokinetic studies of curcumin so far reveal that curcumin is poorly absorbed and rapidly metabolised. To overcome this, different approaches including nanoformulations, co-administration with other drugs, and use of synthetic analogues have been attempted, with some of these approaches having shown a dramatic increase in absorption of curcumin and its metabolites. However, a chemopreventive compound is intended for long term consumption and any formulation approach to enhance the absorption should consider potential long term safety implications. The curcumin-phospholipid formulation, Meriva, satisfies many of the aspects that need to be exhibited by chemopreventive agents, in that it is available in an oral and a safe dosing form.

Clinical pharmacokinetic studies of Meriva have shown this formulation to increase plasma levels of curcumin by up to 29-fold when compared to non-formulated curcumin post enzymatic conversion [252]. A previous preclinical pharmacokinetic study of Meriva performed within the group, investigated levels of curcumin and its metabolites achieved in plasma, liver and intestinal mucosa and it showed that Meriva has superior bioavailability to that of unformulated curcumin if tissues other than the gastrointestinal tract are targeted. [215]. To evaluate the usefulness of Meriva as a chemopreventive agent for lung cancer, a comparative pharmacokinetic study in mice was undertaken. The study aimed to determine whether curcumin in either its formulated or unformulated form reached the lung, and whether Meriva offered a higher concentration of curcumin or its metabolites in lung compared to its unformulated form. Initially, a pharmacokinetic study at a high dose of 240 mg/kg in terms of curcumin equivalents was undertaken. The dose was selected on the basis of previous efficacy studies undertaken within the group [232]. A previously partially

validated HPLC-UV method developed within the group was initially used to analyse these samples [215]. However, when this method was developed authentic curcumin metabolite standards were not available enable accurate quantitation of curcumin conjugates, based on metabolite calibration curves. Instead curcumin calibration curves were used to quantify curcumin metabolites despite the extraction efficiency for the metabolites being unknown, which affords only an estimate of the metabolite concentrations. Considering the potential for metabolites to play a role in the chemopreventive properties of curcumin, it was necessary to test the existing sample processing and HPLC method for its ability to recover and quantify these metabolites. In order to accurately quantify the levels of metabolites, pure curcumin monoglucuronide and curcumin monosulfate standards were synthesised in-house. The existing assay method showed poor extraction efficiency for curcumin monoglucuronide and curcumin monosulfate (48% and 20% respectively) in plasma. The method was thus modified to enhance the extraction of the metabolites, and fully validated as per US-FDA guidelines to ensure its reproducibility in analysing large numbers of samples accurately.

A comparative pharmacokinetic study of curcumin and Meriva at a dose of 70 mg/kg in terms of curcumin was undertaken [264]. The dose was selected on the basis of previous human pharmacokinetic studies and other long term clinical studies of Meriva for inflammatory conditions [252, 266-268]. The samples were analysed using the newly validated and more efficient extraction method. The levels of curcumin and metabolites were accurately quantified using calibration curves obtained from the respective standards and this is the first pharmacokinetic study to our knowledge that reports accurately quantified levels of metabolites.

The rationale for using curcumin as a chemopreventive agent comes mostly from epidemiological evidence which suggest an inverse relation between the incidence of certain cancers and turmeric consumption through food [148]. At the time this study was undertaken, there was insufficient knowledge about uptake and metabolism of curcumin when consumed in turmeric-containing food. It is conceivable that when curcumin as a constituent of turmeric is cooked at high temperature, its chemical properties may be altered resulting in changes to its

absorption. When curcumin is heated at high temperature, it has recently been shown to be transformed into a form called 'deketene curcumin' which was found to be more effective in inducing cell cycle arrest in melanoma cells [269]. In view of this, a healthy volunteer study involving consumption of cooked turmeric-containing foodstuffs was performed.

Overall, the results in this chapter are presented in the following sections:

- 1) Mouse pharmacokinetic study-High dose
- 2) Development and full validation of the modified HPLC-UV method
- 3) Mouse pharmacokinetic study-Low (clinically relevant) dose
- 4) Healthy human volunteer turmeric food study

3.2 Curcumin and metabolite concentration in plasma and lung tissue following a single oral dose - High dose pharmacokinetic study.

Male C57BL/6J mice (3 mice per group) received a single oral gavage dose of curcumin or Meriva at a dose of 240 mg/kg body weight in terms of curcumin equivalent. Following oral administration, plasma and lung tissues were collected at 0.08, 0.25, 0.5, 0.75, 1, 1.5, 3, 6 and 24 hour intervals. The method was focussed on identification and quantification of curcumin and its conjugates only. The peaks were identified putatively on the basis of previous work in the group [215]. The concentration of curcumin and metabolites in plasma and lung was calculated from the curcumin calibration curve obtained from respective matrices and mean concentration vs time curves were plotted. The pharmacokinetic parameters studied were area under the concentration–time curve (AUC), maximum concentration achieved (C_{max}), and time to achieve maximum concentration (T_{max}). The AUC was calculated using the trapezoidal method from time 0 to 24 hours. The extraction efficiency for curcumin was 58% in plasma and 73% which is comparable to previously published values [215].

In plasma, following a single oral dose, parent curcumin was not detected in either of the treatment groups at any of the time points. This was in accordance with previous studies that have mostly failed to detect unconjugated curcumin in human plasma even after the administration of high doses of curcumin [147,

252]. However, the metabolites curcumin glucuronide and DMC glucuronide were present in both treatment groups in varying amounts (Figure 3.1). The AUC values for curcumin glucuronide and DMC glucuronide after administration of Meriva were approximately 18.5 and 16.8 fold higher compared to unformulated curcumin group (Figure 3.2). The average C_{max} values for curcumin glucuronide were $0.29 \pm 0.15 \mu\text{M}$ and $6.12 \pm 2.03 \mu\text{M}$ for unformulated curcumin and Meriva group respectively (Table 3.1). Similarly, the average C_{max} values for DMC glucuronide were $0.57 \pm 0.30 \mu\text{M}$ and $12.34 \pm 3.03 \mu\text{M}$ for unformulated curcumin and Meriva treated mice respectively. The concentrations of both the metabolites were significantly higher for Meriva treated group across all time points ($p > 0.05$). The time to achieve maximum concentration, T_{max} , was 1.5 hours and 1 hour for unformulated curcumin and Meriva group respectively. For DMC glucuronide, the T_{max} was 0.25 hours for unformulated curcumin group whereas in the Meriva group maximum concentration was achieved at 1 hour. The concentration of glucuronide metabolites declined rapidly after 3 hours and were completely eliminated after 24 hours. No other metabolites of curcumin were detected in either group using this method.

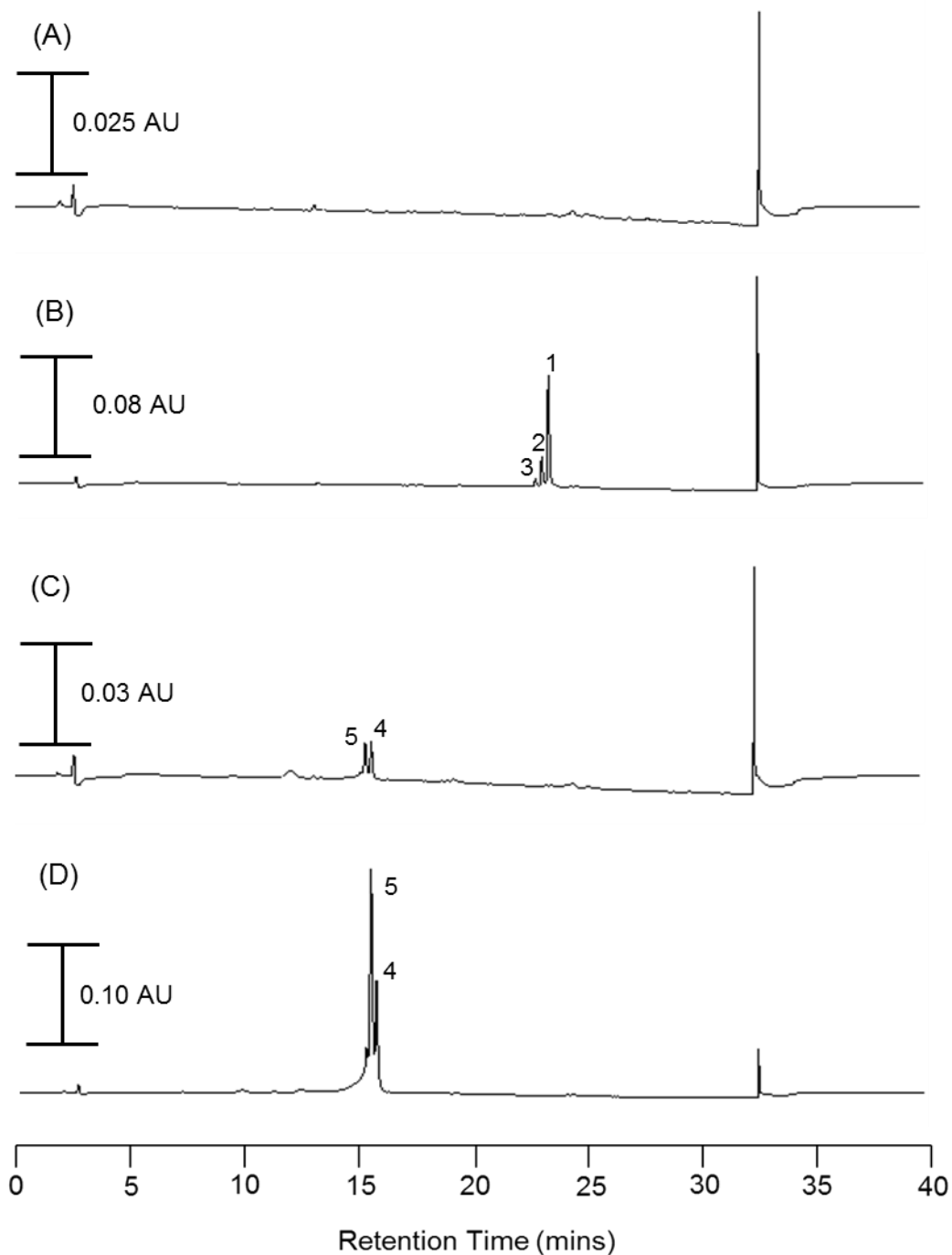


Figure 3.1 Representative HPLC-UV chromatograms of mouse plasma following oral gavage dosing of unformulated curcumin or Meriva.

HPLC-UV chromatograms of plasma taken from mice receiving unformulated curcumin or Meriva at 240 mg/kg by oral gavage obtained 1 hour post dosing. The chromatograms are as follows: (A) Plasma extract from vehicle control mouse (B) Extract from plasma spiked with curcumin standard at 2 $\mu\text{g/mL}$ (C) Plasma extract from mouse receiving unformulated curcumin (D) Plasma extract from mouse receiving Meriva. Peak 1-5 correspond to: (1) curcumin, (2) demethoxycurcumin, (3) bis-demethoxycurcumin, (4) curcumin glucuronide, (5) demethoxycurcumin glucuronide.

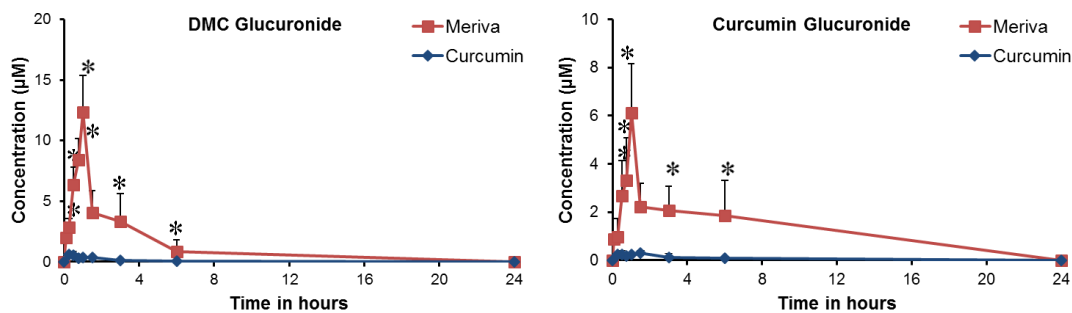


Figure 3.2 Concentrations of curcumin metabolites in mouse plasma following oral dosing with unformulated curcumin or Meriva.

Curcumin metabolite concentration in mouse plasma over 24 hours following Meriva (red line) or unformulated curcumin (blue line) dosing at 240 mg/kg. Values are the mean + SD (n = 3). Statistical comparison between the Meriva and unformulated curcumin at each time point was by student's T-test. Statistically significant differences are indicated as * (p < 0.05).

In lung samples, parent compound curcumin was found to be present in unformulated curcumin group but no major metabolites could be detected at any of the time points. In the Meriva-treated group, free curcumin, curcumin glucuronide and DMC glucuronide could be detected from 15 minutes following dosing up to 6 hours (Figure 3.3 and Figure 3.4). Total exposure to curcumin in the lung tissue was 3.6 times higher for Meriva group than unformulated curcumin group when compared for their AUC values (Figure 3.4 and Table 3.1). The average C_{max} for unformulated curcumin group was $0.09 \pm 0.04 \mu\text{M}$ and $0.36 \pm 0.26 \mu\text{M}$ for Meriva group (concentration values are expressed as micromolar assuming 1 mL equalled 1 gram). For metabolites curcumin glucuronide and DMC glucuronide in Meriva treated group, the average C_{max} values were $0.48 \pm 0.22 \mu\text{M}$ and $0.42 \pm 0.19 \mu\text{M}$ respectively. In Meriva treated mice, after initial rise in the concentrations of curcumin at 0.25 hour, it dipped at 0.5 hour and increased again at 1 hour, to the C_{max} level (Table 3.1). Similar absorption pattern was also observed for curcumin glucuronide where after the initial increase in concentration at 1 hour to the C_{max} level, the concentration dipped at 1.5 hour and again increased at 3 hours. Curcumin and metabolites concentration decreased rapidly after 3 hours and were completely eliminated from the lung after 24 hours.

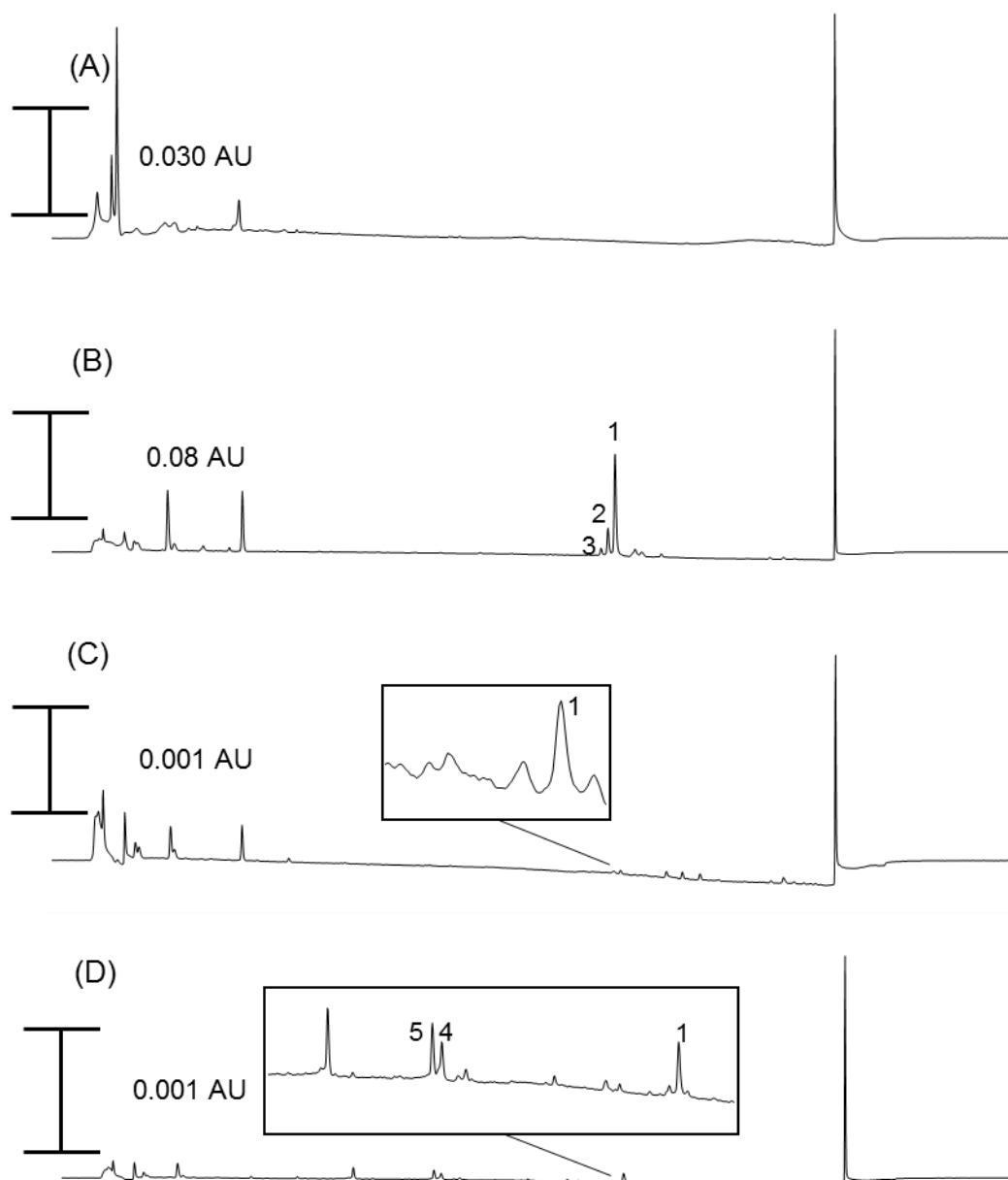


Figure 3.3 Representative HPLC-UV chromatograms of extracts from mouse lung homogenate following oral gavage dosing of unformulated curcumin or Meriva.

HPLC-UV chromatograms of lungs taken from mouse receiving unformulated curcumin or Meriva at 240 mg/kg by oral gavage obtained 1 hour post dosing. The chromatograms are as follows: (A) Lung extract from vehicle control mouse (B) Extract from lung homogenate spiked with curcumin standard at 2 µg/mL (C) Lung homogenate extract from mouse receiving unformulated curcumin (D) Lung homogenate extract from mouse receiving Meriva. Peak 1-5 correspond to: (1) curcumin, (2) demethoxycurcumin (3) *bis*-demethoxycurcumin (4) curcumin glucuronide, (5) demethoxycurcumin glucuronide.

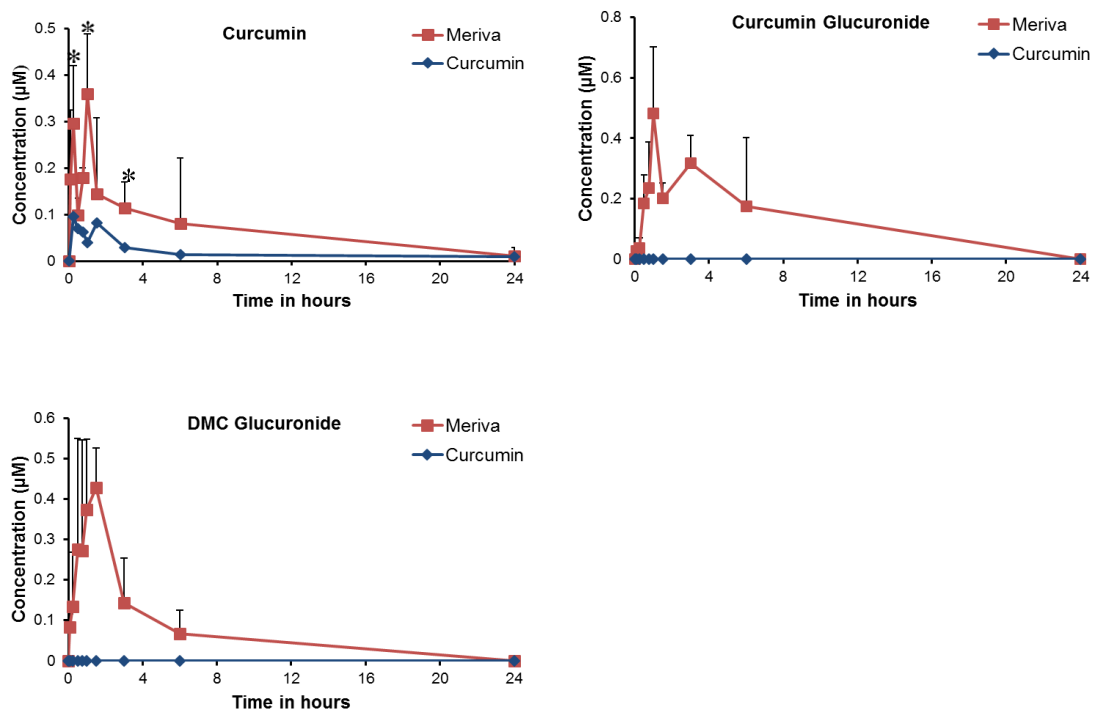


Figure 3.4 Concentrations of curcumin and curcumin metabolites in mouse lungs following oral dosing with unformulated curcumin or Meriva.

Curcumin and curcumin metabolite concentration in mouse lungs over 24 hours following Meriva (red line) or unformulated curcumin (blue line) dosing at 240 mg/kg. Values are mean + SD (n = 3). Statistical comparison between the Meriva and unformulated curcumin at each time point was by student's T-test. Statistically significant differences are indicated as * (p < 0.05).

Table 3.1 Average curcumin and curcumin metabolite concentrations in mouse plasma and lungs following oral dosing at 240 mg/kg dose.

Estimated average plasma peak levels (C_{max}), time of peak levels (T_{max}) and AUC values for unformulated curcumin and Meriva when administered at a dose of 240 mg/kg in terms of curcumin, via oral gavage.

Plasma				
		C_{max} (μM)	T_{max} (hours)	AUC (nmol/h/mL)
Unformulated curcumin	Curcumin	0.29 \pm	1.5	2.19
	glucuronide	0.15 μM		
	Demethoxycurcumin	0.57 \pm	0.25	2.31
	glucuronide	0.30		
Meriva	Curcumin	6.12 \pm	1	40.68
	glucuronide	2.03		
	Demethoxycurcumin	12.34 \pm	1	38.98
	glucuronide	3.03		
Lungs				
Unformulated curcumin	Curcumin	0.09 \pm	0.25	0.459
		0.04 μM		
Meriva	Curcumin	0.36 \pm	1	1.64
	Curcumin	0.48 \pm	1	0.22
	glucuronide	0.22		
	Demethoxycurcumin	0.42 \pm	1.5	1.9
	glucuronide	0.19 μM		

3.2.1 Enzymatic conversion of plasma and lung samples

In order to quantify the overall levels of curcuminoids and to help confirm the identity of observed metabolite peaks, plasma and lung samples were treated with *Helix pomatia* glucuronidase/sulfatase enzyme to convert the metabolites back to their parent curcuminoids.

Following enzymatic conversion of plasma samples, the AUC values of parent curcumin in the plasma were 10 fold higher in the Meriva treated group compared to the unformulated curcumin group. Total systemic exposure to bDMC and DMC were 15.7 and 17.3 fold higher for Meriva compared to unformulated curcumin when comparing the plasma AUC values (Figure 3.5 and Figure 3.6). The average C_{max} increased from $0.20 \pm 0.08 \mu\text{M}$ to $2.04 \pm 0.66 \mu\text{M}$ for bDMC, 1.20 ± 0.40 to $33.02 \pm 12.24 \mu\text{M}$ for DMC and 3.41 ± 1.40 to $38.06 \pm 12.73 \mu\text{M}$ for curcumin for the Meriva group post enzymatic conversion (Table 3.2). The ratio of curcumin, DMC and bDMC in pure unformulated curcumin and Meriva is 1.0/0.25/0.05. In plasma samples this ratio was 1.0/0.29/0.05 for unformulated curcumin and 1.0/0.86/0.05 for the Meriva treated group post enzymatic conversion when compared for their maximum concentration achieved. This shows that demethoxylated forms of curcumin has better intrinsic absorption than parent curcumin when formulated as a phospholipid.

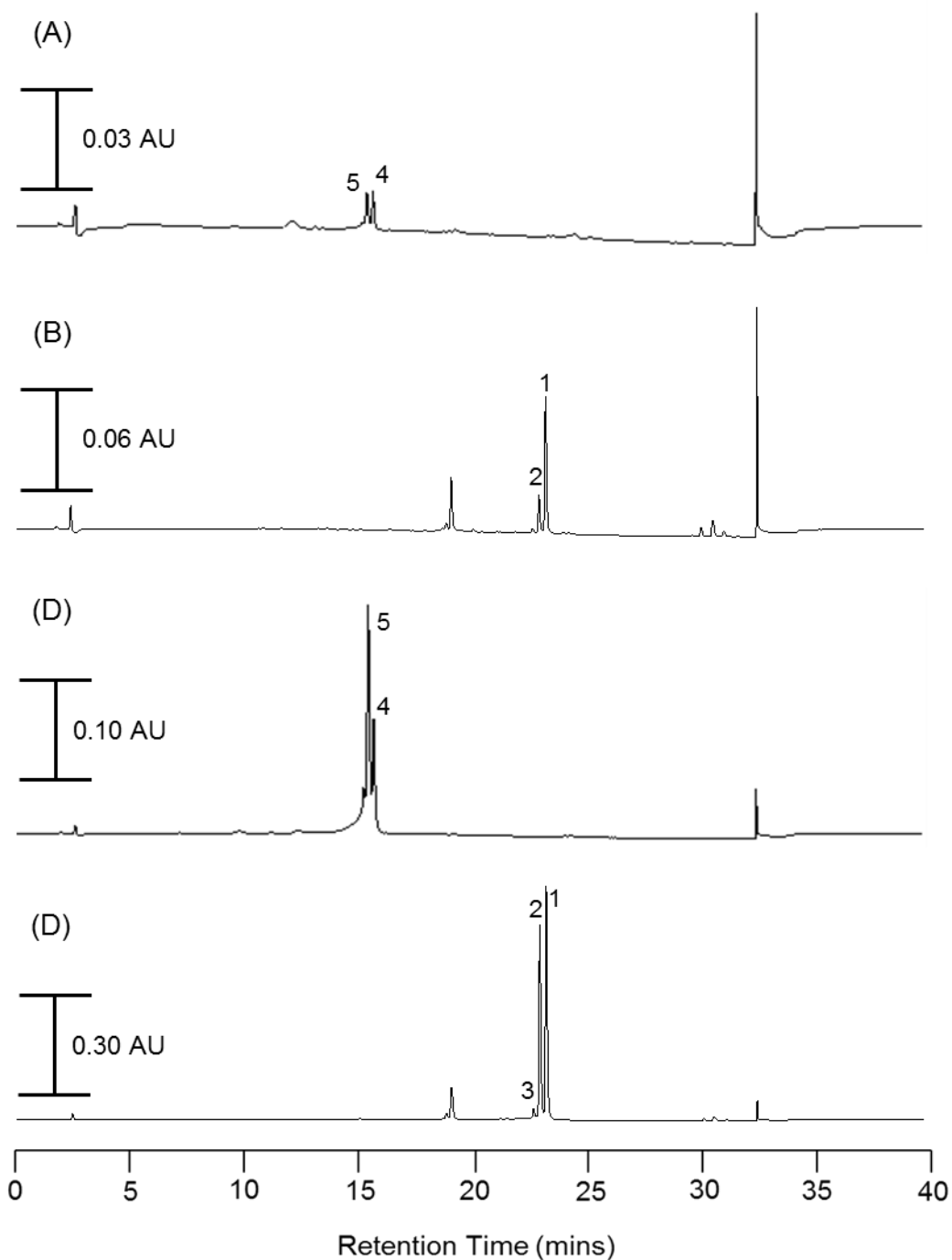


Figure 3.5 Representative HPLC-UV chromatograms of mouse plasma following oral gavage dosing of unformulated curcumin or Meriva and enzymatic conversion.

HPLC-UV chromatograms of plasma taken from mice receiving unformulated curcumin or Meriva at 240 mg/kg by oral gavage obtained 1 hour post dosing. The chromatograms are as follows: (A) Plasma extract from mouse receiving unformulated curcumin (B) Enzymatically converted plasma extract from mouse receiving unformulated curcumin (C) Plasma extract from mouse receiving Meriva. (D) Enzymatically converted plasma extract from mouse receiving Meriva. Peak 1-5 correspond to: (1) curcumin, (2) demethoxycurcumin, (3) *bis*-demethoxycurcumin, (4) curcumin glucuronide, (5) demethoxycurcumin glucuronide.

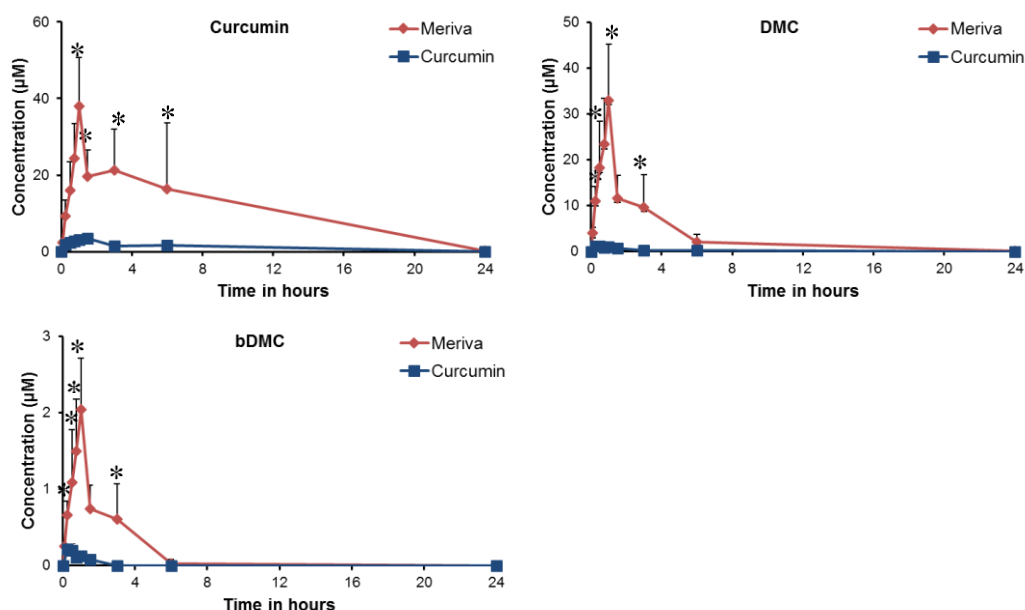


Figure 3.6 Concentrations of curcuminoids in mouse plasma following oral dosing with unformulated curcumin or Meriva and enzymatic conversion.

Curcuminoids concentration in mouse plasma over 24 hours following Meriva (red line) or unformulated curcumin (blue line) dosing at 240 mg/kg and enzymatic conversion. Values are the mean + SD (n = 3). Statistical comparison between the Meriva and unformulated curcumin at each time point was by student's T-test. Statistically significant differences are indicated as * (p < 0.05).

When lung tissues were enzymatically treated, free curcumin was detected in both treatment groups at different time points (Figure 3.7 and Figure 3.8). The AUC value for curcumin was 10.3 fold higher in the Meriva group compared to unformulated curcumin (Table 3.2). DMC and bDMC could be detected in samples from Meriva treated group at different time points (Figure 3.7 and Figure 3.8). DMC was detected only at one time point of 1 hour at 0.04 µM in unformulated curcumin treated mice. No bDMC could be detected across at any time points after enzymatic conversion of lungs in unformulated curcumin treated mice. As seen in plasma, DMC was better absorbed in Meriva treated mice. The ratio of curcumin, DMC and bDMC in lungs was 1/0.77/0.09 post enzymatic conversion when compared for their maximum concentrations achieved.

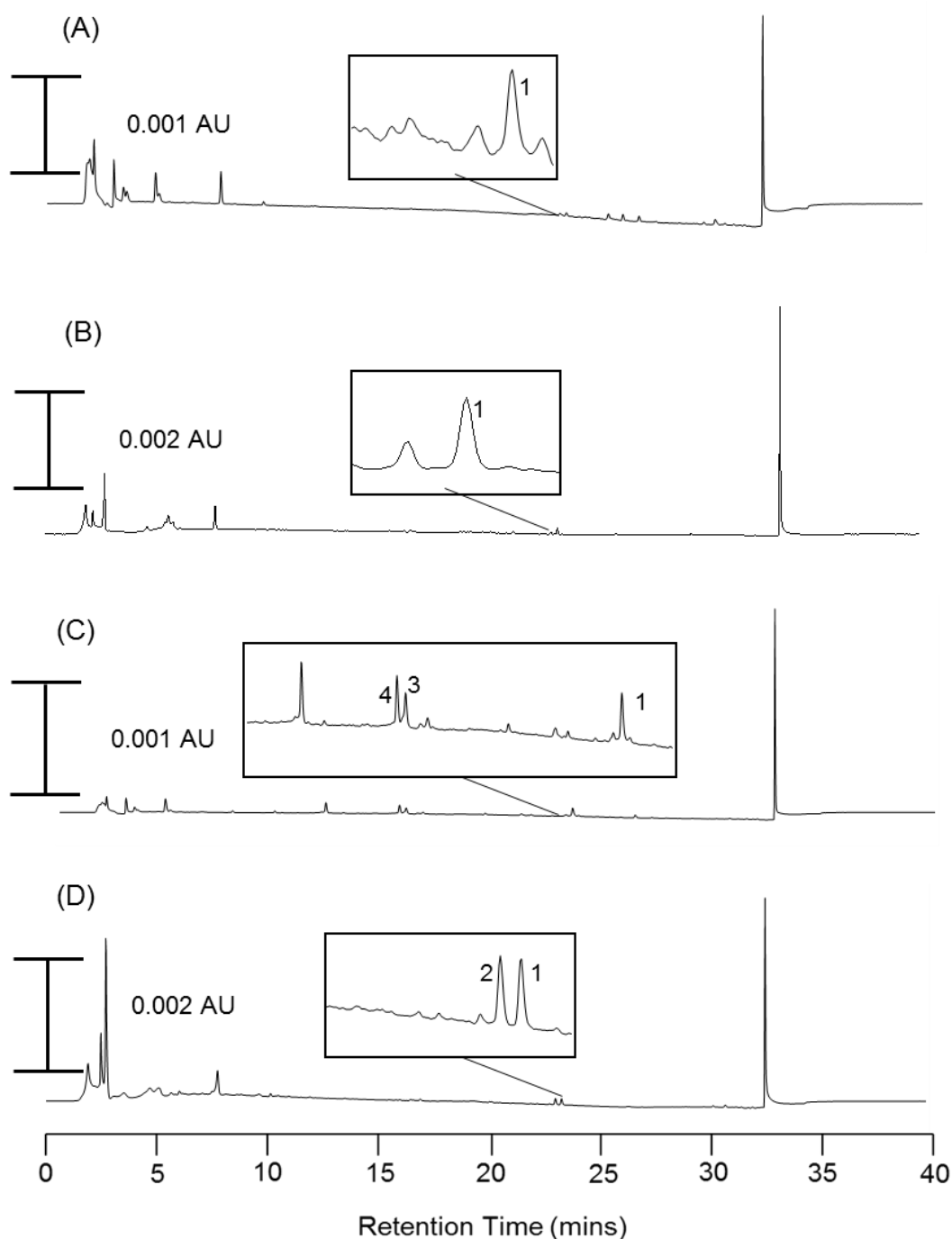


Figure 3.7 Representative HPLC-UV chromatograms of extracts from mouse lung homogenate following oral dosing of unformulated curcumin or Meriva and enzymatic conversion.

HPLC-UV chromatograms of lungs taken from mouse receiving unformulated curcumin or Meriva at 240 mg/kg by oral gavage obtained 1 hour post dosing. The chromatograms are as follows: (A) Lung homogenate extract from mouse receiving unformulated curcumin (B) Enzymatically converted lung homogenate extract from mouse receiving unformulated curcumin (C) Lung homogenate extract from mouse receiving Meriva. (D) Enzymatically converted lung homogenate extract from mouse receiving Meriva. Peak 1-4 correspond to: (1) curcumin, (2) demethoxycurcumin, (3) curcumin glucuronide, (4) demethoxycurcumin glucuronide.

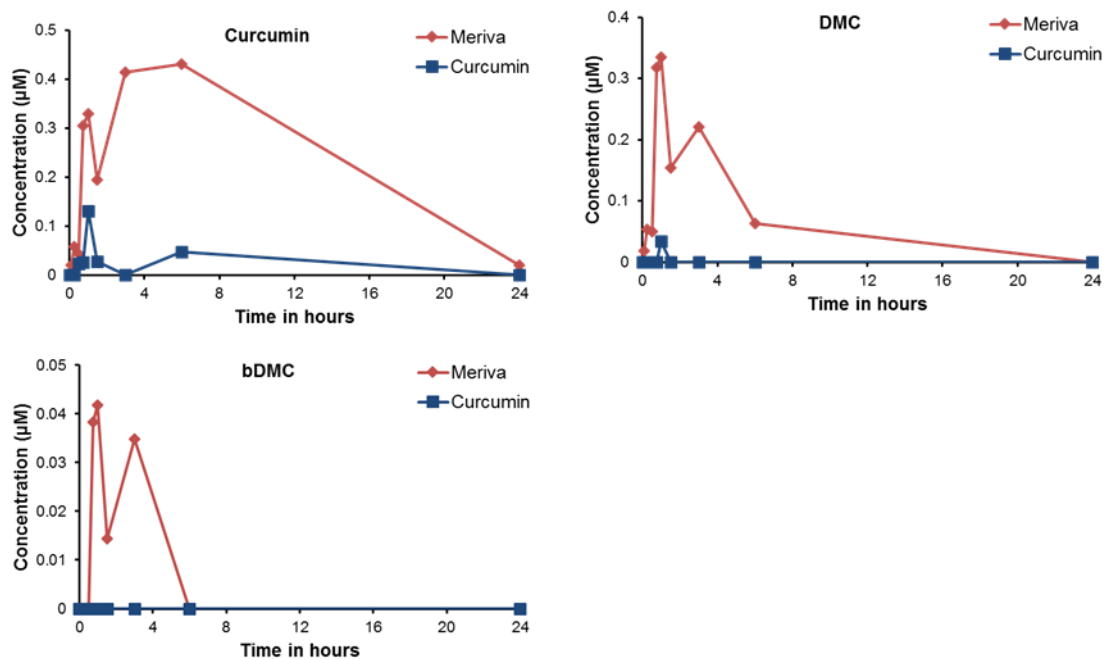


Figure 3.8 Concentrations of curcuminoids in mouse lung homogenate following oral dosing with unformulated curcumin or Meriva and enzymatic conversion.

Curcuminoids concentration in mouse lungs over 24 hours following Meriva (red line) or unformulated curcumin (blue line) dosing at 240 mg/kg and enzymatic conversion. Due to limited sample volume, samples from three mice were pooled together and extracted as single sample.

Table 3.2 Average curcumin and metabolite concentrations in mouse plasma and lungs after 240 mg/kg dose and enzymatic conversion.

Estimated average plasma peak levels (C_{max}), time of peak levels (T_{max}) and AUC values for unformulated curcumin and Meriva when administered at a dose of 240 mg/kg in terms of curcumin via oral gavage.

Plasma				
		C_{max} (μM)	T_{max} (hours)	AUC (nmol/h/mL)
Unformulated curcumin	Curcumin	3.41 \pm 1.40	1.5	26.5
	Demethoxycurcumin	1.20 \pm 0.40	1	4.7
	<i>bis</i> - Demethoxycurcumin	0.20 \pm 0.08	0.25	0.3
Meriva	Curcumin	38.06 \pm 12.73	1	268.6
	Demethoxycurcumin	33.02 \pm 12.24	1	81.3
	<i>bis</i> - Demethoxycurcumin	2.04 \pm 0.66	1	4.0
Lungs				
Unformulated curcumin	Curcumin	0.131	1	0.59
	Demethoxycurcumin	0.045	0.75	0.01
Meriva	Curcumin	0.430	6	6.05
	Demethoxycurcumin	0.334	1	1.54
	<i>bis</i> - Demethoxycurcumin	0.042	1	0.12

Overall, the results suggested that the administration of curcumin in the form of Meriva offers superior bioavailability compared to unformulated curcumin in mouse plasma and the target tissue, lung.

A shortcoming in the pharmacokinetic study described above and previous pharmacokinetic studies is that curcumin calibration curves were used to quantify curcumin metabolites and their extraction efficiencies of metabolites were unknown. The metabolite standards synthesised in-house, showed poor extraction efficiency using current method. Hence, improvements to the previous methodology was required in order to more accurately extract and quantitate curcumin metabolites; these improvements and validation of the resulting assay are described in the following section.

Briefly, the method was modified to include liquid phase extraction for plasma samples and lung homogenates spiked with curcumin, curcumin glucuronide and curcumin sulfate (Refer to Material and Methods section 2.2.3 for detail). To ensure the reproducibility and reliability of the modified HPLC-UV in detecting all of the three analytes, a full method validation was undertaken.

3.3 Full validation of the improved HPLC-UV method for simultaneous detection and quantification of curcumin, curcumin glucuronide and curcumin sulfate

To enhance the extraction efficiency of curcumin metabolites, the existing method was modified to include liquid phase extraction for plasma samples and lung homogenates spiked with curcumin, curcumin glucuronide and curcumin sulfate standards (Refer to Material and Methods section 2.2.3 for detail). The chromatography conditions remained unchanged. To ensure the reproducibility and reliability of the modified HPLC-UV in detecting all of the three analytes, a full method validation was undertaken. The validation was performed in accordance with US-FDA guidelines [270]. A number of parameters have to be met for this validation process; these include accuracy, precision, linearity, recovery, sensitivity and stability. These parameters were measured using sample extraction and the HPLC method outlined in section 2.2.3 and 2.2.2.4 with results described in detail below.

3.3.1 Accuracy and precision

Accuracy of the analytical method describes the closeness of mean test results obtained by the method to the true value of the analyte. Precision describes the closeness of individual measures of an analyte when the procedure is applied repeatedly to multiple aliquots of a single homogenous sample, and is a measure of reproducibility of the whole analytical method. Accuracy and precision were determined by replicate analysis (n=5) of plasma and lung samples spiked with curcumin, curcumin glucuronide and curcumin sulfate at three different concentrations: low, medium and high. Table 3.3 represents the summary of intra-day and inter-day accuracy and precision for plasma and lung samples across three different concentrations. The criterion of mean values within 15% for accuracy and coefficient of variance (CV) not exceeding 15% for precision was successfully met, confirming the reproducibility and repeatability of the method. Accuracy and precision were calculated using the following equations:

$$\text{Accuracy} = \frac{\text{Average concentration of spiked samples}}{\text{Concentration of spiked samples assuming 100\% recovery}} \times 100$$

$$\text{Precision} = \frac{\text{Standard deviation of measured concentration}}{\text{Average of measured concentration}} \times 100$$

3.3.2 Recovery

The recovery of curcumin and curcumin metabolites in plasma and lung was determined by comparing peak area obtained from extracts of spiked samples with that obtained from the direct injection of known amounts of standard solutions. Three different concentrations using three replicate analyses at each concentration was used to determine the recovery. Values for recovery from plasma were in the range of 89%-104% for all three analytes. The ranges for recovery from lung tissue were 98%-106% for curcumin, 53%-60% for curcumin glucuronide and 56%-67% for curcumin sulfate (Table 3.3).

Table 3.3 Recovery, intra-day and inter-day accuracy and precision for determination of curcumin, curcumin glucuronide and curcumin sulfate in mouse plasma and lung

Analyte	Concentration (µg/mL)	Recovery (%)	Inter-day		Intra-day	
			Accuracy (%) ^a	Precision (% CV)	Accuracy (%) ^a	Precision (% CV)
Plasma						
Curcumin	0.1	93.3±6.7	90.1±13.5	14.8	86.3±10.4	11.6
	2	94.8±6.9	84.6±9.2	10.9	89.3±9.3	10.1
	5	88.7±4.6	90.5±9.9	10.9	106.1±3.83	3.6
Curcumin Glucuronide	0.1	90.7±11.0	94.4±8.7	9.2	105.0±8.6	8.2
	2	90.2±4.1	89.7±3.6	4.1	96.6±4.8	5.0
	5	92.2±5.1	100.5±8.7	8.6	108.8±8.0	7.4
Curcumin Sulfate	0.1	104.5±13.2	97.5±6.0	6.23	92.1±6.9	10.3
	2	94.2±9.3	86.5±4.1	4.7	88.4±5.5	6.2
	5	95.0±7.5	95.7±3.6	3.8	90.4±4.4	4.8
Lung						
Curcumin	0.1	105.8±2.75	107.2±12.8	12.0	91.9±4.3	9.1
	2	98.2±3.4	98.5±5.6	5.7	93.2±7.9	7.3
	5	97.6±6.5	93.8±10.3	11.6	98.5±5.7	11.6
Curcumin Glucuronide	0.5	54.2±2.2	112.0±11.1	9.9	113.3±3.9	12.9
	2	53.3±5.1	87.6±10.8	12.3	97.4±9.6	3.9
	5	60.1±3.8	102.8±4.5	4.4	95.7±15.0	3.1
Curcumin Sulfate	0.5	56.4±2.3	105.7±9.1	8.6	112.8±2.4	8.6
	2	62.2±2.0	101.4±15.9	15.6	99.3±3.6	12.3
	5	66.9±7.1	97.7±10.0	10.2	95.34±4.8	10.2

Values are mean ± SD of n=5 determination

3.3.3 Linearity

The linearity of an analytical procedure is its ability to obtain test results which are directly proportional to the concentration of the analyte in the sample. A calibration curve for each analyte was obtained using spiked plasma and lung samples spanning across seven concentrations of analytes (0.1- 10 µg/mL). A calibration curve using the linear regression equation $y=mx+c$ was obtained for each analyte where y = response to concentration, x = concentration of analyte and m = slope of regression line. Calibration curves for all the analytes in both the matrices were linear with an average correlation coefficient (r^2) exceeding 0.998 ($n = 3$). The accuracy values for all the calibration standards were within the acceptable limits of $\pm 15\%$. The relationship between concentrations and responses was continuous and reproducible.

3.3.4 Selectivity and sensitivity

Selectivity is the ability of an analytical method to differentiate and quantify the analyte in the presence of other components in the sample. The selectivity of HPLC analysis was studied by analysing blank plasma and lung samples, which did not show any components interfering with detection of curcuminoids, curcumin glucuronide and curcumin sulfate. Figure 3.9 shows chromatograms of plasma and lung samples, spiked with the analytes in which all the peaks are well separated from each other. The retention times were as follows: 15.7 min for curcumin glucuronide, 19.3 min for curcumin sulfate and 23.4 min for curcumin. The sensitivity of the method was determined by analysing samples at concentrations equal to the lower limit of quantification (LLOQ). The LLOQ of the assay was calculated as the lowest concentration on the standard curve that can be quantitated with accuracy of 80-120% and precision not exceeding 20% CV. The LLOQ for curcumin and metabolites was 0.05 µg/mL in plasma samples and 0.1 µg/mL in lung samples. The values for accuracy and precision at LLOQ are shown in table 3.4. There are other published HPLC-UV methods which have reported five times lower sensitivities and shorter run time however those methods were developed for quantification of curcumin only [233, 235, 271]. Results from previous preclinical and clinical studies reveal that following curcumin administration curcumin metabolites are the major detectable species

in plasma with negligible amounts of parent curcumin. The current method offers an advantage of separation, identification and quantification of all the three curcumin species with good resolution and appreciable LLOQ, making it of particular importance for use in future pharmacokinetic studies, particularly *in vivo* experiments where sample volumes are often low.

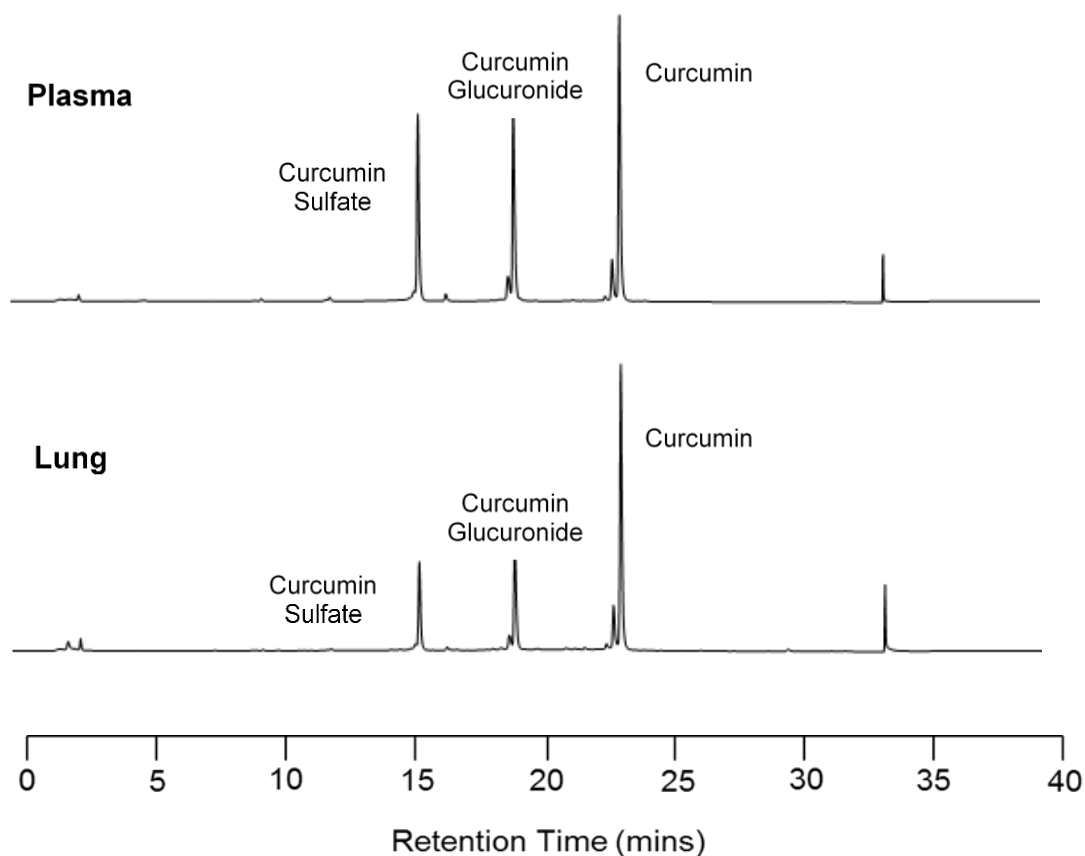


Figure 3.9 Representative HPLC chromatogram of curcumin and metabolites spiked in to plasma and lung homogenate.

Table 3.4 Assay accuracy and precision for the measurement of curcumin, curcumin glucuronide and curcumin sulfate at the lower limit of quantification (LLOQ)

	LLOQ ($\mu\text{g/mL}$)	Plasma ($n=5$)		LLOQ ($\mu\text{g/mL}$)	Lung ($n=5$)	
		Accuracy (%)	Precision (% CV)		Accuracy (%)	Precision (% CV)
Curcumin	0.05	101.4 \pm 4.7	4.5	0.1	101.1 \pm 12.1	12.0
Curcumin Glucuronide	0.05	94.4 \pm 8.7	9.2	0.1	112.8 \pm 14.6	12.9
Curcumin Sulfate	0.05	97.3 \pm 6.0	6.2	0.1	103.6 \pm 13.6	13.2

3.3.5 Stability

Stock solution stability was determined by firstly keeping the stock solution at room temperature for 4 hours and secondly by storing them for 1 month at -20°C. The stock solution was found to be stable under both conditions. Freeze–thaw stability was assessed over three cycles with three different concentrations: 0.2 µg/mL (low), 5 µg/mL (medium) and 10 µg/mL (high) for plasma and: 0.5 µg/mL (low), 5 µg/mL (medium) and 10 µg/mL (high) for lung. Plasma and lung homogenate samples were spiked with curcumin, curcumin glucuronide and curcumin sulfate and stored at -80°C for 24 hours and then thawed unassisted at room temperature. The samples were refrozen at -80°C for 24 hours. This procedure was repeated two more times and the samples were analysed on the first and third cycle. Short term stability was assessed by keeping the standards, diluted in mobile phase, in the autosampler at 4°C for a period of 48 hours and reinjecting them at 0hr, 24hr and 48hr. The curcumin and metabolite content was found to be more than 98% which indicated that the compounds were relatively stable in the autosampler. Long term stability was determined by analysing the samples stored at -80°C after 3 days, 7 days, 14 days and 3 months. Tables 3.5 and 3.6 represent the stability data of curcumin and its metabolites following long term storage and freeze-thaw respectively. The stability studies show that while curcumin and curcumin metabolites are relatively stable in plasma, in lung homogenate curcumin sulfate degrade and possibly convert back to parent curcumin when subjected to multiple freeze thaw cycles. For example, at 0.5 µg/mL concentration in lung the glucuronide and sulfates decrease to 82 and 53% respectively after three freeze thaw cycles, whilst the amount of curcumin in the sample increases to 150%.

Table 3.5 Long term stability of curcumin, curcumin glucuronide and curcumin sulfate in mouse plasma and lung homogenate.

Plasma	Analyte	Concentration (µg/mL)	Content measured as compared to day 0 (%)			
			Day 3	Day 7	Day 14	3 month
Plasma	Curcumin	0.2	96.0±0.9	99.7±13.6	91.2±7.8	91.5±7.0
		5	96.5±7.1	103.2±0.76	105.6±1.7	89.9±8.7
		10	108.6±14.3	96.2±4.4	89.2±1.9	94.2±10.5
	Curcumin Glucuronide	0.2	107.0±12.1	109.8±6.0	102.3±5.0	105.2±8.67
		5	103.5±10.7	102.7±7.4	100.7±4.6	98.1±2.1
		10	97.2±3.5	97.2±1.0	84.7±8.8	96.5±4.7
	Curcumin Sulfate	0.2	101.2±4.0	104.8±9.3	98.5±4.1	77.3±5.6
		5	98.3±13.6	92.2±12.0	96.7±15.6	88.9±13.5
		10	101.3±10.6	85.3±11.1	81.2±6.8	94.2±6.8
Lung	Curcumin	0.5	98.2±5.4	103.5±11.2	93.2±8.3	93.5±1.1
		5	102.2±6.9	89.5±15.3	88.3± 5.6	93.4±9.5
		10	100.3±3.4	87.6±14.9	89.2±7.4	97.3±7.9
	Curcumin Glucuronide	0.5	97.23±4.6	82.8±7.9	86.0±12.0	82.9±5.0
		5	99.5±10.0	87.8±16.01	89.1±0.4	100.7±9.7
		10	92.0±7.66	84.2±3.5	83.9±1.0	96.1±14.6
	Curcumin Sulfate	0.5	62.7±6.2	61.53±10.1	75.2±2.0	75.2±6.3
		5	50.3±4.8	66.3±11.0	67.7±4.1	76.9±6.8
		10	66.5±6.2	62.1±8.8	67.7±6.8	71.4±5.5

Values are mean ± SD of n=3 determination

Table 3.6 Freeze thaw stability of curcumin, curcumin glucuronide and curcumin sulfate in mouse plasma and lung homogenate.

Plasma	Analyte	Concentration (µg/mL)	Content measured (%)	
			Cycle 1	Cycle 3
Plasma	Curcumin	0.2	96.0±0.9	97.4±4.8
		5	96.5±7.1	100.0±1.5
		10	108.6±14.3	102.3±1.6
	Curcumin Glucuronide	0.2	107.0±12.1	101.3±9.3
		5	103.5±10.7	96.5±1.3
		10	97.2±3.5	96.0±3.4
	Curcumin Sulfate	0.2	101.2±4.0	118.3±3.9
		5	98.3±13.6	91.2±1.7
		10	101.3±10.6	108.2±5.0
Lung	Curcumin	0.5	98.2±5.4	149.9±12.5
		5	102.2±6.9	126.5±16.8
		10	100.3±3.4	149.3±4.2
	Curcumin Glucuronide	0.5	97.2±4.6	81.8±7.0
		5	99.5±10.0	91.2±0.3
		10	92.0±7.6	82.2±5.1
	Curcumin Sulfate	0.5	62.7±6.6	53.4±5.7
		5	50.3±4.8	62.9±2.0
		10	66.5±6.2	63.6±1.4

Values are mean ± SD of n=3 determination

3.4 Curcumin and metabolite concentration in plasma and lung tissue following a single oral dose - Low dose pharmacokinetic study

As the new validated method was more efficient in extracting metabolites, the method was applied to a low dose pharmacokinetic study in mice which complimented the dose of Meriva used in clinical trials. This study was intended to investigate and compare the pharmacokinetics of Meriva and unformulated curcumin at a clinically relevant dose and ensure the applicability of the method. The dose used for this study was 3.5 times lower than the previous dose used and was equivalent to a human dose of 2 g for a 70 kg adult (calculated as per body surface area). Male C57BL/6J mice (3 mice per group) received a single oral dose of curcumin or Meriva at 70 mg/kg body weight in terms of curcumin equivalent. Following oral administration, plasma and lung tissues were collected at 0.5, 1, 1.5, 2, 2.5 and 3 hour intervals. Curcumin and metabolite levels were measured using the chromatographic conditions and extraction method described in section 2.2.2.4 and 2.2.3.

Following administration of Meriva or unformulated curcumin at 70 mg/kg by oral gavage, no free curcumin could be detected in the plasma of any mice over the course of the study in either of the treatment groups. However, conjugate metabolites were detectable in both the treatment group, with AUC values for curcumin glucuronide and DMC glucuronide being approximately 4-5 fold higher for the Meriva treated group compared to unformulated curcumin treated group ($p < 0.005$, Figure 3.11 and Figure 3.12). Curcumin sulfate, which was not detected in the previous study due to low extraction efficiency, could be detected in both treatment groups and its AUC values were 14 fold higher in the Meriva treated group compared to the unformulated curcumin treated group ($p < 0.005$). Following Meriva administration, the average C_{max} increased from 0.41 ± 0.29 μM to 2.61 ± 1.89 μM for curcumin glucuronide, 0.39 ± 0.30 μM to 2.81 ± 0.87 μM for DMC glucuronide and 0.24 ± 0.11 μM to 0.46 ± 0.02 μM for curcumin sulfate when compared to unformulated curcumin group (Table 3.7). The metabolites could be detected at all time points investigated from 0.5 hours up to 3 hours in both the treatment groups. In Meriva treated group, after an initial increase in concentration of curcumin glucuronide and DMC glucuronide up to 1 hour, the concentrations plateaued up to 3 hours. For the unformulated curcumin group,

the concentrations for these metabolites declined after initial increase up to 1 hour. In unformulated curcumin group, concentration of curcumin sulfate declined after reaching C_{max} at 1 hour of dosing however in the Meriva group the concentration of curcumin sulfate continued to increase up to 3 hours, to the C_{max} level.

An unidentified peak was detected in both treatment groups across all time points at a retention time of 12.3 minutes. To ascertain the identity of the peak, samples were analysed on LC-MS/MS using existing chromatography conditions. Plasma samples were analysed using multiple reaction monitoring (MRM) to monitor the characteristic fragments of the metabolite in the negative ion mode. In plasma, the peak undergoing transition with m/z of $623 > 134$ was present which corresponded to curcumin glucuronide-sulfate conjugate (Figure 3.10). Due to unavailability of the standard, its levels were quantified using curcumin calibration curves. The AUC values of this glucuronide-sulfate conjugate were 3 fold higher in the Meriva group compared to unformulated curcumin group. The average C_{max} of curcumin glucuronide-sulfate was $0.9 \pm 0.2 \mu\text{M}$ in unformulated curcumin group and $3.15 \pm 0.45 \mu\text{M}$ in Meriva treated group. It was found to be the most predominant metabolite among all the metabolites detected. In the lungs, neither curcumin nor its metabolites could be detected at any of the time points.

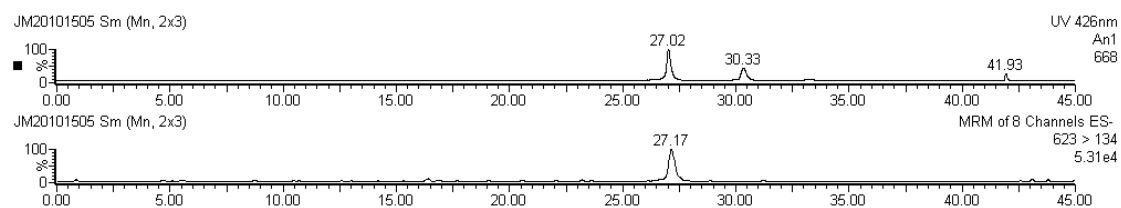


Figure 3.10 LC-MS/MS multiple reaction monitoring (MRM) transition in mouse plasma following oral Meriva dosing.

Identification of curcumin glucuronide-sulfate metabolite in mouse plasma following dosing with 70 mg/kg of curcumin by oral gavage.

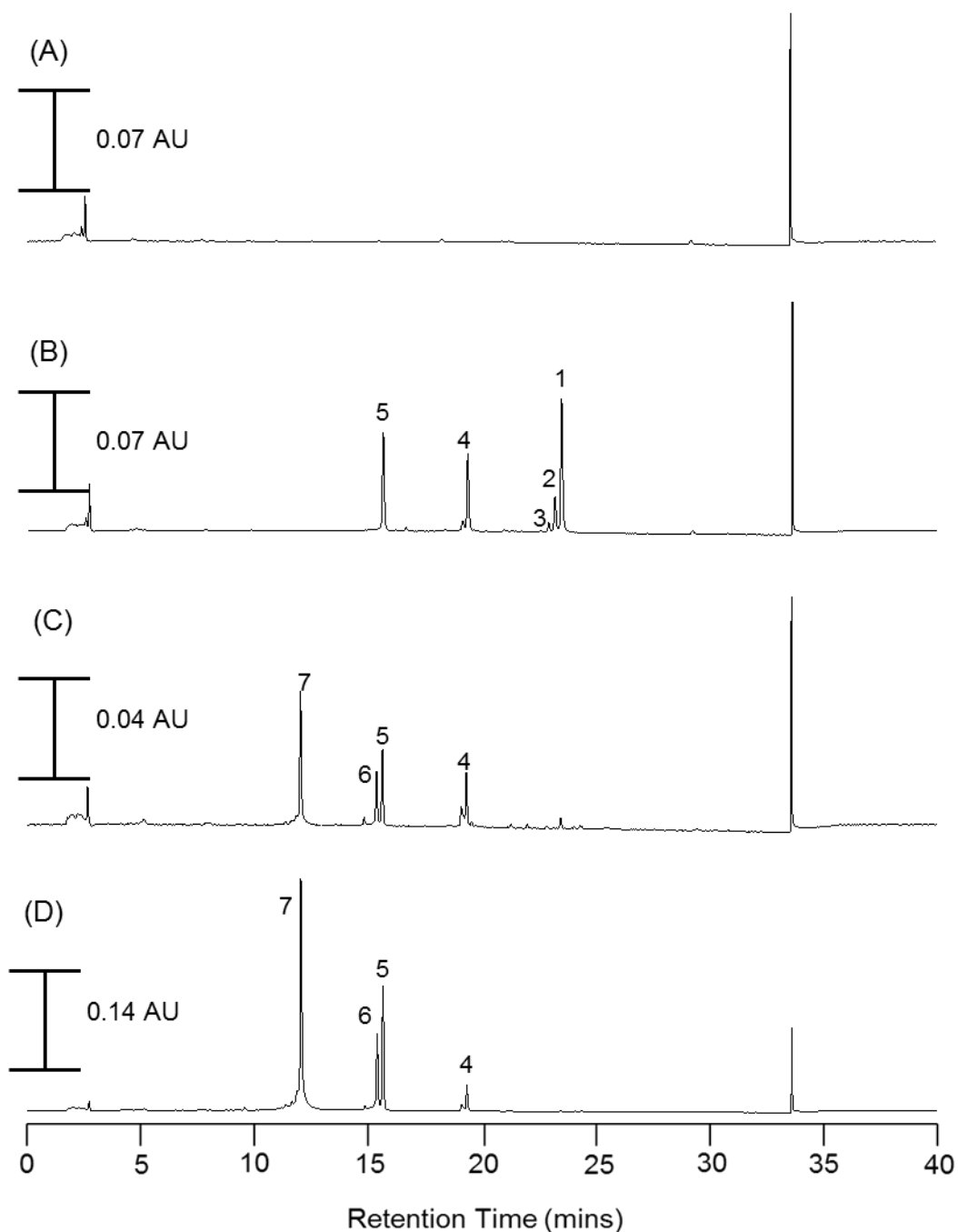


Figure 3.11 Representative HPLC chromatograms of mouse plasma following oral gavage dosing of unformulated curcumin or Meriva (low dose).

HPLC-UV chromatograms of plasma taken from mice receiving unformulated curcumin or Meriva at 70 mg/kg by oral gavage obtained 1 hour post dosing. The chromatograms are as follows: (A) Plasma extract from vehicle control mouse (B) Extract from plasma spiked with curcumin, curcumin sulfate and curcumin glucuronide standards at 2 µg/mL (C) Plasma extract from mouse receiving unformulated curcumin (D) Plasma extract from mouse receiving Meriva. Peak 1-7 correspond to: (1) curcumin, (2) demethoxycurcumin, (3) *bis*-demethoxycurcumin, (4) curcumin sulfate (5) curcumin glucuronide, (6) demethoxycurcumin glucuronide, (7) curcumin glucuronide-sulfate

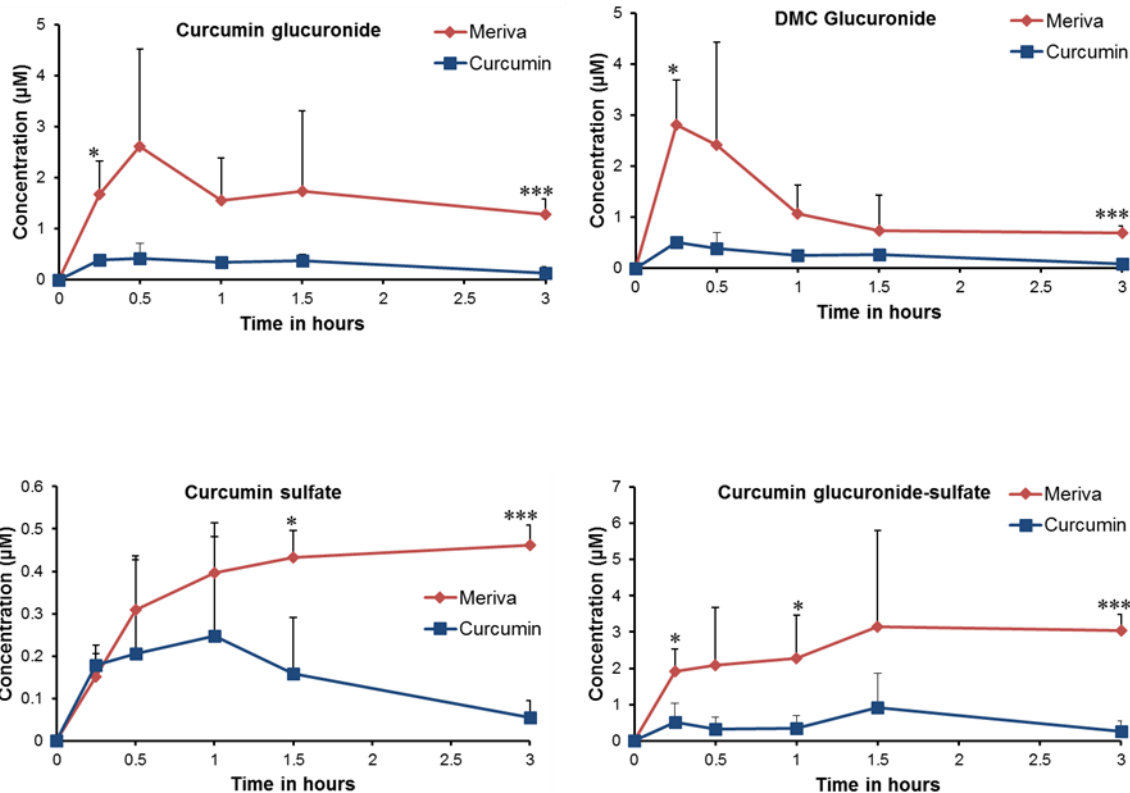


Figure 3.12 Concentrations of curcumin metabolites in mouse plasma following oral dosing with unformulated curcumin or Meriva (low dose).

Curcumin metabolite concentration in mouse plasma over 3 hours following Meriva (red line) or unformulated curcumin (blue line) dosing at 70 mg/kg. Values are the mean + SD (n = 3). Statistical comparison between the Meriva and unformulated curcumin at each time point was by student's T-test. Statistically significant differences are indicated as * (p < 0.05) and *** (p < 0.005).

Table 3.7 Average curcumin metabolite concentrations in mouse plasma following oral dosing at 70 mg/kg dose.

Estimated average plasma peak levels (C_{max}), time of peak levels (T_{max}) and AUC values for unformulated curcumin and Meriva when administered at a dose of 70 mg/kg in terms of curcumin, via oral gavage.

Plasma				
		C_{max} (μM)	T_{max} (hrs)	AUC (nmol/h/mL)
Unformulated curcumin	Curcumin glucuronide	0.41 \pm 0.29	0.5	1.7
	Demethoxycurcumin glucuronide	0.39 \pm 0.30	0.5	3.25
	Curcumin sulfate	0.24 \pm 0.11	1	0.08
	Curcumin glucuronide-sulfate	0.9 \pm 0.2	1.5	3.41
Meriva	Curcumin glucuronide	2.61 \pm 1.89	0.5	9.77
	Demethoxycurcumin glucuronide	2.81 \pm 0.87	0.25	12.54
	Curcumin Sulfate	0.46 \pm 0.02	3	1.12
	Curcumin glucuronide-sulfate	3.15 \pm 0.45	1.5	10.28

3.4.1 Enzymatic conversion of plasma and lung samples

As no free curcumin or its metabolites were detected in lungs in either of the treatment group, it was possible that they may have reached lung tissue but were undetected due to concentrations below the LLOQ. Hence, to determine whether curcumin, either in its free or conjugated form, reached lungs at all and to determine the overall curcuminoid concentrations, plasma and lung samples were subjected to enzymatic conversion with β -glucuronidase/sulfatase.

Post enzymatic conversion, AUC values of DMC and curcumin were approximately 3-4 fold higher in plasma of mice that had received Meriva compared to those administered unformulated curcumin (Figure 3.13 and Figure 3.14). The maximum curcumin concentration achieved in Meriva treated mice was $6.5 \mu\text{M} \pm 3.48 \mu\text{M}$ at 1.5 h post dosing (Table 3.8). bDMC could be detected only in mice in the Meriva group. The curcumin sulfate peaks were still detectable post enzymatic conversion in plasma samples, possibly due to insufficient sulfatase enzyme in the solution. In the lungs, free curcumin could be detected post enzymatic conversion. AUC values of free curcumin measured after enzymatic hydrolysis were 4-times higher in the Meriva group, with maximum concentrations of $0.41 \mu\text{M} \pm 0.05 \mu\text{M}$ reached at 3 hours after dosing (Table 3.8). The average C_{max} of curcumin in unformulated group was $0.09 \pm 0.01 \mu\text{M}$ achieved at a T_{max} of 3 hours. DMC was detected only in mice that received Meriva. A maximum concentration of $0.22 \pm 0.06 \mu\text{M}$ was achieved at 0.25 hours post dosing. bDMC could not be detected in either treatment group. These results suggest that curcumin given in the form of Meriva, furnishes both plasma and lung tissues of mice with detectable levels of curcuminoids, even at clinically relevant doses.

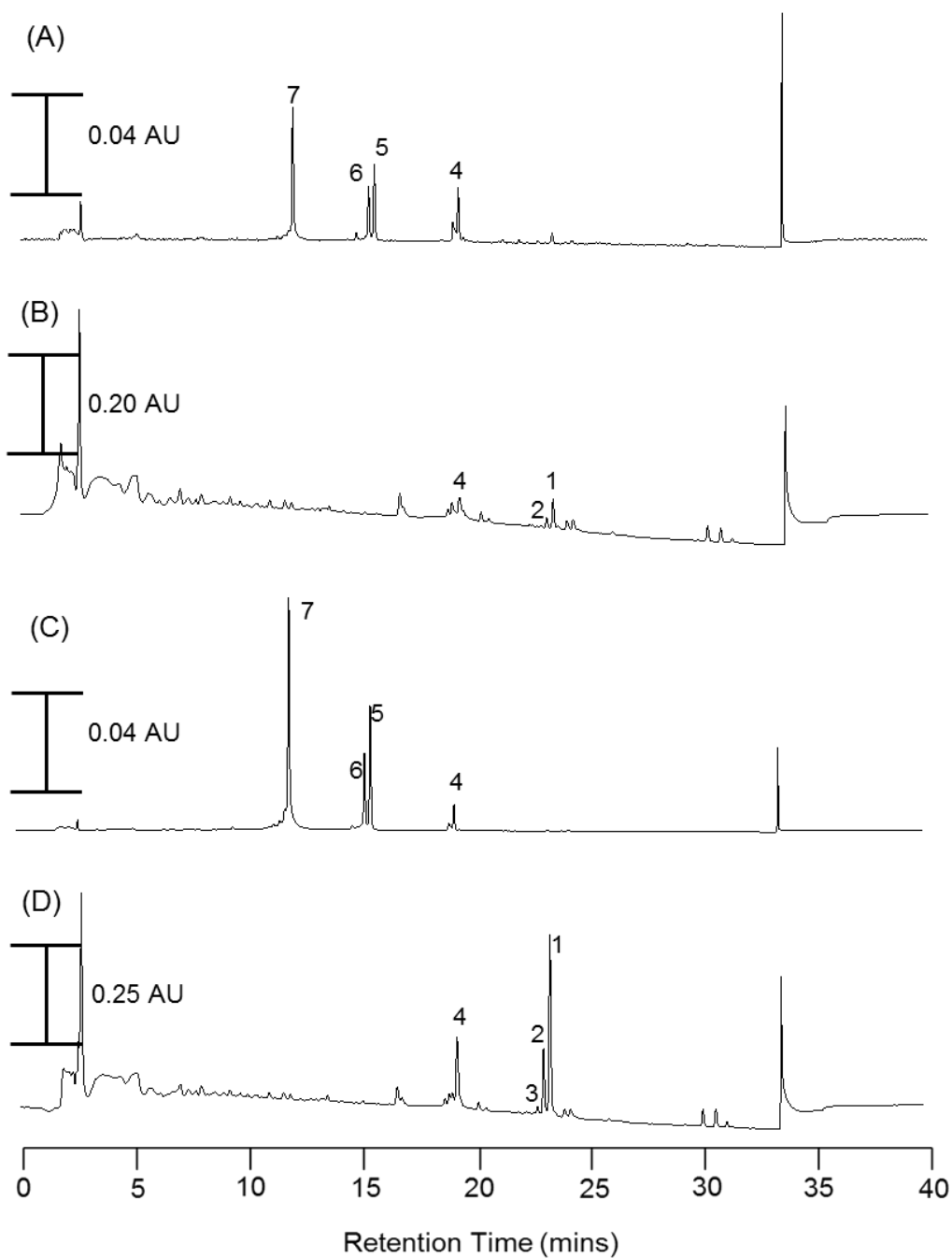


Figure 3.13 Representative HPLC-UV chromatograms of mouse plasma following oral gavage dosing of unformulated curcumin or Meriva and enzymatic conversion.

HPLC-UV chromatograms of plasma taken from mice receiving unformulated curcumin or Meriva at 70 mg/kg by oral gavage obtained 1 hour post dosing. The chromatograms are as follows: (A) Plasma extract from mouse receiving unformulated curcumin (B) Enzymatically converted plasma extract from mouse receiving unformulated curcumin (C) Plasma extract from mouse receiving Meriva. (D) Enzymatically converted plasma extract from mouse receiving Meriva. Peak 1-7 correspond to: (1) curcumin, (2) demethoxycurcumin, (3) *bis*-demethoxycurcumin, (4) curcumin sulfate, (5) curcumin glucuronide, (6) demethoxycurcumin glucuronide, (7) curcumin glucuronide-sulfate

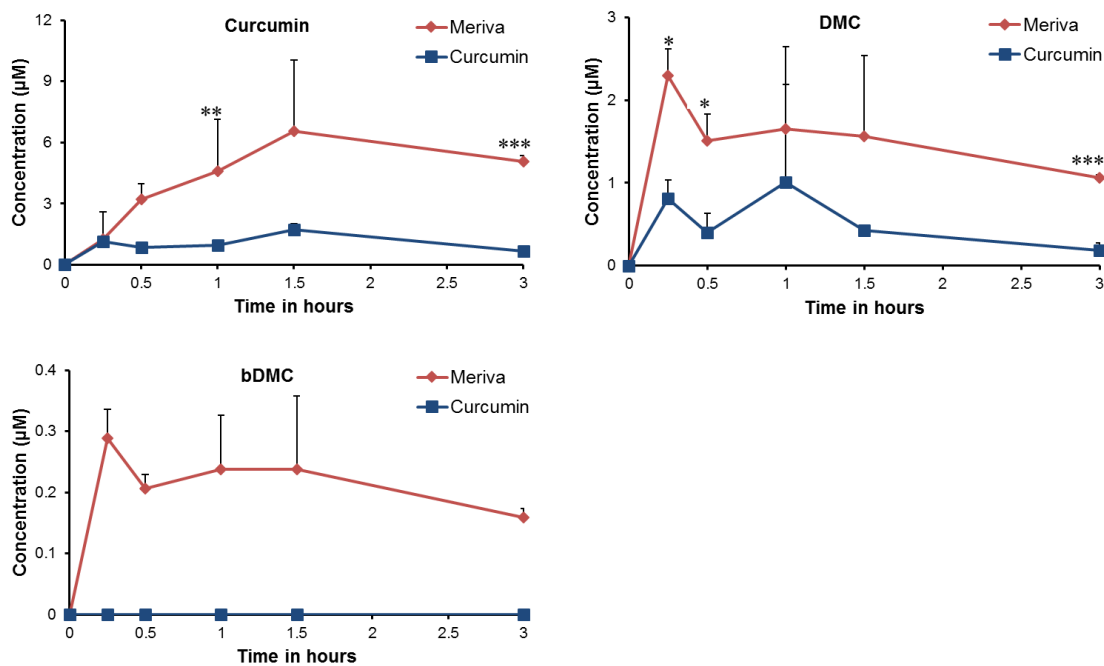


Figure 3.14 Concentrations of curcuminoids in mouse plasma following oral dosing with unformulated curcumin or Meriva and enzymatic conversion (low dose).

Curcuminoid concentration in mouse plasma over 3 hours following Meriva (red line) or unformulated curcumin (blue line) dosing at 70 mg/kg and enzymatic conversion. Values are the mean + SD (n = 3). Statistical comparison between the Meriva and unformulated curcumin at each time point was by student's T-test. Statistically significant differences are indicated as * (p < 0.05), ** (p < 0.01) and *** (p < 0.005).

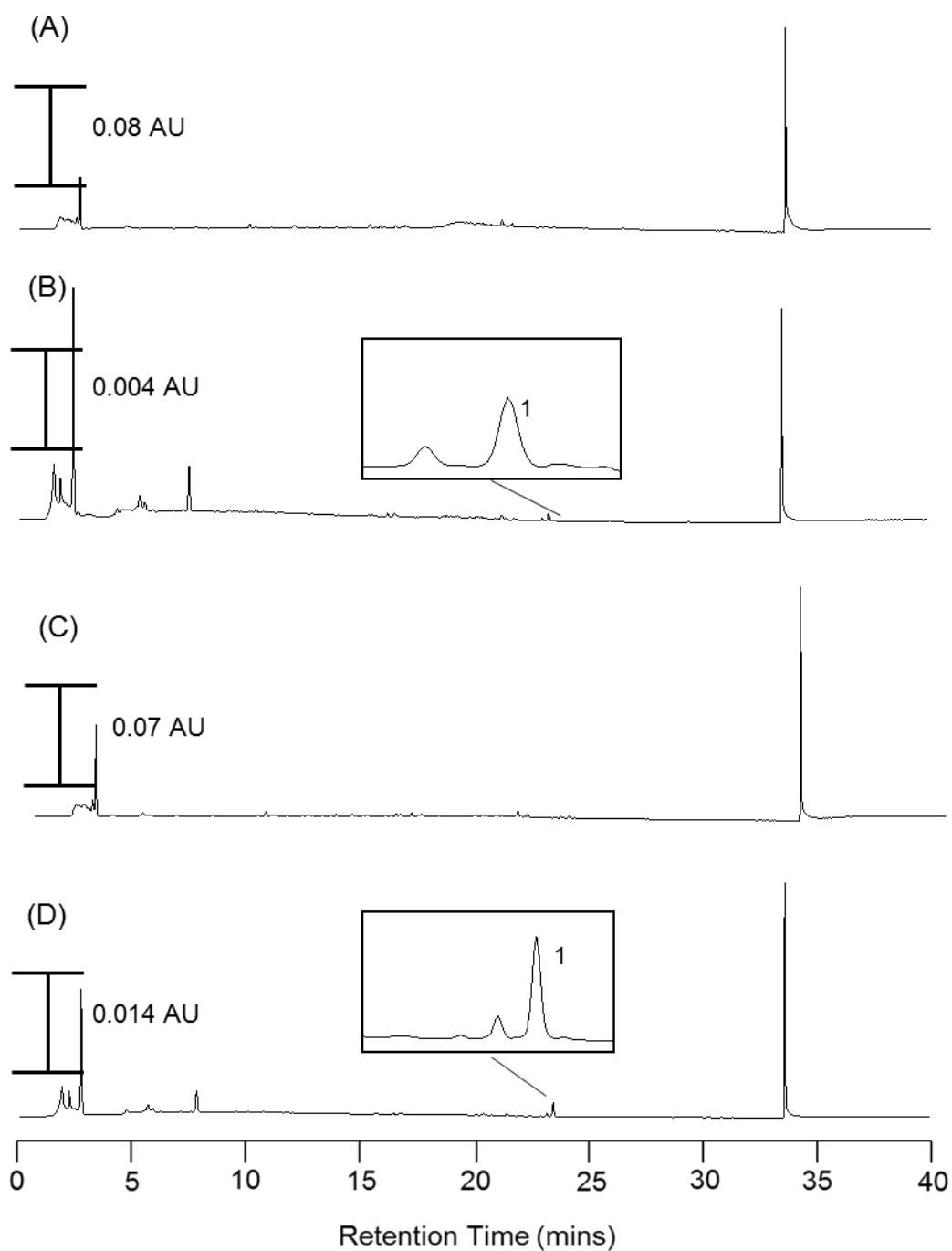


Figure 3.15 Representative HPLC-UV chromatograms of mouse lung homogenate following oral gavage dosing of unformulated curcumin or Meriva and enzymatic conversion.

HPLC-UV chromatograms of plasma taken from mice receiving unformulated curcumin or Meriva at 70 mg/kg by oral gavage obtained 3 hour post dosing. The chromatograms are as follows: (A) Lung homogenate extract from mouse receiving unformulated curcumin (B) Enzymatically converted lung homogenate extract from mouse receiving unformulated curcumin (C) Lung homogenate extract from mouse receiving Meriva. (D) Enzymatically converted lung homogenate extract from mouse receiving Meriva. Peak 1 corresponds to curcumin.

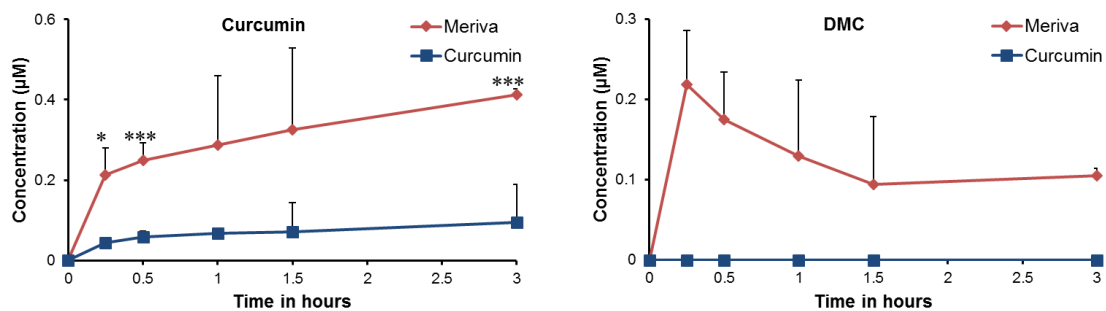


Figure 3.16 Concentrations of curcuminoids in mouse lung homogenate following oral dosing with unformulated curcumin or Meriva and enzymatic conversion (low dose).

Curcuminoid concentration in mouse lung homogenate over 3 hours following Meriva (red line) or unformulated curcumin (blue line) dosing at 70 mg/kg and enzymatic conversion. Values are the mean + SD (n = 3). Statistical comparison between the Meriva and unformulated curcumin at each time point was by student's T-test. Statistically significant differences are indicated as * (p < 0.05) and *** (p < 0.005).

Table 3.8 Average curcuminoid concentrations in mouse plasma and lungs after 70 mg/kg oral dosing and enzymatic conversion.

Estimated average plasma peak levels (C_{max}), time of peak levels (T_{max}) and AUC values for unformulated curcumin and Meriva when administered at a dose of 70 mg/kg in terms of curcumin, via oral gavage.

Plasma				
		C_{max} (μ M)	T_{max} (hours)	AUC (nmol/h/mL)
Unformulated curcumin	Curcumin	1.71±0.57	1.5	3.29
	demethoxycurcumin	1.00±0.04	1	1.41
Meriva	<i>bis</i> - demethoxycurcumin	1.18±1.00	0.25	0.62
	demethoxycurcumin	2.29±0.32	0.25	4.32
	Curcumin	6.53±3.48	1.5	14.14
Lungs				
Unformulated curcumin	Curcumin	0.09±0.01	3	0.20
Meriva	Curcumin	0.41±0.05	3	1.07
	demethoxycurcumin	0.21±0.06	0.25	0.41

3.5 Healthy human volunteer turmeric food Study

The aim of this study was to determine whether ingestion of food containing a defined dose of curcumin could generate detectable concentrations of curcuminoids in plasma of healthy human volunteers. Four healthy volunteers (fasted overnight) consumed three portions of turmeric-containing food consisting of soup, sandwich and a sweet (flapjack) (Figure 3.17). Each portion of food contained 1 gram of turmeric. Blood samples were taken at 0.5, 1, 2, 4, 8 and 24 hours post food consumption. The turmeric used in food preparation and the food was analysed to determine curcumin content and presence of any breakdown products of curcumin post cooking.



Figure 3.17 Turmeric containing sandwich, flapjack and soup used for the healthy human volunteer study.

In, turmeric curcumin content was 3.25% (approximately 4.25% curcuminoids) (Figure 3.18). Therefore, curcumin consumed by each volunteer in these three portions was approximately 100 mg. The curcumin content was found to be 71%, 52% and 48% of the expected levels in soup, bread and flapjack respectively (Figure 3.18). The lower than expected values might be due to extraction difficulties from a food matrix. Apart from the curcuminoid peaks, no other peak could be detected.

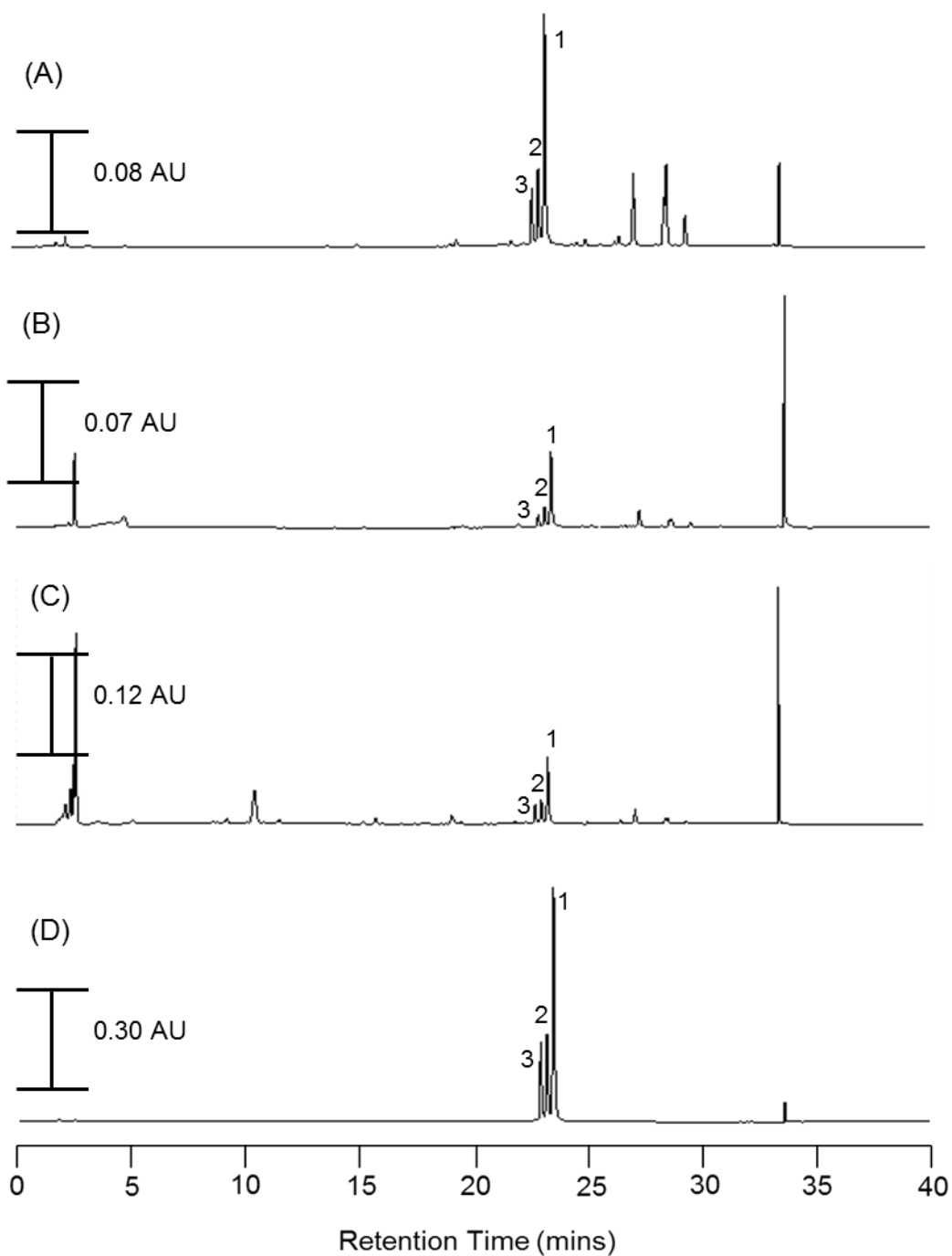


Figure 3.18 Representative HPLC-UV chromatograms of turmeric and turmeric food.

HPLC-UV chromatograms of turmeric and turmeric containing food used for the healthy volunteer study. Each portion of food contained 1 gram of turmeric. The chromatograms are as follows: (A) Turmeric (B) Extracted bread (C) Extracted flapjack (D) Extracted soup. Peak 1-3 correspond to: (1) curcumin, (2) demethoxycurcumin, (3) bis-demethoxycurcumin.

The extraction efficiencies of curcumin, curcumin glucuronide and curcumin sulfate from human plasma were 90.2 ± 13.1 , 98.3 ± 13.2 and 83.9 ± 10.2 respectively, consistent with results in murine plasma. The values are from single injection and calculated across three different concentration. No free curcumin could be detected in plasma samples of any of the volunteers at any of the time points analysed. In plasma samples from two volunteers, a small peak at 1 hour could be tentatively ascribed to curcumin glucuronide (Figure 3.19). However, levels were too low for unambiguous identification. An unidentified peak was seen at approximately 27 minutes. The samples were subjected to enzymatic hydrolysis but no free curcumin could be detected in any of the samples.

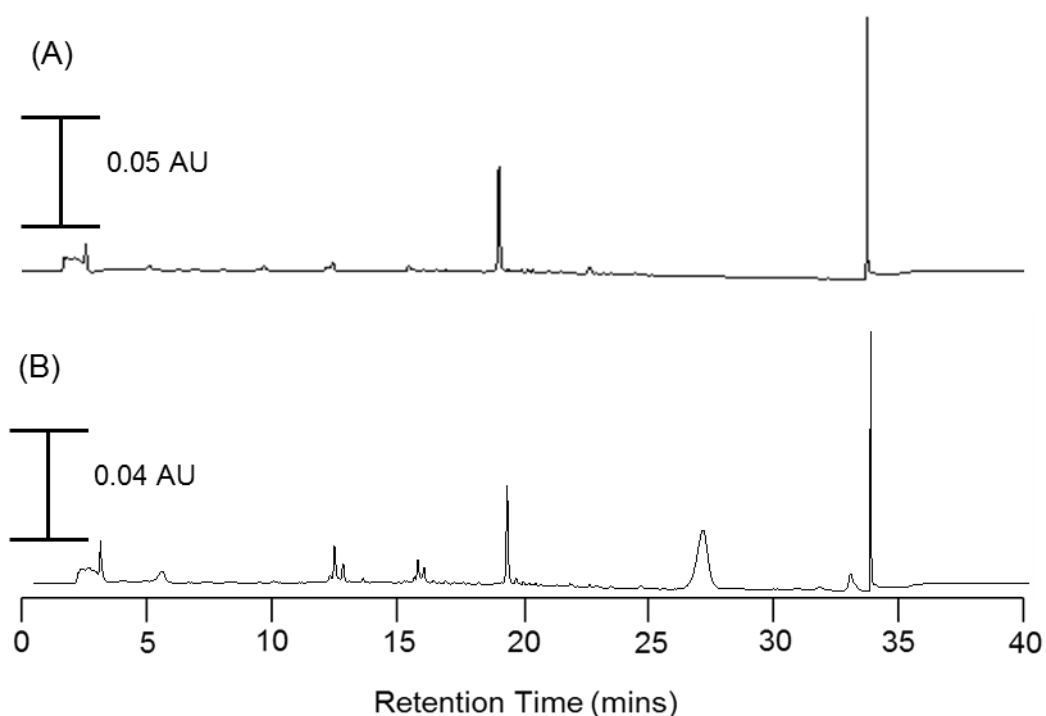


Figure 3.19 Representative HPLC-UV chromatograms of healthy human plasma following consumption of turmeric containing food.

HPLC-UV chromatograms of plasma taken from healthy human volunteer following consumption of turmeric containing food at an estimated dose of 1.5 mg/kg. The chromatograms are as follows: (A) Extract of plasma taken before consumption of food (B) Extract of plasma taken 1 hour after consumption of food.

3.6 Discussion

Despite compelling evidence for efficacy of curcumin in a wide variety of *in vitro* and *in vivo* cancer models, evidence for clinical efficacy is lacking. Several phase II trials have been completed in a variety of indications, alluding to its safety, tolerability and acceptability, with some limited evidence of potential for benefit. However, on oral administration, curcumin undergoes effective first pass metabolism in the small intestine and liver by phase 2 metabolising enzymes, furnishing higher levels of glucuronide and sulfate metabolites than the parent compound itself. The conjugate metabolites are hydrophilic in nature and hence are quickly eliminated from the body. To overcome this difficulty, various formulation strategies are being developed that protect curcumin from getting extensively metabolised and increase its absorption. To this end, a formulation called Meriva has been developed which complexes curcumin with phosphatidylcholine which imparts a lipophilic character and improves its absorption. Phosphatidylcholine forms the major molecular building block of cell membranes and is miscible in both water and in oil/lipid environments and well absorbed orally.

As a first part of this study, a comparative pharmacokinetic study between unformulated curcumin and Meriva was undertaken to determine whether Meriva offered a better pharmacokinetic profile for its potential use as a chemopreventive agent for lung cancer. Plasma and lung tissue levels were determined by using a previously partially validated HPLC-UV method [215]. The pharmacokinetic profile over the 24 hour period in plasma was similar to that seen in previous studies. No free curcumin could be detected in either of the treatment groups and only the conjugate metabolites curcumin monoglucuronide and DMC glucuronide could be detected - levels of which were 16-18 fold higher in mice that received Meriva compared to those administered standard curcumin. The lipophilic character of the curcumin-phosphatidylcholine complex may facilitate diffusion of curcumin across biological membranes in the gastrointestinal tract via formation of a phospholipid monolayer on the mucosal surface, thus supporting the transition of curcumin from the hydrophilic gut content across lipophilic membranes and into cells [215]. The curcumin-phosphatidylcholine complex shields curcumin from hydrolytic degradation and increases its cellular

accumulation. Interestingly, the major metabolite was DMC glucuronide and not curcumin glucuronide in both the treatment groups, the reasons for which are unknown. A possible explanation could be that the hydrolytic stabilization of curcumin at intestinal pH might, in fact, translate into a significant curcumin load for the gut microflora, known to be able to reductively demethoxylate dietary phenolics [252].

Glucuronidation is a major route of phase 2 metabolism for curcumin and takes place by adding the glycosyl group of uridine-5'-diphosphoglucuronic acid (UDPGA) preferentially at the phenolic hydroxyl group. This reaction is catalysed by the enzyme superfamily of uridine-5'-diphosphoglucuronosyltransferases (UGTs) which are predominantly found in the gastrointestinal tract. The UGT enzymes mainly involved in glucuronidation of curcumin and DMC are UGT1A1, 1A8, and 1A10 [213]. Although glucuronidation is usually dominant in phase II conjugated metabolism, sulfonation of curcumin also takes place to some extent. The sulfotransferases (SULTs) enzymes involved in sulfonation of curcumin are SULT1A3, 1B1, 1C4 and 1E1 [212]. No sulfate metabolites were detected in either treatment group. There was no evidence of other curcumin metabolites such as dihydro, tetrahydro, hexahydro, octahydro curcumin formed by phase 1 metabolising enzymes cytochrome P450s and alcohol dehydrogenase were also undetectable. However, the assay wasn't set up to detect these so they may not be efficiently extracted or indeed detected with the chromatographic system employed.

In lungs, free curcumin was detected in both treatment groups and levels of free curcumin were 3.6 times higher in the Meriva treated mice. A possible explanation for the presence of free curcumin in lungs but not in plasma could be that curcumin metabolites get converted back to their parent form once they reach the lung. A study by Liu *et al* 2015 demonstrated the conversion of curcumin glucuronide to curcumin *in vivo*. Following a single intravenous dose of curcumin glucuronide at 2 mg/kg, a peak curcumin concentration of 2 μ M was detected in lungs, whereas curcumin concentration in plasma was negligible [272]. This possibly suggests that β -glucuronidase enzymes expressed in lungs allow back conversion of curcumin glucuronide to curcumin but not in plasma. Studies have already shown that β -glucuronidase enzyme is expressed in normal

mouse lungs [273]. *In vitro* studies with isolated, perfused human lung have shown significantly higher β -glucuronidase expression and activity in the tumour bearing lungs as compared to normal lungs [274]. Theoretically, increased β -glucuronidase activity due to elevated levels of the enzyme in tumour tissue will increase the rate at which curcumin glucuronide is converted to active curcumin, and thus increase the overall concentration of curcumin in the tumour which would be beneficial for the use of this compound in the management of lung cancer.

A closer look at the concentration vs time curve shows that while the metabolites are eliminated by a steadily decreasing concentration in plasma and lungs, free curcumin concentration in lung decreases at 0.5 and 1 hour and increases at 0.75 and 1.5 hours post dosing. From this biphasic response, it can be speculated that curcumin metabolites, on reaching lung tissue through systemic circulation, may get converted to curcumin and some are excreted back into the systemic circulation unchanged with this exchange continuing until conjugates are completely eliminated. A similar pattern was also observed for enzymatically converted samples. The results from this study showed that even if no free curcumin is detected in plasma, curcumin metabolites can still play an important role in providing parent curcumin in target tissues.

It is now a widely conceived notion that even if curcumin has poor systemic bioavailability, its beneficial properties can be attributed partly to bioactivity possessed by its minor metabolites including THC, in addition to the potential conjugated metabolite back-conversion phenomenon described above. This is of particular importance for curcumin formulations such as Meriva which generate high concentrations of conjugated metabolites at an equivalent curcumin dose. This can be helpful in deciding future dosing strategies for Meriva which may be used at a much lower dosage as compared to unformulated curcumin where dosing of curcumin in clinical studies is currently limited by the bulk of tablets.

A limitation of the metabolite concentration data in in this high dose pharmacokinetic study was the fact the values were calculated using a curcumin calibration curve, which provides an approximate estimation only and does not account for any differences in extraction efficiency. Considering this, it was

imperative to ascertain whether the conjugated metabolites were efficiently recovered using this method and subsequently develop an improved assay that enabled accurate determination of metabolite concentrations rather than estimates based on curcumin equivalents. To this end, authentic curcumin monoglucuronide and curcumin monosulfate were synthesised in house and their identity confirmed by NMR and mass spectrometry. The current method was modified to increase the extraction efficiency and was fully validated to confirm its reproducibility and reliability.

The modified method not only improved extraction efficiencies of metabolites but also shed light on relative instability of curcumin metabolites in lung homogenates when subjected to frequent freezing and thawing. On long term storage of up to 3 months, curcumin sulfate degraded by a maximum of 32% and curcumin glucuronide degraded by a maximum of 18%. Even though maximum degradation of curcumin in lung homogenate was 13%, it can be hypothesised that it degrades to a greater extent than this, as curcumin formed by back conversion of metabolites would increase the total curcumin content in the sample.

The pharmacokinetic study repeated at a low dose using the new method showed the presence of glucuronide conjugates, in addition to previously undetected curcumin sulfate and curcumin glucuronide-sulfate metabolites. Due to the unavailability of a curcumin glucuronide-sulfate standard, it was quantified using the curcumin calibration curve and was found to be the most predominant metabolite in plasma. The levels of these metabolites were 3-5 fold higher in the Meriva treated mice compared to those that received standard curcumin.

In lung, no curcumin or metabolites were detected in either treatment group at low dose. Following enzymatic conversion, curcumin and DMC could be detected in the Meriva group and only curcumin was detected in the unformulated curcumin group. Encouragingly, this suggests that even at a low dose, curcumin either in its free or conjugated form had reached the lung, but levels were below the limit of detection. It was interesting to find that the levels of curcumin post enzymatic conversion were similar to those detected in the high dose study for

both treatments. This may be partly due to slightly higher extraction efficiency of the method.

The amounts of curcumin/curcuminoids from pure formulations of curcumin found in the blood of healthy volunteers have previously been established [146, 198, 231, 234]. However, much of the evidence for potential health benefits of curcumin are extrapolated from epidemiological data. These data are not based on ingestion of curcumin supplements, rather, they are derived from the intake of turmeric through food consumption in populations that consume turmeric-rich foods. Here, a study was undertaken in healthy volunteers using food containing known quantities of turmeric to determine whether measurable levels of curcuminoids could be detected in plasma. Following consumption of turmeric containing food, very low levels of curcumin glucuronide (tentatively assigned) were detected at 1 hour for 2 volunteers. Even at this extremely low dose (approximately 1.5 mg/kg for a 70 kg adult) of curcumin, it was encouraging that this method was sufficient for detection of a circulating metabolite. At the point of thesis submission, assay sensitivity was being further refined, and a MS-based method is currently under validation for the detection of curcumin and its metabolites down to a picomolar sensitivity. Early results from the experiments indicate at the presence of free curcumin, curcumin glucuronide and curcumin sulfate in all volunteers. One of the other aims of the study was to determine whether any curcumin breakdown products were formed after cooking it in different matrices and temperature. However, no such products could be identified when extracted food samples were analysed using HPLC-UV.

Overall, from this study we can conclude that Meriva offers superior levels of curcumin metabolites and curcumin in lungs and in plasma compared to its unformulated form. A number of clinical studies have already established the safety of Meriva for prolonged human consumption [203, 251, 266, 275-277]. A sensitive and specific HPLC-UV method has been developed for the determination of curcumin and curcumin metabolites in murine plasma and lung tissue. At the time of undertaking this study, it was the only HPLC-UV method to be validated using curcumin glucuronide and curcumin sulfate standards allowing precise quantification of the metabolites. This study sheds light on relative stability and potential conversion of curcumin metabolites to parent

compound in lung homogenates. The method was successfully applied to an *in vivo* pharmacokinetic study and human healthy volunteer study. This *in vivo* study showed that curcumin glucuronide-sulfate is the major metabolite of curcumin following oral administration which was not reported in previous studies. For the first time in a curcumin pharmacokinetic study, metabolite concentrations are expressed as authentic concentration and not equivalents.

4 *In-vitro* effect of curcumin on HGF/MET signalling axis

4.1 Introduction

Two dimensional (2D) cell culture has been routinely used for decades, and provides valuable high-throughput information regarding drug effects and mechanisms of action in short time frames and at low cost. However, the culture of cells in two dimensions is arguably primitive and does little to represent the complexity and heterogeneity of diseases like cancer, especially in lung cancer which exhibits dense stroma. Recently, there have been attempts to better mimic the tumour microenvironment by generation of 3D models which incorporate important elements of the tumour stroma such as fibroblasts. In order to try and address some of the concerns arising from the use of 2D models, a 3D organotypic co-culture model combining lung cancer cells with lung fibroblasts was used in order to see assess whether chemopreventive effects of curcumin observed in 2D culture systems, could be recapitulated in 3D models.

The HGF-MET axis pathway has been frequently implicated as a driving factor in cancer cell invasion and metastasis. In lung cancer, HGF and MET are often found to be overexpressed, and so provide a potential target by which curcumin could elicit its anti-invasive properties. The role of the HGF-MET axis in invasion is particularly influenced by stromal constituents such as fibroblasts.

The overall aim of this chapter was to investigate the role of fibroblasts in lung cancer cell invasion, and to determine whether curcumin was able to modify the invasive capacity of lung cancer cells in a 3D organotypic model which incorporated a fibroblastic component. Further, we wished to identify whether curcumin could directly affect the properties of lung fibroblasts in a way which might directly influence their role in invasive processes. A549 human lung adenocarcinoma cells and MRC5 normal human fibroblasts were used for these investigations.

4.2 Effect of curcumin on proliferation of A549 and MRC5 cells

Sustained chronic cell proliferation is one of the most fundamental traits of cancer cells [278]. Suppression of cell proliferation is one of the mechanisms by which a chemopreventive or chemotherapeutic agent could exert its effect. Although, previous studies have shown anti-proliferative effect of curcumin on A549 cells, no study has reported the effect of curcumin on proliferation of MRC5 fibroblasts. Therefore, in order to ascertain a working concentration for further *in vitro* work, cell proliferation assays were performed on A549 and MRC5 cells (see section 2.2.6.4). To perform this study, A549 cells were exposed to curcumin (2, 4, 6, 8 or 10 μM) or to DMSO (vehicle control) for up to 144 h. For MRC5 cells lower concentrations of curcumin (0.25, 0.5, 1, 2.5 or 5 μM) were used as concentration above 5 μM were found to be excessive and toxic to the cells.

Curcumin had a significant dose dependent growth inhibitory effect on A549 cells from 120 hours of treatment, but growth inhibition was most marked following 144 hours of treatment. Exposure of these cells to 4 μM of curcumin at 144 hours significantly reduced the cell numbers compared to the control cell population (Figure 4.1). The MRC5 lung fibroblasts also exhibited a dose-dependent response to curcumin, albeit at lower doses. A dose as low as 0.25 μM significantly decreased cell number as compared to control and at a dose of 2.5 μM , > 50% reduction in cell number was observed (Figure 4.2). The IC_{50} value for A549 at 144 hours was 4.16 ± 0.20 and for MRC5 was 1.49 ± 0.30 . Proliferation results for both the cell lines suggested that longer exposure to curcumin made the cell lines more sensitive to its growth inhibitory effect.

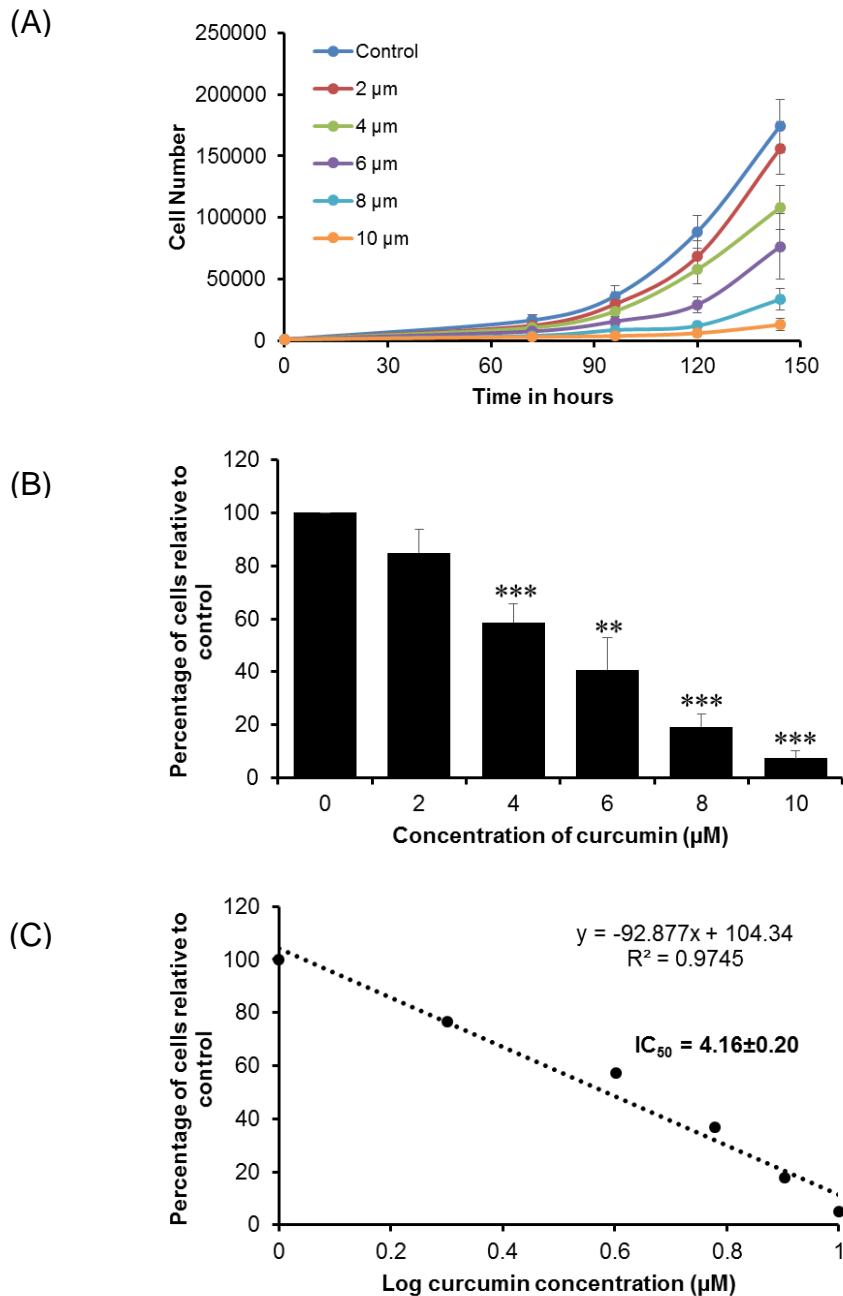


Figure 4.1 Effect of curcumin on the growth of A549 lung cancer cells.

(A) Growth curve of A549 cells following treatment with curcumin at 72, 96, 120 and 144 hours. (B) Cell number expressed as percentage relative to control following treatment with curcumin for 144 hours. Each column represents the mean \pm SD of three independent experiments, each performed in triplicate. Statistical comparison between the control and curcumin treatment was by Student's T-test. Statistically significant differences are indicated as * ($p < 0.05$) and *** ($p < 0.005$). (C) demonstrates how the IC_{50} value was calculated for the 144 h time point, as outlined in chapter 2.

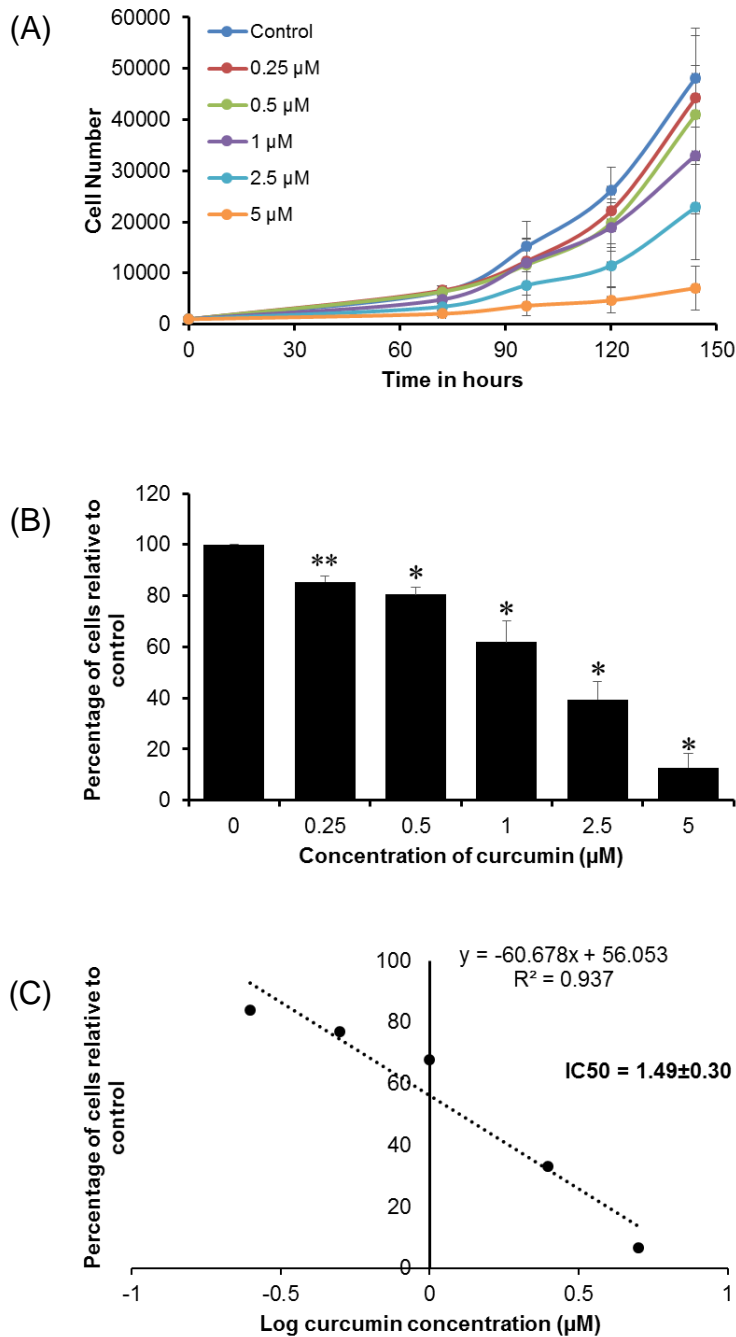


Figure 4.2 Effect of curcumin on the growth of MRC5 lung fibroblasts.

(A) Growth curve of MRC5 fibroblasts following treatment with curcumin at 72, 96, 120 and 144 hours. (B) Cell number expressed as percentage relative to control following treatment with curcumin for 144 hours. Each column represents the mean \pm SD of three independent experiments, each performed in triplicate. Statistical comparison between the control and curcumin treatment was by Student's T-test. Statistically significant differences are indicated as * ($p < 0.05$) and ** ($p < 0.01$). (C) demonstrates how the IC_{50} value was calculated for the 144 h time point, as outlined in chapter 2.

4.3 Optimisation of Organotypic Assay conditions and Effect of MRC5 fibroblasts on invasiveness of A549 cells

In a tumour microenvironment, various growth factors, chemokines and extracellular matrix secreted by stromal components influence the ability of cancer cells to invade locally or metastasize to a different organ. One of the predominant stromal components of the tumour microenvironment are fibroblasts, which are thought to influence the behaviour of cancer cells at all stages of cancer progression. To investigate how the fibroblasts impact upon the invasive behaviour of lung cancer cells, organotypic co-cultures were utilised. The organotypics co-cultures were set-up as described in material and methods section 2.2.6.5. In these co-culture models, stromal constituents (in this case, fibroblasts) are 3-dimensionally co-cultured with cancer cells in a collagen/matrigel gel, containing essential extracellular matrix components. These models enable invasion and cancer-stroma interactions to be studied in conditions that better represent those observed in vivo than more simplistic 2D cultures.

After 12 days of incubation, the top layer of the cells was found to be firmly attached to the gel. Small invading island of cells were clearly seen in gels of all cell ratios (Figure 4.3). However, with decreasing number of fibroblasts, the number of invading cell islands decreased and could be seen only near the top layer of the gel. The gel that had A549 and MRC5 cells in the ratio 1:5 on top, showed maximum invasion of cell islands into the gel (Figure 4.3 A). The matrix degradation in this 1:5 ratio was greater than that observed for the other ratios. Although equal number of cells were seeded on each gel, the cell layer thickness on top of gel decreased with decreasing number of fibroblasts in the ratio, indicating higher cell proliferation in the presence of fibroblasts.

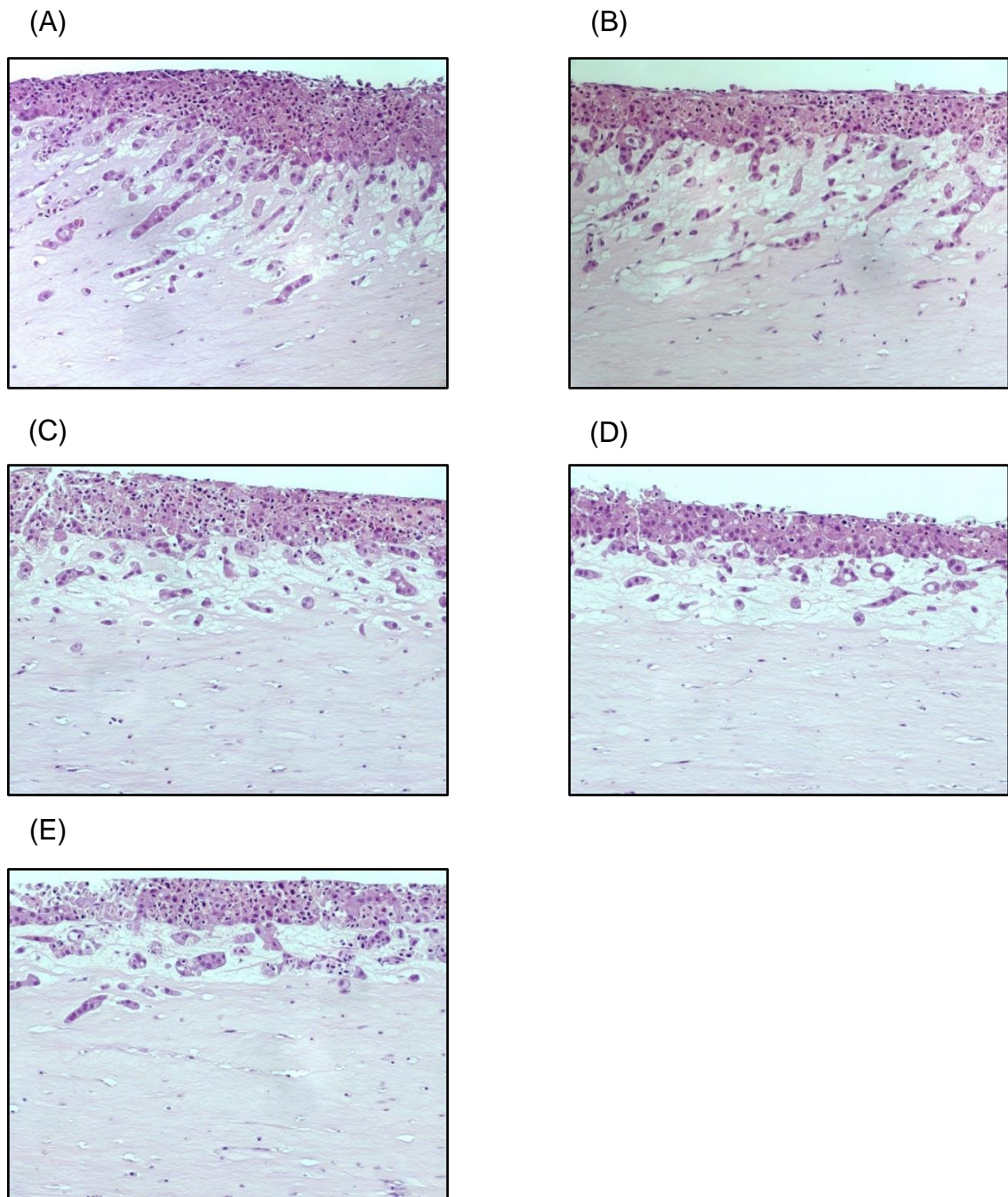


Figure 4.3 Effect of different tumour cell:fibroblast ratios on tumour cell invasion.

Representative cross-sections of organotypic co-cultures in which MRC5 lung fibroblast-embedded gels are seeded with an epithelial cell layer consisting of A549 lung cancer cells and MRC5 fibroblasts in ratios of (A) 1:5, (B) 1:2, (C) 1:1, (D) 2:1, (E) 5:1. Models were produced in triplicate and cultured for 12 days before being fixed in formalin, sectioned and stained. Images were taken under 20X magnification.

The 1:5 ratio was used with other lung cancer cell lines such as H1299 and H2228 in combination with MRC5 fibroblasts but not much invasion was observed (Figure 4.4 A, C and E). Thus all further experiments were performed using A549 cells in 1:5 ratio.

Further investigation was undertaken to determine whether the presence of fibroblasts was crucial for lung cancer cells to exhibit an invasive phenotype. Lung cancer cells were thus seeded on to the gel in the absence of fibroblasts and cultured for 12 days. None of the lung cancer cell lines (A549, H1299 and H2228) invaded in the absence of fibroblasts (Figure 4.4 B, D and F). The gels also appeared to be 'flattened out' in the absence of fibroblasts as opposed to in the presence of fibroblasts where they retain their rounded shape even after 12 days of incubation. This indicates that fibroblasts offer stiffness to the gel matrix.

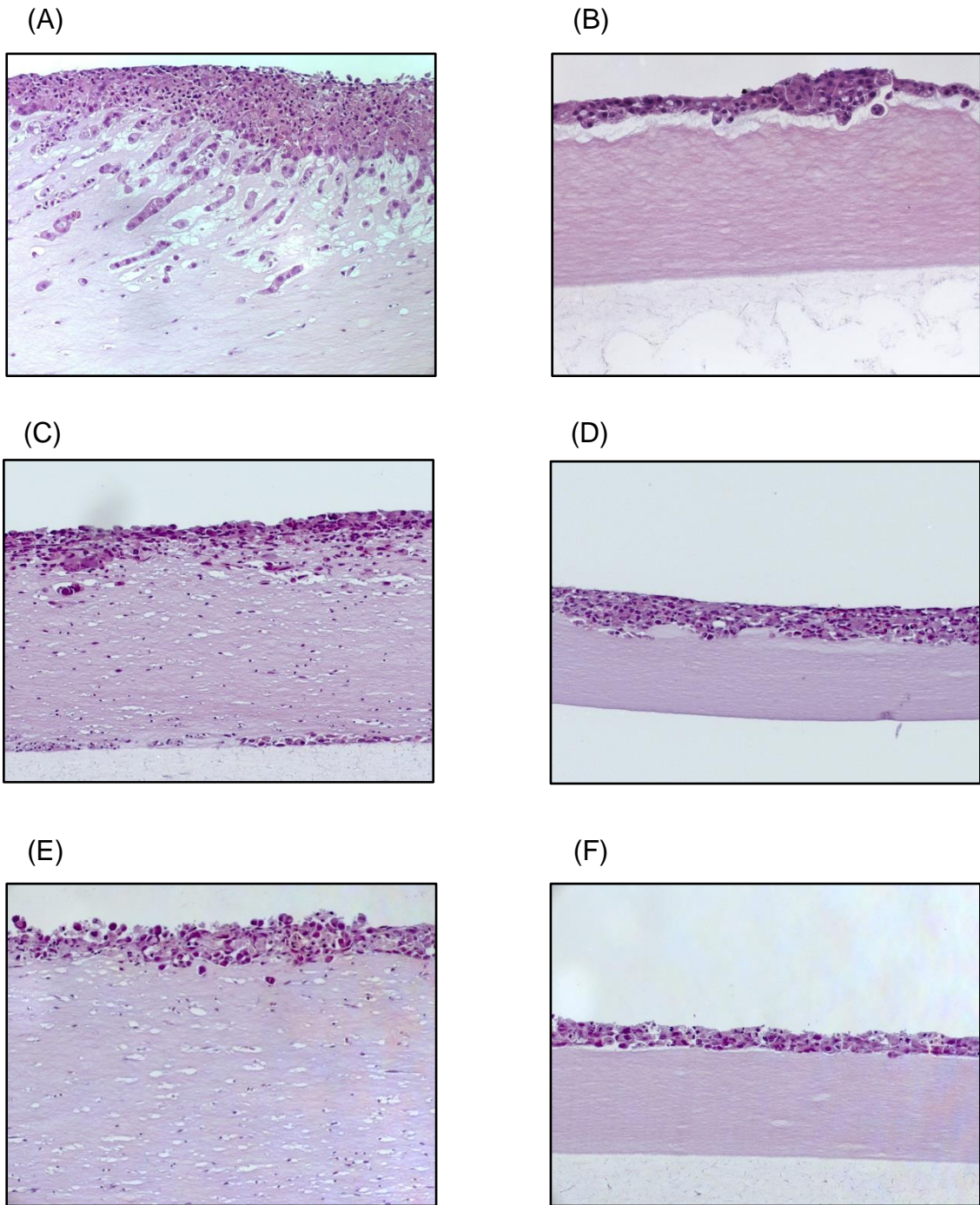


Figure 4.4 Effect of fibroblasts on invasion on different lung cancer cell invasion.

Representative cross-sections of organotypic co-cultures in the presence of MRC5 fibroblasts for (A) A549, (C) H1299 (E) H2228 lung cancer lines and in absence of MRC5 fibroblasts for (B) A549, (D) H1299 (F) H2228 cell lines. Models were produced in triplicate and cultured for 12 days before being fixed in formalin, sectioned and stained (H/E). A549 cells in combination with MRC5 fibroblasts in the ration of 1:5 produced well defined invasion. Images were taken under 20X magnification.

To further investigate how fibroblasts and tumour cells behave in the absence of a tumour-stroma interaction, A549 only and MRC5 only embedded gels were prepared and incubated for 12 days (Figure 4.5). The results showed that A549 cells degraded the gel matrix and formed clusters even though cells were homogeneously suspended in the gel mixture. The MRC5 gels did not degrade the matrix nor did they form any clusters. This suggested that the invading cells islands may consist of tumour cells only or a combination of both cell types, but would not contain MRC5 fibroblasts only.

The organotypic co-culture was further modified firstly, by seeding A549 and MRC5 cells together on top of the gel but with no MRC5 fibroblasts embedded in the gel and secondly, by seeding A549 cells only on top of an MRC5 fibroblast-embedded gel (Figure 4.5). In both circumstances A549 cells invaded into the gel which suggested that only the presence of fibroblasts either in direct or indirect contact was sufficient to stimulate cancer cells to invade. However, there was more invasion observed in the organotypic where the A549 cells were in direct contact with MRC5 fibroblasts on the top of the gel.

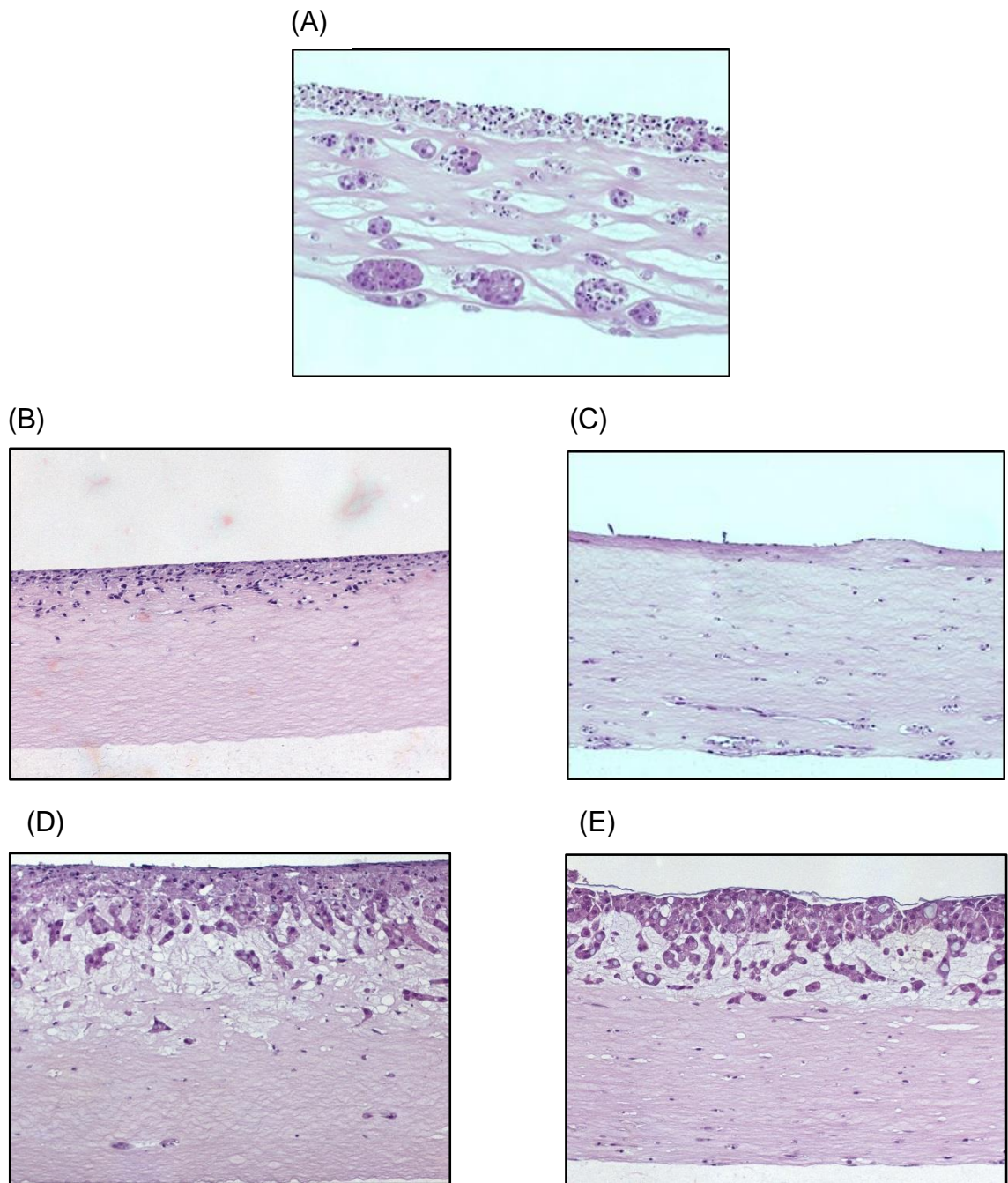


Figure 4.5 Invasive behaviour of A549 tumour cells and MRC5 fibroblasts under different organotypic conditions.

Representative cross-sections of organotypic co-cultures of A549 and MRC5 cells when seeded in different conditions. Models were produced in triplicate and cultured for 12 days before being fixed in formalin, sectioned and stained (H/E). Organotypic cross-sections (A) A549 only in the gel and on top, (B) MRC5 only on top of gel, (C) MRC5 only in the gel (D) A549 and MRC5 on the gel with blank gel and (E) A549 and MRC5 on the gel with MRC5 in the gel. Images were taken under 20X magnification.

To differentiate invading tumour cells from fibroblasts, the sections were immunohistochemically stained with MNF116 cytokeratin antibody (Figure 4.6). MNF16 cytokeratin was expressed exclusively by A549 cells which was confirmed by western blotting (Figure 4.6 D). H1299, H2228 and MRC5 did not express MNF 16 cytokeratin.

Immunohistochemical staining of A549 only gel sections showed positive staining whereas staining of the MRC5 only gel was negative. However, in co-culture organotypics of A549 and MRC5 cells, the entire epithelial layer and the invading cell islands were stained. This implies that after 12 days of incubation, there is either an alteration in the phenotype of MRC5 fibroblasts which may cause them to express MNF 116 cytokeratin after being in contact with tumour cells, or, MRC5 fibroblasts are completely replaced by proliferating A549 tumour cells. Interestingly, the MRC5 fibroblasts embedded in the gel of A549 and MRC5 co-culture, did not show positive staining for MNF 116 cytokeratin which suggests staining of MRC5, if any, is only when they are in direct contact with A549 tumour cells.

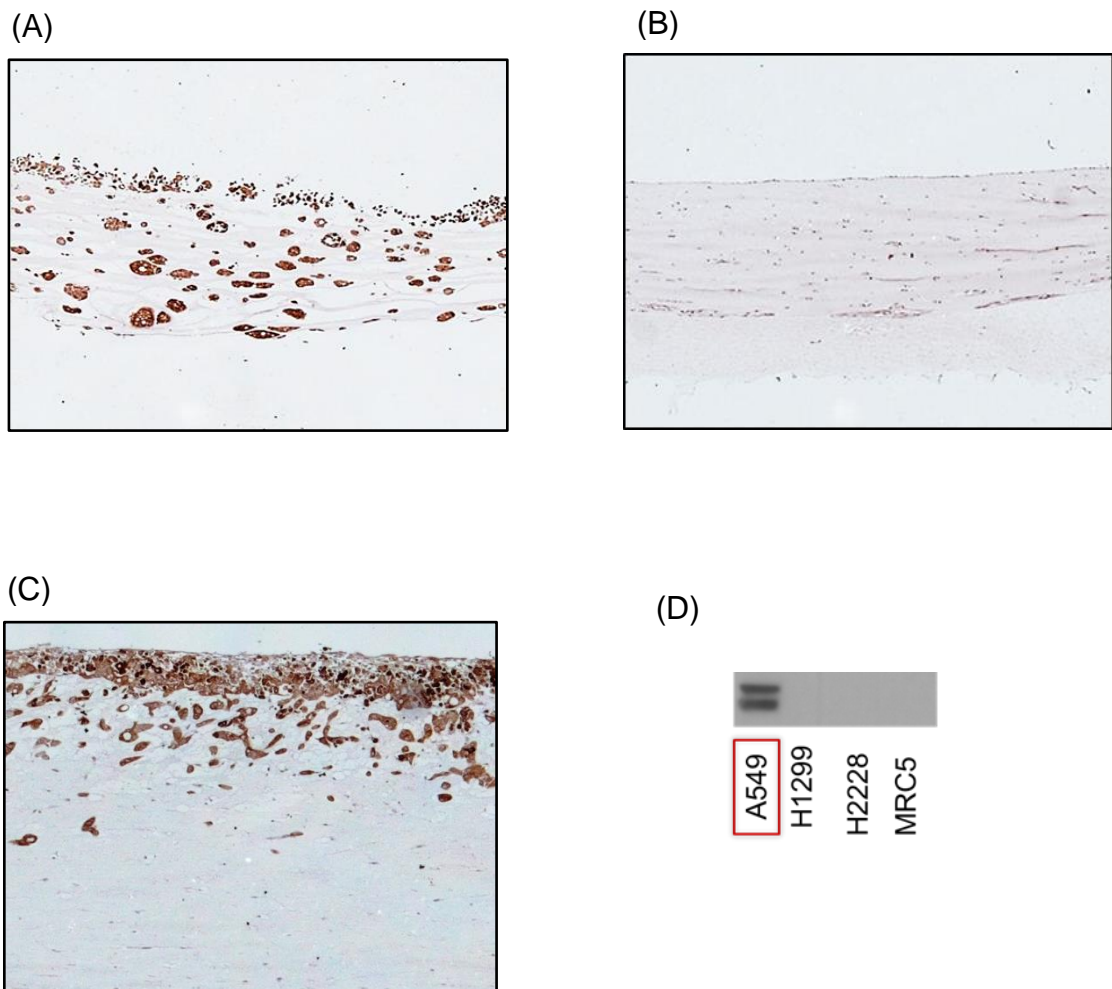


Figure 4.6 Immunohistochemical staining of organotypics with MNF 116 cytochrome.

Representative cross-sections of organotypic co-cultures of (A) A549 only, (B) MRC5 only and (C) A549:MRC5 co-culture in ratio of 1:5. Models were produced in triplicate and cultured for 12 days before being fixed in formalin, sectioned and stained. Immunohistochemical staining with MNF 116 cytochrome antibody produces a brown chromogenic reaction which highlights cancer cells. Images were taken at 20X magnification. (D) Western blot of A549, H1299 and MRC5 cell lysates to determine expression of MNF 116 cytochrome.

4.4 Effect of curcumin treatment on invasion of A549 cells

After optimising the assay conditions, the organotypic co-culture assay was used to assess whether curcumin could inhibit the invasion of tumour cells when in the presence of fibroblasts. The A549 cells and MRC5 fibroblasts were seeded in the ratio of 1:5. The KGM media added in the wells was treated with different concentrations of curcumin (0.25, 0.5, 1, 2.5 and 5 μM) with a DMSO vehicle control, and plates were incubated for 12 days. The highest dose was selected on the basis of results from cell proliferation assay. The media was changed every two days. After 12 days, the gels were processed for haematoxylin and eosin staining.

To enable the comparison of the degree of invasion between different treatment groups, a semi-quantitative method was used. Individual images across the whole sections were taken and invasion was quantified using the equation below. Imaging software ImageJ (Version 1.4) was used to score the invading area.

$$\text{Percentage Invasion} = \frac{\text{Total invading area}}{\text{Total invading area} + \text{Total non-invading area}} \times 100$$

Curcumin treatment inhibited invasion of A549 cells by 15% at a dose of 0.5 μM as compared to control (Figure 4.7). Even though the inhibition was small, it was statistically significant. Further increase in curcumin concentration did have much effect on A549 cell invasion. Curcumin concentrations of 1 and 2.5 μM inhibited cell invasion only by 18 and 19%. The highest concentration of 5 μM showed a decrease in cell invasion by 25% but was statistically non-significant. Overall, the results suggest that even though curcumin treatment inhibited A549 cell invasion, increasing concentrations of curcumin resulted in only a modest increase in this anti-invasive capacity.

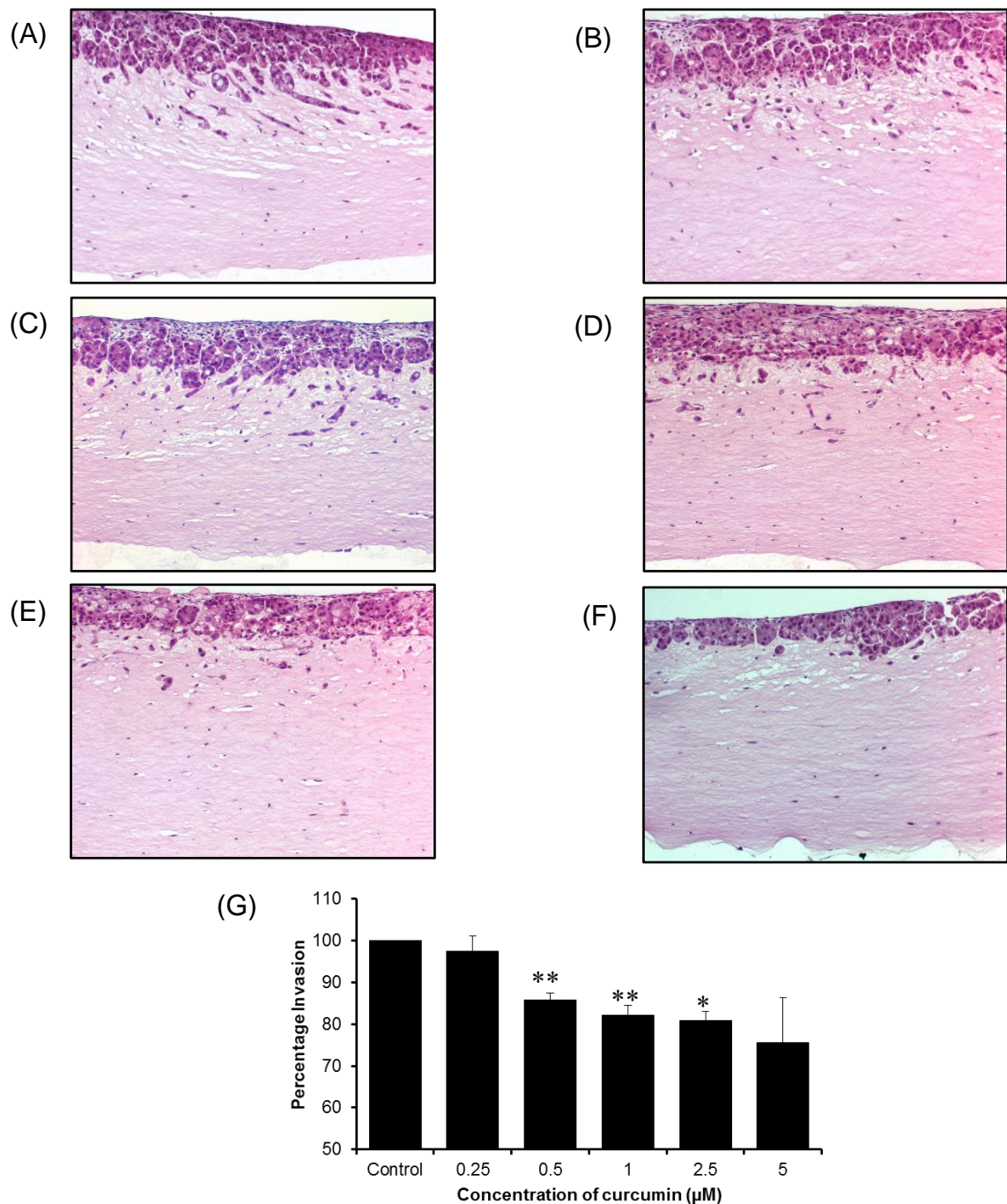


Figure 4.7 Effect of curcumin treatment on invasion of A549 cells in a 3D organotypic co-culture model.

Representative cross-sections of organotypic co-cultures treated with DMSO control or curcumin. Figures are represented as follows: (A) DMSO control, (B) 0.25 μM , (C) 0.5 μM , (D) 1 μM , (E) 2.5 μM and (F) 5 μM curcumin. Models were produced in triplicate and cultured for 12 days before being fixed in formalin, sectioned and stained. Images were taken in 20X magnification. (G) represents the mean \pm SD of three independent experiments, each performed in triplicate. Statistical comparison between the control and curcumin treatment was by Student's T-test. Statistically significant differences are indicated as * ($p < 0.05$) and ** ($p < 0.01$).

4.5 Effect of conditioned media on the HGF/MET pathway

The organotypic co-culture assay showed that fibroblasts, as an integral component of tumour stroma, play an important role in stimulating the invasive behaviour of tumour cells. The presence of MRC5 fibroblasts either in, or on top of the gel was sufficient to stimulate invasion of A549 cells, with this invasion inhibited by curcumin treatment. This suggests that there are factors secreted by fibroblasts which activate the pathways involved in cell invasion, migration and metastasis of cancer cells. Aberrant HGF/MET signalling has been frequently implicated in cell proliferation, invasion and metastasis of lung cancer. Hence, in this study we sought to determine the involvement of HGF/MET signalling and its downstream targets in invasion of lung cancer cells, and a possible mechanism of action for the anti-invasive activity of curcumin.

Serum starved A549 cells were stimulated with fibroblast-conditioned media at time points up to 4 hours. Cell lysates were analysed by Western blotting to determine the expression of the MET receptor and its phosphorylated form. Further key effector proteins downstream of MET including Akt, pAkt, MAPK and pMAPK were also analysed.

Following serum starvation of A549 cells, basal level expression of c-MET did not change significantly (figure 4.8). The expression remained unchanged after treatment with conditioned media. However, serum starvation reduced phosphorylation of the c-MET receptor at the pMET1003 and pMET1349 sites. Phospho-MET1234 was not expressed by A549 cells at a basal level. On treatment with conditioned media, the expression of pMET1003 and pMET1349 increased by 3 and 5 fold respectively compared to the serum starved control. The phospho-MET1234 site was also phosphorylated following treatment with conditioned media. Phosphorylation of the c-MET receptor was prolonged, being observed even after 4 hours of treatment. The highest effect of phosphorylation could be seen at 0.5 hours for pMET1003 and pMET1234 and at 4 hours for pMET1349.

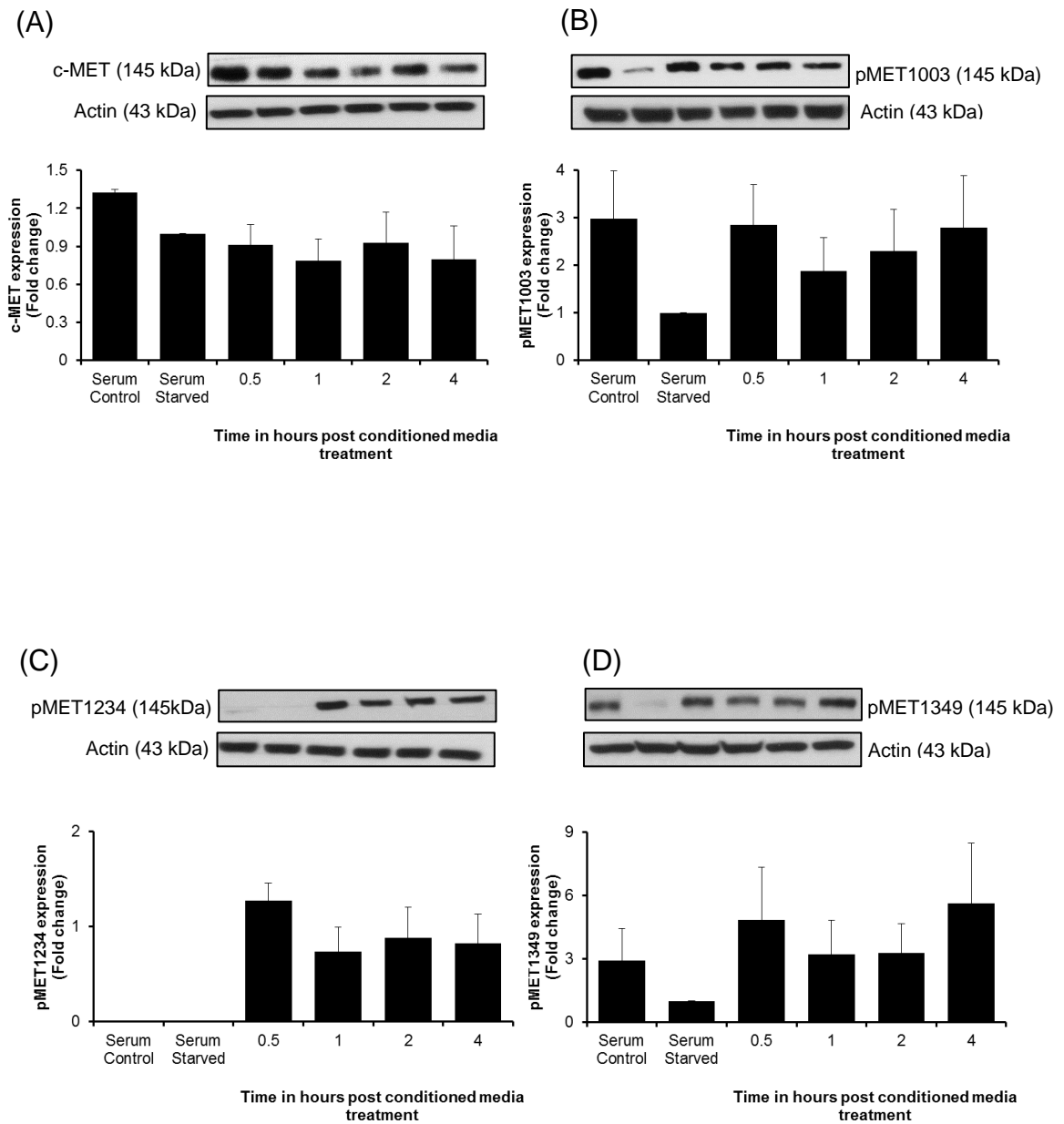


Figure 4.8 Expression of MET receptor related proteins in A549 cells treated with MRC5 conditioned media

The expression of (A) c-MET, (B) pMET1003, (C) pMET1234 and (D) pMET1349 was analysed by Western blotting. Each graph is based on densitometric analysis of Western blots after normalisation to actin. Each column represents mean \pm SD of three independent experiments. Statistical comparison between the serum starved and conditioned media treatment was by Student's T-test.

Among the downstream proteins of the HGF-MET pathway, total protein expression of Akt and MAPK did not change upon serum starvation and following treatment with conditioned media (figure 4.9). The expression of phosphorylated protein pAkt and pMAPK decreased upon serum starvation, and treatment with MRC5 conditioned media increased the expression up to 4 fold for pAkt ($p < 0.005$) and up to 8 fold for pMAPK ($p < 0.001$). The highest effect on phosphorylation was observed at 0.5 hours and was persistent even after 4 hours of conditioned media treatment.

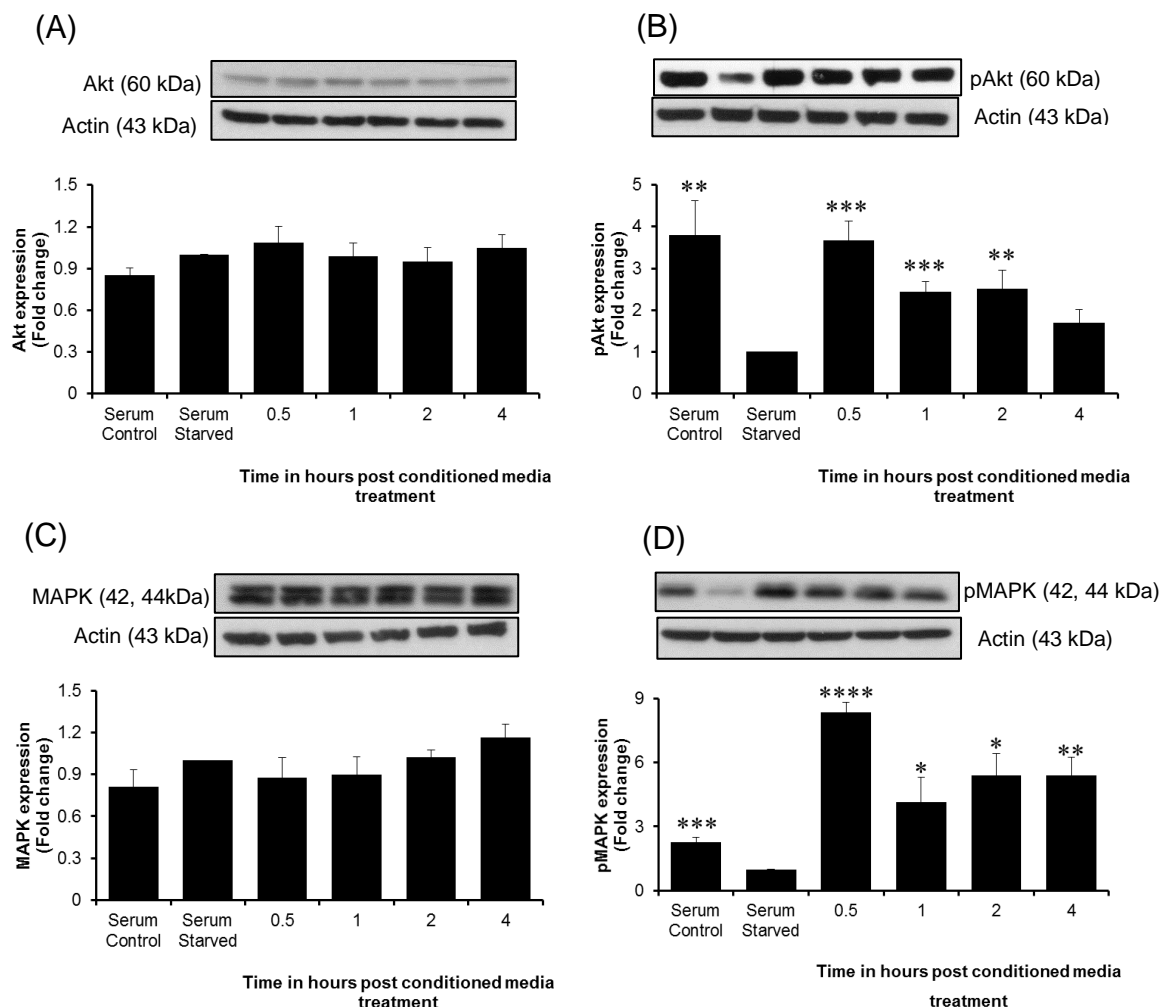


Figure 4.9 Expression of downstream proteins of HGF-MET pathway in A549 cells treated with MRC5 conditioned media.

The expression of (A) Akt, (B) pAkt, (C) MAPK and (D) pMAPK was analysed by Western blotting. Each graph is based on densitometric analysis of Western blots after normalisation to actin. Each column represents mean \pm SD of three independent experiments. Statistical comparison between the serum starved and conditioned media treatment was by Student's T-test. Statistically significant differences are indicated as * ($p < 0.05$), *** ($p < 0.005$) and **** ($p < 0.001$).

4.6 Effect of curcumin treatment on the HGF-MET pathway

Having established that conditioned media generated from MRC5 fibroblasts was able to stimulate the HGF-MET pathway, we further wanted to investigate whether curcumin was able to inhibit this stimulated HGF-MET pathway. To achieve this, we first looked at the effect of curcumin treatment on basal expression levels of MET/pMET in A549 cancer cells and MRC5 fibroblasts. This was to gain insight into how curcumin may be modulating the HGF-MET pathway to inhibit lung cancer invasion and metastasis.

Whole cell lysates from the lung cancer cell line A549 and fibroblasts MRC5 treated with 5 μ M curcumin for 1, 2, 4, 8 16 and 24 hours were analysed by western blotting to determine the expression of proteins in HGF-MET pathway.

In A549 cells, curcumin treatment did not cause any change in expression of the c-MET receptor protein. Expression of pMET1003 increased by 44% after 16 hours of curcumin treatment but the difference was statistically non-significant (Figure 4.10 B). The most predominant effect of curcumin treatment was on pMET1349, with expression significantly inhibited by 85% after 16 hours of treatment ($p < 0.001$) (Figure 4.10 C).

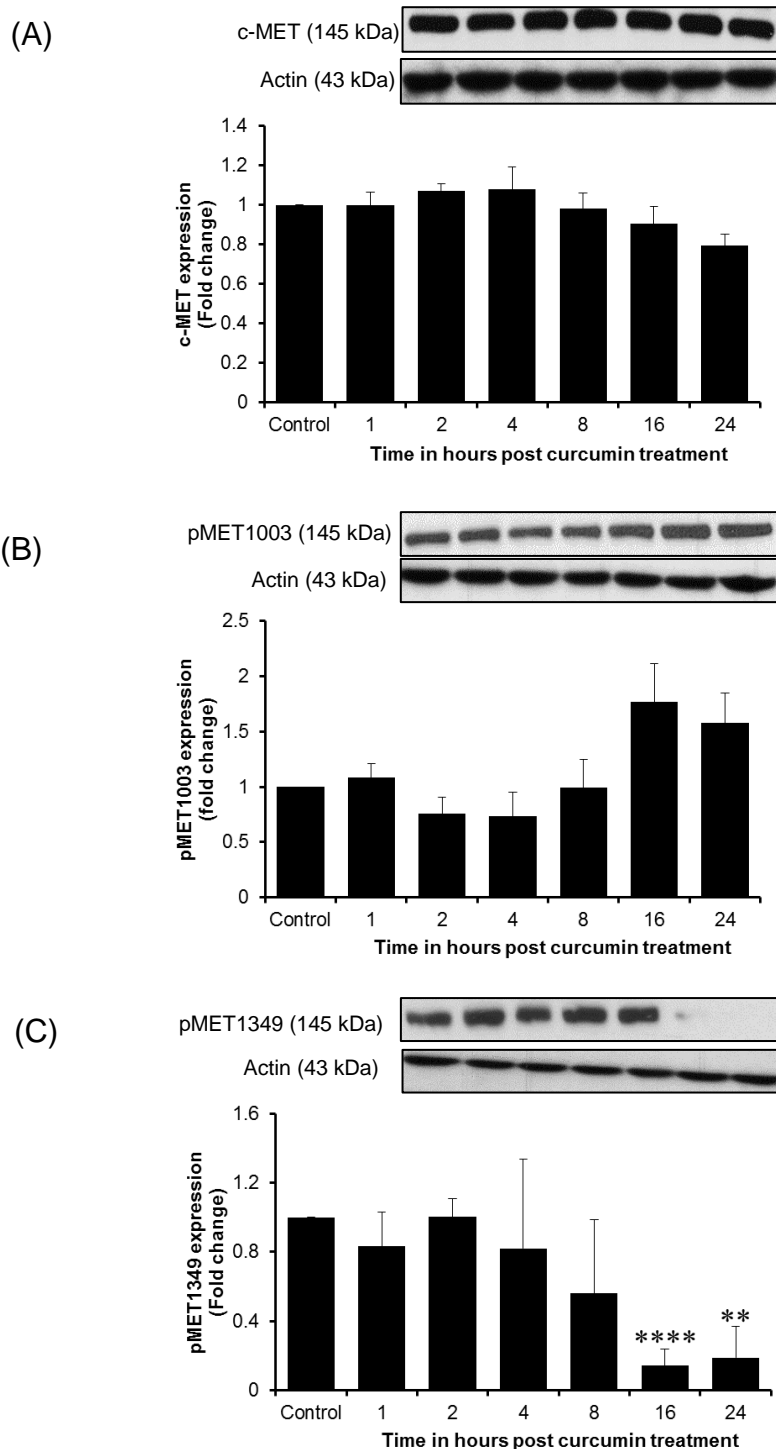


Figure 4.10 Expression of MET receptor related proteins in A549 cells treated with curcumin.

The expression of (A) c-MET, (B) pMET1003 and (C) pMET1349 was analysed by Western blotting. A549 cells were treated with DMSO vehicle or 5 μ M curcumin for 1-24 hours. Each graph is based on densitometric analysis of Western blots after normalisation to actin. Each column represents mean \pm SD of three independent experiments. Statistical comparison between the control and curcumin treatment was by Student's T-test. Statistically significant differences are indicated as ** ($p < 0.01$) and **** ($p < 0.001$).

For the downstream proteins, curcumin treatment did not change expression of Akt, MAPK and pMAPK (figure 4.11). However, expression of pAkt was inhibited by 32% after 4 hours of curcumin treatment at 5 μ M concentration.

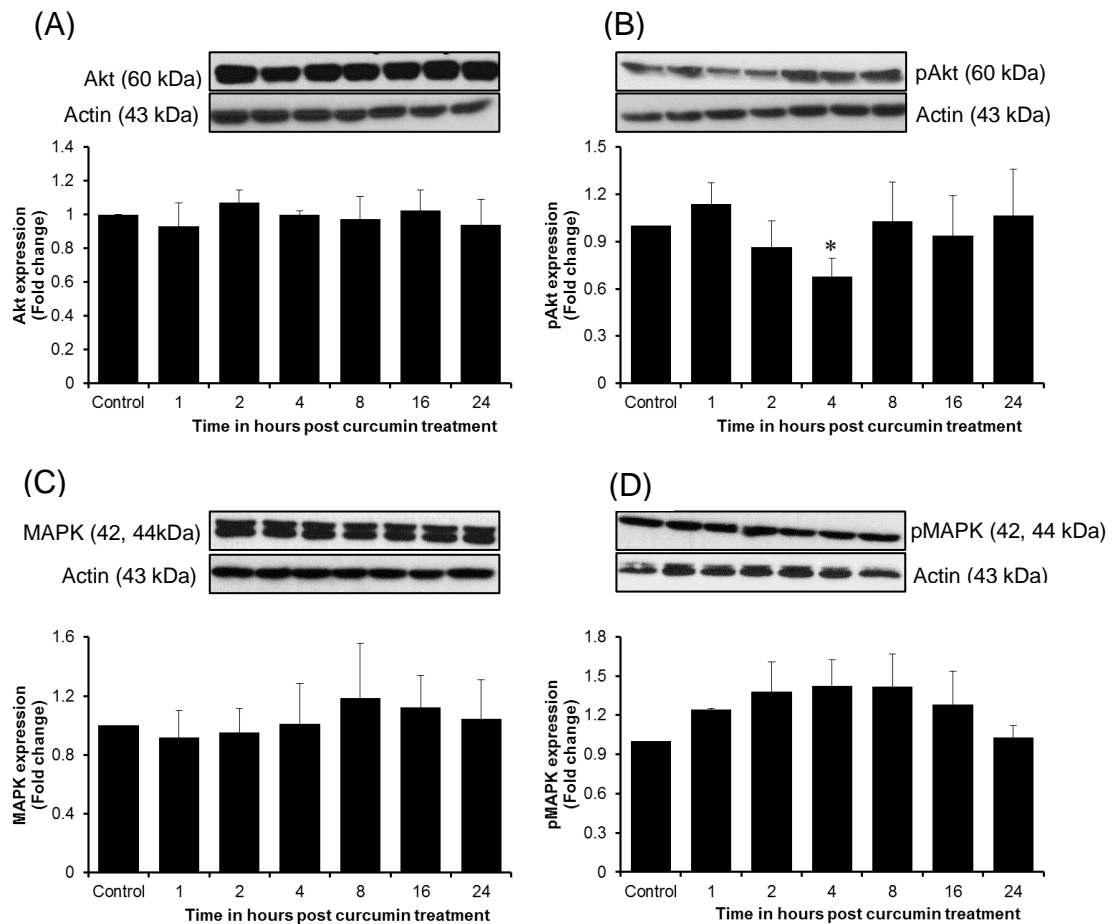


Figure 4.11 Expression of downstream proteins of HGF-MET pathway in A549 cells treated with curcumin.

The expression of (A) Akt, (B) pAkt, (C) MAPK and (D) pMAPK was analysed by Western blotting. A549 cells were treated with DMSO vehicle or 5 μ M curcumin for 1-24 hours. Each graph is based on densitometric analysis of Western blots after normalisation to actin. Each column represents mean \pm SD of three independent experiments. Statistical comparison between the control and curcumin treatment was by Student's T-test. Statistically significant differences are indicated as ** ($p < 0.01$).

In MRC5 fibroblasts, curcumin treatment did not affect the expression of c-MET receptor and pMET1003 (Figure 4.12). However, curcumin treatment reduced the expression of pMET1349 to approximately 48-68% following curcumin between 8 to 24 hours ($p < 0.005$).

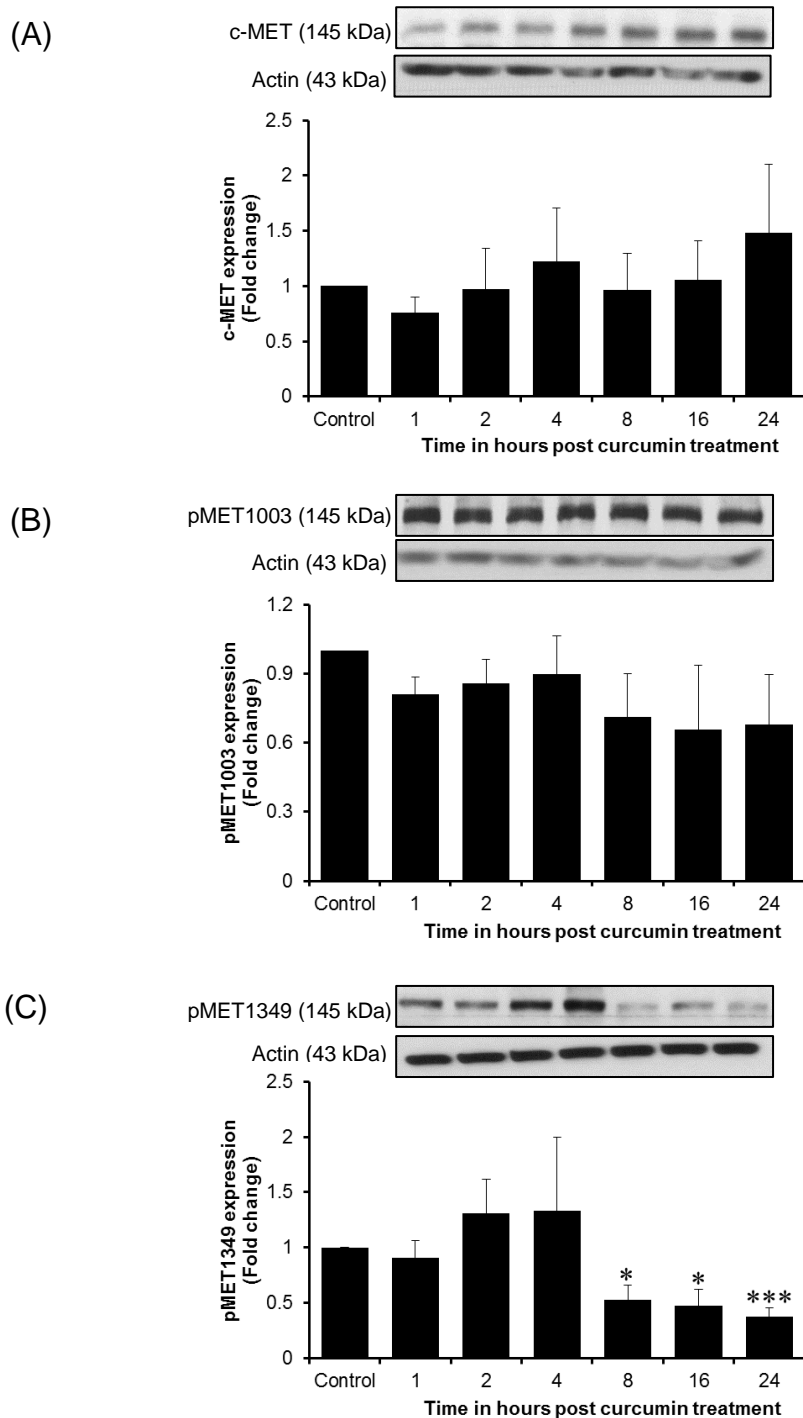


Figure 4.12 Expression of MET receptor related proteins in MRC5 fibroblasts treated with curcumin.

The expression of (A) c-MET, (B) pMET1003 and (C) pMET1349 was analysed by Western blotting. MRC5 fibroblasts were treated with DMSO vehicle or 5 μ M curcumin for 1-24 hours. Each graph is based on densitometric analysis of Western blots after normalisation to actin. Each column represents mean \pm SD of three independent experiments. Statistical comparison between the control and curcumin treatment was by Student's T-test. Statistically significant differences are indicated as * ($p < 0.05$) and *** ($p < 0.005$).

For the downstream proteins of the HGF-MET pathway in MRC5 cells, curcumin treatment did not have any effect on expression of Akt, pAkt or MAPK. Curcumin treatment significantly increased the expression of pMAPK by approximately 2.5 fold following exposure of 1 hours ($p < 0.05$). Post 1 hours, the expression of pMAPK decreased in a time dependent manner and was restored to its basal levels after 24 hours of curcumin treatment (Figure 4.13).

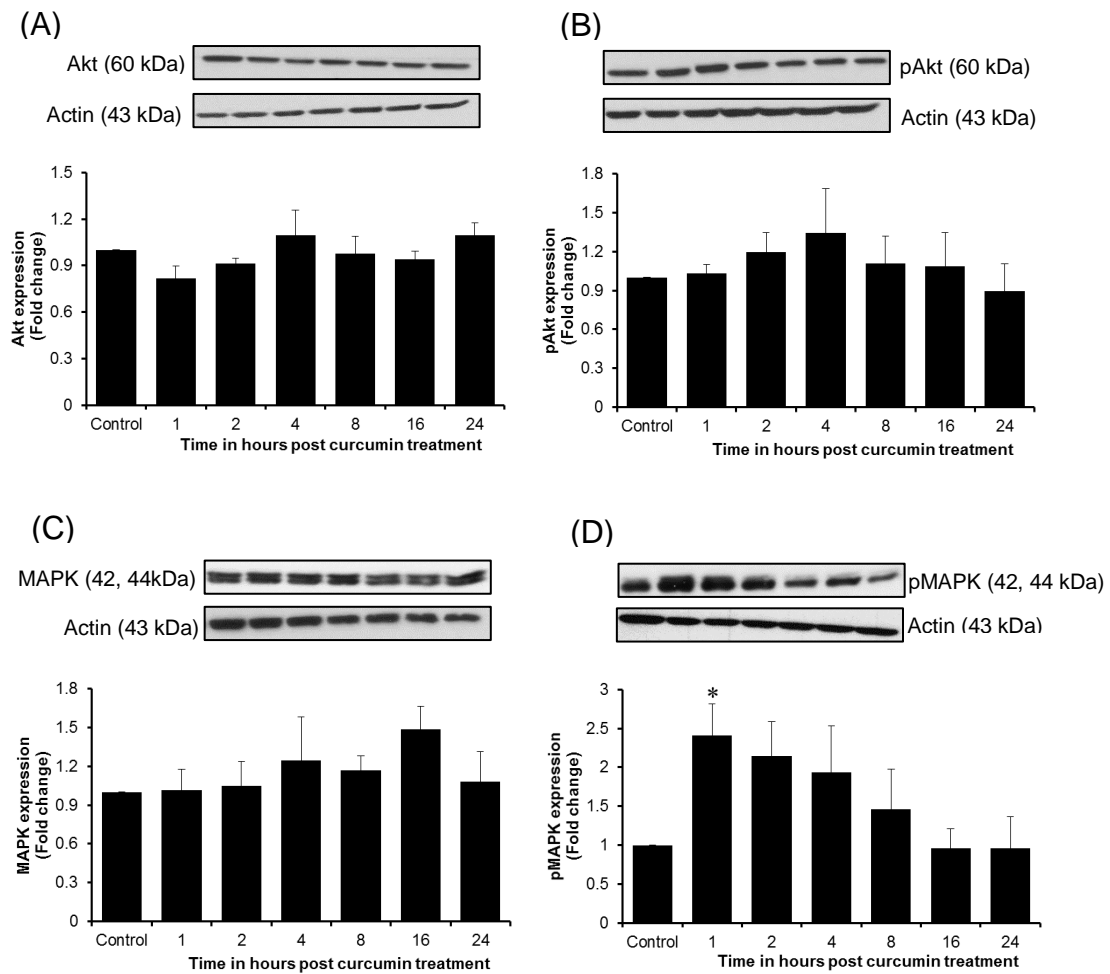


Figure 4.13 Expression of downstream proteins of HGF-MET pathway in MRC5 fibroblasts treated with curcumin.

The expression of (A) Akt, (B) pAkt, (C) MAPK and (D) pMAPK was analysed by Western blotting. MRC5 fibroblasts were treated with DMSO vehicle or 5 μ M curcumin for 1-24 hours. Each graph is based on densitometric analysis of Western blots after normalisation to actin. Each column represents mean \pm SD of three independent experiments. Statistical comparison between the control and curcumin treatment was by Student's T-test. Statistically significant differences are indicated as * ($p < 0.05$).

4.7 Effect of curcumin treatment on HGF stimulated HGF-MET pathway

From our results so far we can conclude that MRC5 conditioned media stimulates the HGF-MET pathway, and that curcumin treatment could significantly inhibit basal expression levels of important targets like pMET1349 and pAkt. However, in a tumour microenvironment, there is increased production of many growth factors (including HGF) which can cause constitutive signalling of the HGF-MET pathway. Hence, our next goal was to determine the effect of curcumin on the HGF-MET pathway specifically under HGF-stimulated conditions. To achieve this it was necessary to optimise conditions for external stimulation of the HGF-MET pathway.

4.7.1 Optimisation of HGF stimulation conditions

To determine optimal conditions for HGF-mediated stimulation of the HGF-MET pathway, two factors for consideration were concentration of HGF to be used and time of exposure. Initially a 100 ng/mL concentration of HGF was tested which was found to be too high. The concentration was then reduced to 50 ng/mL. A549 cells were serum starved overnight and the media was replaced with serum-free media containing HGF at a concentration of 50 ng/mL. The cells were harvested at time-points up to 4 hours and cell lysates analysed by western blotting.

As seen in previous results, serum starvation did not affect expression of c-MET receptor (Figure 4.14). Upon HGF treatment, expression of c-MET remained unchanged and expression of pMET1003 increased by 2 fold but the increase was not statistically significant. HGF treatment induced phosphorylation of pMET1234 which could not be detected at basal level, corroborating data observed in the conditioned media experiment. HGF treatment significantly increased expression of pMET1349 up to 3 fold as compared to serum starved expression levels ($p < 0.05$). Phosphorylation of the c-MET receptor by HGF treatment could be seen at four post treatment, with the effect being greatest at 0.25, 0.5 and 4 hours for pMET1003, pMET1234 and pMET1349 respectively.

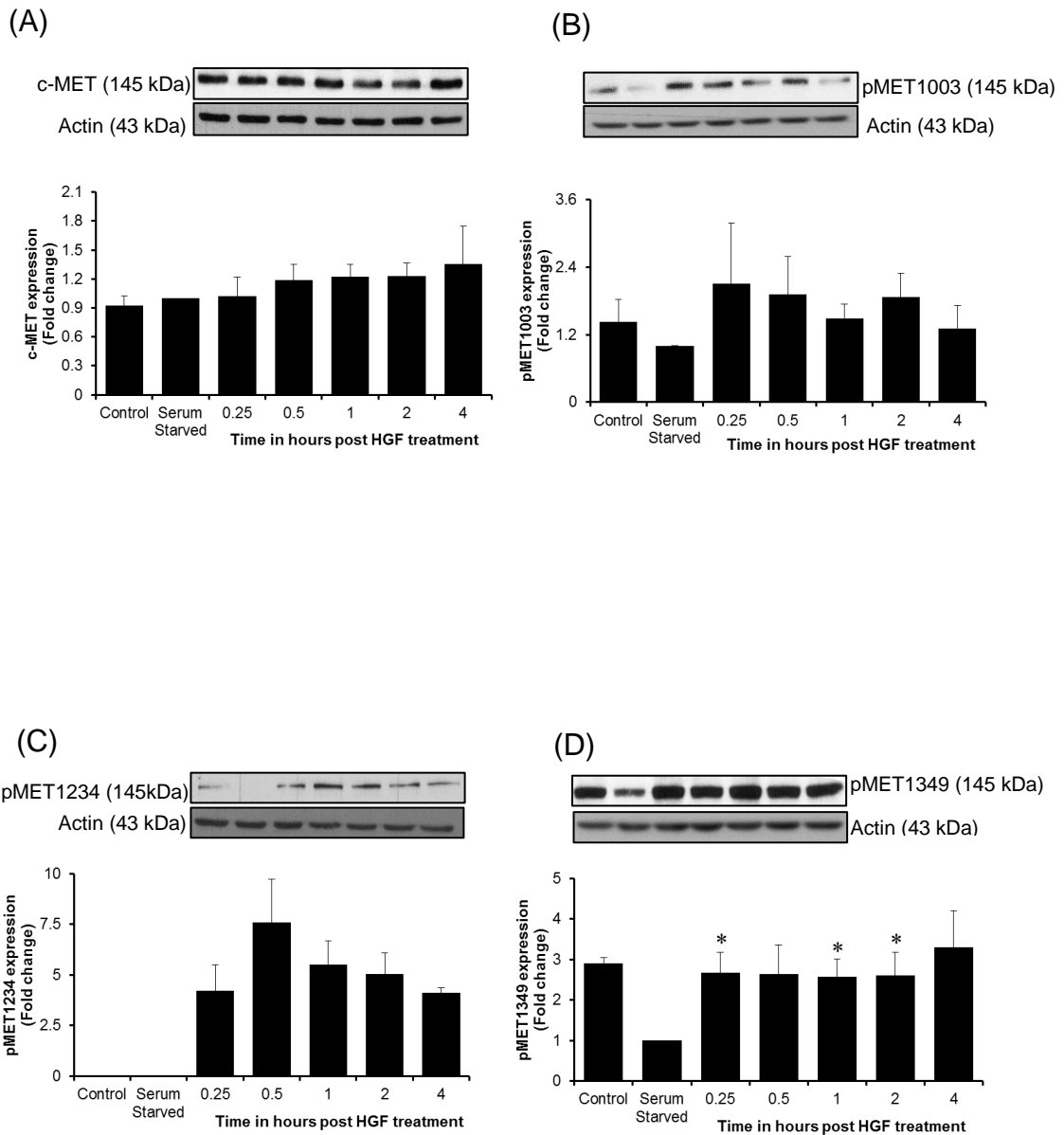


Figure 4.14 Expression of MET receptor related proteins in A549 cells after stimulation with HGF.

The expression of (A) c-MET, (B) pMET1003, (C) pMET1234 and (D) pMET1349 was analysed by Western blotting. A549 cells were treated with vehicle control or 50 ng/mL HGF for 0.25-4 hours. Each graph is based on densitometric analysis of Western blots after normalisation to actin. Each column represents mean \pm SD of three independent experiments. Statistical comparison between the serum starved and HGF (50 ng/mL) treatment was by Student's T-test. Statistically significant differences are indicated as * ($p < 0.05$).

For the downstream proteins, as previously observed in the conditioned media experiment, serum starvation did not affect total protein expression of Akt and MAPK. Expression of pAkt increased by more than 50% following HGF stimulation (Figure 4.15). The effect of HGF treatment was most pronounced on phosphorylation of MAPK which increased the expression levels by up to 9 fold after 0.25 hours of treatment ($p < 0.005$). The phosphorylation of Akt and MAPK was highest at 0.5 and 0.25 hours respectively post HGF induction, with the effect reduced in a time dependent manner.

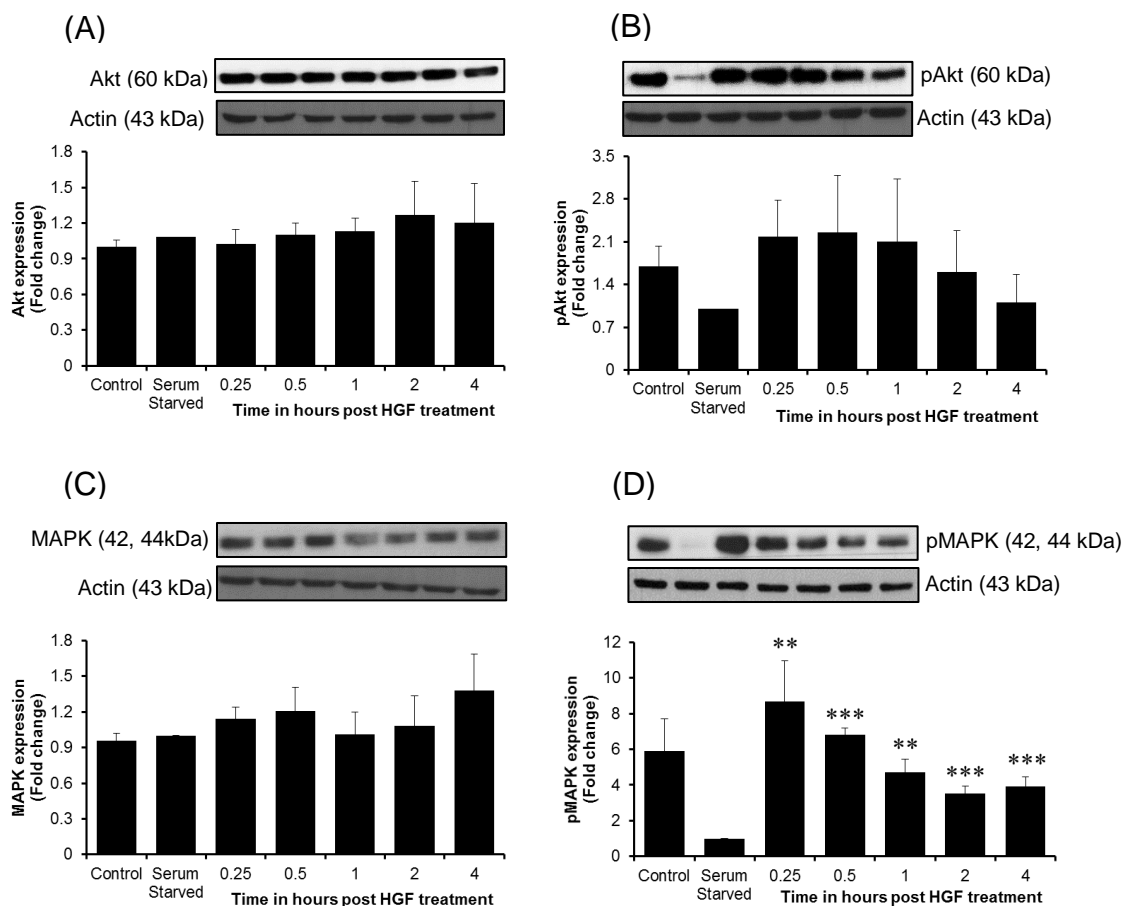


Figure 4.15 Expression of downstream proteins of HGF-MET pathway in A549 cells after stimulation with HGF.

The expression of (A) Akt, (B) pAkt, (C) MAPK and (D) pMAPK was analysed by Western blotting. A549 cells were treated with vehicle control or 50 ng/mL HGF for 0.25-4 hours. Each graph is based on densitometric analysis of Western blots after normalisation to actin. Each column represents mean \pm SD of three independent experiments. Statistical comparison between the serum starved and HGF (50 ng/mL) treatment was by Student's T-test. Statistically significant differences are indicated as ** ($p < 0.01$) and *** ($p < 0.005$).

Having optimised the conditions for HGF stimulation, A549 cells were serum starved overnight and then stimulated with serum-free media containing 50 ng/mL HGF for 0.5 hours. This was used as control. For curcumin treatments, A549 cells were pre-treated with 5 μ M curcumin for 1, 2, 4, and 8 hours and then stimulated with HGF (50 ng/mL) for 30 minutes. The cell lysates were then analysed by western blotting.

Following curcumin pre-treatment and HGF stimulation, c-MET expression in A549 cells remained unchanged (Figure 4.16). Expression of pMET1003 was significantly inhibited by 57-63% after 4 and 8 hours of curcumin treatment. This result was contradictory to curcumin treatment results in section 4.6 which caused increased in expression of pMET1003. Curcumin pre-treatment significantly inhibited phosphorylation of pMET1234 and pMET1349 by approximately 70 and 30% respectively ($p < 0.005$).

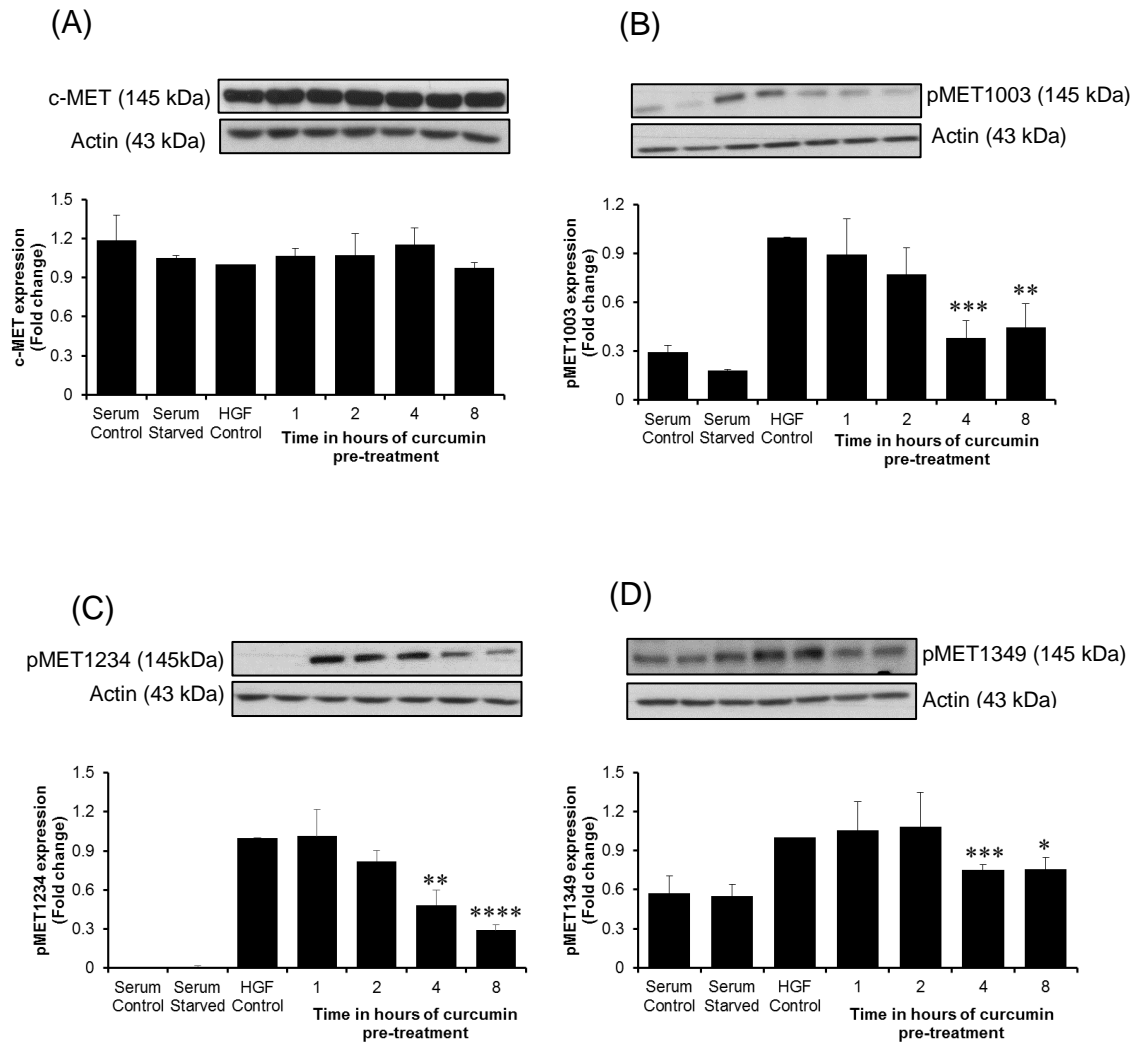


Figure 4.16 Expression of MET receptor related proteins in A549 cells after pre-treatment with curcumin and stimulation by HGF.

The expression of (A) c-MET, (B) pMET1003, (C) pMET1234 and (D) pMET1349 was analysed by Western blotting. A549 cells were pre-treated with DMSO vehicle or 5 μ M curcumin for 1-8 hours and then stimulated with 50 ng/mL of HGF. Each graph is based on densitometric analysis of Western blots after normalisation to actin. Each column represents mean \pm SD of three independent experiments. Statistical comparison between HGF control and curcumin pre-treatment treatment was by Student's T-test. Statistically significant differences are indicated as * ($p < 0.05$), ** ($p < 0.01$) and *** ($p < 0.01$).

Curcumin treatment did not cause any significant changes to downstream proteins Akt, MAPK and pMAPK (Figure 4.17). The only significant change was seen in pAkt expression which was inhibited by approximately 32% as compared to HGF control after 8 hours of curcumin pre-treatment ($p < 0.05$). These results were consistent with the curcumin treatment results in section 4.6.

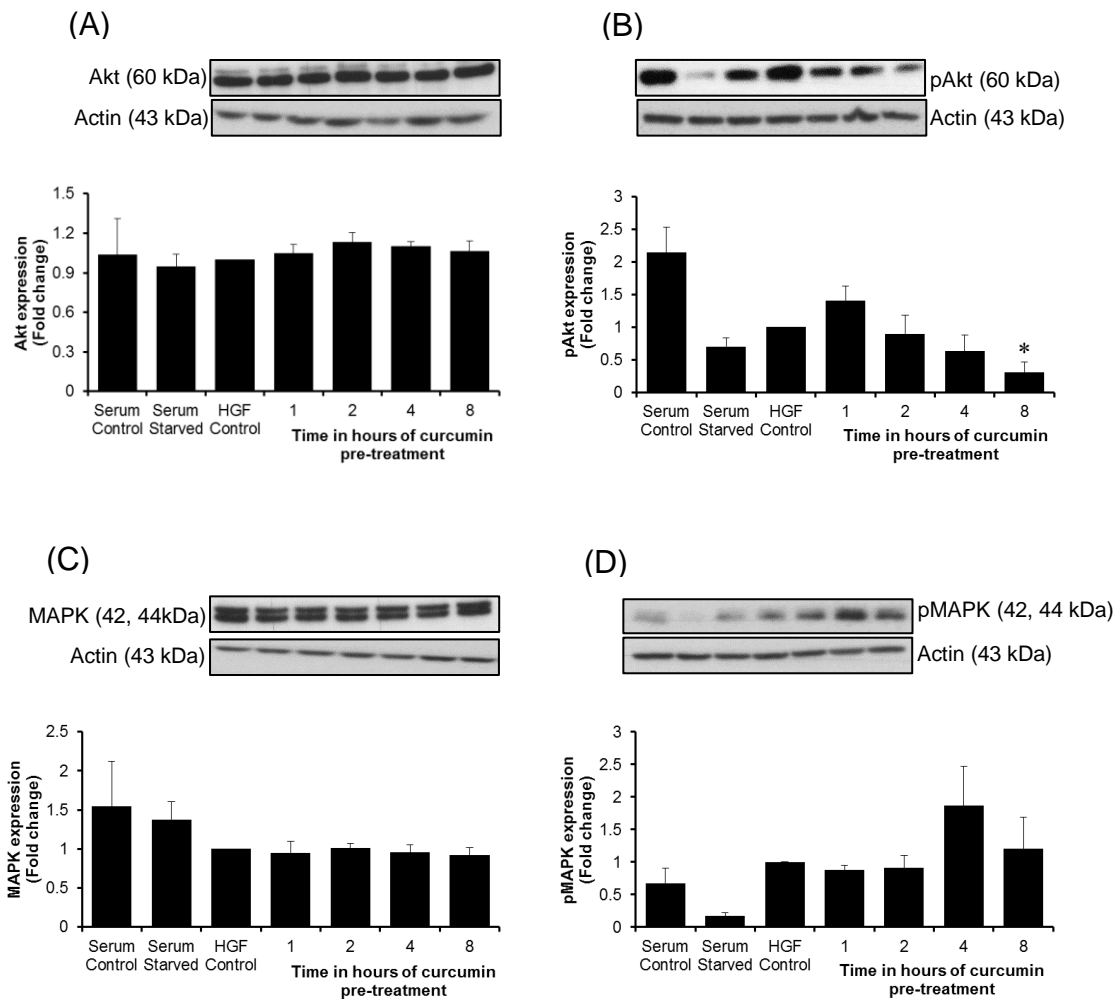


Figure 4.17 Expression of downstream proteins of HGF-MET pathway in A549 cells after pre-treatment with curcumin and stimulation by HGF.

The expression of (A) Akt, (B) pAkt, (C) MAPK and (D) pMAPK was analysed by Western blotting. A549 cells were pre-treated with DMSO vehicle or 5 μ M curcumin for 1-8 hours and then stimulated with 50 ng/mL of HGF. Each graph is based on densitometric analysis of Western blots after normalisation to actin. Each column represents mean \pm SD of three independent experiments. Statistical comparison between HGF control and curcumin pre-treatment treatment was by Student's T-test. Statistically significant differences are indicated as * ($p < 0.05$).

4.8 Effect of curcumin treatment on HGF expression in MRC5 fibroblasts

The results from the preceding sections of this chapter showed that curcumin treatment significantly inhibited phosphorylation of the c-MET receptor induced by its ligand HGF. To support our hypothesis that HGF secreted by MRC5 fibroblasts caused A549 cancer cells to invade and that curcumin treatment inhibited cell invasion by disrupting the HGF-MET pathway, we investigated the effects of curcumin treatment on HGF expression in MRC5 fibroblasts.

To measure HGF levels, MRC5 fibroblasts were seeded in a 24 well plate and treated with different concentrations of curcumin (0.25, 0.5, 1, 2.5 and 5 μM) for 6 days. On the sixth day, the media was collected to measure HGF levels by ELISA, and cell numbers were counted for each treatment group. The HGF concentration was normalised to cell number and expressed as picograms (pg) of HGF/5000 cells.

Curcumin treatment of MRC5 fibroblasts for 6 days had a significant effect on HGF levels with a reduction of approximately 70% at a very low dose of 0.25 μM ($p < 0.005$). At concentration above 0.25 μM , HGF expression could not be detected in the media of MRC5 fibroblasts.

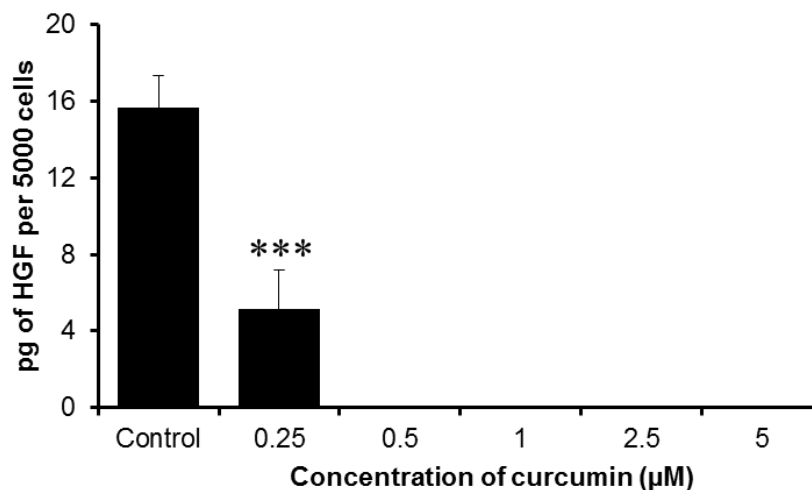


Figure 4.18 Expression of HGF in MRC5 fibroblasts after treatment with curcumin.

The expression of HGF was analysed by ELISA. MRC5 fibroblasts were incubated with DMSO vehicle or curcumin (0.25-5 μM) for 6 days. The graph represents mean \pm SD of three independent experiments normalised to cell number. Statistical comparison between control and treatment was by Student's T-test. Statistically significant differences are indicated as *** ($p < 0.001$).

4.9 Discussion

The work described in this chapter was aimed at investigating the effect of curcumin treatment on potential targets that could explain its *in vivo* efficacy. To facilitate this, *in vitro* studies including a three dimensional (3D) organotypic co-culture assay were used as models for secondary or tertiary chemoprevention. It is now well-accepted that cancer cells interact with stromal cells, extracellular matrix proteins, and neighbouring normal epithelial cells to generate feedback mechanisms that are essential for tumour progression. The traditionally used two dimensional (2D) models are helpful in testing possible mechanism hypotheses, but they fail to capture disease complexity. Often, promising results obtained from monolayer 2D cell cultures cannot be translated into *in vivo* settings. The treatment applied to a monolayer cell culture typically reaches cells without passing through any physical barriers, whereas the *in vivo* environment significantly restricts the partition of drugs throughout the entire tumour [279]. Therefore, *in vitro* 3D cancer models which allow the study of cell–cell and cell–matrix interactions has gained increasing utility for a wide variety of preventive and therapeutic investigations.

The 3D organotypic model used in the current study incorporated two crucial features of a tumour microenvironment. First is the stromal component which was represented by addition of fibroblasts, and second is the extracellular matrix (ECM) which was achieved by using hydrogels made up of collagen, matrigel and growth factors. Initial experiments were designed to determine the effect of MRC5 lung fibroblasts on A549 lung cancer cells. The results showed the critical role fibroblasts play in regulating cancer cell invasion. The importance of fibroblasts in tumourigenesis has been described in detail in the introduction section 1.3.1.4.1. The process of invasion and metastasis is dependent on contributions of the cellular and molecular biology of tumour and stromal cells in the tumour microenvironment. The fibroblasts surrounding the tumour cells have been shown to be particularly important for regulating migration and invasion of tumour cells [280]. Fibroblasts which form the non-ECM component of the tumour are responsible for the deposition of ECM components such as collagen,

fibronectin, laminin and several growth factors including VEGF, EGF, FGF, PDGF and HGF [281, 282]. It is conceivable that when fibroblasts are incorporated in to the model, the factors secreted by them activate pathways which are involved in cell invasion and proliferation. This stimulatory effect of fibroblasts has been shown in similar models involving pancreatic, breast and colon cancer cells [283]. One of the striking feature of the results shown here, is that invasion of A549 cells depended on the tumour cell: fibroblasts ratio. The invasive capacity of A549 cells increased with an increasing number of fibroblasts. These results reveal the importance of incorporating stromal components in designing and optimising future *in vitro* studies. Intriguingly, organotypic models constructed, incubated and processed in an identical fashion using H1299 and H2228 cell lines, did not exhibit much invasion. While the exact reason for this is unknown, the difference in invasive behaviour might be due to *KRAS* mutation status in these cell lines. The A549 cell line harbour a *KRAS* mutation whereas H1299 and H2228 express wild-type *KRAS* [284, 285]. Constitutive *KRAS* signalling activates downstream pathways such as MAPK and PI3K/Akt that promote cell proliferation and migration [286]. Additionally, H1299 cells do not express MET receptor [75].

Curcumin treatment of organotypics inhibited invasion of A549 cells by 25%. The results are significant considering that A549 cells were not in direct contact of curcumin treatment. It can be postulated that the hydrogels containing MRC5 fibroblasts, when are in contact with curcumin treated media, curcumin permeates through the gel which ultimately comes in contact with fibroblast and tumour cells, resulting in reduced invasion by disrupting growth factor secretion and paracrine signalling involved in the invasion process.

To elucidate a possible mechanism for the stimulatory effect of fibroblasts and inhibitory effects of curcumin treatment on A549 cell invasion, the HGF/MET pathway was investigated. At the time this work was undertaken, there was very little published evidence for the effect of curcumin on the HGF/MET pathway in lung cancer cells. A study by Lee et al. had investigated effect of curcumin on c-MET receptor using A549 xenograft model [287]. A very recent paper showed that curcumin inhibited HGF-induced EMT and angiogenesis through regulating c-MET dependent PI3K/Akt/mTOR signalling pathways in lung cancer [288]. The

c-MET receptor and its ligand HGF are frequently associated with lung cancer invasion and metastasis and its downstream signalling pathway are involved cell proliferation and differentiation [289]. Multiple studies have reported primary MET amplification in NSCLC adenocarcinoma ranging from 2% to 20% [290-292]. MET amplification leads to overexpression of the MET receptor and to activation of downstream signal transduction. In particular, the MAPK and PI3K/AKT pathways are activated [84]. HGF was also found to be overexpressed in approximately 50% of NSCLC cases [74, 293, 294]. Considering the central role HGF/MET pathway plays in lung cancer proliferation, invasion and metastasis, its role was investigated in the current work.

To determine how MRC5 fibroblasts might have stimulated A549 cell invasion in organotypics, serum starved A549 cells were treated with MRC5 conditioned media. The MRC5 conditioned media activated the MET receptor and the downstream MAPK and Akt signalling. As HGF is the only known agonist of MET receptor, it is likely that HGF secreted by MRC5 fibroblasts caused A549 cells to invade by stimulating the HGF/MET pathway.

To investigate how curcumin treatment of organotypics reduced cell invasion, A549 cells and MRC5 fibroblasts were treated with curcumin and expression of proteins in HGF/MET pathway were determined. At the basal level (i.e., under standard culture conditions), curcumin treatment significantly downregulated expression of pMET1349 in both cell types and expression of pAkt in A549 cells only. To simulate the conditions of organotypics, we next investigated whether curcumin treatment could inhibit HGF stimulation of the HGF/MET pathway in A549 cells. HGF treatment dramatically induced phosphorylation of c-MET at its major tyrosine sites 1003, 1234 and 1349. Curcumin treatment abrogated the HGF stimulated expression of pMET1349, pAkt and pMET1234.

The phosphorylation site Tyr1234 and Tyr1349 of c-MET receptor are central to its downstream activity. Tyr1234 is located within the activation loop of the tyrosine kinase domain and it activates the intrinsic kinase activity of the receptor. Tyr1349 is located in the C-terminus of MET and acts as a multifunctional docking site for intracellular adaptors that transmit signals further downstream [68]. Curcumin treatment inhibiting these sites is particularly significant

considering that most of the anti-MET therapies (cabozantinib, crizotinib, foretinib, tivantinib) currently under clinical investigation for lung cancer have similar targets [295].

HGF has been identified as a fibroblast-derived factor which is capable of causing epithelial cell scattering and stimulating the migration and invasion of cancer cells [296, 297]. Having established the effect of curcumin on the MET receptor, we further investigated the effect of curcumin on its ligand HGF. From the literature, HGF is not expressed by A549. Therefore, the curcumin effect on HGF levels was tested only in MRC5 fibroblasts. HGF levels were significantly reduced at a very low concentration of curcumin (0.25 μ M) after 6 days of treatment. This concentration is less than the 0.4 μ M concentration achieved in mouse lungs following a single oral dose in the pharmacokinetic study. The intervention pathways that been followed in developing anti-MET therapies include either inhibiting HGF from binding to MET or inhibiting activation at tyrosine kinase domain. In our study, curcumin treatment not only targeted the activation of MET receptor but also inhibited expression of its ligand HGF.

Blocking HGF or c-MET activation is emerging as an important target as it is highly expressed in a wide variety of tumours including lung. In A549 cells, c-MET silenced by siRNA inhibited cell growth and viability and also substantially inhibited HGF induced phosphorylation of MET and Akt [70]. This validates the role of c-MET as therapeutic target in lung cancer. pAKT is a crucial target downstream of c-MET that regulates cell proliferation, survival, migration, and cell invasion into the stroma. In our study curcumin treatment inhibited pAkt expression in A549 cell line under different experimental conditions such as basal expression, conditioned media induced stimulation and HGF induced stimulation.

The current work has some limitations but presents further opportunity to enhance our knowledge of the potential for curcumin in a preventive setting. The organotypic co-culture assay can be further used to investigate markers of epithelial mesenchymal transition (EMT), angiogenesis and invasion such as β -catenin, E-cadherin and matrix metalloproteinase (MMPs). The quantitation method could be improved by using techniques such as zymography and

immunofluorescent laser detection which can be more precise and accurate in determining tumour cell invasion. The model can be further optimised by including other stromal components such as endothelial cells and immune cells. Patient derived tumour cells and cancer associated fibroblasts can be used to produce personalised tumour facsimiles for individual patients and to test the utility of curcumin. This model can be used in conjunction with genetically manipulated tumour and stromal cells targeting the HGF and MET protein to further investigate their role in a tumour microenvironment-like settings. Further work should be aimed at investigating the exact mechanisms of action by which curcumin inhibits HGF and c-MET.

Overall the results from this chapter show that curcumin is able to inhibit KRAS mutant lung tumour cell invasion by targeting the HGF-MET pathway and its downstream signalling pathways. Inhibition of HGF production by stromal fibroblasts was achievable at concentrations observed in mouse lung following a 70 mg/kg dose, which is equivalent to a dose of 2 g/daily in humans. Current therapeutics in trials targeting the MET pathway in lung cancer include cabozantinib, crizotinib, foretinib, tivantinib and are associated with significant toxicities such as fistula, respiratory failure, haemorrhage, sepsis, and cardiopulmonary failure making further investigation of curcumin as a potential MET inhibitor attractive within a preventive setting.

5 *In vivo* efficacy of Meriva in lung cancer xenograft

5.1 Introduction

For successful translation of any potential chemopreventive or chemotherapeutic compound from the preclinical to clinical stage, extensive *in vivo* studies are required to establish safety, the pharmacokinetic/pharmacodynamic relations and to evaluate the mechanism of action. These findings are used to estimate clinical dosing regimens and determine safety margins and toxicity. *In vivo* models provide a greater understanding of how a new drug acts and undergoes metabolism in a biological system, which cannot yet be recapitulated in *in vitro* systems. With the knowledge of both pharmacologically active concentrations *in vitro* and target tissue levels achievable *in vivo*, conclusions can be drawn regarding whether compounds will be active in efficacy models. These models also allow drugs to be administered via a regimen most likely to mimic human dosing strategies. In the case of curcumin, oral administration to animals can thus be compared to capsule consumption in humans.

The curcumin pharmacokinetic studies described in this thesis (Chapter 3) at both, high and low doses, suggested that Meriva furnishes higher metabolite and parent curcumin levels in mouse plasma and lungs as compared to unformulated curcumin. Curcumin also showed potent anti-proliferative activity on lung cancer cells *in vitro* (Chapter 4). Although preclinical efficacy of curcumin has been demonstrated in several *in vivo* studies (Section 1.4.2), there are no published studies investigating the efficacy of Meriva against lung cancer. Hence, it was reasonable to investigate the efficacy of Meriva in an *in vivo* model.

Having established the important role that fibroblasts play in the tumour microenvironment using an organotypic model (Chapter 4), it was decided to incorporate fibroblasts in combination with tumour cells in an *in vivo* xenograft model. The conditions of a 1:5 ratio of tumour cells to fibroblasts were extrapolated to the *in vivo* study.

5.2 Effect of MRC5 fibroblasts on A549 lung cancer cells growth in nude mice

To extrapolate the findings from our in vitro organotypic assay, A549 cells with or without MRC5 fibroblasts and MRC5 fibroblasts on their own were inoculated subcutaneously in to nude mice with 5 animals per group. After tumours first became palpable they were measured every 5 days.

As expected, MRC5 fibroblasts alone did not form any tumours after 30 days of inoculation and were found to be non-tumorigenic. The A549:MRC5 co-culture xenografts grew at a significantly higher rate compared to A549 cells alone ($p < 0.05$). At the end of 37 days post inoculation, the mean tumour volume for A549:MRC5 xenografts was $760 \pm 104 \text{ mm}^3$ whereas the mean tumour volume for A549 cells only was $413 \pm 102 \text{ mm}^3$.

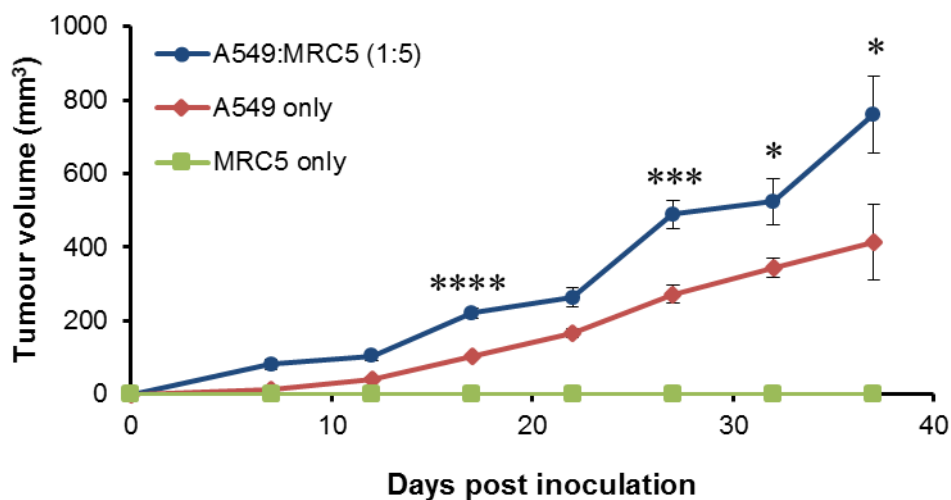


Figure 5.1 Effect of MRC5 fibroblasts on growth of A549 tumour cells in nude mice

Animals were divided into three groups ($n=5$). Tumour formation was initiated by inoculating mouse flanks with A549 cells (8×10^5), MRC5 fibroblasts (4×10^6) or a combination of both in a ratio of 1:5 (4.8×10^6). Tumour volumes were measured every 5 days once they became palpable. Graph represents the volume of tumours over 37 days. Data points are the mean \pm SEM of tumour volumes. Statistical comparison between the A549:MRC5 and A549 only group was by Student's T-test. Statistically significant differences are indicated as * ($p < 0.05$), *** ($p < 0.005$) and **** ($p < 0.001$).

5.3 Determination of cell population sub-type in co-culture xenograft tumours

The results from the organotypic co-culture assay described in the previous chapter suggested that fibroblasts in the epithelial layer might be replaced by tumour cells after incubation with tumour cells for 12 days. To ascertain whether this may also be the case in vivo, the tumours from mice inoculated with the 1:5 ratio of A549:MRC5 cells was analysed by flow cytometry to determine the population of each cell type.

A single cell suspension of xenograft tumour samples obtained from three different mice after 37 days of growth was prepared and stained with MNF 116 cytokeratin antibody, a marker for tumour cells, as described in sections 2.2.7.1 and 2.2.7.2. The samples were then analysed by flow cytometry. The results showed that $92.3 \pm 0.6\%$ of the cell population consisted of tumour cells (Figure 5.2). Furthermore, the haematoxylin and eosin stained sections when observed under the microscope, showed tumour cells to be the major cell population, confirming the findings from flow cytometry (Figure 5.3). Apart from tumour cells, other cell types observed included stromal cells (seen mostly in the periphery of the tumour section), basophils and neutrophils. The slides were observed with the help of histopathologist Dr David Moore.

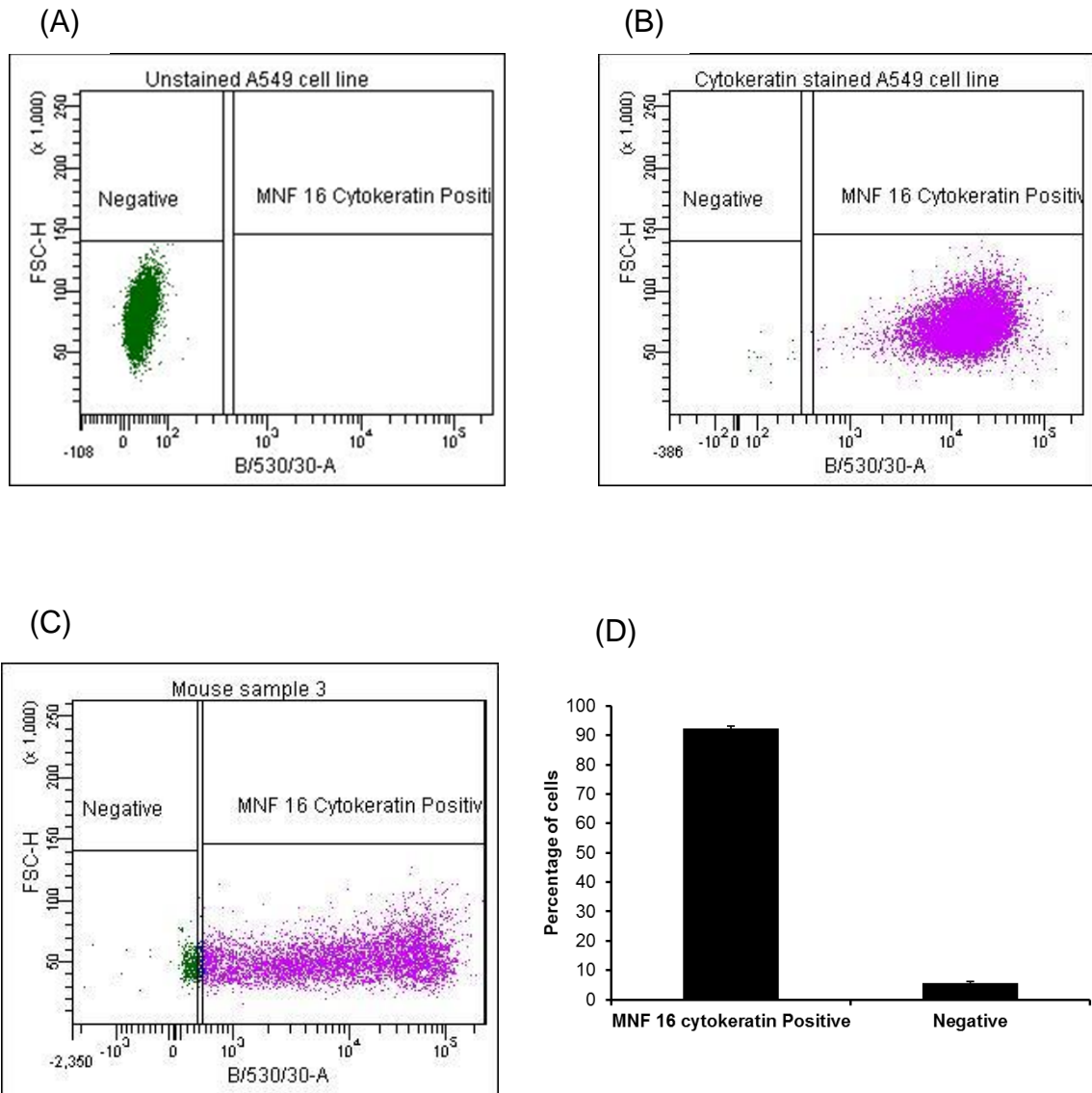


Figure 5.2 Representative flow cytometry scatter plots for the MNF 116 cytokeratin assay in mouse tumour xenograft cells.

The cells were stained with primary MNF 16 cytokeratin and secondary FITC conjugated antibody. (A) Negative control showing unstained A549 cells. (B) Positive control showing A549 cells stained with MNF 116 cytokeratin. (C) Representative scatter plot from one of the mouse samples showing tumour cells stained positively and negatively with MNF 116 cytokeratin. (D) Each column represents the mean \pm SEM of three independent mouse tumour samples collected after 37 days of growth.

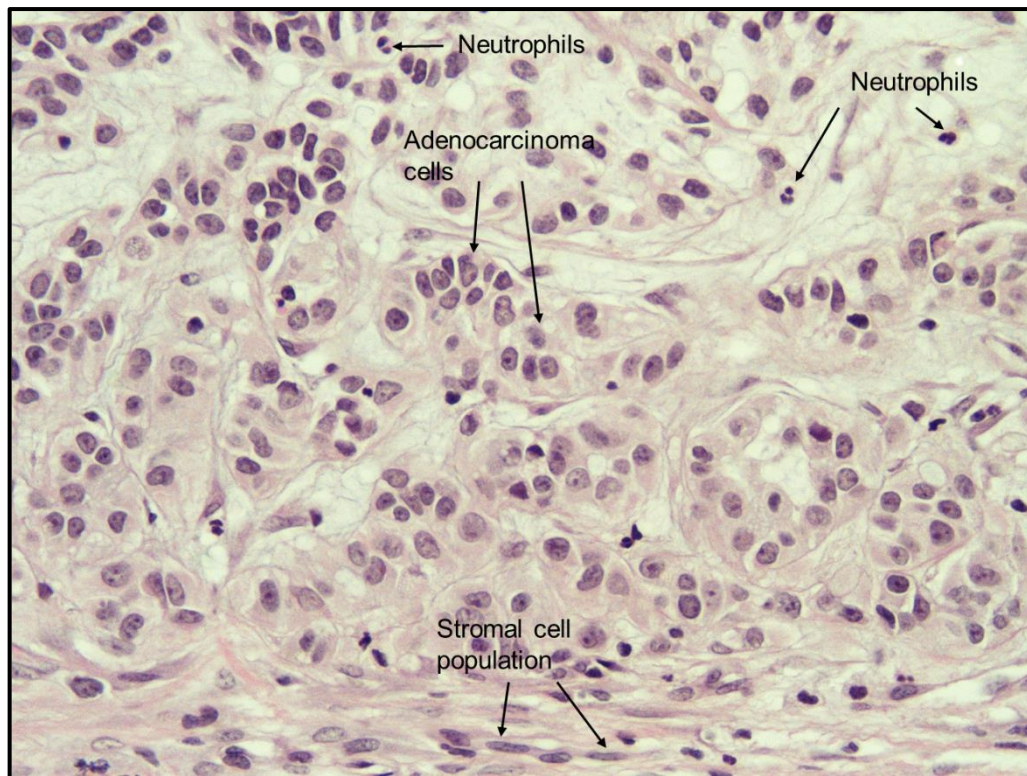


Figure 5.3 Histological appearance of A549:MRC5 (1:5) co-culture xenograft tumours.

Paraffin embedded sections of tumours from co-culture xenograft tumour bearing nude mice. The tumours were allowed to grow for 37 days. Arrows indicate different cell sub types. Cell types were identified with the help of histopathologist Dr David Moore. Image taken at 40x magnification.

5.4 Effect of Meriva consumption on A549:MRC5 co-culture xenografts in nude mice.

Animals were divided into two groups of ten mice each. A total of 4.8×10^6 A549 and MRC5 cells in the ratio of 1:5 were suspended in a 100 μ L mixture of matrigel and serum free media (1:1, v:v) and subcutaneously injected into the right dorsal flank of the mice under isoflurane inhalation anaesthesia. Once the tumours become palpable (7 days post injection) animals were randomly distributed to study diet groups and this was subsequently designated as day 0. The treatment groups were AIN93G diet supplemented with Meriva (0.226%) and the equivalent control dose of Epikuron (0.180%). The dose was selected on the basis of completed clinical studies of Meriva for inflammatory conditions which used dose of 1-2 grams per day. The dose was calculated using body surface area factor and assuming a 20 gram mouse eats 3 grams of diet daily. Tumour volume was measured every 5 days using digital Vernier callipers. The study was initially planned to monitor tumour growth for 35 days based on the preliminary experiments. However, at day 28 two animals from control group had to be culled due to tumour ulceration. Therefore, the study duration was reduced to 30 days. As all the mice from the Meriva were still alive until day 30, the study was continued as a survival study on their respective diets and the mice culled when they showed signs of illness, or, when the tumour size reached 17 mm in diameter. The objectives were to evaluate the efficacy of Meriva against the growth of lung tumour xenografts and to determine whether consumption of the Meriva-containing diet provided any survival benefits.

Dietary Meriva inhibited tumour growth and the difference could be seen as early as 10 days when compared to control diet. This trend continued until day 30, when Meriva caused a significant decrease in tumour volume compared to animal on control diet when compared for their growth curves ($p < 0.03$). However, the difference between single data points was found to be non-significant when compared by student's *t* test. At day 30, tumour volumes in the Meriva group were reduced by 29.5% in comparison to control (Figure 5.4). Murine body weight was not affected by Meriva over the course of the study, suggesting that Meriva did not cause any toxicity that stopped the animals from eating (Figure 5.5).

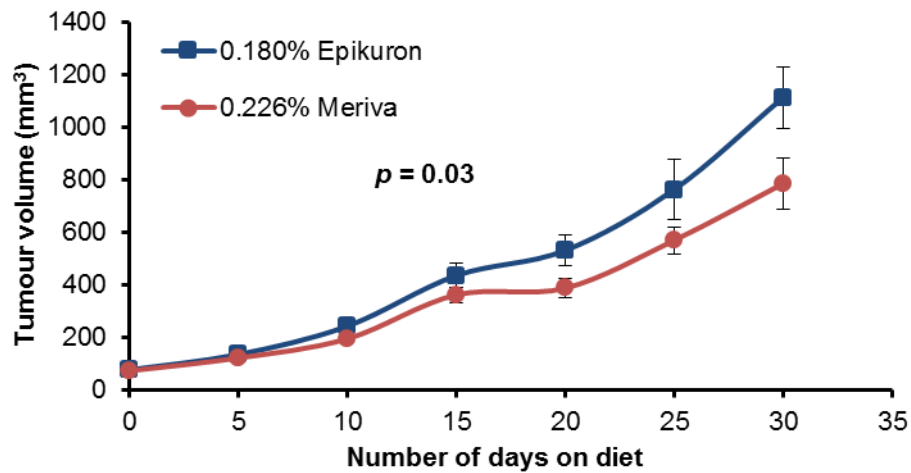


Figure 5.4 Effect of dietary Meriva or Epikuron on tumour growth in nude mice.

Animals were divided into two equal groups (n=10). Tumour formation was initiated by inoculating the flank of each mouse with A549 and MRC5 cells (4.8×10^6) in 1:5 ratio. One week after tumours became palpable, animals were switched to study diet consisting of either Meriva (0.226%) or control Epikuron (0.180%) diet and this point was designated as day 0. At day 30, there were 8 mice in Epikuron group and 10 in Meriva group. Tumour volumes were measured every 5 days. Data points are the mean \pm SEM of tumour volumes for either control or treatment. Statistical comparison was by a mixed effects linear regression. The difference between growth curves for Epikuron and Meriva diet was statistically significant.

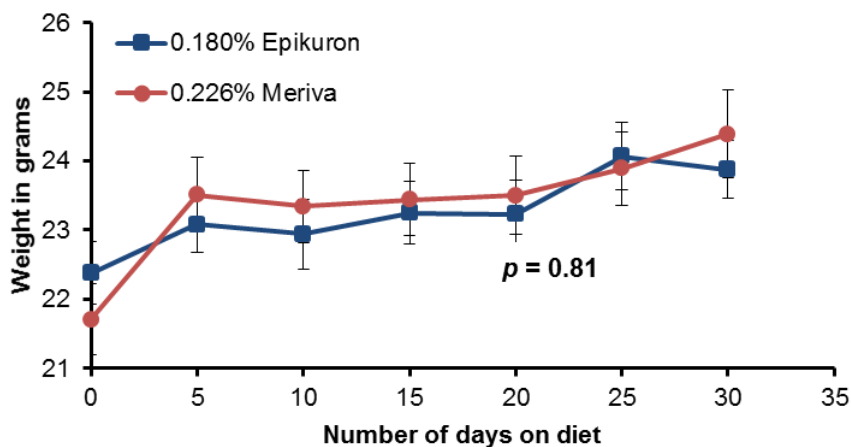


Figure 5.5 Effect of dietary Meriva or Epikuron on body weight in nude mice.

Body weights were measured every 5 days. Graphs represent body weights of mice over 30 days on Meriva or control Epikuron diet. Values represent the mean \pm SD. On day 30 there 8 mice in Epikuron group and 10 mice in Meriva group. Statistical comparison was by a mixed effects linear regression.

After determining the effect of Meriva on tumour volumes for 30 days, the animals were observed to determine whether Meriva imparted any survival benefits. For the survival, Kaplan-Meier analysis was used to compare the survival of tumour bearing nude mice on control and Meriva diets (Figure 5.6). The mice were culled when they showed signs of illness or when the tumour size reached 17 mm in diameter. The median survival time for animals on Meriva diet (39 days) was higher than that of animals on Epikuron diet (33 days) and the difference was statistically significant by Log-rank test. The last mouse in the Meriva treated group survived 2 weeks longer than the last control mouse.

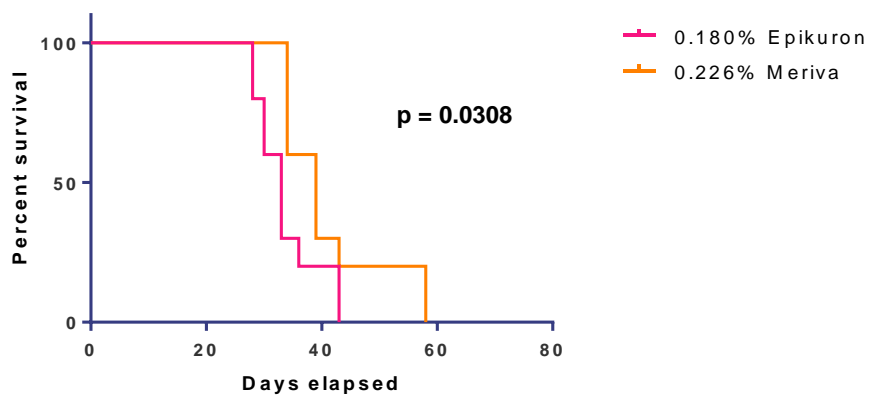


Figure 5.6 Kaplan-Meier survival curves for nude mice on 0.226% Meriva diet or control Epikuron diet.

n = 10 mice per group. Statistical comparison was by Log-rank test.

5.5 Modulation of HGF/MET pathway and downstream proteins by Meriva in tumour tissue

The *in vitro* data detailed in Chapter 4 suggested that curcumin treatment downregulated the expression of pMET1234, pMET1349 and pAkt in A549 cells when treated under different experimental conditions. Therefore, the expression of these proteins in xenograft tumours of Meriva treated and control animals was investigated. One of the animals in the Meriva group was found dead in the cage and was stored in formalin. Hence, samples from nine mice from each group were available from this group for Western blot analysis.

As observed in the *in vitro* experiments (Section 4.6), Meriva treatment did not affect the expression of c-MET protein in the tumours (Figure 5.7). Intriguingly, no expression of any of the phosphorylated MET receptor was detected in either of the treatment groups. For the downstream proteins, MAPK and pMAPK, the levels of both were downregulated by approximately 40 and 30%, respectively however, only the change in MAPK was statistically significant (Figure 5.8). These results contradict the previous *in vitro* data where curcumin treatment did not affect the expression of total MAPK protein. However, there was a non-significant change in the expression of Akt whereas expression of pAkt was reduced significantly by more than 50% in Meriva treated tumour tissues relative to control mice (Figure 5.8). The ratio of pAkt/Akt expression between controls and treated animals was also compared, revealing a significant difference of 43% in treated compared to control groups. This suggests that the decrease in pAkt expression was not mediated purely by changes in total Akt expression.

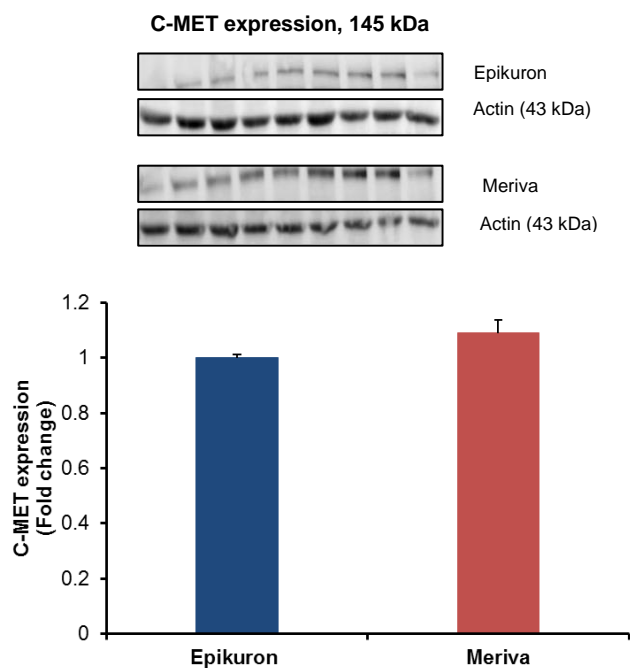


Figure 5.7 Effect of Meriva on the expression c-MET in A549:MRC5 co-culture xenograft tumours in nude mice

Protein levels were measured after sacrificing the animals which received either 0.226% w/w Meriva or 0.180% w/w Epikuron by western blotting of tumour xenograft tissue for C-MET. Each graph is based on densitometric analysis of Western blots after normalisation to actin. Each lane represents single animal. Each column represents the mean \pm SEM of 9 animals for the Meriva and Epikuron group. Statistical comparison between the control and Meriva treatment was by Student's T-test.

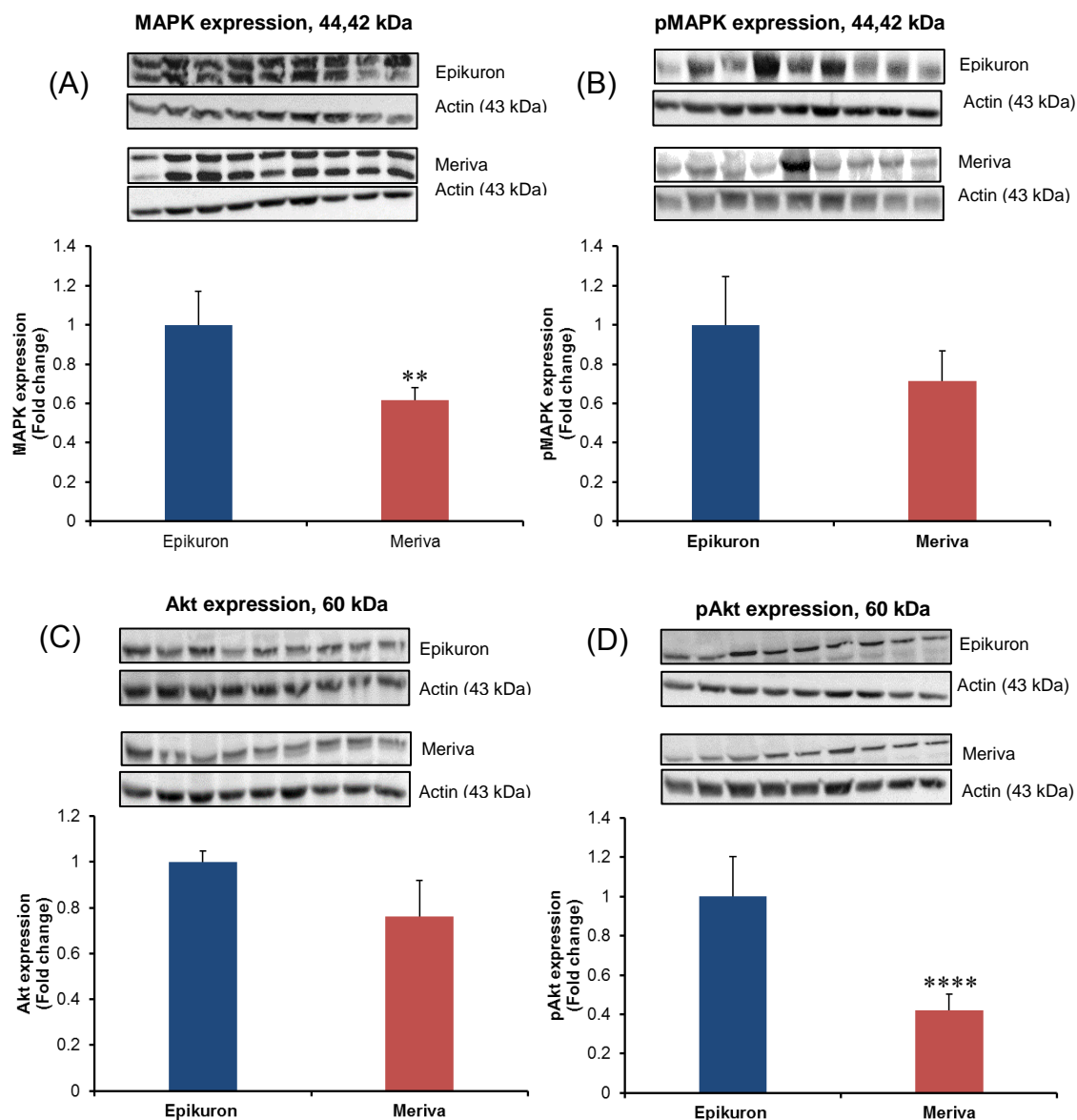


Figure 5.8 Effect of Meriva on the expression MAPK, pMAPK, Akt and pAkt in A549:MRC5 co-culture xenograft tumours in nude mice

Protein levels were measured after sacrificing the animals which received either 0.226% w/w Meriva or 0.180% w/w Epikuron by western blotting of tumour xenograft tissue for (A) MAPK, (B) pMAPK (C) Akt and (D) pAkt. Each graph is based on densitometric analysis of Western blots after normalisation to actin. Each lane represents single animal. Each column represents the mean \pm SEM of 9 animals for the Meriva and Epikuron group. Statistical comparison between the control and Meriva treatment was by Student's T-test. Statistically significant differences are indicated as ** ($p < 0.01$) and **** ($p < 0.001$).

5.6 Modulation of the apoptotic proteins, p21, p27, p53, Bax and Bcl-2 by Meriva in tumour tissue

Induction of apoptosis and autophagy represent two of the mechanisms through which curcumin exhibits its growth inhibitory activity. As dietary Meriva treatment inhibited tumour growth in nude mice, these mechanisms were also investigated in the xenograft tumour tissue. To this end, expression of apoptotic proteins p21, p27, p53, Bax and Bcl-2 in the tumour xenograft tissue was determined in control and Meriva treated samples.

Dietary Meriva caused non-significant changes in expression of p21, p27 and only expression of p53 was significantly upregulated as compared to control group (Figure 5.9). Expression of p53 increased approximately 2 fold in the Meriva treated group as compared to control (Figure 5.9). Meriva treatment did not cause induce any significant changes in expression of Bax and Bcl-2 (Figure 5.10).

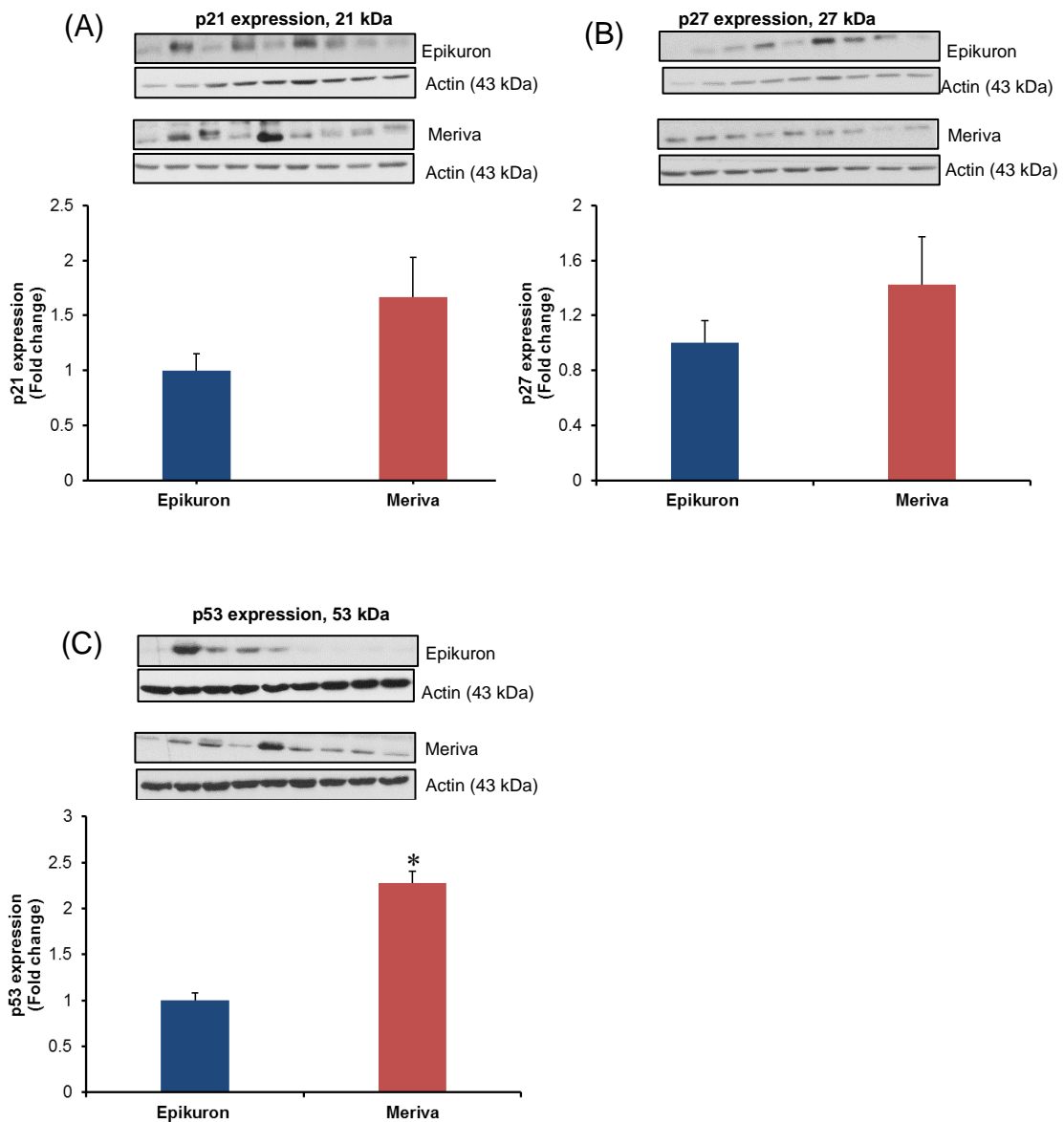


Figure 5.9 Effect of Meriva on the expression of p21, p27 and p53 in A549:MRC5 co-culture xenograft tumours in nude mice.

Protein levels were measured after sacrificing the animals which received either 0.226% w/w Meriva or 0.180% w/w Epikuron by western blotting of tumour xenograft tissue for (A) p21, (B) p27 and (C) p53. Each lane represents single animal. Each graph is based on densitometric analysis of Western blots after normalisation to actin. Each column represents the mean \pm SEM of 9 animals for the Meriva and Epikuron group. Statistical comparison between the control and Meriva treatment was by Student's T-test. Statistically significant differences are indicated as * ($p < 0.05$).

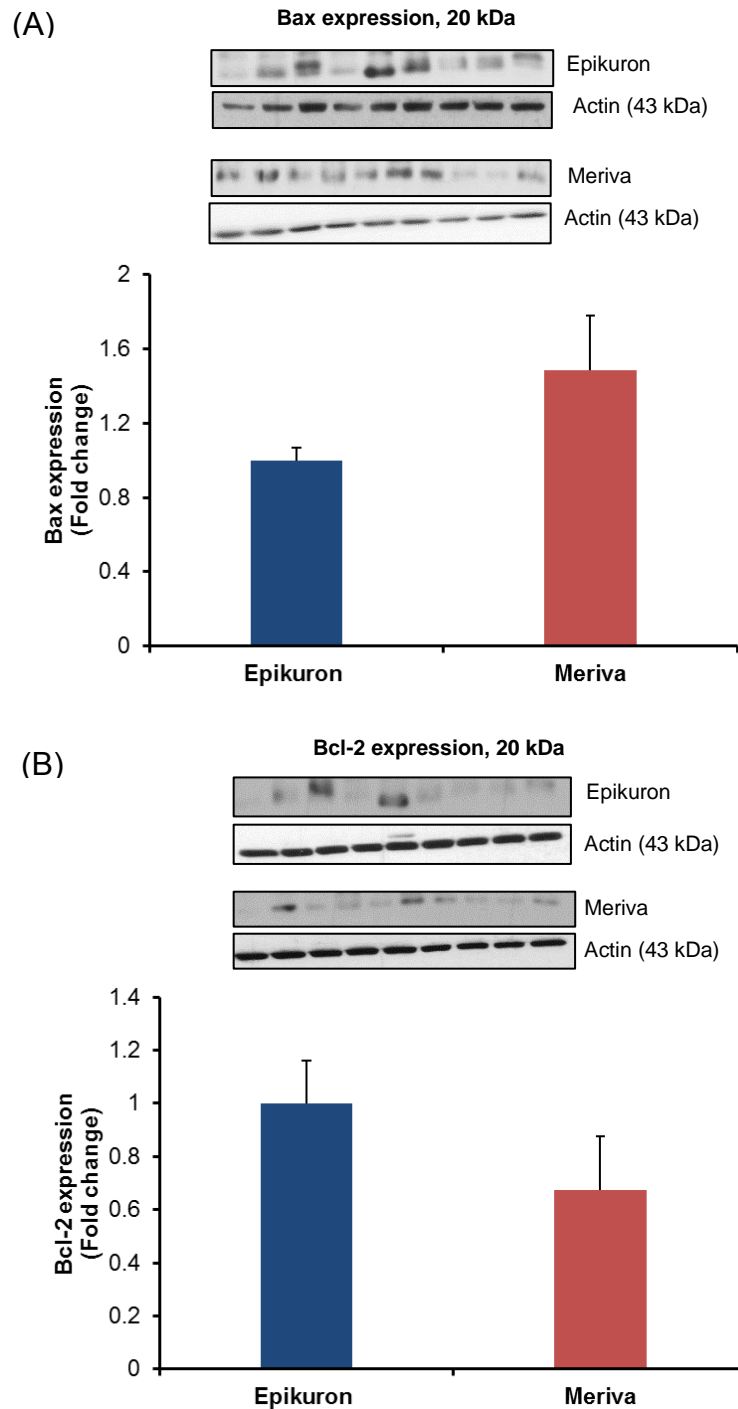


Figure 5.10 Effect of Meriva on the expression of Bax and Bcl-2 in A549:MRC5 co-culture xenograft tumours in nude mice.

Protein levels were measured after sacrificing the animals which received either 0.226% w/w Meriva or 0.180% w/w Epikuron by western blotting of tumour xenograft tissue for (A) Bax and (B) Bcl-2. Each graph is based on densitometric analysis of Western blots after normalisation to actin. Each lane represents single animal. Each column represents the mean \pm SEM of 9 animals for the Meriva and Epikuron group. Statistical comparison between the control and Meriva treatment was by Student's T-test.

5.7 Modulation of the autophagy proteins LC3-I, LC3-II and inflammatory marker COX-2 by Meriva in tumour tissue

Microtubule-associated protein light chain 3 (LC3) is widely used as a marker for autophagy and the ratio of LC3-II:LC3-I protein is indicative of autophagy rate. Meriva treatment caused a 20% increase in the ratio of LC3-II/LC3-I protein expression but the change was statistically non-significant. The expression of inflammatory marker COX-2 remained unchanged by dietary Meriva (Figure 5.11).

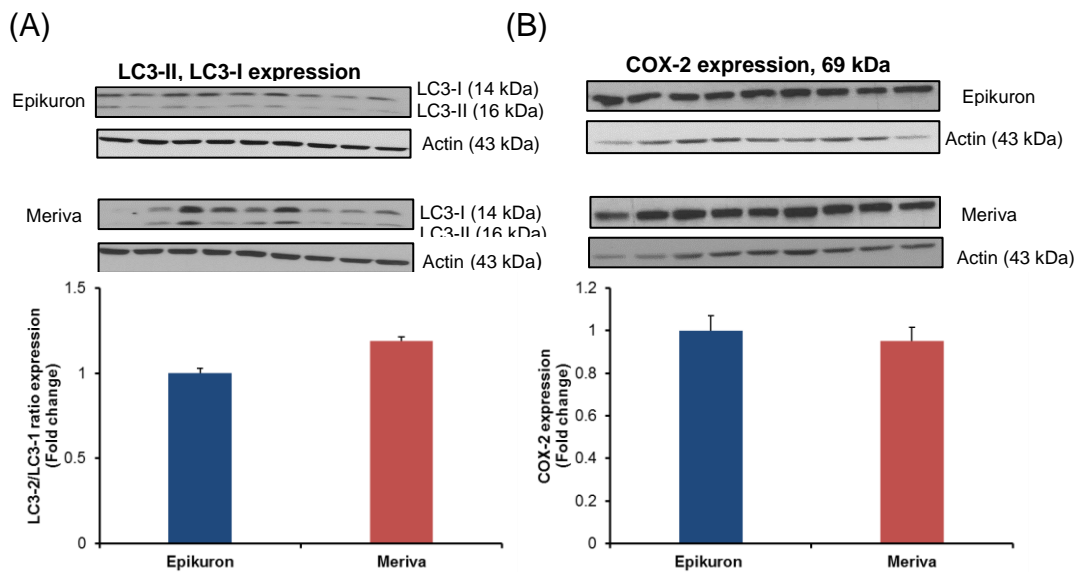


Figure 5.11 Effect of Meriva on the expression of LC3 and COX-2 in A549:MRC5 co-culture xenograft tumours bearing nude mice.

Protein levels were measured after sacrificing animals which received either 0.226% w/w Meriva or 0.180% w/w Epikuron by western blotting of tumour xenograft tissue for (A) LC3 and (B) COX-2. Each graph is based on densitometric analysis of Western blots after normalisation to actin. Each lane represents single animal. Each column represents the mean \pm SEM of 9 animals for the Meriva and Epikuron group. Statistical comparison between the control and Meriva treatment was by Student's T-test.

5.8 Effect of Meriva on cell proliferation and apoptosis in paraffin-embedded xenograft tumour tissue using immunohistochemical staining

The nuclear protein Ki-67 is a validated marker for cell proliferation. Similarly, activated caspase 3 is a well-defined marker for apoptosis and the anti-cleaved caspase 3 antibody is used to detect activated caspase 3. Therefore, the expression of Ki-67 and cleaved caspase 3 were investigated in control and treated tumours, in order to assess the effect of Meriva on tumour cell proliferation.

The tumour sections from the mice on Epikuron and Meriva diets were immunostained for Ki-67 and cleaved caspase-3. The slides were scanned with a Hamamatsu slide scanner and the counting was done by imaging software ImageJ (version 1.49). Meriva treatment caused a significant change in the expression of Ki-67 and cleaved caspase 3 (Figure 5.12 and Figure 5.13). The expression of Ki-67 was reduced by approximately 30% and that of cleaved caspase 3 was increased by 80%.

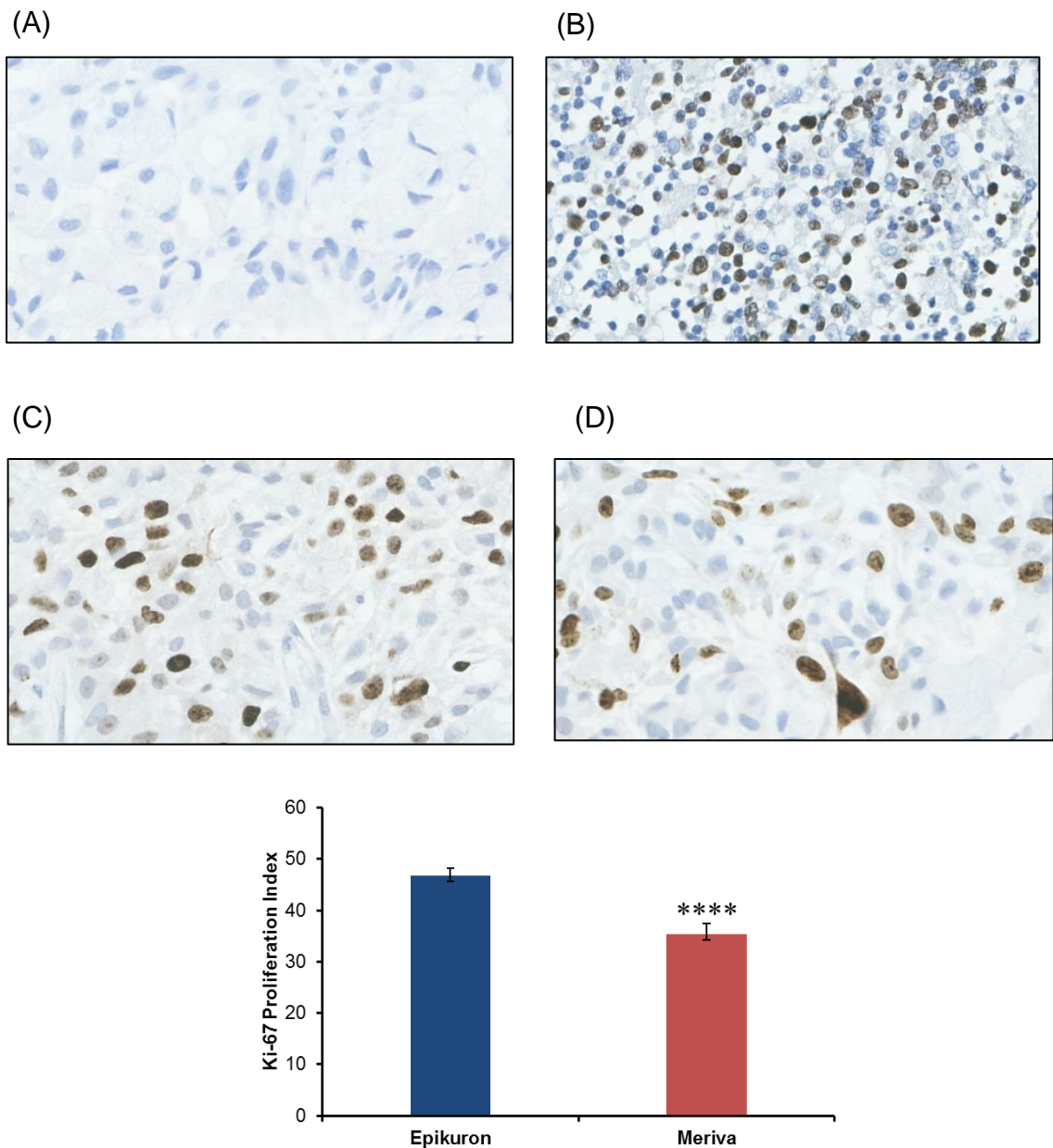


Figure 5.12 Effect of 0.226% Meriva diet on Ki-67 expression in A549:MRC5 co-culture xenograft tumours bearing nude mice.

Immunostaining was performed on paraffin-embedded tumour sections (n = 10 mice per group). The images are representative of samples from the (A) negative control (tumour tissue without antibody) (B) positive control (human tonsil) (C) control-fed groups and (D) Meriva fed group. Sections were immunohistochemically stained for Ki-67 (1:500). The cytoplasmic and perinuclear immunoreactions (brown) were regarded as positive for Ki-67 and counted using automated ImageJ software. The bar chart represents the mean of the positively stained cells \pm SEM as a percentage of the total number of cells. Statistical comparison between the control and Meriva treatment was by Student's T-test. Statistically significant differences are indicated as **** ($p < 0.005$).

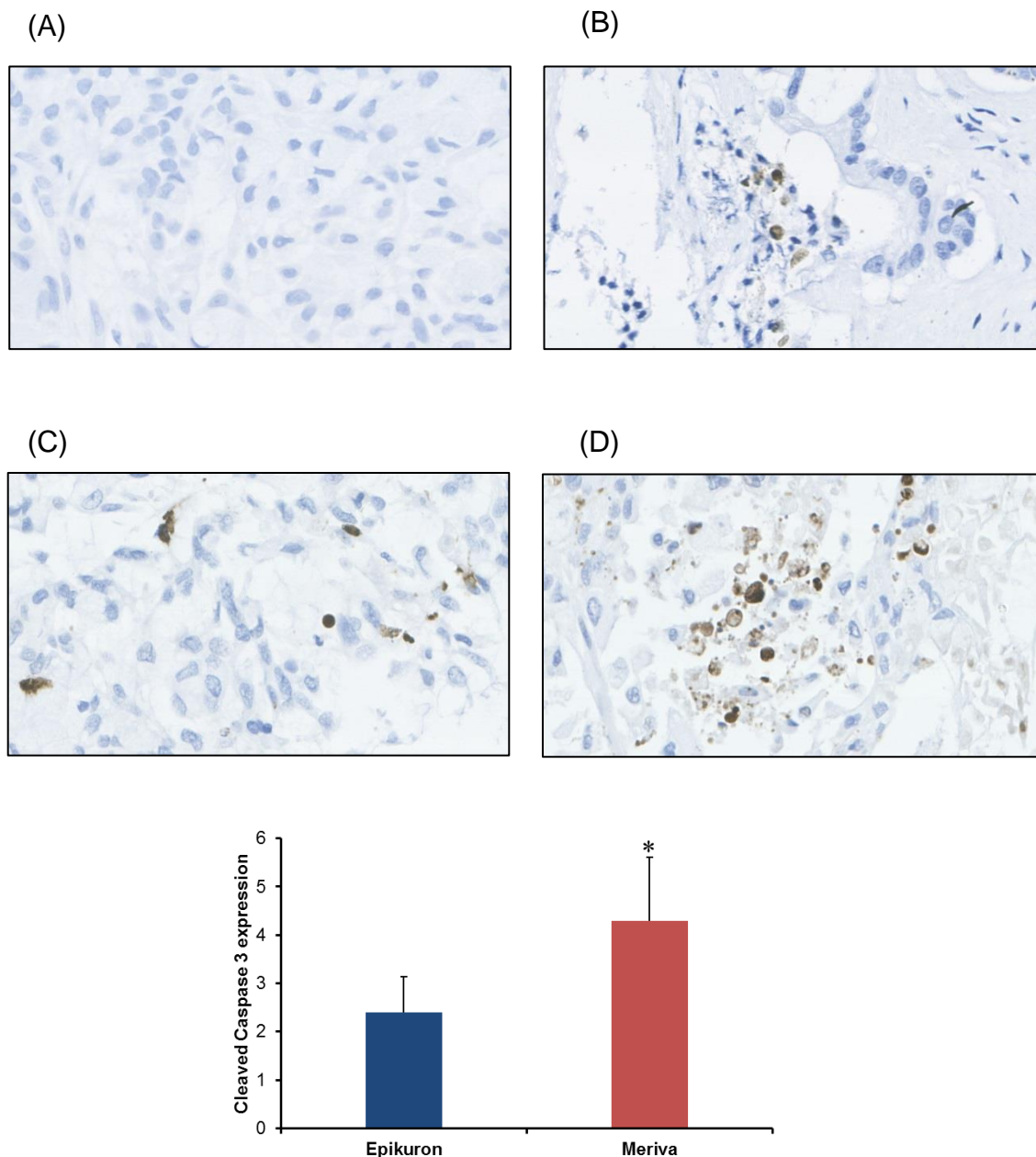


Figure 5.13 Effect of 0.226% Meriva diet on cleaved caspase 3 expression in A549:MRC5 co-culture xenograft tumours bearing nude mice.

Immunostaining was performed on paraffin-embedded tumour sections (n = 10 mice per group). The images are representative of samples from the (A) negative control (tumour tissue without antibody) (B) positive control (human tonsil) (C) control-fed groups and (D) Meriva fed group. Sections were immunohistochemically stained for cleaved caspase 3 (1:100). The cytoplasmic and perinuclear immunoreactions (brown) were regarded as positive for cleaved caspase (red arrows) and counted using ImageJ software. The bar chart represents the mean of the positively stained cells \pm SEM as a percentage of the total number of cells. Statistically significant differences are indicated as * ($p < 0.05$).

5.9 Curcumin and metabolite levels in xenograft tumours and lung tissue following consumption of Meriva.

The tumours and lung tissue from the xenograft study were analysed to determine the levels achieved post dietary feeding. The samples were prepared, extracted and analysed using HPLC-UV as per procedure described in Material and Method section 2.2.2.4 and 2.2.3. Curcuminoids or their metabolites could not be detected in either of the tissues. As curcuminoids were detectable only after post-enzymatic conversion in our previous low dose pharmacokinetic study, tumours and lung tissue were subjected to enzymatic conversion (Material and Method section 2.2.2.3) to ascertain whether curcumin in either its free or conjugated form reached the tissues. Post enzymatic conversion, curcumin was detected in 4 out of 10 tumour samples ($0.14 \pm 0.01\mu\text{M}$ for 4 samples). In lungs no curcuminoids could be detected even after enzymatic conversion (Figure 5.14).

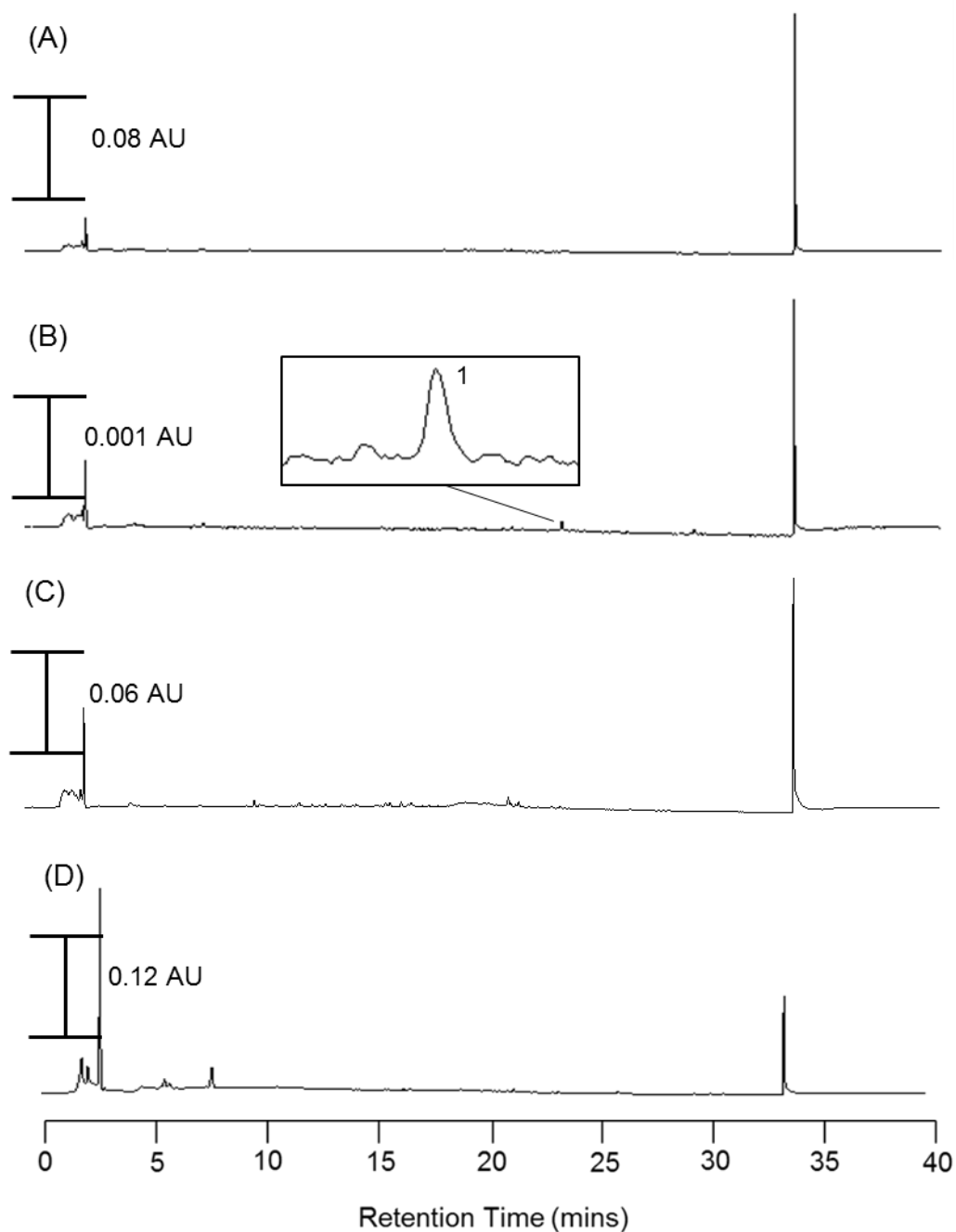


Figure 5.14 Representative HPLC-UV chromatogram of mouse xenograft tumour and lungs post Meriva feeding.

HPLC-UV chromatograms of xenograft tumours or lungs taken from mice receiving Meriva (0.226%) through diet. The chromatograms are as follows: (A) Tumour homogenate extract from Meriva treated mice (B) Extract of enzymatically converted tumour homogenate from Meriva treated mice (C) Lung homogenate extract from Meriva treated mice. (D) Extract of enzymatically converted lung homogenate from Meriva treated mice. Peak 1 to curcumin.

5.10 Discussion

The primary focus of the work described in this chapter was to determine the *in vivo* efficacy of Meriva when given in the diet, and to investigate the potential mechanism of action for its efficacy. The xenograft model used in the study was an extension of the *in vitro* 3D organotypic model where a co-culture of A549 and MRC5 cells was used. This is one of only a few studies using co-cultures of lung tumour cells and fibroblasts in a xenograft efficacy study. The A549 cells used for the xenograft study is a NSCLC adenocarcinoma cell line harbouring a KRAS mutation and is one of the most widely used cell lines for lung cancer xenograft studies [258, 263]. KRAS mutation is the most common type of mutation detected in approximately 25% of all NSCLC cases [298].

Subcutaneous implantation of tumour cells in nude mice is the most common method implemented in early phases of pre-clinical efficacy studies. Most of the xenograft studies described in the literature to date have only used cancer cells to initiate tumour formation. However, it is now well established that tumours are complex tissues comprised of a heterogeneous mixture of cells including endothelial cells, mesenchymal cells, leukocytes, pericytes and extra cellular matrix [299]. The major component of tumour stroma is fibroblasts which have been shown to play important roles during cancer progression and metastasis. They stimulate tumorigenesis, angiogenesis, and invasion in a variety of solid tumours including lung, by secreting various extracellular matrix proteins, proteases, chemokines, and angiogenic factors [300]. Hence, in the current xenograft study, fibroblasts were incorporated with tumour cells to initiate tumour formation.

We first sought to determine the effect of MRC5 fibroblasts on tumour growth. The data from organotypic cultures described in the previous chapter suggested that MRC5 fibroblasts stimulated the invasive capacity of A549 cells. Hence, to explore whether MRC5 fibroblasts could stimulate tumorigenesis, they were subcutaneously co-transplanted with A549 tumour cells. Growth of the resulting tumours was compared against subcutaneous growth of A549 or MRC5 cells alone.

In vitro studies have shown that fibroblasts promote the proliferation of lung cancer cells including A549. A study which co-cultured A549 cells with CCD-19Lu fibroblasts (from a healthy donor) and HLF-A fibroblasts (from a patient with epidermoid carcinoma of the lung) showed that both types of fibroblasts increased proliferation of A549 cells, and the rate of proliferation increased with increasing number of fibroblasts. The proliferation effect was more prominent in the HLF-A co-culture. These effects were exerted by activation of mitogen-activated protein kinases (MAPK) and Akt and via stimulation of TGF- α , EGF and amphiregulin [301]. Similarly, activated forms of fibroblasts known as cancer associated fibroblasts (CAFs) are also known to stimulate proliferation. CAFs stimulated the proliferation of A549 cell when co-cultured together [302]. In addition, conditioned media generated from CAFs also stimulated A549 cell proliferation [303]. The effect of CAFs on promoting tumour growth and metastasis have been shown in models of breast cancer, however there are no in vivo studies demonstrating the same for lung cancer [304]. Fibroblasts secrete an array of paracrine factors including stromal derived factor-1 (SDF-1), PDGF, bFGF, TGF- β , interleukins and HGF which may cause transcriptional changes in cancer cells, enhancing cell proliferation and thus playing an important role in tumorigenesis [297]. The data shown in Chapter 4 section 4.3 demonstrated activation of the HGF/MET pathway and downstream MAPK and Akt signalling in A549 cells by MRC5 conditioned media. As these pathways play an important role in the regulation of cell growth and proliferation, it can be postulated that various growth factors secreted by fibroblasts contribute to tumour growth.

Further analysis of the tumour cell population by FACS and histology indicated that cancer cells form the major cell population (90%) in the tumour even though their initial cell number was only one-fifth of that for fibroblasts. This correlated with organotypic results which also suggested the predominant presence of A549 cells in the upper surface layer. It is possible that as A549 cells are more aggressive in growth compared to MRC5, they outgrow the MRC5 cell population. It can be postulated that when A549 cells are co-cultured with MRC5 fibroblasts, they acquire a more aggressive phenotype which provides a growth and invasive advantage to A549 cells both in vivo and in vitro.

This scenario however is different from human disease where tumours are characterized by extensive development of stroma and tumour cells together. It would have been interesting to assess how co-cultured cells would have behaved in orthotopic lung implantation. An orthotopic xenograft mouse model of breast cancer showed that the fibroblast population actually increases when co-cultures of breast cancer cells and human fibroblasts are orthotopically injected in to mammary fat pads [305]. This suggests that properties of tumour growth in a xenograft study depends greatly on the site of implantation and potentially the type of cancer cells used. In another xenograft model with A549 cells only, curcumin significantly decreased tumour growth and had a suppressing effect of the expression of MMPs, including MMP-2, MMP-9 and -14 [171]. For the current study, further investigations on expression of cytokines, marker of angiogenesis, metastasis and fibroblast markers such as laminin and fibronectin could shed more light on tumour properties and possibly explain differential growth patterns of tumours. Nonetheless, from our findings, we speculate that the presence of fibroblasts initially promotes tumour growth through secretion of an array of growth factors, prior to them being outcompeted by the tumour cells themselves.

The 100% tumour take in this current study demonstrates the reason for A549 cells being the most widely used cell line for lung cancer xenograft models. Preclinical evidence for in vivo efficacy of curcumin against lung cancer has already been reviewed in our publication by Howells et al. [106]. Within these studies, curcumin administration was mostly via oral gavage, intraperitoneal or intravenous route of administration as opposed dietary consumption. Also, amongst the xenograft studies, none used a co-culture of cells to initiate tumour growth. To date only two studies have been performed to test the in vivo efficacy of Meriva. One study aimed at evaluating the efficacy of Meriva on colorectal tumour-bearing mice and the other at lung metastasis of murine mammary gland adenocarcinoma [306],[307]. Both studies demonstrated effectiveness of Meriva in inhibiting tumour growth and lung metastasis. However, the doses of Meriva used were 1.13% and 6% in the diet. This would give a human equivalent dose (when calculated using body surface area) of approximately 8.5 and 51 grams/day respectively for a 70 kg adult. Such high doses are not suitable for

long term human consumption and hence a clinically relevant dose of 0.226% Meriva w/w in the diet was used for this study which equates to approximately a 2 g/day human dose.

The *in vivo* efficacy study showed that dietary Meriva consumption caused a statistically significant inhibition of xenograft lung tumour growth and enhanced the overall survival at this clinically relevant dose. This may be as a consequence of steady levels of curcumin or its conjugates in tumour tissue and the systemic circulation furnished through Meriva consumption. Even though the curcuminoids could be detected only in 4 tumour samples, it is possible that the curcuminoids or their metabolites may be present in the rest of the tumour sample as well, albeit below the limit of detection. The levels will also be dependent on when the mouse last ate, which will vary among animals and could account for the failure to detect curcuminoids in all mice. The same may also be possible for lungs where no curcuminoids could be detected even after enzymatic conversion. Current work in our laboratory includes developing a more sensitive LC-MS/MS technique which can detect quantities as low as femtomolar concentrations.

On investigating the potential mechanism of action by which Meriva exerted its efficacy it was shown not to affect total c-MET levels, but there was no expression of phosphorylated forms of the MET receptor. One of the possible reasons for this may be the low abundance of the phosphorylated form of MET receptor making it difficult to detect its expression by Western blotting. Immunohistochemical staining might have helped in detecting the phosphorylated proteins but due to time constraints no further work was undertaken. Among the downstream proteins, pAkt expression was significantly downregulated in tumour tissues from Meriva treated animals. Oncogenic activation of Akt through phosphorylation is a major and common event in tumourigenesis. *In vitro* studies have shown that curcumin-induced apoptosis in lung cancer cell lines is mediated via inhibition of pAkt [308].

The expression of proteins associated with apoptosis, cell survival and autophagy was further examined. In Meriva treated tissues, a significant increase in p53 expression was observed, with an overall trend for an increase in expression of p21 and p27. The p53 gene is a tumour suppressor and its loss of

function is a frequent event in tumorigenesis. Wild-type p53 inhibits cell proliferation by arresting cells in the G1 phase of the cell cycle, and is also involved in inducing apoptosis, autophagy and senescence.[309]. Meriva induced non-significant changes in other targets such as apoptotic proteins Bax, Bcl-2 and the autophagy marker LC3-I/II.

The decrease in Ki-67 proliferation index indicates that Meriva treatment inhibited tumour cell proliferation. Ki-67 is associated with ribosomal RNA transcription and reduction in its activity leads to inhibition of ribosomal RNA synthesis [310]. The Ki-67 reduction by Meriva observed in our study is consistent with other studies using curcumin against A549 xenograft, K-Ras transgenic and Lewis lung carcinoma mice models of lung cancer [162, 311, 312]. Meriva treatment also induced apoptosis in tumour cells which was evident by increased cleaved caspase 3 expression. Cleavage of caspase 3 is a hallmark of apoptosis which is activated by mitochondrial release of cytochrome C into the cytosol and is a recommended biomarker of apoptosis for clinical and in vivo studies [313].

In summary, the data presented here is the first report of in vivo efficacy of Meriva in a model of lung cancer following a clinically relevant oral dosing regimen. Meriva significantly reduced the growth of tumours derived from A549-MRC5 cell co-culture in the nude mouse xenograft model. We showed that efficacy of Meriva can potentially be via modulation of pAkt and p53 in tumour tissue. Additional studies with Meriva in a transgenic model of lung cancer are therefore warranted to elucidate its potential for use in the management of the disease in humans.

6. Concluding Discussion

Smoking prevention and cessation are at the heart of an overall strategy for lung cancer prevention, but they do not address the problem of the increasing population of former smokers and successfully treated patients who remain at elevated risk. To tackle this issue, there has been an increasing focus on chemoprevention. Despite extensive efforts, agents evaluated in the majority of lung cancer chemoprevention trials have been found to be ineffective or even harmful. As a result, no single agent has been proven to be clinically effective for lung cancer chemoprevention to date. There is therefore a pressing need to investigate and develop new agents for the chemoprevention of lung cancer.

As previously described, the dietary polyphenol, curcumin, represents a well-suited candidate to investigate within the context of lung cancer chemoprevention. In spite of extensive preclinical studies, there have not been many clinical studies demonstrating efficacy within this paradigm. Meriva, a phosphatidylcholine complex formulation of curcumin, offers improved pharmacokinetic properties and enhanced bioavailability in numerous pre-clinical models. Therefore, the research undertaken in this thesis was designed to establish preclinical evidence for the development of curcumin (in the form of Meriva) as a chemopreventive agent for lung cancer.

Previous work within the department had explored the levels of curcumin and its metabolites achieved in intestine and liver of murine models following Meriva administration [215]. The levels achieved in the lung remained to be investigated. Our pharmacokinetic studies showed that Meriva offered superior oral absorption in lungs and in plasma compared to its unformulated form. The possible reasons for these results are: 1) The Meriva formulation increases hydrolytic stability of curcumin at physiological pH, resulting in reduced degradation within an aqueous environment 2) The lipophilic character of the curcumin–phosphatidylcholine complex facilitates rapid exchange of curcumin across biological membranes, boosting its absorption and cellular uptake from the gastrointestinal tract after oral ingestion.

There have been other successful attempts to increase the bioavailability of curcumin, such as co-administration with other drugs, delivery as nanoparticles,

or use of nano-emulsions to improve the pharmacokinetics of curcumin albeit with concerns of safety and toxicity for long term consumption (see section 1.12.4.3). An advantage of Meriva is that it complexes curcumin with phosphatidylcholine which is naturally derived from soy lecithin. Clinical studies of Meriva so far have shown it to be safe for long term human consumption without any significant toxicity. Meriva doses in the range of 1-2 g for an extended period of up to 8 months showed excellent tolerability [251, 266, 268, 276, 314]. This suggests that Meriva is worth considering for the long-term prevention and management of diseases including lung cancer.

Even though phosphatidylcholine is extracted from soy and itself does not contain soy protein, an alternative formulation called Meriva-SF containing phospholipids derived from sunflower oil has been developed by Indena in order to circumvent adverse reactions in individuals who may exhibit soy sensitivity. Simultaneously, a sustained release formulation has also been developed which complexes Meriva with high and low viscosity hydroxypropyl methylcellulose and magnesium citrate laurate (Time-Sorb®). This formulation claims to slow the release and furnish steady-state blood levels of curcumin, although there are as yet, no published data to support this. Nonetheless, these developments are exciting and further enhance the prospects of Meriva being developed as a successful agent for long term management of disease.

In our high dose pharmacokinetic study we observed that curcumin was detected in lung tissues even though no free curcumin could be detected in plasma. This suggests that parent curcumin is regenerated from the glucuronide conjugate in lung tissue probably by intrinsic activity of β -glucuronidase enzyme. This finding is supported by findings by Garvey et al., [272] who demonstrated specifically that intravenous administration of curcumin glucuronide generated parent curcumin in mouse lungs. This possibly explain how curcumin exhibits its biological effects despite not being absorbed in systemic circulation in its active parent form. Metabolite concentrations in this study, as well as several others have been reported as curcumin equivalents, based on the extraction and UV absorption characteristics of curcumin. However, a pharmacokinetic study of resveratrol within our department showed that metabolite concentrations are underestimated by doing so. The estimated resveratrol metabolite concentration

increased 3-4 fold in plasma and up to 1.5 fold in human colon tumour tissue when samples were reanalysed using the metabolite standard curve [315]. Hence, curcumin monoglucuronide and curcumin monosulfate standards were synthesized and the method was revalidated using these standards. At the time when this work was undertaken, there was no HPLC-UV method validated using curcumin and its major metabolites. The new method not only significantly improved the extraction efficiency but also shed light on the relative instability of curcumin metabolites in lungs and in plasma when subjected to frequent freezing and thawing.

The second pharmacokinetic study in this project was performed with a clinically relevant dose of Meriva (equivalent to a human dose of approximately 2 g) utilising the newly validated method. Post enzymatic conversion, the total exposure to curcumin in lungs was 0.4 μM for Meriva treated mice, which was approximately 4.5 fold higher than for unformulated curcumin. The results from this study are of particular significance, as for any potential chemopreventive agent it is important to demonstrate its ability to reach target tissues at a clinically acceptable dose. These levels are still significantly lower than the concentration of curcumin used for virtually all published *in vitro* studies demonstrating potency against lung cancer cell lines. Unpublished data from our lab has shown that, for *in vitro* experiments, repeated daily treatment of cells with curcumin for longer periods significantly reduces the concentration of curcumin required to observe a similar effect. For example, single treatment of A549 cells for 6 days had an IC₅₀ value of 4.1 μM , but treating cells each day reduced the IC₅₀ to 2.5 μM . Therefore, consumption of Meriva for longer periods could possibly exert a pharmacological effect even at low doses.

The second part of this thesis focussed on evaluating the mechanisms of action potentially underlying the *in vivo* efficacy of Meriva. Figure 1.12 in the introduction of the thesis shows the ability of curcumin to modulate multiple cancer related targets. Until recently, there was no published evidence suggesting that curcumin may modulate the HGF-MET pathway. However, Hu et al., [316] have recently reported that curcumin can inhibit c-MET activation in prostate cancer cells. The proto-oncogene MET and its ligand HGF interact and activate downstream signalling via the MAPK/Akt pathway. Aberrant HGF-MET signalling thus

enhances the emergence of an oncogenic phenotype by promoting cellular proliferation, survival, migration, invasion and angiogenesis.

Multiple studies have reported primary MET amplification in NSCLC adenocarcinoma ranging from 2% to 21% [317]. MET amplification leads to overexpression of the MET receptor and activation of downstream signal transduction pathways such as MAPK and Akt. HGF/MET overexpression has also been associated with resistance against *anti-EGFR* and *anti-VEGF* targeted therapies for lung cancer. Considering the range of roles that the HGF/MET axis plays in lung carcinogenesis, HGF/MET makes an attractive target. To date there have been a number of clinical trials targeting HGF/MET inhibition. Onartuzumab, a monovalent antibody that blocks binding of HGF to the MET receptor, in combination with erlotinib, resulted in clinically and statistically improved progression-free survival and overall survival in lung cancer patients [318]. Similarly, Tivantinib, which inhibits auto-phosphorylation of MET, prolonged progression free survival with erlotinib in lung cancer patients [319]. Crizotinib, approved for patients with NSCLC harbouring *EML4-ALK* gene rearrangement exhibited clinical benefit in patients with NSCLC with an absence of *ALK* rearrangement but presence of MET amplification [67]. There are several other drug candidates targeting MET such as Rilotumumab, Ficlatusumab, Cabozantinib and Foretinib which are currently under clinical development for the treatment of lung cancer [295].

The data from *in vitro* experiments in Chapter 4 showed that curcumin treatment inhibited invasion of lung cancer cells in a 3D organotypic co-culture model and suppressed expression of HGF in lung fibroblasts at doses as low as 0.25 μ M. Curcumin treatment also inhibited phosphorylation of the c-MET receptor and Akt. In clinical studies, treatment with erlotinib and cabozantinib in patients with NSCLC resulted in a substantial decreases in pMET and pERK [83]. LY2801653, an oncokinase inhibitor, inhibited tumour growth and metastasis in the H441 NSCLC cell line by inhibition of pMET, pAkt and pMAPK *in vitro* and *in vivo* [75]. Similarly, in the SCLC cell line NCI-H69, treatment by a selective MET inhibitor SU11274 reduced the phosphorylation of MET along with other oncokinases such as pERK1/2, pMAPK and pAkt [70]. Considering that curcumin treatment modulated these targets in A549 lung cancer cells, its clinical development could

similarly be targeted towards combination, adjuvant or maintenance therapies for the potential management of lung cancer in a secondary or tertiary prevention setting.

The final part of this project attempted to demonstrate the *in vivo* efficacy of Meriva in an A549-MRC5 co-culture xenograft mouse model. Although the current study and several other previously reported studies utilised an established A549 lung cancer line, the data generated from such studies may have potential within the context tertiary prevention for use in adjuvant or maintenance regimens. The two important features of this study were co-culturing tumour cells with fibroblasts for tumour initiation, and Meriva treatment through dietary consumption at a clinically achievable dosing regimen. A questionnaire study previously undertaken by Iwuji *et al.* in our group suggested that patients would be hesitant to take large single doses for oral administration of a chemopreventive agent over long periods of time, and would prefer small divided doses [320]. Thus the human equivalent dose of 2 g used in the study could be distributed into 4 doses of 500 mg to enhance patient compliance.

The overarching aim of this project was to provide the groundwork for the development of Meriva as a potential agent for chemoprevention of lung cancer. The models used in our studies were most pertinent to tertiary chemopreventive settings but they also suggest a possible role for curcumin in the therapeutic management of lung cancer. It can be developed as an adjuvant therapy after primary treatment of lung cancer. In reality there would be significant overlap between the use of curcumin for tertiary prevention in previously treated cancer patients and as adjuvant therapy and in fact the two scenarios could be considered the same in lung cancer management. In any event, it is likely that curcumin would have to be used in combination with a maintenance drug therapy rather than as a single agent in cancer patients (or for tertiary prevention), therefore it would be essential to assess the activity and efficacy of curcumin/Meriva in combination with current and emerging therapies before translating to the clinic.

Lung cancer chemoprevention has been a 'forbidden fruit' since the harmful results of CARET and ATBC trials and subsequent failures of other

chemopreventive agents to show positive results. Lessons learnt from these trials have changed the approach to designing large scale chemoprevention trials, and it is now deemed essential to take numerous factors into account during this process. This includes: smoking history; age; genetic makeup; lifestyle; family history; gender differences and non-linear dose related effects. It is thought that one of the critical reasons for failure of chemoprevention trials is selection of the wrong dose. The majority of the preclinical and clinical studies of curcumin have administered impractically high doses in order to demonstrate pharmacokinetic and pharmacodynamic properties of curcumin. This is mainly due to the safe toxicity profile observed with curcumin even at these very high doses. However, in addition to potentially compromising compliance, high dose consumption does not necessarily equate with better efficacy and may even prove detrimental. For example, one of the reasons cited for failure of the ATBC and CARET studies was the dose of β -carotene, which was 5-10 times higher than the normal dietary intake [321]. Similarly, a chemopreventive study from our group using resveratrol showed a non-linear dose response relationship in a mouse model of colorectal carcinogenesis with a lower dose of resveratrol being more effective at suppressing intestinal adenoma development than a dose 200-fold higher [322]. The doses used in pharmacokinetic and *in vivo* studies described in this thesis were clinically relevant, but the failure to confidently detect the presence of curcumin and its metabolites in lung and tumour tissue without enzymatic conversion warrants the development of a more sensitive method. The current method is still useful for analysing curcuminoids and metabolites concentration in plasma and possibly gastrointestinal sites but a more sensitive method is required for distant organs such as lungs and xenograft sites where the analytes reach target tissues by passing through the systemic circulation. Current work in the department is focussed on developing an LC-MS/MS method for simultaneous detection of curcuminoids and their metabolites which can detect analytes in femtomolar concentrations as opposed to nanomolar concentration using HPLC.

Although work in this project has tried to identify the mechanisms of action of curcumin on the HGF/MET pathway, more work is required to assess the effect of curcumin on markers of cellular invasion including β -catenin, E-cadherin and

MMPs. Ongoing work within the Department includes use of other lung cancer cell line such as PC9 and PC9-ER (erlotinib resistant) to determine the effect of curcumin on invasion and markers of EMT. HGF-silenced MRC5 fibroblasts will also be used in the organotypic model to further establish the role that fibroblasts have in causing HGF-stimulated migration of tumour cells.

In summary, the findings of this project demonstrate the superior ability of Meriva to reach lung target tissue. The presence of a curcumin glucuronide-sulfate conjugate which has not previously been reported, was detected in this study. The HPLC-UV assay is the first method to have been validated using curcumin, curcumin monoglucuronide and curcumin monosulfate and allowed accurate plasma and tissue concentrations to be determined. The HGF/MET pathway has been established as a potential target of curcumin in lung cancer, with invasion thought to be mediated via fibroblast-related production of growth factors including HGF, which could be inhibited by curcumin. Furthermore, co-culture of lung cancer cells with fibroblasts in a xenograft model enhanced the rate of tumour growth. A low, clinically relevant dose of Meriva inhibited tumour growth in this co-culture model.

Future work should evaluate the efficacy of Meriva as a single agent or in combination with other agents using different models such as transgenic models of lung cancer to provide better insight as to whether efficacy of Meriva could be maintained at the correct pathologic site. There is also a need to assess the *in vitro* effects of curcumin across more extensive cellular models. Such systems should include explant cultures using primary tissue and cell cultures from primary tissues. Use of such models would allow greater insight into the effects of curcumin across clinically relevant models. These approaches are now commonly used for investigation into molecular mechanisms for targeted agents, and should also be incorporated into preclinical strategies for chemopreventive agents. This would be a rational approach for improving the chances of translating observations of preclinical efficacy into the clinic.

Prior to undertaking large scale chemoprevention trials for curcumin/Meriva, it is necessary to understand the mechanisms to identify pharmacodynamic biomarkers to evaluate its efficacy in targeting potential targets in short term

trials, for example pre-surgical window trials - as a relatively quick way of getting evidence of activity in humans. A better understanding of mechanisms of action might also help identify which types of individual's curcumin might have efficacy in.

In summary, curcumin meets many of the criteria necessary to be successfully taken forward to the clinic but there is much work still to be done to bridge the knowledge gaps prior to entering it into large-scale prevention studies for lung cancer. This is critical if the failings of other trials championing diet-derived agents are not to be repeated.

7 References

1. Doll, R. and A.B. Hill, *Smoking and carcinoma of the lung; preliminary report*. Br Med J, 1950. **2**(4682): p. 739-48.
2. Graham, E.A., *Primary carcinoma of the lung*. Dis Chest, 1950. **18**(1): p. 1-9.
3. Torre, L.A., et al., *Global cancer statistics, 2012*. CA Cancer J Clin, 2015. **65**(2): p. 87-108.
4. Hecht, S.S., *Cigarette smoking and lung cancer: chemical mechanisms and approaches to prevention*. Lancet Oncol, 2002. **3**(8): p. 461-9.
5. Hecht, S.S., *Tobacco smoke carcinogens and lung cancer*. J Natl Cancer Inst, 1999. **91**(14): p. 1194-210.
6. Harris, J.E., et al., *Cigarette tar yields in relation to mortality from lung cancer in the cancer prevention study II prospective cohort, 1982-8*. BMJ, 2004. **328**(7431): p. 72.
7. Kiyohara, C. and Y. Ohno, *Sex differences in lung cancer susceptibility: a review*. Gen Med, 2010. **7**(5): p. 381-401.
8. Jemal, A., E. Ward, and M.J. Thun, *Contemporary lung cancer trends among U.S. women*. Cancer Epidemiol Biomarkers Prev, 2005. **14**(3): p. 582-5.
9. Crispo, A., et al., *The cumulative risk of lung cancer among current, ex- and never-smokers in European men*. Br J Cancer, 2004. **91**(7): p. 1280-6.
10. Services, U.S.D.o.H.a., *The Health Consequences of Involuntary Exposure to Tobacco Smoke: A Report to the Surgeon General*. 2006.
11. Oberg., M., *Worldwide burden of disease from exposure to second-hand smoke: a retrospective analysis of data from 192 countries*. Lancet 2011. **377**: p. 8.
12. Brownson, R.C., et al., *Passive smoking and lung cancer in nonsmoking women*. Am J Public Health, 1992. **82**(11): p. 1525-30.
13. Hecht, S.S., *Tobacco carcinogens, their biomarkers and tobacco-induced cancer*. Nat Rev Cancer, 2003. **3**(10): p. 733-44.
14. Cancer, I.A.f.R.o., *AIR POLLUTION AND CANCER*. 2010.
15. Cohen, A.J. and C.A. Pope, 3rd, *Lung cancer and air pollution*. Environ Health Perspect, 1995. **103 Suppl 8**: p. 219-24.
16. Pershagen, G., *Air pollution and cancer*. IARC Sci Publ, 1990(104): p. 240-51.
17. Doll, R., *Mortality from lung cancer in asbestos workers*. Br J Ind Med, 1955. **12**(2): p. 81-6.
18. Dela Cruz, C.S., L.T. Tanoue, and R.A. Matthay, *Lung cancer: epidemiology, etiology, and prevention*. Clin Chest Med, 2011. **32**(4): p. 605-44.
19. Wright, C.M., et al., *MS4A1 dysregulation in asbestos-related lung squamous cell carcinoma is due to CD20 stromal lymphocyte expression*. PLoS One, 2012. **7**(4): p. e34943.
20. Field, R.W. and B.L. Withers, *Occupational and environmental causes of lung cancer*. Clin Chest Med, 2012. **33**(4): p. 681-703.
21. Sarigiannis, D., et al., *Lung cancer risk from PAHs emitted from biomass combustion*. Environ Res, 2015. **137**: p. 147-56.

22. Armstrong, B., et al., *Lung cancer risk after exposure to polycyclic aromatic hydrocarbons: a review and meta-analysis*. Environ Health Perspect, 2004. **112**(9): p. 970-8.
23. Boffetta, P., N. Jourenkova, and P. Gustavsson, *Cancer risk from occupational and environmental exposure to polycyclic aromatic hydrocarbons*. Cancer Causes Control, 1997. **8**(3): p. 444-72.
24. Jung, K.H., et al., *Assessment of benzo(a)pyrene-equivalent carcinogenicity and mutagenicity of residential indoor versus outdoor polycyclic aromatic hydrocarbons exposing young children in New York City*. Int J Environ Res Public Health, 2010. **7**(5): p. 1889-900.
25. Cassidy, A., et al., *The LLP risk model: an individual risk prediction model for lung cancer*. Br J Cancer, 2008. **98**(2): p. 270-6.
26. Cote, M.L., et al., *Increased risk of lung cancer in individuals with a family history of the disease: a pooled analysis from the International Lung Cancer Consortium*. Eur J Cancer, 2012. **48**(13): p. 1957-68.
27. You, M., et al., *Fine mapping of chromosome 6q23-25 region in familial lung cancer families reveals RGS17 as a likely candidate gene*. Clin Cancer Res, 2009. **15**(8): p. 2666-74.
28. Tomoshige, K., et al., *Germline mutations causing familial lung cancer*. J Hum Genet, 2015. **60**(10): p. 597-603.
29. Voorrips, L.E., et al., *Vegetable and fruit consumption and lung cancer risk in the Netherlands Cohort Study on diet and cancer*. Cancer Causes Control, 2000. **11**(2): p. 101-15.
30. Brennan, P., et al., *Effect of cruciferous vegetables on lung cancer in patients stratified by genetic status: a mendelian randomisation approach*. Lancet, 2005. **366**(9496): p. 1558-60.
31. Fontham, E.T., *Protective dietary factors and lung cancer*. Int J Epidemiol, 1990. **19** Suppl 1: p. S32-42.
32. Mursu, J., et al., *Intake of flavonoids and risk of cancer in Finnish men: The Kuopio Ischaemic Heart Disease Risk Factor Study*. Int J Cancer, 2008. **123**(3): p. 660-3.
33. Xue, X.J., et al., *Red and processed meat consumption and the risk of lung cancer: a dose-response meta-analysis of 33 published studies*. Int J Clin Exp Med, 2014. **7**(6): p. 1542-53.
34. Travis, W.D., et al., *The 2015 World Health Organization Classification of Lung Tumors: Impact of Genetic, Clinical and Radiologic Advances Since the 2004 Classification*. J Thorac Oncol, 2015. **10**(9): p. 1243-60.
35. Gridelli, C., et al., *Treatment of Elderly Patients With Non-Small-Cell Lung Cancer: Results of an International Expert Panel Meeting of the Italian Association of Thoracic Oncology*. Clin Lung Cancer, 2015. **16**(5): p. 325-33.
36. Beasley, M.B., E. Brambilla, and W.D. Travis, *The 2004 World Health Organization classification of lung tumors*. Semin Roentgenol, 2005. **40**(2): p. 90-97.
37. Travis, W.D., et al., *International Association for the Study of Lung Cancer/American Thoracic Society/European Respiratory Society: international multidisciplinary classification of lung adenocarcinoma: executive summary*. Proc Am Thorac Soc, 2011. **8**(5): p. 381-5.
38. Weichert, W. and A. Warth, *Early lung cancer with lepidic pattern: adenocarcinoma in situ, minimally invasive adenocarcinoma, and lepidic*

- predominant adenocarcinoma*. *Curr Opin Pulm Med*, 2014. **20**(4): p. 309-16.
39. Cancer, I.A.f.R.o., *Pathology and Genetics of Tumours of the Lung, Pleura, Thymus and Heart*. IARC Publications.
 40. John, T.M.S., *With Every Breath: A Lung Cancer Guidebook*. 2009.
 41. Hamilton, W. and D. Sharp, *Diagnosis of lung cancer in primary care: a structured review*. *Fam Pract*, 2004. **21**(6): p. 605-11.
 42. Fontana, R.S., et al., *Lung cancer screening: the Mayo program*. *J Occup Med*, 1986. **28**(8): p. 746-50.
 43. Brett, G.Z., *Earlier diagnosis and survival in lung cancer*. *Br Med J*, 1969. **4**(5678): p. 260-2.
 44. National Lung Screening Trial Research, T., et al., *The National Lung Screening Trial: overview and study design*. *Radiology*, 2011. **258**(1): p. 243-53.
 45. Pinsky, P.F., *Assessing the benefits and harms of low-dose computed tomography screening for lung cancer*. *Lung Cancer Manag*, 2014. **3**(6): p. 491-498.
 46. Ganti, A.K. and J.L. Mulshine, *Lung cancer screening*. *Oncologist*, 2006. **11**(5): p. 481-7.
 47. Detterbeck, F.C., P.E. Postmus, and L.T. Tanoue, *The stage classification of lung cancer: Diagnosis and management of lung cancer, 3rd ed: American College of Chest Physicians evidence-based clinical practice guidelines*. *Chest*, 2013. **143**(5 Suppl): p. e191S-210S.
 48. Mirsadraee, S., et al., *The 7th lung cancer TNM classification and staging system: Review of the changes and implications*. *World J Radiol*, 2012. **4**(4): p. 128-34.
 49. Howington, J.A., et al., *Treatment of stage I and II non-small cell lung cancer: Diagnosis and management of lung cancer, 3rd ed: American College of Chest Physicians evidence-based clinical practice guidelines*. *Chest*, 2013. **143**(5 Suppl): p. e278S-313S.
 50. Join Y. Luh, C.R.T., *Radiation Therapy for Non-Small Cell Lung Cancer*. *Caring Ambassadors Lung Cancer Choices*, 2014. **2**.
 51. Luo, S.Y. and D.C. Lam, *Oncogenic driver mutations in lung cancer*. *Transl Respir Med*, 2013. **1**(1): p. 6.
 52. Siegelin, M.D. and A.C. Borczuk, *Epidermal growth factor receptor mutations in lung adenocarcinoma*. *Lab Invest*, 2014. **94**(2): p. 129-37.
 53. Jorge, S.E., S.S. Kobayashi, and D.B. Costa, *Epidermal growth factor receptor (EGFR) mutations in lung cancer: preclinical and clinical data*. *Braz J Med Biol Res*, 2014. **0**: p. 0.
 54. Pao, W. and J. Chmielecki, *Rational, biologically based treatment of EGFR-mutant non-small-cell lung cancer*. *Nat Rev Cancer*, 2010. **10**(11): p. 760-74.
 55. Sharma, S.V., et al., *Epidermal growth factor receptor mutations in lung cancer*. *Nat Rev Cancer*, 2007. **7**(3): p. 169-81.
 56. Engelman, J.A., et al., *MET amplification leads to gefitinib resistance in lung cancer by activating ERBB3 signaling*. *Science*, 2007. **316**(5827): p. 1039-43.
 57. Kobayashi, S., et al., *EGFR mutation and resistance of non-small-cell lung cancer to gefitinib*. *N Engl J Med*, 2005. **352**(8): p. 786-92.

58. Keating, G.M., *Afatinib: a review of its use in the treatment of advanced non-small cell lung cancer*. *Drugs*, 2014. **74**(2): p. 207-21.
59. Cheng, L., et al., *Molecular pathology of lung cancer: key to personalized medicine*. *Mod Pathol*, 2012. **25**(3): p. 347-69.
60. Karachaliou, N., et al., *KRAS mutations in lung cancer*. *Clin Lung Cancer*, 2013. **14**(3): p. 205-14.
61. Pao, W., et al., *KRAS mutations and primary resistance of lung adenocarcinomas to gefitinib or erlotinib*. *PLoS Med*, 2005. **2**(1): p. e17.
62. Reinersman, J.M., et al., *Frequency of EGFR and KRAS mutations in lung adenocarcinomas in African Americans*. *J Thorac Oncol*, 2011. **6**(1): p. 28-31.
63. Soda, M., et al., *Identification of the transforming EML4-ALK fusion gene in non-small-cell lung cancer*. *Nature*, 2007. **448**(7153): p. 561-6.
64. El-Telbany, A. and P.C. Ma, *Cancer genes in lung cancer: racial disparities: are there any?* *Genes Cancer*, 2012. **3**(7-8): p. 467-80.
65. Shaw, A.T., et al., *Clinical features and outcome of patients with non-small-cell lung cancer who harbor EML4-ALK*. *J Clin Oncol*, 2009. **27**(26): p. 4247-53.
66. Sasaki, T., et al., *The biology and treatment of EML4-ALK non-small cell lung cancer*. *Eur J Cancer*, 2010. **46**(10): p. 1773-80.
67. Shaw, A.T., et al., *Effect of crizotinib on overall survival in patients with advanced non-small-cell lung cancer harbouring ALK gene rearrangement: a retrospective analysis*. *Lancet Oncol*, 2011. **12**(11): p. 1004-12.
68. Cecchi, F., D.C. Rabe, and D.P. Bottaro, *Targeting the HGF/Met signaling pathway in cancer therapy*. *Expert Opin Ther Targets*, 2012. **16**(6): p. 553-72.
69. Christensen, J.G., J. Burrows, and R. Salgia, *c-Met as a target for human cancer and characterization of inhibitors for therapeutic intervention*. *Cancer Lett*, 2005. **225**(1): p. 1-26.
70. Ma, P.C., et al., *Functional expression and mutations of c-Met and its therapeutic inhibition with SU11274 and small interfering RNA in non-small cell lung cancer*. *Cancer Res*, 2005. **65**(4): p. 1479-88.
71. Cappuzzo, F., et al., *Increased MET gene copy number negatively affects survival of surgically resected non-small-cell lung cancer patients*. *J Clin Oncol*, 2009. **27**(10): p. 1667-74.
72. Okuda, K., et al., *Met gene copy number predicts the prognosis for completely resected non-small cell lung cancer*. *Cancer Sci*, 2008. **99**(11): p. 2280-5.
73. Bean, J., et al., *MET amplification occurs with or without T790M mutations in EGFR mutant lung tumors with acquired resistance to gefitinib or erlotinib*. *Proc Natl Acad Sci U S A*, 2007. **104**(52): p. 20932-7.
74. Sierra, J.R. and M.S. Tsao, *c-MET as a potential therapeutic target and biomarker in cancer*. *Ther Adv Med Oncol*, 2011. **3**(1 Suppl): p. S21-35.
75. Wu, W., et al., *Inhibition of tumor growth and metastasis in non-small cell lung cancer by LY2801653, an inhibitor of several oncokinasases, including MET*. *Clin Cancer Res*, 2013. **19**(20): p. 5699-710.
76. Puri, N., et al., *A selective small molecule inhibitor of c-Met, PHA665752, inhibits tumorigenicity and angiogenesis in mouse lung cancer xenografts*. *Cancer Res*, 2007. **67**(8): p. 3529-34.

77. Yang, Y., et al., *A selective small molecule inhibitor of c-Met, PHA-665752, reverses lung premalignancy induced by mutant K-ras*. *Mol Cancer Ther*, 2008. **7**(4): p. 952-60.
78. Jung, H.Y., et al., *The Blocking of c-Met Signaling Induces Apoptosis through the Increase of p53 Protein in Lung Cancer*. *Cancer Res Treat*, 2012. **44**(4): p. 251-61.
79. Ozasa, H., et al., *Significance of c-MET overexpression in cytotoxic anticancer drug-resistant small-cell lung cancer cells*. *Cancer Sci*, 2014. **105**(8): p. 1032-9.
80. Munshi, N., et al., *ARQ 197, a novel and selective inhibitor of the human c-Met receptor tyrosine kinase with antitumor activity*. *Mol Cancer Ther*, 2010. **9**(6): p. 1544-53.
81. Bodmer, A., et al., *[The potential of monoclonal antibodies in cancer : established trastuzumab and cetuximab and promising targets IGF-1R and c-MET]*. *Med Sci (Paris)*, 2009. **25**(12): p. 1090-8.
82. Kishi, Y., et al., *Systemic NK4 gene therapy inhibits tumor growth and metastasis of melanoma and lung carcinoma in syngeneic mouse tumor models*. *Cancer Sci*, 2009. **100**(7): p. 1351-8.
83. Padda, S., J.W. Neal, and H.A. Wakelee, *MET inhibitors in combination with other therapies in non-small cell lung cancer*. *Transl Lung Cancer Res*, 2012. **1**(4): p. 238-53.
84. Sadiq, A.A. and R. Salgia, *MET as a possible target for non-small-cell lung cancer*. *J Clin Oncol*, 2013. **31**(8): p. 1089-96.
85. Wang, X., et al., *Does hepatocyte growth factor/c-Met signal play synergetic role in lung cancer?* *J Cell Mol Med*, 2010. **14**(4): p. 833-9.
86. Yano, S., et al., *Hepatocyte growth factor induces gefitinib resistance of lung adenocarcinoma with epidermal growth factor receptor-activating mutations*. *Cancer Res*, 2008. **68**(22): p. 9479-87.
87. Raghav, K.P., A.M. Gonzalez-Angulo, and G.R. Blumenschein, Jr., *Role of HGF/MET axis in resistance of lung cancer to contemporary management*. *Transl Lung Cancer Res*, 2012. **1**(3): p. 179-93.
88. Dong, G., et al., *Hepatocyte growth factor/scatter factor-induced activation of MEK and PI3K signal pathways contributes to expression of proangiogenic cytokines interleukin-8 and vascular endothelial growth factor in head and neck squamous cell carcinoma*. *Cancer Res*, 2001. **61**(15): p. 5911-8.
89. Stabile, L.P., et al., *Targeting of Both the c-Met and EGFR Pathways Results in Additive Inhibition of Lung Tumorigenesis in Transgenic Mice*. *Cancers (Basel)*, 2010. **2**(4): p. 2153-70.
90. Zhang, Y.W., et al., *MET kinase inhibitor SGX523 synergizes with epidermal growth factor receptor inhibitor erlotinib in a hepatocyte growth factor-dependent fashion to suppress carcinoma growth*. *Cancer Res*, 2010. **70**(17): p. 6880-90.
91. Tang, Z., et al., *Dual MET-EGFR combinatorial inhibition against T790M-EGFR-mediated erlotinib-resistant lung cancer*. *Br J Cancer*, 2008. **99**(6): p. 911-22.
92. Robinson, K.W. and A.B. Sandler, *The role of MET receptor tyrosine kinase in non-small cell lung cancer and clinical development of targeted anti-MET agents*. *Oncologist*, 2013. **18**(2): p. 115-22.

93. U.S. Department of Health and Human Services. *How Tobacco Smoke Causes Disease. The Biology and Behavioral Basis for Smoking-Attributable Disease. A Report of the Surgeon General.* 2010. Atlanta, GA: U.S. Department of Health and Human Services, Centers for Disease Control and Prevention, National Center for Chronic Disease Prevention and Health Promotion, Office on Smoking and Health. 2010.
94. Okuyemi, K.S., N.L. Nollen, and J.S. Ahluwalia, *Interventions to facilitate smoking cessation.* Am Fam Physician, 2006. **74**(2): p. 262-71.
95. Nakamura, M., et al., *Effects of stage-matched repeated individual counseling on smoking cessation: A randomized controlled trial for the high-risk strategy by lifestyle modification (HISLIM) study.* Environ Health Prev Med, 2004. **9**(4): p. 152-60.
96. Winterhalder, R.C., et al., *Chemoprevention of lung cancer--from biology to clinical reality.* Ann Oncol, 2004. **15**(2): p. 185-96.
97. Szabo, E., et al., *Chemoprevention of lung cancer: Diagnosis and management of lung cancer, 3rd ed: American College of Chest Physicians evidence-based clinical practice guidelines.* Chest, 2013. **143**(5 Suppl): p. e40S-60S.
98. Greenwald, P., et al., *Chemoprevention.* CA Cancer J Clin, 1995. **45**(1): p. 31-49.
99. Kelsey, C.R., et al., *Local recurrence after surgery for early stage lung cancer: an 11-year experience with 975 patients.* Cancer, 2009. **115**(22): p. 5218-27.
100. Sugimura, H., et al., *Survival after recurrent nonsmall-cell lung cancer after complete pulmonary resection.* Ann Thorac Surg, 2007. **83**(2): p. 409-17; discussion 417-8.
101. Casto, B.C. and M.A. Pereira, *Prevention of mouse lung tumors by combinations of chemopreventive agents using concurrent and sequential administration.* Anticancer Res, 2011. **31**(10): p. 3279-84.
102. Stewart, D., *Lung Cancer: Prevention, Management, and Emerging Therapies.* Current Clinical Oncology, 2010.
103. Albini, A. and M.B. Sporn, *The tumour microenvironment as a target for chemoprevention.* Nat Rev Cancer, 2007. **7**(2): p. 139-47.
104. Madar, S., I. Goldstein, and V. Rotter, *'Cancer associated fibroblasts'--more than meets the eye.* Trends Mol Med, 2013. **19**(8): p. 447-53.
105. Deep, G. and R. Agarwal, *Targeting tumor microenvironment with silibinin: promise and potential for a translational cancer chemopreventive strategy.* Curr Cancer Drug Targets, 2013. **13**(5): p. 486-99.
106. Howells, L.M., et al., *Translating curcumin to the clinic for lung cancer prevention: evaluation of the preclinical evidence for its utility in primary, secondary, and tertiary prevention strategies.* J Pharmacol Exp Ther, 2014. **350**(3): p. 483-94.
107. Tang, P.H., et al., *Effective and sustained delivery of hydrophobic retinoids to photoreceptors.* Invest Ophthalmol Vis Sci, 2010. **51**(11): p. 5958-64.
108. Hong, W.K., et al., *13-cis-retinoic acid in the treatment of oral leukoplakia.* N Engl J Med, 1986. **315**(24): p. 1501-5.
109. Wald, N.J., et al., *Serum beta-carotene and subsequent risk of cancer: results from the BUPA Study.* Br J Cancer, 1988. **57**(4): p. 428-33.

110. Albanes, D., et al., *Alpha-Tocopherol and beta-carotene supplements and lung cancer incidence in the alpha-tocopherol, beta-carotene cancer prevention study: effects of base-line characteristics and study compliance*. J Natl Cancer Inst, 1996. **88**(21): p. 1560-70.
111. Omenn, G.S., et al., *Risk factors for lung cancer and for intervention effects in CARET, the Beta-Carotene and Retinol Efficacy Trial*. J Natl Cancer Inst, 1996. **88**(21): p. 1550-9.
112. Hennekens, C.H., et al., *Lack of effect of long-term supplementation with beta carotene on the incidence of malignant neoplasms and cardiovascular disease*. N Engl J Med, 1996. **334**(18): p. 1145-9.
113. Pekmezci, D., *Vitamin E and immunity*. Vitam Horm, 2011. **86**: p. 179-215.
114. Traber, M.G. and J. Atkinson, *Vitamin E, antioxidant and nothing more*. Free Radic Biol Med, 2007. **43**(1): p. 4-15.
115. Byers, T. and N. Guerrero, *Epidemiologic evidence for vitamin C and vitamin E in cancer prevention*. Am J Clin Nutr, 1995. **62**(6 Suppl): p. 1385S-1392S.
116. Clark, L.C., et al., *Effects of selenium supplementation for cancer prevention in patients with carcinoma of the skin. A randomized controlled trial. Nutritional Prevention of Cancer Study Group*. JAMA, 1996. **276**(24): p. 1957-63.
117. Reid, M.E., et al., *Selenium supplementation and lung cancer incidence: an update of the nutritional prevention of cancer trial*. Cancer Epidemiol Biomarkers Prev, 2002. **11**(11): p. 1285-91.
118. Dunn, B.K., A. Ryan, and L.G. Ford, *Selenium and Vitamin E Cancer Prevention Trial: a nutrient approach to prostate cancer prevention*. Recent Results Cancer Res, 2009. **181**: p. 183-93.
119. Kamangar, F., et al., *Lung cancer chemoprevention: a randomized, double-blind trial in Linxian, China*. Cancer Epidemiol Biomarkers Prev, 2006. **15**(8): p. 1562-4.
120. Karp, D.D., et al., *Randomized, double-blind, placebo-controlled, phase III chemoprevention trial of selenium supplementation in patients with resected stage I non-small-cell lung cancer: ECOG 5597*. J Clin Oncol, 2013. **31**(33): p. 4179-87.
121. Forceville, X., et al., *Effects of high doses of selenium, as sodium selenite, in septic shock: a placebo-controlled, randomized, double-blind, phase II study*. Crit Care, 2007. **11**(4): p. R73.
122. Van Schooten, F.J., et al., *Effects of oral administration of N-acetyl-L-cysteine: a multi-biomarker study in smokers*. Cancer Epidemiol Biomarkers Prev, 2002. **11**(2): p. 167-75.
123. Izzotti, A., et al., *Inhibition by N-acetylcysteine of carcinogen-DNA adducts in the tracheal epithelium of rats exposed to cigarette smoke*. Carcinogenesis, 1995. **16**(3): p. 669-72.
124. van Zandwijk, N., et al., *EUROSCAN, a randomized trial of vitamin A and N-acetylcysteine in patients with head and neck cancer or lung cancer. For the European Organization for Research and Treatment of Cancer Head and Neck and Lung Cancer Cooperative Groups*. J Natl Cancer Inst, 2000. **92**(12): p. 977-86.
125. Keith, R.L., et al., *Oral iloprost improves endobronchial dysplasia in former smokers*. Cancer Prev Res (Phila), 2011. **4**(6): p. 793-802.

126. Mao, J.T., et al., *Lung cancer chemoprevention with celecoxib in former smokers*. *Cancer Prev Res (Phila)*, 2011. **4**(7): p. 984-93.
127. Cook, N.R., et al., *Low-dose aspirin in the primary prevention of cancer: the Women's Health Study: a randomized controlled trial*. *JAMA*, 2005. **294**(1): p. 47-55.
128. Brasky, T.M., et al., *Non-steroidal anti-inflammatory drugs and small cell lung cancer risk in the VITAL study*. *Lung Cancer*, 2012. **77**(2): p. 260-4.
129. Gray, J.E., et al., *Phase 2 randomized study of enzastaurin (LY317615) for lung cancer prevention in former smokers*. *Cancer*, 2013. **119**(5): p. 1023-32.
130. Limburg, P.J., et al., *Randomized phase II trial of sulindac for lung cancer chemoprevention*. *Lung Cancer*, 2013. **79**(3): p. 254-61.
131. Kelly, K., et al., *A randomized phase II chemoprevention trial of 13-CIS retinoic acid with or without alpha tocopherol or observation in subjects at high risk for lung cancer*. *Cancer Prev Res (Phila)*, 2009. **2**(5): p. 440-9.
132. Kelley, M.J., et al., *Safety and efficacy of weekly oral oltipraz in chronic smokers*. *Cancer Epidemiol Biomarkers Prev*, 2005. **14**(4): p. 892-9.
133. Veronesi, G., et al., *Randomized phase II trial of inhaled budesonide versus placebo in high-risk individuals with CT screen-detected lung nodules*. *Cancer Prev Res (Phila)*, 2011. **4**(1): p. 34-42.
134. Lam, S., et al., *A randomized phase IIb trial of anethole dithiolethione in smokers with bronchial dysplasia*. *J Natl Cancer Inst*, 2002. **94**(13): p. 1001-9.
135. Kurie, J.M., et al., *N-(4-hydroxyphenyl)retinamide in the chemoprevention of squamous metaplasia and dysplasia of the bronchial epithelium*. *Clin Cancer Res*, 2000. **6**(8): p. 2973-9.
136. McLarty, J.W., et al., *Beta-Carotene, vitamin A, and lung cancer chemoprevention: results of an intermediate endpoint study*. *Am J Clin Nutr*, 1995. **62**(6 Suppl): p. 1431S-1438S.
137. Lee, J.S., et al., *Randomized placebo-controlled trial of isotretinoin in chemoprevention of bronchial squamous metaplasia*. *J Clin Oncol*, 1994. **12**(5): p. 937-45.
138. Saito, M., et al., *Chemoprevention effects on bronchial squamous metaplasia by folate and vitamin B12 in heavy smokers*. *Chest*, 1994. **106**(2): p. 496-9.
139. Arnold, A.M., et al., *The effect of the synthetic retinoid etretinate on sputum cytology: results from a randomised trial*. *Br J Cancer*, 1992. **65**(5): p. 737-43.
140. Heimbürger, D.C., et al., *Improvement in bronchial squamous metaplasia in smokers treated with folate and vitamin B12. Report of a preliminary randomized, double-blind intervention trial*. *JAMA*, 1988. **259**(10): p. 1525-30.
141. Steward, W.P. and K. Brown, *Cancer chemoprevention: a rapidly evolving field*. *Br J Cancer*, 2013. **109**(1): p. 1-7.
142. Mayne, S.T., G.J. Handelman, and G. Beecher, *Beta-Carotene and lung cancer promotion in heavy smokers--a plausible relationship?* *J Natl Cancer Inst*, 1996. **88**(21): p. 1513-5.
143. Russell, R.M., *The enigma of beta-carotene in carcinogenesis: what can be learned from animal studies*. *J Nutr*, 2004. **134**(1): p. 262S-268S.

144. Greenberg, A.K., et al., *Chemoprevention of lung cancer: prospects and disappointments in human clinical trials*. *Cancers (Basel)*, 2013. **5**(1): p. 131-48.
145. Sozzi, G. and M. Boeri, *Potential biomarkers for lung cancer screening*. *Transl Lung Cancer Res*, 2014. **3**(3): p. 139-48.
146. Prasad, S., et al., *Curcumin, a component of golden spice: from bedside to bench and back*. *Biotechnol Adv*, 2014. **32**(6): p. 1053-64.
147. Lao, C.D., et al., *Dose escalation of a curcuminoid formulation*. *BMC Complement Altern Med*, 2006. **6**: p. 10.
148. Hutchins-Wolfbrandt, A. and A.M. Mistry, *Dietary turmeric potentially reduces the risk of cancer*. *Asian Pac J Cancer Prev*, 2011. **12**(12): p. 3169-73.
149. Sinha, R., et al., *Cancer risk and diet in India*. *J Postgrad Med*, 2003. **49**(3): p. 222-8.
150. Ali, R., et al., *Cancer incidence in British Indians and British whites in Leicester, 2001-2006*. *Br J Cancer*, 2010. **103**(1): p. 143-8.
151. Tayyem, R.F., et al., *Curcumin content of turmeric and curry powders*. *Nutr Cancer*, 2006. **55**(2): p. 126-31.
152. Kwon, Y., *Estimation of curcumin intake in Korea based on the Korea National Health and Nutrition Examination Survey (2008-2012)*. *Nutr Res Pract*, 2014. **8**(5): p. 589-94.
153. Anand, P., et al., *Curcumin and cancer: an "old-age" disease with an "age-old" solution*. *Cancer Lett*, 2008. **267**(1): p. 133-64.
154. Perrone, D., et al., *Biological and therapeutic activities, and anticancer properties of curcumin*. *Exp Ther Med*, 2015. **10**(5): p. 1615-1623.
155. Rahmani, A.H., et al., *Curcumin: a potential candidate in prevention of cancer via modulation of molecular pathways*. *Biomed Res Int*, 2014. **2014**: p. 761608.
156. Sreejayan and M.N. Rao, *Nitric oxide scavenging by curcuminoids*. *J Pharm Pharmacol*, 1997. **49**(1): p. 105-7.
157. Singh, S. and B.B. Aggarwal, *Activation of transcription factor NF-kappa B is suppressed by curcumin (diferuloylmethane) [corrected]*. *J Biol Chem*, 1995. **270**(42): p. 24995-5000.
158. Iqbal, M., et al., *Dietary supplementation of curcumin enhances antioxidant and phase II metabolizing enzymes in ddY male mice: possible role in protection against chemical carcinogenesis and toxicity*. *Pharmacol Toxicol*, 2003. **92**(1): p. 33-8.
159. Karunaweera, N., et al., *Plant polyphenols as inhibitors of NF-kappaB induced cytokine production-a potential anti-inflammatory treatment for Alzheimer's disease?* *Front Mol Neurosci*, 2015. **8**: p. 24.
160. Aggarwal, S., et al., *Curcumin (diferuloylmethane) down-regulates expression of cell proliferation and antiapoptotic and metastatic gene products through suppression of I kappa B alpha kinase and Akt activation*. *Mol Pharmacol*, 2006. **69**(1): p. 195-206.
161. Yang, C.L., et al., *Curcumin blocks small cell lung cancer cells migration, invasion, angiogenesis, cell cycle and neoplasia through Janus kinase-STAT3 signalling pathway*. *PLoS One*, 2012. **7**(5): p. e37960.
162. Xu, Y., et al., *Curcumin inhibits tumor proliferation induced by neutrophil elastase through the upregulation of alpha 1-antitrypsin in lung cancer*. *Mol Oncol*, 2012. **6**(4): p. 405-17.

163. Aggarwal, B.B., A. Kumar, and A.C. Bharti, *Anticancer potential of curcumin: preclinical and clinical studies*. *Anticancer Res*, 2003. **23**(1A): p. 363-98.
164. Hasima, N. and B.B. Aggarwal, *Cancer-linked targets modulated by curcumin*. *Int J Biochem Mol Biol*, 2012. **3**(4): p. 328-51.
165. Liu, H., et al., *Identification of potential pathways involved in the induction of cell cycle arrest and apoptosis by a new 4-arylidene curcumin analogue T63 in lung cancer cells: a comparative proteomic analysis*. *Mol Biosyst*, 2014. **10**(6): p. 1320-31.
166. Wu, S.H., et al., *Curcumin induces apoptosis in human non-small cell lung cancer NCI-H460 cells through ER stress and caspase cascade- and mitochondria-dependent pathways*. *Anticancer Res*, 2010. **30**(6): p. 2125-33.
167. Lev-Ari, S., et al., *Curcumin induces apoptosis and inhibits growth of orthotopic human non-small cell lung cancer xenografts*. *J Nutr Biochem*, 2014. **25**(8): p. 843-50.
168. Li, F., et al., *Curcumin induces p53-independent necrosis in H1299 cells via a mitochondria-associated pathway*. *Mol Med Rep*, 2015. **12**(5): p. 7806-14.
169. Alevizakos, M., S. Kaltsas, and K.N. Syrigos, *The VEGF pathway in lung cancer*. *Cancer Chemother Pharmacol*, 2013. **72**(6): p. 1169-81.
170. Lin, S.S., et al., *Curcumin inhibits the migration and invasion of human A549 lung cancer cells through the inhibition of matrix metalloproteinase-2 and -9 and Vascular Endothelial Growth Factor (VEGF)*. *Cancer Lett*, 2009. **285**(2): p. 127-33.
171. Tsai, J.R., et al., *Curcumin Inhibits Non-Small Cell Lung Cancer Cells Metastasis through the Adiponectin/NF-kappaB/MMPs Signaling Pathway*. *PLoS One*, 2015. **10**(12): p. e0144462.
172. Li, R., et al., *Curcumin inhibits transforming growth factor-beta1-induced EMT via PPARgamma pathway, not Smad pathway in renal tubular epithelial cells*. *PLoS One*, 2013. **8**(3): p. e58848.
173. Starok, M., et al., *EGFR Inhibition by Curcumin in Cancer Cells: A Dual Mode of Action*. *Biomacromolecules*, 2015. **16**(5): p. 1634-42.
174. Mohan, R., et al., *Curcuminoids inhibit the angiogenic response stimulated by fibroblast growth factor-2, including expression of matrix metalloproteinase gelatinase B*. *J Biol Chem*, 2000. **275**(14): p. 10405-12.
175. Xu, J., et al., *Bisdemethoxycurcumin suppresses migration and invasion of highly metastatic 95D lung cancer cells by regulating E-cadherin and vimentin expression, and inducing autophagy*. *Mol Med Rep*, 2015. **12**(5): p. 7603-8.
176. Jiang, A.P., et al., *Down-regulation of epidermal growth factor receptor by curcumin-induced UBE1L in human bronchial epithelial cells*. *J Nutr Biochem*, 2014. **25**(2): p. 241-9.
177. Sakurai, R., et al., *Curcumin protects the developing lung against long-term hyperoxic injury*. *Am J Physiol Lung Cell Mol Physiol*, 2013. **305**(4): p. L301-11.
178. Zhang, Z., et al., *The effect of curcumin on human bronchial epithelial cells exposed to fine particulate matter: a predictive analysis*. *Molecules*, 2012. **17**(10): p. 12406-26.

179. Tourkina, E., et al., *Curcumin-induced apoptosis in scleroderma lung fibroblasts: role of protein kinase cepsilon*. Am J Respir Cell Mol Biol, 2004. **31**(1): p. 28-35.
180. Rennolds, J., et al., *Curcumin regulates airway epithelial cell cytokine responses to the pollutant cadmium*. Biochem Biophys Res Commun, 2012. **417**(1): p. 256-61.
181. Shishodia, S., et al., *Curcumin (diferuloylmethane) down-regulates cigarette smoke-induced NF-kappaB activation through inhibition of IkkappaBalpha kinase in human lung epithelial cells: correlation with suppression of COX-2, MMP-9 and cyclin D1*. Carcinogenesis, 2003. **24**(7): p. 1269-79.
182. Li, S., et al., *Curcumin lowers erlotinib resistance in non-small cell lung carcinoma cells with mutated EGF receptor*. Oncol Res, 2013. **21**(3): p. 137-44.
183. Xiao, K., et al., *Curcumin induces autophagy via activating the AMPK signaling pathway in lung adenocarcinoma cells*. J Pharmacol Sci, 2013. **123**(2): p. 102-9.
184. Kaushik, G., et al., *Curcumin sensitizes lung adenocarcinoma cells to apoptosis via intracellular redox status mediated pathway*. Indian J Exp Biol, 2012. **50**(12): p. 853-61.
185. Chen, H.W., et al., *Curcumin inhibits lung cancer cell invasion and metastasis through the tumor suppressor HLJ1*. Cancer Res, 2008. **68**(18): p. 7428-38.
186. Tamakoshi, A., et al., *Cigarette smoking and serum soluble Fas levels: Findings from the JACC study*. Mutat Res, 2009. **679**(1-2): p. 79-83.
187. Nemmar, A., D. Subramanian, and B.H. Ali, *Protective effect of curcumin on pulmonary and cardiovascular effects induced by repeated exposure to diesel exhaust particles in mice*. PLoS One, 2012. **7**(6): p. e39554.
188. Xu, F., et al., *Curcumin attenuates staphylococcus aureus-induced acute lung injury*. Clin Respir J, 2015. **9**(1): p. 87-97.
189. Sehgal, A., et al., *Synergistic effects of piperine and curcumin in modulating benzo(a)pyrene induced redox imbalance in mice lungs*. Toxicol Mech Methods, 2012. **22**(1): p. 74-80.
190. Sehgal, A., et al., *Combined effects of curcumin and piperine in ameliorating benzo(a)pyrene induced DNA damage*. Food Chem Toxicol, 2011. **49**(11): p. 3002-6.
191. Yin, H., et al., *Synergistic antitumor efficiency of docetaxel and curcumin against lung cancer*. Acta Biochim Biophys Sin (Shanghai), 2012. **44**(2): p. 147-53.
192. Tung, Y.T., et al., *Curcumin reduces pulmonary tumorigenesis in vascular endothelial growth factor (VEGF)-overexpressing transgenic mice*. Mol Nutr Food Res, 2011. **55**(7): p. 1036-43.
193. Lee, J.C., et al., *Dietary curcumin increases antioxidant defenses in lung, ameliorates radiation-induced pulmonary fibrosis, and improves survival in mice*. Radiat Res, 2010. **173**(5): p. 590-601.
194. Su, C.C., et al., *Curcumin inhibits human lung large cell carcinoma cancer tumour growth in a murine xenograft model*. Phytother Res, 2010. **24**(2): p. 189-92.

195. Rocks, N., et al., *Curcumin-cyclodextrin complexes potentiate gemcitabine effects in an orthotopic mouse model of lung cancer*. Br J Cancer, 2012. **107**(7): p. 1083-92.
196. Xu, M., et al., *Effects of curcumin in treatment of experimental pulmonary fibrosis: a comparison with hydrocortisone*. J Ethnopharmacol, 2007. **112**(2): p. 292-9.
197. Puliappadamba, V.T., et al., *Curcumin inhibits B[a]PDE-induced procarcinogenic signals in lung cancer cells, and curbs B[a]P-induced mutagenesis and lung carcinogenesis*. Biofactors, 2015. **41**(6): p. 431-42.
198. Teong, B., et al., *Enhanced anti-cancer activity by curcumin-loaded hydrogel nanoparticle derived aggregates on A549 lung adenocarcinoma cells*. J Mater Sci Mater Med, 2015. **26**(1): p. 5357.
199. Ryan, J.L., et al., *Curcumin for radiation dermatitis: a randomized, double-blind, placebo-controlled clinical trial of thirty breast cancer patients*. Radiat Res, 2013. **180**(1): p. 34-43.
200. Carroll, R.E., et al., *Phase IIa clinical trial of curcumin for the prevention of colorectal neoplasia*. Cancer Prev Res (Phila), 2011. **4**(3): p. 354-64.
201. Cheng, A.L., et al., *Phase I clinical trial of curcumin, a chemopreventive agent, in patients with high-risk or pre-malignant lesions*. Anticancer Res, 2001. **21**(4B): p. 2895-900.
202. Sharma, R.A., et al., *Effects of dietary curcumin on glutathione S-transferase and malondialdehyde-DNA adducts in rat liver and colon mucosa: relationship with drug levels*. Clin Cancer Res, 2001. **7**(5): p. 1452-8.
203. Ledda, A., et al., *Meriva(R), a lecithinized curcumin delivery system, in the control of benign prostatic hyperplasia: a pilot, product evaluation registry study*. Panminerva Med, 2012. **54**(1 Suppl 4): p. 17-22.
204. Ghalaut, V.S., et al., *Effect of imatinib therapy with and without turmeric powder on nitric oxide levels in chronic myeloid leukemia*. J Oncol Pharm Pract, 2012. **18**(2): p. 186-90.
205. He, Z.Y., et al., *Upregulation of p53 expression in patients with colorectal cancer by administration of curcumin*. Cancer Invest, 2011. **29**(3): p. 208-13.
206. Epelbaum, R., et al., *Curcumin and gemcitabine in patients with advanced pancreatic cancer*. Nutr Cancer, 2010. **62**(8): p. 1137-41.
207. Bayet-Robert, M., et al., *Phase I dose escalation trial of docetaxel plus curcumin in patients with advanced and metastatic breast cancer*. Cancer Biol Ther, 2010. **9**(1): p. 8-14.
208. Dhillon, N., et al., *Phase II trial of curcumin in patients with advanced pancreatic cancer*. Clin Cancer Res, 2008. **14**(14): p. 4491-9.
209. Prasad, S., A.K. Tyagi, and B.B. Aggarwal, *Recent developments in delivery, bioavailability, absorption and metabolism of curcumin: the golden pigment from golden spice*. Cancer Res Treat, 2014. **46**(1): p. 2-18.
210. Wang, K. and F. Qiu, *Curcuminoid metabolism and its contribution to the pharmacological effects*. Curr Drug Metab, 2013. **14**(7): p. 791-806.
211. Wahlstrom, B. and G. Blennow, *A study on the fate of curcumin in the rat*. Acta Pharmacol Toxicol (Copenh), 1978. **43**(2): p. 86-92.

212. Lu, X., et al., *Sulfonation of curcuminoids: characterization and contribution of individual SULT enzymes*. Mol Nutr Food Res, 2015. **59**(4): p. 634-45.
213. Hoehle, S.I., E. Pfeiffer, and M. Metzler, *Glucuronidation of curcuminoids by human microsomal and recombinant UDP-glucuronosyltransferases*. Mol Nutr Food Res, 2007. **51**(8): p. 932-8.
214. Pan, M.H., T.M. Huang, and J.K. Lin, *Biotransformation of curcumin through reduction and glucuronidation in mice*. Drug Metab Dispos, 1999. **27**(4): p. 486-94.
215. Marczylo, T.H., et al., *Comparison of systemic availability of curcumin with that of curcumin formulated with phosphatidylcholine*. Cancer Chemother Pharmacol, 2007. **60**(2): p. 171-7.
216. Metzler, M., et al., *Curcumin uptake and metabolism*. Biofactors, 2013. **39**(1): p. 14-20.
217. Priyadarsini, K.I., *The chemistry of curcumin: from extraction to therapeutic agent*. Molecules, 2014. **19**(12): p. 20091-112.
218. Hoehle, S.I., et al., *Metabolism of curcuminoids in tissue slices and subcellular fractions from rat liver*. J Agric Food Chem, 2006. **54**(3): p. 756-64.
219. Shoji, M., et al., *Comparison of the effects of curcumin and curcumin glucuronide in human hepatocellular carcinoma HepG2 cells*. Food Chem, 2014. **151**: p. 126-32.
220. Choudhury, A.K., et al., *Synthesis and Evaluation of the Anti-Oxidant Capacity of Curcumin Glucuronides, the Major Curcumin Metabolites*. Antioxidants (Basel), 2015. **4**(4): p. 750-67.
221. Pal, A., et al., *Curcumin glucuronides: assessing the proliferative activity against human cell lines*. Bioorg Med Chem, 2014. **22**(1): p. 435-9.
222. Ireson, C., et al., *Characterization of metabolites of the chemopreventive agent curcumin in human and rat hepatocytes and in the rat in vivo, and evaluation of their ability to inhibit phorbol ester-induced prostaglandin E2 production*. Cancer Res, 2001. **61**(3): p. 1058-64.
223. Wu, J.C., et al., *Chemopreventative effects of tetrahydrocurcumin on human diseases*. Food Funct, 2014. **5**(1): p. 12-7.
224. Lai, C.S., et al., *Tetrahydrocurcumin is more effective than curcumin in preventing azoxymethane-induced colon carcinogenesis*. Mol Nutr Food Res, 2011. **55**(12): p. 1819-28.
225. Kang, N., et al., *Tetrahydrocurcumin induces G2/M cell cycle arrest and apoptosis involving p38 MAPK activation in human breast cancer cells*. Food Chem Toxicol, 2014. **67**: p. 193-200.
226. Yoysungnoen, B., et al., *Effects of tetrahydrocurcumin on hypoxia-inducible factor-1alpha and vascular endothelial growth factor expression in cervical cancer cell-induced angiogenesis in nude mice*. Biomed Res Int, 2015. **2015**: p. 391748.
227. Wu, J.C., et al., *Tetrahydrocurcumin, a major metabolite of curcumin, induced autophagic cell death through coordinative modulation of PI3K/Akt-mTOR and MAPK signaling pathways in human leukemia HL-60 cells*. Mol Nutr Food Res, 2011. **55**(11): p. 1646-54.
228. Chen, C.Y., W.L. Yang, and S.Y. Kuo, *Cytotoxic activity and cell cycle analysis of hexahydrocurcumin on SW 480 human colorectal cancer cells*. Nat Prod Commun, 2011. **6**(11): p. 1671-2.

229. Pan, M.H., S.Y. Lin-Shiau, and J.K. Lin, *Comparative studies on the suppression of nitric oxide synthase by curcumin and its hydrogenated metabolites through down-regulation of IkappaB kinase and NFkappaB activation in macrophages*. *Biochem Pharmacol*, 2000. **60**(11): p. 1665-76.
230. Patel, K.R., et al., *Sulfate metabolites provide an intracellular pool for resveratrol generation and induce autophagy with senescence*. *Sci Transl Med*, 2013. **5**(205): p. 205ra133.
231. Ravindranath, V. and N. Chandrasekhara, *Absorption and tissue distribution of curcumin in rats*. *Toxicology*, 1980. **16**(3): p. 259-65.
232. Perkins, S., et al., *Chemopreventive efficacy and pharmacokinetics of curcumin in the min/+ mouse, a model of familial adenomatous polyposis*. *Cancer Epidemiol Biomarkers Prev*, 2002. **11**(6): p. 535-40.
233. Maiti, K., et al., *Curcumin-phospholipid complex: Preparation, therapeutic evaluation and pharmacokinetic study in rats*. *Int J Pharm*, 2007. **330**(1-2): p. 155-63.
234. Shoba, G., et al., *Influence of piperine on the pharmacokinetics of curcumin in animals and human volunteers*. *Planta Med*, 1998. **64**(4): p. 353-6.
235. Yang, K.Y., et al., *Oral bioavailability of curcumin in rat and the herbal analysis from *Curcuma longa* by LC-MS/MS*. *J Chromatogr B Analyt Technol Biomed Life Sci*, 2007. **853**(1-2): p. 183-9.
236. Sharma, R.A., et al., *Phase I clinical trial of oral curcumin: biomarkers of systemic activity and compliance*. *Clin Cancer Res*, 2004. **10**(20): p. 6847-54.
237. Garcea, G., et al., *Consumption of the putative chemopreventive agent curcumin by cancer patients: assessment of curcumin levels in the colorectum and their pharmacodynamic consequences*. *Cancer Epidemiol Biomarkers Prev*, 2005. **14**(1): p. 120-5.
238. Irving, G.R., et al., *Prolonged biologically active colonic tissue levels of curcumin achieved after oral administration--a clinical pilot study including assessment of patient acceptability*. *Cancer Prev Res (Phila)*, 2013. **6**(2): p. 119-28.
239. Kanai, M., et al., *A phase I/II study of gemcitabine-based chemotherapy plus curcumin for patients with gemcitabine-resistant pancreatic cancer*. *Cancer Chemother Pharmacol*, 2011. **68**(1): p. 157-64.
240. Basnet, P. and N. Skalko-Basnet, *Curcumin: an anti-inflammatory molecule from a curry spice on the path to cancer treatment*. *Molecules*, 2011. **16**(6): p. 4567-98.
241. Sarada, S.K., et al., *Curcumin prophylaxis mitigates the incidence of hypobaric hypoxia-induced altered ion channels expression and impaired tight junction proteins integrity in rat brain*. *J Neuroinflammation*, 2015. **12**: p. 113.
242. Garcea, G., et al., *Detection of curcumin and its metabolites in hepatic tissue and portal blood of patients following oral administration*. *Br J Cancer*, 2004. **90**(5): p. 1011-5.
243. Saxena, A., et al., *Pharmacovigilance: effects of herbal components on human drugs interactions involving cytochrome P450*. *Bioinformation*, 2008. **3**(5): p. 198-204.

244. Song, W., et al., *Stable loading and delivery of disulfiram with mPEG-PLGA/PCL mixed nanoparticles for tumor therapy*. *Nanomedicine*, 2015.
245. Sreenivasan, S., et al., *Modulation of multidrug resistance 1 expression and function in retinoblastoma cells by curcumin*. *J Pharmacol Pharmacother*, 2013. **4**(2): p. 103-9.
246. Shahani, K., et al., *Injectable sustained release microparticles of curcumin: a new concept for cancer chemoprevention*. *Cancer Res*, 2010. **70**(11): p. 4443-52.
247. Khalil, N.M., et al., *Pharmacokinetics of curcumin-loaded PLGA and PLGA-PEG blend nanoparticles after oral administration in rats*. *Colloids Surf B Biointerfaces*, 2013. **101**: p. 353-60.
248. Sercombe, L., et al., *Advances and Challenges of Liposome Assisted Drug Delivery*. *Front Pharmacol*, 2015. **6**: p. 286.
249. Helson, L., et al., *Infusion pharmacokinetics of Lipocurc (liposomal curcumin) and its metabolite tetrahydrocurcumin in Beagle dogs*. *Anticancer Res*, 2012. **32**(10): p. 4365-70.
250. Nayyer Karimi, B.G., Hamed Hamishehkar, Fatemeh Keivani, Akram Pezeshki, Mohammad Mahdi Gholian, *Phytosome and Liposome: The Beneficial Encapsulation Systems in Drug Delivery and Food Application*. *APPLIED FOOD BIOTECHNOLOGY*, 2015. **2**(3): p. 17-27.
251. Belcaro, G., et al., *Efficacy and safety of Meriva(R), a curcumin-phosphatidylcholine complex, during extended administration in osteoarthritis patients*. *Altern Med Rev*, 2010. **15**(4): p. 337-44.
252. Cuomo, J., et al., *Comparative absorption of a standardized curcuminoid mixture and its lecithin formulation*. *J Nat Prod*, 2011. **74**(4): p. 664-9.
253. Gazdar, A.F., B. Gao, and J.D. Minna, *Lung cancer cell lines: Useless artifacts or invaluable tools for medical science?* *Lung Cancer*, 2010. **68**(3): p. 309-18.
254. Nyga, A., U. Cheema, and M. Loizidou, *3D tumour models: novel in vitro approaches to cancer studies*. *J Cell Commun Signal*, 2011. **5**(3): p. 239-48.
255. Hughes, C.S., L.M. Postovit, and G.A. Lajoie, *Matrigel: a complex protein mixture required for optimal growth of cell culture*. *Proteomics*, 2010. **10**(9): p. 1886-90.
256. Orkin, R.W., et al., *A murine tumor producing a matrix of basement membrane*. *J Exp Med*, 1977. **145**(1): p. 204-20.
257. Edmondson, R., et al., *Three-dimensional cell culture systems and their applications in drug discovery and cell-based biosensors*. *Assay Drug Dev Technol*, 2014. **12**(4): p. 207-18.
258. Kellar, A., C. Egan, and D. Morris, *Preclinical Murine Models for Lung Cancer: Clinical Trial Applications*. *Biomed Res Int*, 2015. **2015**: p. 621324.
259. Meuwissen, R., et al., *Induction of small cell lung cancer by somatic inactivation of both Trp53 and Rb1 in a conditional mouse model*. *Cancer Cell*, 2003. **4**(3): p. 181-9.
260. Jackson, E.L., et al., *Analysis of lung tumor initiation and progression using conditional expression of oncogenic K-ras*. *Genes Dev*, 2001. **15**(24): p. 3243-8.
261. Fisher, G.H., et al., *Induction and apoptotic regression of lung adenocarcinomas by regulation of a K-Ras transgene in the presence and*

- absence of tumor suppressor genes. *Genes Dev*, 2001. **15**(24): p. 3249-62.
262. Zhao, B., et al., *Transgenic mouse models for lung cancer*. *Exp Lung Res*, 2000. **26**(8): p. 567-79.
263. Liu, J. and M.R. Johnston, *Experimental Animal Models for Studying Lung Cancer*. 2009: p. 241-265.
264. Reagan-Shaw, S., M. Nihal, and N. Ahmad, *Dose translation from animal to human studies revisited*. *FASEB J*, 2008. **22**(3): p. 659-61.
265. Hill, K., *Identification of potential mechanisms of action of 3',4',5'-Trimethoxyflavonol in the inhibition of prostate cancer (Doctoral dissertation)*. University of Leicester. 2015.
266. Antiga, E., et al., *Oral Curcumin (Meriva) Is Effective as an Adjuvant Treatment and Is Able to Reduce IL-22 Serum Levels in Patients with Psoriasis Vulgaris*. *Biomed Res Int*, 2015. **2015**: p. 283634.
267. Drobic, F., et al., *Reduction of delayed onset muscle soreness by a novel curcumin delivery system (Meriva(R)): a randomised, placebo-controlled trial*. *J Int Soc Sports Nutr*, 2014. **11**: p. 31.
268. Di Pierro, F., et al., *Comparative evaluation of the pain-relieving properties of a lecithinized formulation of curcumin (Meriva((R))), nimesulide, and acetaminophen*. *J Pain Res*, 2013. **6**: p. 201-5.
269. Dahmke, I.N., et al., *Cooking enhances curcumin anti-cancerogenic activity through pyrolytic formation of "deketene curcumin"*. *Food Chem*, 2014. **151**: p. 514-9.
270. U.S. Department of Health and Human Services, F.a.D.A., *Guidance for Industry: Bioanalytical Method Validation*. 2013.
271. Jager, R., et al., *Comparative absorption of curcumin formulations*. *Nutr J*, 2014. **13**: p. 11.
272. Garvey, L., *Role of β -Glucuronidase in the chemopreventive efficacy of oral curcumin: A Prodrug hypothesis*. 2015.
273. Shi, Q., et al., *Inflammation-associated extracellular beta-glucuronidase alters cellular responses to the chemical carcinogen benzo[a]pyrene*. *Arch Toxicol*, 2016. **90**(9): p. 2261-73.
274. Murdter, T.E., et al., *Enhanced uptake of doxorubicin into bronchial carcinoma: beta-glucuronidase mediates release of doxorubicin from a glucuronide prodrug (HMR 1826) at the tumor site*. *Cancer Res*, 1997. **57**(12): p. 2440-5.
275. Belcaro, G., et al., *Product-evaluation registry of Meriva(R), a curcumin-phosphatidylcholine complex, for the complementary management of osteoarthritis*. *Panminerva Med*, 2010. **52**(2 Suppl 1): p. 55-62.
276. Belcaro, G., et al., *Meriva(R)+Glucosamine versus Chondroitin+Glucosamine in patients with knee osteoarthritis: an observational study*. *Eur Rev Med Pharmacol Sci*, 2014. **18**(24): p. 3959-63.
277. Steigerwalt, R., et al., *Meriva(R), a lecithinized curcumin delivery system, in diabetic microangiopathy and retinopathy*. *Panminerva Med*, 2012. **54**(1 Suppl 4): p. 11-6.
278. Hanahan, D. and R.A. Weinberg, *Hallmarks of cancer: the next generation*. *Cell*, 2011. **144**(5): p. 646-74.

279. Goodman, T.T., C.P. Ng, and S.H. Pun, *3-D tissue culture systems for the evaluation and optimization of nanoparticle-based drug carriers*. *Bioconjug Chem*, 2008. **19**(10): p. 1951-9.
280. Schauer, I.G., et al., *Cancer-associated fibroblasts and their putative role in potentiating the initiation and development of epithelial ovarian cancer*. *Neoplasia*, 2011. **13**(5): p. 393-405.
281. Wood, S.L., et al., *The role of the tumor-microenvironment in lung cancer-metastasis and its relationship to potential therapeutic targets*. *Cancer Treat Rev*, 2014. **40**(4): p. 558-66.
282. De Vlieghere, E., et al., *Cancer-associated fibroblasts as target and tool in cancer therapeutics and diagnostics*. *Virchows Arch*, 2015. **467**(4): p. 367-82.
283. Froeling, F.E., et al., *Organotypic culture model of pancreatic cancer demonstrates that stromal cells modulate E-cadherin, beta-catenin, and Ezrin expression in tumor cells*. *Am J Pathol*, 2009. **175**(2): p. 636-48.
284. Sunaga, N., et al., *Knockdown of oncogenic KRAS in non-small cell lung cancers suppresses tumor growth and sensitizes tumor cells to targeted therapy*. *Mol Cancer Ther*, 2011. **10**(2): p. 336-46.
285. Guin, S., et al., *Contributions of KRAS and RAL in non-small-cell lung cancer growth and progression*. *J Thorac Oncol*, 2013. **8**(12): p. 1492-501.
286. Bhattacharya, S., M.A. Socinski, and T.F. Burns, *KRAS mutant lung cancer: progress thus far on an elusive therapeutic target*. *Clin Transl Med*, 2015. **4**(1): p. 35.
287. Lee, J.Y., et al., *Curcumin induces EGFR degradation in lung adenocarcinoma and modulates p38 activation in intestine: the versatile adjuvant for gefitinib therapy*. *PLoS One*, 2011. **6**(8): p. e23756.
288. Jiao, D., et al., *Curcumin inhibited HGF-induced EMT and angiogenesis through regulating c-Met dependent PI3K/Akt/mTOR signaling pathways in lung cancer*. *Molecular Therapy — Oncolytics*, 2016. **3**: p. 16018.
289. Agwa, E.S. and P.C. Ma, *Targeting the MET receptor tyrosine kinase in non-small cell lung cancer: emerging role of tivantinib*. *Cancer Manag Res*, 2014. **6**: p. 397-404.
290. Onozato, R., et al., *Activation of MET by gene amplification or by splice mutations deleting the juxtamembrane domain in primary resected lung cancers*. *J Thorac Oncol*, 2009. **4**(1): p. 5-11.
291. Onitsuka, T., et al., *Comprehensive molecular analyses of lung adenocarcinoma with regard to the epidermal growth factor receptor, K-ras, MET, and hepatocyte growth factor status*. *J Thorac Oncol*, 2010. **5**(5): p. 591-6.
292. Onitsuka, T., et al., *Acquired resistance to gefitinib: the contribution of mechanisms other than the T790M, MET, and HGF status*. *Lung Cancer*, 2010. **68**(2): p. 198-203.
293. Tsao, M.S., et al., *Differential expression of Met/hepatocyte growth factor receptor in subtypes of non-small cell lung cancers*. *Lung Cancer*, 1998. **20**(1): p. 1-16.
294. Tsao, M.S., et al., *Hepatocyte growth factor is predominantly expressed by the carcinoma cells in non-small-cell lung cancer*. *Hum Pathol*, 2001. **32**(1): p. 57-65.

295. Landi, L., et al., *Targeting c-MET in the battle against advanced nonsmall-cell lung cancer*. *Curr Opin Oncol*, 2013. **25**(2): p. 130-6.
296. Grugan, K.D., et al., *Fibroblast-secreted hepatocyte growth factor plays a functional role in esophageal squamous cell carcinoma invasion*. *Proc Natl Acad Sci U S A*, 2010. **107**(24): p. 11026-31.
297. Nakamura, T., et al., *Induction of hepatocyte growth factor in fibroblasts by tumor-derived factors affects invasive growth of tumor cells: in vitro analysis of tumor-stromal interactions*. *Cancer Res*, 1997. **57**(15): p. 3305-13.
298. Shames, D.S. and Wistuba, II, *The evolving genomic classification of lung cancer*. *J Pathol*, 2014. **232**(2): p. 121-33.
299. Whipple, C.A., *Tumor talk: understanding the conversation between the tumor and its microenvironment*. *Cancer Cell Microenviron*, 2015. **2**(2): p. e773.
300. Jeon, E.S., et al., *Mesenchymal stem cells stimulate angiogenesis in a murine xenograft model of A549 human adenocarcinoma through an LPA1 receptor-dependent mechanism*. *Biochim Biophys Acta*, 2010. **1801**(11): p. 1205-13.
301. Cekanova, M., et al., *Pulmonary fibroblasts stimulate the proliferation of cell lines from human lung adenocarcinomas*. *Anticancer Drugs*, 2006. **17**(7): p. 771-81.
302. Li, J., et al., *mir-1-mediated paracrine effect of cancer-associated fibroblasts on lung cancer cell proliferation and chemoresistance*. *Oncol Rep*, 2016. **35**(6): p. 3523-31.
303. Kinoshita, K., et al., *Imatinib mesylate inhibits the proliferation-stimulating effect of human lung cancer-associated stromal fibroblasts on lung cancer cells*. *Int J Oncol*, 2010. **37**(4): p. 869-77.
304. Liao, D., et al., *Cancer associated fibroblasts promote tumor growth and metastasis by modulating the tumor immune microenvironment in a 4T1 murine breast cancer model*. *PLoS One*, 2009. **4**(11): p. e7965.
305. Olsen, C.J., et al., *Human mammary fibroblasts stimulate invasion of breast cancer cells in a three-dimensional culture and increase stroma development in mouse xenografts*. *BMC Cancer*, 2010. **10**: p. 444.
306. Ibrahim, A., et al., *Effect of curcumin and Meriva on the lung metastasis of murine mammary gland adenocarcinoma*. *In Vivo*, 2010. **24**(4): p. 401-8.
307. Howells, L.M., et al., *Curcumin ameliorates oxaliplatin-induced chemoresistance in HCT116 colorectal cancer cells in vitro and in vivo*. *Int J Cancer*, 2011. **129**(2): p. 476-86.
308. Amin, A.R., et al., *Curcumin induces apoptosis of upper aerodigestive tract cancer cells by targeting multiple pathways*. *PLoS One*, 2015. **10**(4): p. e0124218.
309. Liu, X., et al., *Association between smoking and p53 mutation in lung cancer: a meta-analysis*. *Clin Oncol (R Coll Radiol)*, 2014. **26**(1): p. 18-24.
310. Bullwinkel, J., et al., *Ki-67 protein is associated with ribosomal RNA transcription in quiescent and proliferating cells*. *J Cell Physiol*, 2006. **206**(3): p. 624-35.
311. Ranjan, A.P., et al., *Curcumin-ER Prolonged Subcutaneous Delivery for the Treatment of Non-Small Cell Lung Cancer*. *J Biomed Nanotechnol*, 2016. **12**(4): p. 679-88.

312. Moghaddam, S.J., et al., *Curcumin inhibits COPD-like airway inflammation and lung cancer progression in mice*. *Carcinogenesis*, 2009. **30**(11): p. 1949-56.
313. Bressenot, A., et al., *Assessment of apoptosis by immunohistochemistry to active caspase-3, active caspase-7, or cleaved PARP in monolayer cells and spheroid and subcutaneous xenografts of human carcinoma*. *J Histochem Cytochem*, 2009. **57**(4): p. 289-300.
314. Belcaro, G., et al., *A controlled study of a lecithinized delivery system of curcumin (Meriva(R)) to alleviate the adverse effects of cancer treatment*. *Phytother Res*, 2014. **28**(3): p. 444-50.
315. Patel, K., *Potential cancer chemopreventive properties of Resveratrol metabolites*. 2011.
316. Hu, H.J., et al., *Curcumin mediates reversion of HGF-induced epithelial-mesenchymal transition via inhibition of c-Met expression in DU145 cells*. *Oncol Lett*, 2016. **11**(2): p. 1499-1505.
317. Pao, W. and N. Girard, *New driver mutations in non-small-cell lung cancer*. *Lancet Oncol*, 2011. **12**(2): p. 175-80.
318. Koeppen, H., et al., *Biomarker analyses from a placebo-controlled phase II study evaluating erlotinib+/-onartuzumab in advanced non-small cell lung cancer: MET expression levels are predictive of patient benefit*. *Clin Cancer Res*, 2014. **20**(17): p. 4488-98.
319. Sequist, L.V., et al., *Randomized phase II study of erlotinib plus tivantinib versus erlotinib plus placebo in previously treated non-small-cell lung cancer*. *J Clin Oncol*, 2011. **29**(24): p. 3307-15.
320. Iwujii, C., et al., *Cancer chemoprevention: factors influencing attitudes towards chemopreventive agents in high-risk populations*. *European journal of cancer prevention : the official journal of the European Cancer Prevention Organisation (ECP)*, 2014. **23**(6): p. 594-601.
321. Greenwald, P., *Beta-carotene and lung cancer: a lesson for future chemoprevention investigations?* *J Natl Cancer Inst*, 2003. **95**(1): p. E1.
322. Cai, H., et al., *Cancer chemoprevention: Evidence of a nonlinear dose response for the protective effects of resveratrol in humans and mice*. *Sci Transl Med*, 2015. **7**(298): p. 298ra117.